Elucidating the mechanism of localised mRNA translation during *Drosophila* oogenesis

DPhil Thesis
University of Oxford
Christ Church
DPhil Chromosome and Developmental Biology

Alexander Davidson
Supervisor: Professor Ilan Davis
49,745 words

21/08/2015
Trinity Term 2015

Elucidating the mechanism of localised mRNA translation during *Drosophila* oogenesis.

Alexander Davidson, Christ Church, DPhil Chromosome and Developmental Biology, Trinity Term 2015

Abstract

mRNA localisation and translational control is a conserved, universal process involved in a number of essential cellular processes. Localised mRNAs are processed throughout their life cycle from transcription to degradation. How and where key mRNA remodelling steps occur is unclear. Furthermore, how mRNAs are translationally repressed during their transport, but translationally activated once localised, is a key question in the field. The *Drosophila* oocyte is a well used model system, and is patterned by the differential localisation of *gurken*, *bicoid*, *oskar* and *nanos*, which are all transcribed in the nuclei of the adjacent supporting nurse cell tissue. Here, I image localised mRNAs in live nurse cells and detect *gurken* with single molecule fluorescent *in-situ* hybridisation techniques for the first time. I use these assays to characterise the properties of *gurken* and *oskar* mRNAs in the nurse cells, and show they are strikingly different to the oocyte. I find that Processing bodies, which are key sites of translational regulation in the oocyte, contain significantly lower levels of the translational activator and *Drosophila* CPEB homolog, Orb. I show that, in contrast to *oskar,* whose translation is prevented during transport mainly by repressor proteins, *gurken* mRNA translation in the nurse cells is not prevented by a single repressor, but rather the absence of its translational activator, Orb/CPEB, in this tissue. Ectopic expression of Orb in the nurse cells is sufficient for the association of *gurken* with Processing bodies and premature *gurken* translation. These data highlight a new model for translational regulation through restricted spatial access to a translational activator, and I propose that such a mechanism could be widely deployed in other tissues.

Declaration

I hereby declare that this Thesis is my own work and the experiments described in the following pages were performed by myself, unless otherwise stated. The experiments were carried out in the Department of Biochemistry, University of Oxford. This Thesis has not been submitted for any other degree or professional qualification.

The following parts of this Thesis were completed by others.

1.) Cloning of the *grk-MS2-24* constructs used in Chapter 3 was performed by B. Steinkraus, Fulga lab, Weatherall Institute of Molecular Medicine, University of Oxford, John Radcliffe Hospital, Headington, Oxford, OX3 9DS, UK. This relates to the following figures:

Figure 3-10: The majority of *grk*GFP-24* particles are retained in the nurse cell nuclei.

Movie 3-10: *grk*GFP-24* particles are retained in the nurse cell nuclei

Movie 3-12: *grk* particles which are exported from the nurse cell nuclei in *grk*GFP-24* egg chambers do localise to the oocyte DA corner

2.) All Electron Microscopy data displayed in Chapters 5 and 7 was collected by T. Weil, B. Herpers and C. Rabouille at the Department of Cell biology, UMC Utrecht,

Heidelberglaan 100, 3584 CX Utrecht, The Netherlands. This relates to the following figures:

Figure 5-1: Nurse cell P bodies visualized by EM have a similar protein complement to those in the oocyte

Figure 5-3: Sqd is detected in nurse cell P bodies by EM but not fluorescence

Figure 5-4: Orb is expressed at much lower levels in the nurse cells than in the oocyte

Figure 7-14: P bodies throughout the oocyte contain Sqd and Orb

Alex Davidson

21/08/2015

Acknowledgements

I would like to thank my supervisor, Ilan Davis, for allowing me to undertake my DPhil in his lab, and for his supervision, advice, and patience. I am indebted to Tim Weil for his help in steering the project, teaching me all of the techniques involved, discussions of the data, immeasurable quantities of life advice, and for continuing to supervise me after moving to Cambridge. My thanks also go to Richard Parton for teaching me the finer details of microscopy and the importance of being pedantic. I am extremely grateful to Catherine Rabouille for her work with the EM and for allowing me to present her data in this Thesis, and discussions of the data. I am thankful to Bruno Steinkraus for his help with cloning, to Lu Yang for her help with the sPAT, and Kirsty Gill for help with *Drosophila* protocols.

I am enormously grateful to all of the other members of the Davis lab past and present for their help and advise, and to collaborators: A. Ephrussi (EMBL, Germany), A. Nakamura (RIKEN, Japan), P. Macdonald (University of Texas at Austin, USA), M. Buszczak (University of Texas SouthWestern Medical Center, USA), T. Schüpbach (Princeton University, USA) and J. van Minne (University of Calgary, Canada) for fly stocks, antibodies and reagents; P. Schedl (Princeton University, USA), D. Ish-Horowicz, and T. Schupbach (Princeton University USA) for experimental advice; L. Shermelleh (Department of Biochemistry, University of Oxford) and Micron Oxford for help and advice with 3D-SIM, and Bram Herpers (Leiden, NL) for the egg chamber IEM sections.

Finally I am grateful to the Wellcome Trust for funding me, and to Christ Church, Amber, my friends and family, and the OUBC for their support outside of the lab.

List of abbreviations

AA	Amino Acid
aret	*arrest*
AT	Actively transported
BBR	Bicoid binding region
bcd	*bicoid*
Bic C	Bicaudal C
BicD	Bicaudal-D
BIE	*bicoid* instability element
BLE	*bicoid* localisation element
BRE	Bruno Response Element
Bru	Bruno
BSA	Bovine Serum Albumin
BSF	*bicoid* stability factor
bwk	*bullwinkle*
cDNA	Complementrary deoxyribonucleic acid
CPE	Cytoplasmic polyadenylation element
CPEB	Cytoplasmic polyadenylation element binding protein
CPSF	Cleavage and polyadenylation specficity factor
DA	Dorsoanterior
dFMR1	*Drosophila* Fragile X mental retardation protein
DICE	Differential control element
DIG	Digoxygenin
DNA	Deoxyribonucleic acid
DSB	Double strand break

dsRBP	Double stranded RNA binding protein
D-TACC	*Drosophila* transforming acidic coiled-coil protein
EDTA	Ethylenediaminetetraacetic acid
EGFR	Epidermal growth factor receptor
Egl	Egalitarian
eIF	Eukaryotic initation factor
EJC	Exon-exon Junction Complex
Enc	Encore
Exu	Exuperantia
FFS	Fluorescence fluctuation microscopy
FISH	Fluorescent *in situ* hybridisation
Flp	Flipase
fps	Frames per second
FRT	Flipase - recognition target sequence
GFP	Green fluorescent protein
Gld2	Germline development 2
Glo	Glorund
GSC	Germline stem cell
h	Hour(s)
grk	*gurken*
Heph	Hephaestus
hnRNP	Heterogenous nuclear ribonucleoprotein
iCLIP	Individual-nucleotide resolution Cross-linking and Immuno-Precipitation
IEM	Immuno-electron microscopy
IRES	Internal ribosome entry site

ISH	*in situ* hybridisation
Klar	Klarsicht
mCherry	Monomeric Cherry
MCP	MS2 coat protein
MCP-FP	MCP fused to a fluorophore
Me31B	Maternal expression at 31B
min	Minute(s)
mKO2	Monomeric Kusabira Orange 2
mm	millimetre
mM	milliMol
ml	mililitre
mRNA	Messenger Ribonucleic Acid
MZT	Maternal-to-zygotic transition
NA	Numerical aperture
NGD	No-go decay
NLS	Nuclear localisation signal
NMD	Nonsense-mediated decay
NMJ	Neuromuscular junction
NMR	Nuclear magnetic resonance
nos	*nanos*
NPC	Nuclear pore complex
NRE	Nanos response element
NSD	Non-stop decay
OES	Oocyte entry signal
orb	*oo18 RNA binding protein*
osk	*oskar*

Otu	Ovarian tumour
PABP	Poly(A) binding protein
PAP	Poly(A) polymerase
PARN	Poly(A) ribonuclease
PBS	Phosphate Buffered Saline
PBST	PBS with Tween 20 (0.2%)
PBTX	PBS with Triton-X 100 (0.1%)
PCP	PP7 coat protein
PCR	Polymerase Chain Reaction
PFA	Paraformaldehyde
piRNA	PIWI interacting RNA
PKA	Protein Kinase A
pros	*prospero*
PTB	Polypyrimidine tract binding protein
Pum	Pumilio
P-bodies	Processing bodies
RBP	RNA binding protein
RINGO	Rapid inducer of G2-M in oocytes
RNA	Ribonucleic Acid
RNAse	Ribonuclease
RNP	Ribonucleoprotein
rpm	revolutions per minute
RRM	RNA recognition motif
RT-PCR	Reverse Transcription PCR
s	Second(s)
SELEX	Selected evolution of ligands by exponential enrichment

siRNA	Short interfering RNA
SOLE	Spliced *oskar* localisation element
sPAT	Splint mediated poly(A) test assay
spindle-B	*spn-B*
SRE	Smaug recognition element
Sqd	Squid
Stau	Staufen
S^{1}	*Star*^{1}
TIRF	Total internal reflection microscopy
TSA	Tyramide signal amplification
Tral	Trailerhitch
TRICK	Translating RNA imaging by coat protein knock-off
Tris	tris(hydroxymethyl)aminomethane
Triton-X 100	Octylphenoxypolyethoxyethanol
Tween 20	Polyoxyethylene sorbitan monolaurate
UTR	Untranslated region
UV	Ultraviolet
UAS	Upstream activator sequence
Vas	Vasa
Wisp	Wispy
YFP	Yellow fluorescent protein
YPS	Ypsilon Schachtel
4E-BP	eIF4E binding protein
4E-HP	eIF4E homology proteins
μl	Microlitre
μm	Micrometre

Table of Contents

Results

Discussion

List of Figures

List of Tables

Chapter 1: Introduction

Localised mRNA translation

Targeting protein expression to different areas of the cell is essential for many biological processes. The view that intracellular protein localisation is mediated exclusively by signal regions within the peptides themselves was challenged when *actin* mRNA was found to be asymmetrically localised in ascidian eggs (Jeffery et al. 1983). Since then, the role of mRNA localisation and localised translation has been uncovered as a universal and conserved mechanism for controlling protein expression in time and space (Buxbaum et al. 2015, Lécuyer et al. 2007, Medioni et al. 2012, Parton et al. 2014, St Johnston 2005, Weil 2014).

Localising mRNAs, rather than proteins, to different sub-cellular locations offers many advantages. First, mRNA can undergo numerous rounds of translation once localised, so it is more efficient to localise a small amount of mRNA than move large amounts of protein. Second, transporting translationally repressed mRNA ensures that the protein is expressed in one subcellular domain, and not in another. Third, it removes the risk of proteins signalling prematurely and promiscuously during their transport. Finally, delegating control of translation to specific regions of the cytoplasm permits rapid, flexible responses to external stimuli, and protein expression in different subcellular locations independently of one another.

Functions of mRNA localisation and localised translation

mRNA localisation is important for cellular function in many tissues and organisms. In differentiating neurons, axonal growth cone guidance depends on the translation of axonally localised mRNAs (Jung et al. 2012, Leung et al. 2013, Yoon et al. 2012),

including *RhoA* (Wu et al. 2005) and *β-actin* (Leung et al. 2006*,* Zhang et al. 2001). In mature neurons, mRNAs including *CaMKIIα*, *MAP2, Arc*, and *β-actin* (Blichenberg et al. 1999, Blichenberg et al. 2001, Lyford et al. 1995, Tiruchinapalli et al. 2003) are localised to the dendrites. The translation of a number of mRNAs at the neuromuscular junction (NMJ) including *msp-300* and *discs large* is thought to regulate synaptic growth and function (McDermott et al. 2014). mRNA localisation at the synapse is also important for synaptic plasticity and learning and memory (Steward & Schuman 2001, Sutton & Schuman 2006).

Cell fate decisions and stem cell development can also be regulated by mRNA localisation. In neurogenesis of the fruit fly *Drosophila*, *prospero* (*pros*) mRNA is asymmetrically localised in neuroblasts (neural stem cells) and is inherited specifically by ganglion mother cells, whose differentiation requires *pros* mRNA (Broadus et al. 1998, Doe et al. 1991, Spana & Doe 1995). In *Saccharomyces cerevisiae*, localisation of *ASH1* mRNA to the bud tip, and inheritance of this mRNA only by the daughter cell, regulates mating type switching (Bertrand et al. 1998, Long et al. 1997, Takizawa et al. 1997). Egg activation and fertilisation in a number of animals coincides with the translation of localised mRNAs. For example, the *Drosophila* embryo is initially patterned by opposing morphogen gradients of *bicoid* (*bcd*) and *nanos* (*nos*) mRNA, which are localised during oogenesis but not translated until egg activation (Lehmann & Nüsslein-Volhard 1991, St Johnston et al. 1989).

Localised mRNAs control motility in some differentiated cells. Chick embryo fibroblasts are polarised by the localisation and translation of *β-actin* mRNA at the leading edge. This localisation is required for correct adhesion of the leading edge to

the substrate, and is crucial for cell motility (Katz et al. 2012, Kislauskis et al. 1997, Lawrence & H 1986, Sundell & H 1991).

Localised mRNA translation has been extensively studied in symmetry breaking, establishment of polarity, and subsequent tissue patterning during development. In the oocytes of the frog *Xenopus laevis*, the localisation of mRNAs including *Vg1* to the oocyte vegetal cortex is required for mesoderm induction (Thomsen & Melton 1993, Weeks & Melton 1987). Localisation of mRNAs in ascidian development specifies muscle, mesodermal, and endodermal tissue fates (Nishida & Sawada 2001, Takatori et al. 2010). In zebrafish embryos, vegetal localisation of *squint* mRNA patterns dorsal fates (Lim et al. 2012). Symmetry breaking and establishment of polarity during *Drosophila* oogenesis is determined by the differential localisation of *gurken* (*grk*), *oskar* (*osk*) and *bcd* mRNAs (Weil 2014).

Failure of mRNA localisation is also involved in a number of diseases (Cody et al. 2013), including Fragile X syndrome (Bassell & Warren 2008), Schizophrenia (Lauriat et al. 2008), Spinal Muscular Atrophy (Fallini et al. 2012, Rossoll et al. 2003) and Cancer (Gu et al. 2012).

Key outstanding questions in the field

Despite extensive research on localised mRNA translation, key questions still remain. How are transcripts which share the same origin (the nucleus), sorted and transported to distinct subcellular locations? At which point during the life of the mRNA are these sorting decisions made, and which proteins and cis-acting elements regulate this process? What is the molecular mechanism by which mRNAs are translationally repressed during transport and activated once they are localised?

Does the diversity of regulatory mechanisms for mRNA localisation represent different ways of localising diverse transcripts, or redundancy in these mechanisms to safeguard important processes?

The life cycle of mRNA

mRNA is regulated throughout its life cycle, and the processing of mRNA during each step of its journey influences where it is localised and translated. Once transcribed in the nuclei, mRNA is exported into the cytoplasm, transported to its final destination and then anchored, translated, and degraded (Parton et al. 2014).

Cis-acting regions and trans-acting factors

mRNA localisation requires different mRNAs to be specifically targeted to distinct subcellular locations, and translationally regulated in time and space. This specificity is defined by both regions within the mRNA, and factors which associate with it.

Cis-acting regions

mRNAs targeting specificity can be controlled by regions of the mRNA known as “cis-acting elements”. These often comprise double-stranded secondary structures including hairpins, stem loops and bulges, which are necessary for their function (Amrute-Nayak & Bullock 2012, Ferrandon 1997, Hamilton & Davis 2007, Van De Bor et al. 2005, Wilhelm & Vale 1993).

These “localisation elements” are often necessary and sufficient to target mRNAs to a specific subcellular location. These localisation elements vary in size, from 11 to 625 nucleotides (Ainger et al. 1993, Macdonald & Struhl 1988, Müller et al. 2013). Distinct regions of the localisation element can also regulate different steps of mRNA transport. For example, multiple cis-acting elements are necessary for the localisation of *oo18 RNA binding protein* (*orb*) and *osk* mRNA during oogenesis in *Drosophila* (Kim-Ha et al. 1993, Lantz & Schedl 1994), and localisation of *xcat2*

mRNA to the mitochondrial cloud in *Xenopus* oogenesis requires six repeated motifs in the 3' untranslated region (UTR, Chang et al. 2004).

Cis-acting elements are also involved in translational control. The *nos* translational control element (TCE) contains multiple regions, which are required for translational repression of the mRNA at different stages during *Drosophila* oogenesis and embryogenesis (Crucs et al. 2000, Forrest et al. 2004). In *Xenopus*, the translation of cell cycle mRNAs like *mos* and *cyclin A1*, *cyclin B1* and *Cyclin B* is regulated by cytoplasmic polyadenylation element binding protein (CPEB) interaction with cytoplasmic polyadenylation (CPE) sites in their 3'UTRs, (Barkoff et al. 2000, Fox et al. 1988, Hake & Richter 1994, de Moor & Richter 1997, Sarkissian et al. 2004).

Trans-acting proteins

mRNAs are not transported alone, and are packaged in ribonucleoprotein (RNP) complexes with trans-acting factors, (Kato & Nakamura 2011). Zipcode binding protein (ZBP1) is required for the localisation of *β actin* mRNA in chick fibroblasts through interactions with the "zipcode" mRNA sequence (Farina et al. 2003, Ross et al. 1997). The RNA binding protein (RBP) She2p is required for the localisation of *ASH1* mRNA to the bud tip in yeast, and interacts with conserved motifs in the mRNA and the Myosin V motor (Olivier et al. 2005, Takizawa & Vale 2000).

Specific trans-acting proteins also mediate mRNA translational control. Translational repression of *ASH1* mRNA during transport in yeast requires Khd1p, Loc1p and Puf6p proteins binding in the nucleus (Gu et al. 2004, Irie et al. 2002). The *Xenopus* protein Maskin cooperates with CPEB in immature oocytes to repress translation of mRNAs by binding eukaryotic initiation factor 4E (eIF4E) and preventing its

association with the 5' Cap translation initation machinery (Cao & Richter 2002, Richter & Sonenberg 2005, Stebbins-Boaz et al. 1999). Bruno protein translationally represses *osk* mRNA in *Drosophila* oocytes by interacting with Bruno response elements (BREs) in its 3' UTR (Kim-Ha et al. 1995).

Although some mRNAs can be directed to different regions by interacting with different proteins (Cha et al. 2001), many trans-acting factors associate with more than one transcript. The highly conserved double stranded RBP (dsRBP) Staufen (Stau) is required for the localisation of *bcd* and *osk* mRNAs to opposite ends of the *Drosophila* oocyte (Ephrussi et al. 1991, St Johnston et al. 1989, St Johnston et al. 1991). During *Drosophila* oogenesis and embryogenesis, Bicaudal-D (BicD) and Egalitarian (Egl) proteins are required to link cargoes, including multiple localised mRNAs, to the motor protein Dynein (Bullock & Ish-Horowicz 2001, Liu et al. 2013, Mach & Lehmann 1997, Navarro et al. 2004). For mRNAs which localise to distinct regions using the Dynein motor, like *grk* and *bcd*, other mechanisms presumably confer specificity. Recent evidence suggests that each mRNA contains a unique complement of proteins, rather than being controlled by single proteins binding specific mRNAs (Castello et al. 2012, Castello et al. 2013, McDermott et al. 2012).

Transcription and nuclear export

Once transcribed in the nucleus, pre-mRNAs are co-transcriptionally spliced (Baurén & Wieslander 1994, Shandilya & Roberts 2012), which often involves the association of proteins that are necessary for mRNA regulation (Holt & Bullock 2009, Natalizio & Wente 2013). For example, deposition of the exon-exon junction complex (EJC) on mRNA after splicing is necessary for export and localisation of many transcripts (Le Hir 2000, Natalizio & Wente 2013, Saulière et al. 2012, Singh et al. 2012). Alternative

splicing can also shuffle cis-acting sequences, so different splice variants interact with distinct proteins and are differentially localised (Horne-Badovinac & Bilder 2008, Trcek & Singer 2010). Moreover, introns can be retained in certain transcripts, regulating mRNA levels through nuclear retention, transcript turnover, and nonsense-mediated decay (NMD, Braunschweig et al. 2014). mRNAs then diffuse through inter-chromatin tracks to the nuclear pore complex (NPC) where they are exported (Grünwald & Singer 2010, Mor et al. 2010, Natalizio & Wente 2013, Valkov et al. 2012). Nuclear export involves remodelling of the RNP complex and is facilitated by RNA helicases, which interact with nucleoporin proteins to promote export (Figure 1-1, Montpetit et al. 2011, Powrie et al. 2011, Rodríguez-Navarro & Hurt 2011, Valkov et al. 2012).

Transport and anchoring

Once exported, the RNP is remodelled to include motor linkers and adaptors, motor proteins, and translational repressors (Figure 1-2). The best characterised mechanism for localising mRNA is through active transport of the transcript, followed by its anchoring to the cytoskeleton (Figures 1-2 and 1-3). Myosin motors localise mRNAs on the actin cytoskeleton, including; *ASH1* mRNA to the bud tip in yeast (Long et al. 1997, Takizawa et al. 1997); *β actin* to the leading edge of fibroblasts (Katz et al. 2012, Sundell & H 1991) and *pros* mRNA to the basal cortex of *Drosophila* neuroblasts (Barros et al. 2003, Broadus et al. 1998). *grk* (MacDougall et al. 2003), *bcd* (Weil et al. 2006) and pair rule transcripts (Bullock & Ish-Horowicz 2001) in the *Drosophila* oocyte and embryo are transported to the minus end of microtubules by Dynein, and *osk* (Zimyanin et al. 2008), *MBP* (Carson et al. 1997) and *CamKIIα* (Kanai et al. 2004) mRNAs are transported to the plus ends of microtubules by Kinesin in the *Drosophila* oocyte and developing oligodendrocytes.

Figure 1-1: Nuclear export

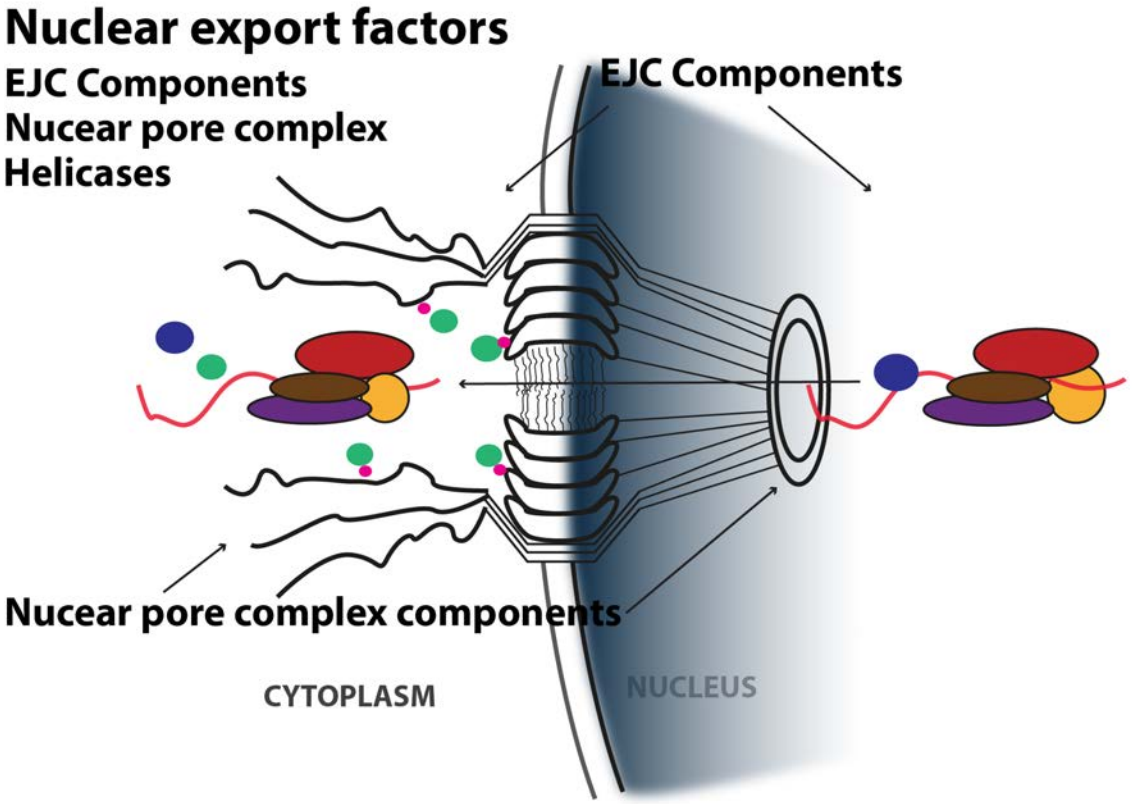

Figure 1-1:

mRNAs (red line) are packaged with a number of proteins in the nucleus, like the EJC (components in red, brown, orange and purple). The protein complement of the RNP is remodelled as it passes through the nuclear pore, with certain proteins (blue) being removed by helicases (green) tethered to nucleoporin proteins (pink).

EJC, exon-exon junction complex.

Figure 1-2: RNP formation and transport

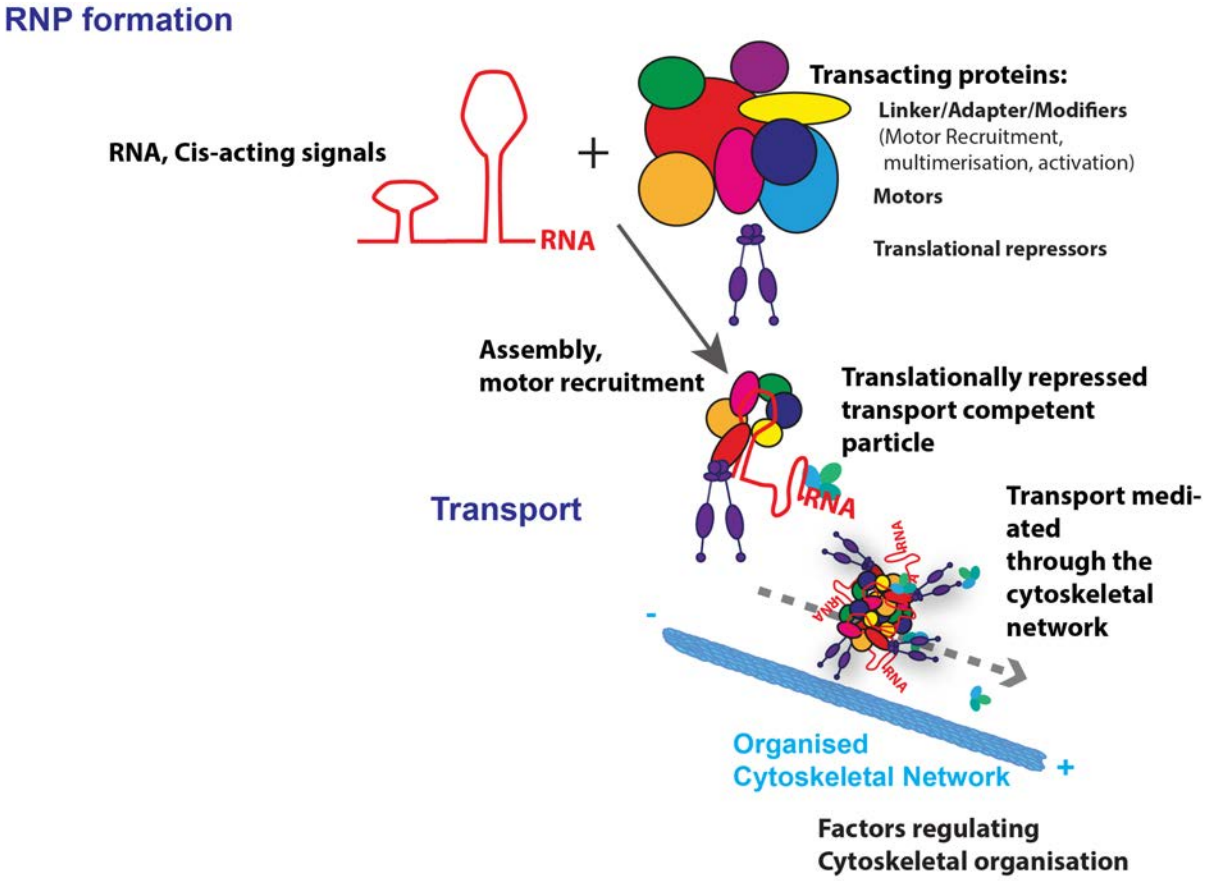

Figure 1-2:

The RNP which is exported from the nucleus is further remodelled in the cytoplasm, with the addition of proteins required for active transport on the cytoskeleton and translational repressor proteins. In this instance, mRNA is transported to the plus end of microtubules by Kinesin.

The microtubule cytoskeleton and motor proteins

Microtubule-mediated transport involves the motor proteins Dynein and Kinesin. Dynein is the major minus end directed microtubule motor. Its two heavy chain domains are AAA ATPases, and interact with the microtubule in an ATP dependent manner (Burgess & Knight 2004, Gennerich & Vale 2009, Nishiura et al. 2004, Reck-Peterson et al. 2006, Sakato & King 2004, Samsó et al. 1998). This requires the accessory proteins Dynactin (Chowdhury et al. 2015, King 2000, Schroer 2004, Waterman-Storer & Karki 1995) and Dynamitin (Eckley et al. 1999, Wilkie & Davis 2001). Egl binds to cis-acting regions on the mRNA, and BicD links this complex to the Dynein motor (Bullock & Ish-Horowicz 2001, Liu et al. 2013).

Kinesins are the major plus end directed microtubule motors (Caviston & Holzbaur 2006, Tekotte & Davis 2002). Members of the Kinesin 1 family contain two force-generating Kinesin heavy chains (KHC), the motor domain of which can bind the microtubule in an ATP dependent manner, whilst the Kinesin light chain (KLC) proteins bind the globular tail domain of KHC, and link the cargoes to the motor complex (Goldstein 2001, Vale 2003, Yildiz et al. 2004).

Transport on motors is not always unidirectional. Dynein is capable of reversing direction (Gross 2004), and mRNAs like *Vg1* mRNA in *Xenopus* oocytes can be transported bidirectionally by multiple motors (Gagnon et al. 2013). The number and activity of motors recruited to an RNP complex, and the degree of mRNA oligomerisation, affects the state of transport, both of which can be affected by cis-acting regions within the mRNA (Amrute-Nayak & Bullock 2012, Bullock et al. 2003, Soundararajan & Bullock 2014).

The cytoskeleton is also highly complex. Contrary to models of a highly polarised cytoskeletal network (Clark et al. 1994, Clark et al. 1997, Theurkauf et al. 1992), in the *Drosophila* oocyte microtubules are oriented randomly with a slight posterior bias (Parton et al. 2011, Zimyanin et al. 2008). Furthermore, numerous proteins regulate the cytoskeleton and motor proteins, including Pat1, which regulates the motility of Kinesin in *osk* localisation (Loiseau et al. 2010), and Ensconsin, the microtubule-associated protein (MAP) which increases the efficiency of kinesin recruitment to microtubules (Sung et al. 2008).

Anchoring

mRNA is often anchored to the cytoskeleton at its final destination (Figure 1-3). In the *Drosophila* oocyte, *grk* mRNA is anchored at the dorsoanterior (DA) corner, which requires the Squid (Sqd) protein to convert Dynein from an ATP dependent active motor to a static anchor (Delanoue et al. 2007, Jaramillo et al. 2008). Both this and anchoring of apically localised mRNAs in the *Drosophila* embryo requires microtubules and Dynein, but not actin (Bullock & Ish-Horowicz 2001, Delanoue & Davis 2005, Wilkie & Davis 2001). *nos* mRNA, which diffuses through the ooplasm is enriched at the posterior pole of the oocyte by being trapped by the actin cytoskeleton and Osk protein (Forrest & Gavis 2003, Jankovics et al. 2002, Lantz et al. 1999, Sinsimer et al. 2011, Vanzo et al. 2007), and both *bcd* and *Vg1* mRNAs are anchored on the actin cytoskeleton in *Drosophila* and *Xenopus* oocytes respectively (Weil et al. 2008, Weil et al. 2010b, Yisraeli et al. 1990).

Figure 1-3: Anchoring

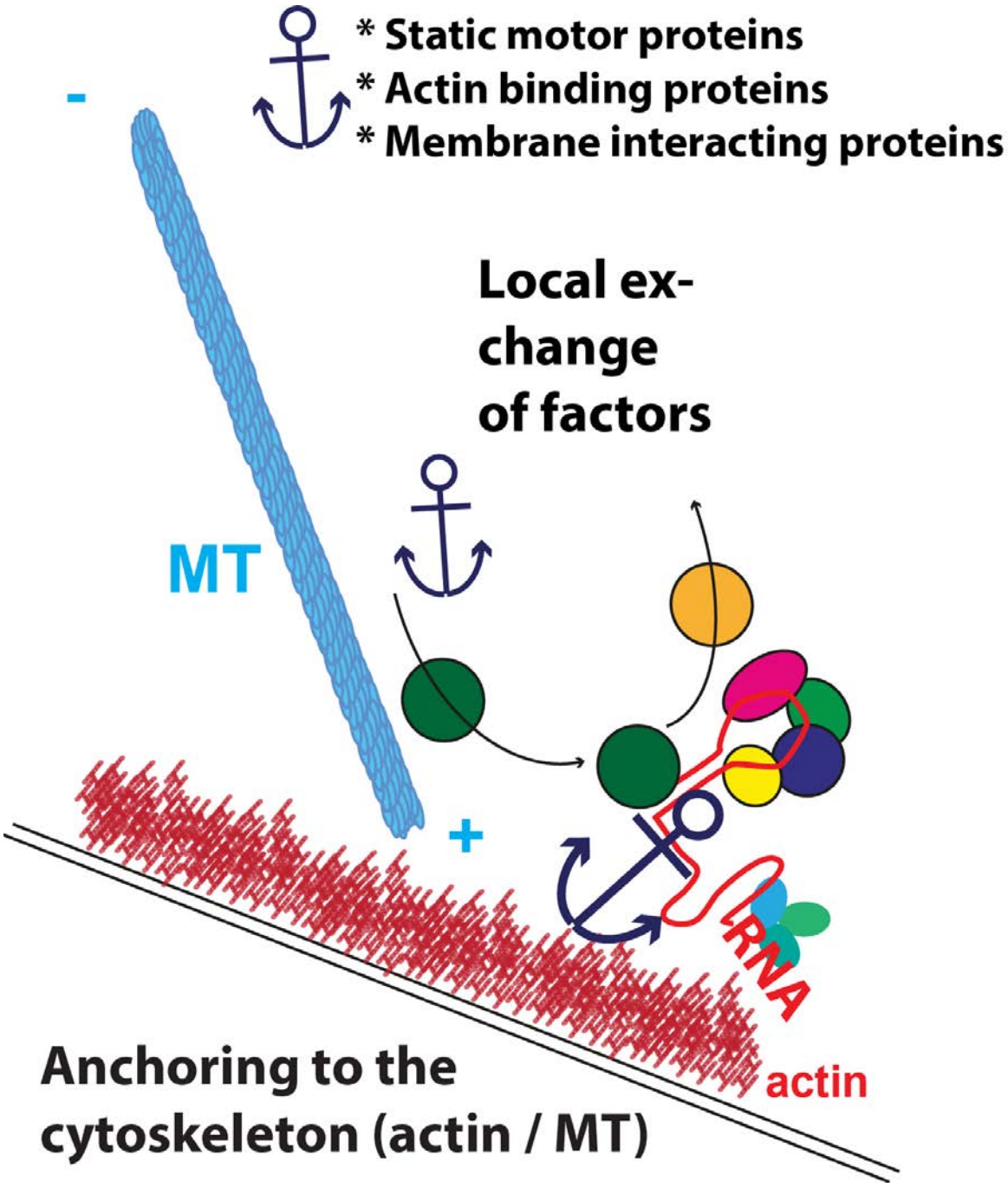

Figure 1-3:

Once localised at its final destination, the RNP is once again remodelled and proteins anchor the mRNA to the cytoskeleton. In this case, the mRNA is anchored to the actin cytoskeleton.

Translation

Most localised mRNAs are only translated once localised or in response to temporal cues. Although a number of mechanisms have been identified for translationally regulating certain mRNAs (Ivshina et al. 2014, Richter & Lasko 2011, Slaidina & Lehmann 2014, Weil 2015), it is not clear how numerous transcripts are translationally repressed during their transport, and then activated once localised. The molecular interactions between the proteins involved, how these are coordinated in time and space, and why there are so many diverse mechanisms for translationally regulating mRNAs in different organisms and tissues, are key questions in the field.

Canonical eukaryotic translational initiation involves assembling the translation machinery at the 5' Cap or at internal ribosome entry sites (IRES). In the canonical pathway (Figure 1-4, Jackson et al. 2010), a 43S preinitation complex (including eIF3, eIF1, eIF1A, eIF5 and eIF2 complexed with GTP and the Met-tRNA, and a 40S ribosomal subunit) binds to the 5' Cap, mediated by the alteration of the 5' mRNA secondary structure by eIF4A, eIF4B, eIF4F and eIF4G. This 43S complex then scans the 5'UTR until it reaches the initiation codon. This is followed by the formation of the 48S complex, hydrolysis of the eIF2-GTP complex, and eIF5B mediated displacement of most eIF proteins by the joining of the 48S and 60S ribosomal subunits. This 80S recognition complex elongates and terminates translation, and is recycled following termination to generate separated ribosomal subunits ready for initiation on another transcript.

Figure 1-4: Translation

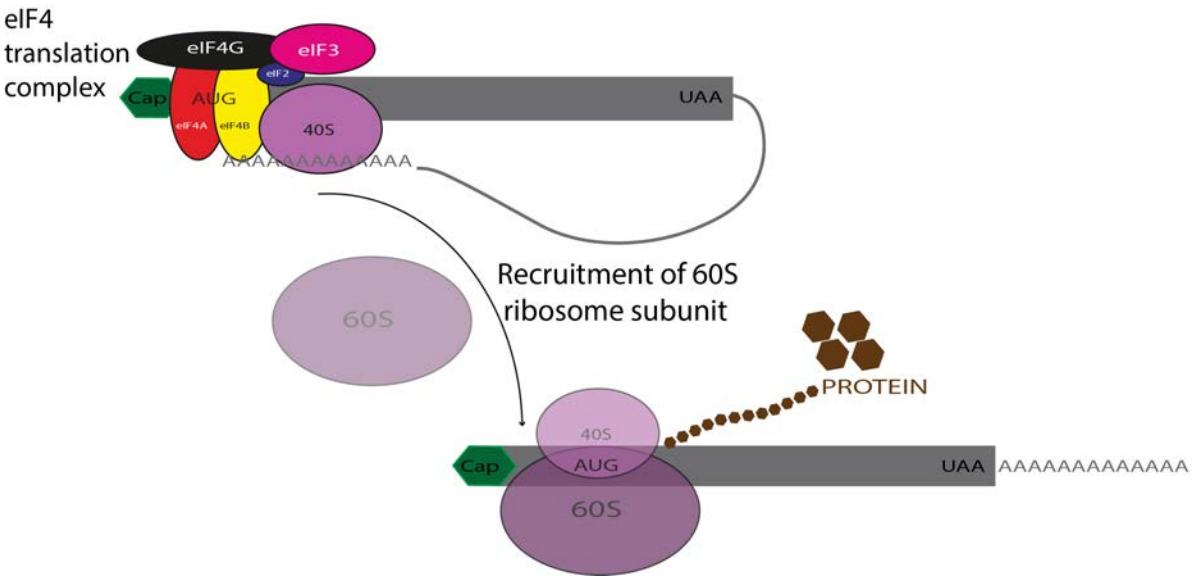

Figure 1-4:

A simplified schematic of translation initiation. The 43S pre-initation complex (including the eIF4 proteins, only some of which are shown here for simplicity) is assembled at the 5' Cap. Following scanning and reaching the AUG start codon, the 60S subunit is recruited, the eIF proteins are displaced, and translation elongation begins, producing the protein. 40S, ribosome small subunit; 60S, ribosome large subunit; AUG, start codon (coding sequence); CAP, 7-methylguanylate cap; eIF, eukaryotic translation initiation factor; RNA pol II, RNA polymerase II; UAA, stop codon (coding sequence).

3'-5' interactions of mRNA

The 3' and 5' ends of the mRNA can interact to stimulate or repress translation. Poly(A) binding protein (PABP) binds the 3' poly adenosine (A) tail of mRNA and to eIF4G, which also binds eIF4E at the 5' mRNA Cap, creating a closed loop (Méndez & Richter 2001, Richter & Lasko 2011). Similarly Paip1, a PABP interacting protein, binds to eIF4A at the 5' end of the mRNA and PABP at the poly(A) tail simultaneously (Craig et al. 1998, Wells et al. 1998). Here, the closed loop complex increases the rate of formation of the translational initiation machinery and aids translational activation. mRNA circularisation can also repress translation. Heterogenous nuclear ribonucleoproteins (hnRNPs) can bind the differential control element (DICE) in the 3' UTR of certain mRNAs, and initiate a loop preventing joining of the 60S ribosomal subunit to the 43S complex (Ostareck et al. 2001).

CPEB-mediated translational control

Xenopus oocytes have been used extensively to biochemically investigate translational control. Here, the translational repression and activation of a subset of mRNAs like *mos* and *cyclin A1*, *cyclin B1* and *Cyclin B2* is mediated by 3' and 5' mRNA interactions, controlled by CPEB (Figure 1-5 (A), Barkoff et al. 2000, Frank-Vaillant et al 1999 Ivshina et al. 2014, Méndez & Richter 2001, de Moor & Richter 1997, Richter & Lasko 2011).

In the nucleus CPEB binds the CPE (consensus UUUUUAU Fox et al. 1989, Hake & Richter 1994) sequence in the 3' UTR of these mRNAs, and cleavage and polyadenylation specificity factor (CPSF) binds the conserved hexanucleotide sequence roughly 30 bases downstream of the CPE (consensus AAUAAA, Bilger et al. 1994, Dickson et al. 1999, McGrew et al 1989, Paris & Richter 1990).

Figure 1-5: Translational control by CPEB and eIF4E binding proteins

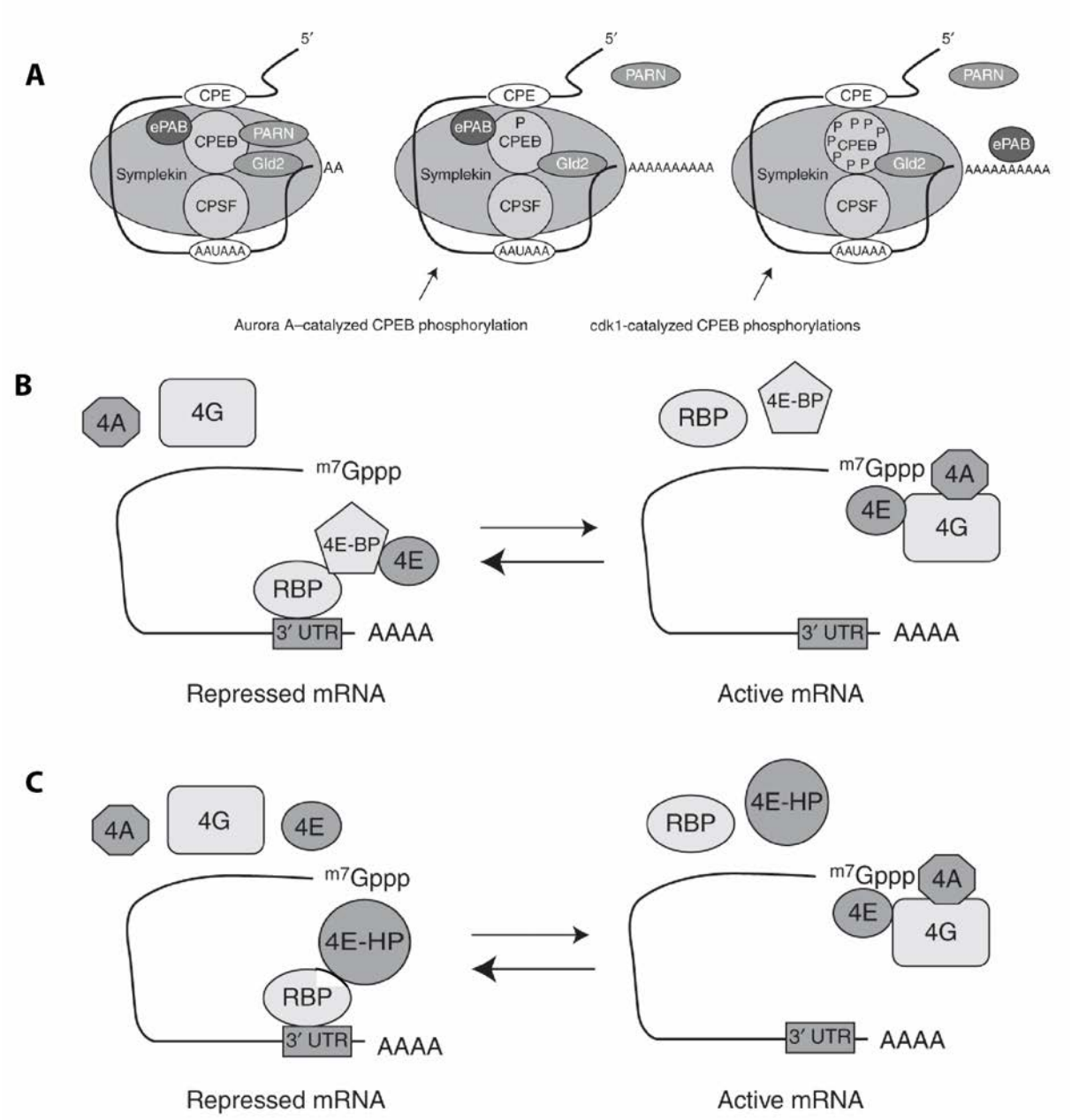

Figure 1-5: (Adapted from Richter & Lasko 2011). For simplicity, only the 3'UTR is shown in these diagrams.

(A): Regulation of translation by CPEB proteins. In immature oocytes, the polyadenylation hexanucleotide is bound by CPSF and the CPE by CPEB. CPEB is

(Figure 1-5 continued)

associated with Gld2 which attempts to elongate the poly(A) tail, and PARN which keeps it shortened. The whole complex is assembled on the scaffold protein Symplekin. Progesterone secretion activates the Aurora-A kinase, which phosphorylates CPEB and causes the removal of PARN from the complex. Gld2 now elongates the poly(A) tail, and cdk1 kinase activation further phosphorylates CPEB and causes ePAB to bind to the poly(A) tail. For simplicity, not all proteins are shown. The Maskin/CPEB interaction is detailed in (B).

(B): Translational repression by eIF4E binding proteins (4E-BPs), for example Cup in Drosophila and Maskin in *Xenopus*. 4E-BPs bind eIF4E (4E) and prevent its association with eIF4G (4G) and eIF4A (4A) and at the 5' Cap (m7Gppp) and repress translation. The 4E-BP is recruited by an RNA binding protein (RBP), such as Bruno and Smaug in *Drosophila* and CPEB in *Xenopus*.

(C): Translational repression by eIF4E homology proteins (4E-HP), which bind the 5' Cap but cannot bind eIF4E, preventing assembly of the intiation complex at the 5' Cap. 4E-HPs are recruited by RBPs, for example Bicoid or the Pumilio/Nanos/Brain tumor complex in *Drosophila*.

CPSF, with other proteins, cleaves the primary transcript 20-30 bases downstream of the hexanucleotide sequence (Mandel et al. 2006), where the poly(A) tail is added by poly(A) polymerase (PAP, Huarte et al. 1992, Kim & Richter 2006, Sachs & Wahle 1993).

Once exported from the nucleus, additional proteins are added to this complex on Symplekin, a scaffold protein (Shatkin & Manley 2000). CPEB associates with two enzymes; Germline development 2 (Gld2), a poly(A) polymerase, attempts to elongate the poly(A) tail, whereas poly(A) ribonuclease (PARN), a deadenylating enzyme, attempts to trim it (Barnard et al. 2004, Kim & Richter 2006). In immature oocytes, PARN is more active than Gld2 and the poly(A) tail is maintained in a shortened state (approximately 40 nucleotides). CPEB is also bound by ePAB, a poly(A) binding protein (Padmanabhan & Richter 2006) and Maskin, which simultaneously binds eIF4E. This prevents assembly of the translation initiation complex and creates a repressive closed loop (Cao & Richter 2002, Richter & Sonenberg 2005, Stebbins-Boaz et al. 1999).

At oocyte maturation, progesterone secretion stimulates re-entry into meiosis and activates the protein kinase Aurora A, which phosphorylates CPEB (Mendez et al. 2000a). This phosphorylation leads to the removal of PARN and allows Gld2 to elongate the poly(A) tail (approximately 150 nucleotides, Kim & Richter 2006), and induces a stronger affinity between CPEB and CPSF (Mendez et al. 2000b). Simultaneously, progesterone stimulation releases the translational repression of *rapid inducer of G2-M in oocytes* (*RINGO*) mRNA by Pumilio (Pum), causing translation of RINGO protein (Cao et al. 2010, Padmanabhan & Richter 2006). RINGO binds and activates cdk1 kinase, which further phosphorylates CPEB,

allowing ePAB to dissociate from CPEB and bind the poly(A) tail (Kim & Richter 2007). Maskin phosphorylation and the ePAB - poly(A) tail interaction facilitate the removal of Maskin from eIF4E (Barnard et al. 2005, Cao et al. 2006, Cao & Richter 2002, Kim & Richter 2007). At this point, the mRNA is translated. However, polyadenylation-induced translation does not occur en masse. Waves of polyadenylation are controlled by the number and position of CPEs in the 3' UTR, the presence of additional proteins in the complex, and the rate of ubiquitination and destruction of CPEB (Lin et al. 2010, Mendez et al. 2002, Piqué et al. 2008, Reverte et al. 2001, Setoyama et al. 2007).

CPEB independent regulation of the poly(A) tail and translation

mRNA can be translationally repressed by being consistently deadenylated by other proteins. Cup and Bicaudal C (BicC) recruit the CCR4 deadenylase in the *Drosophila* oocyte to repress *osk* translation (Igreja & Izaurralde 2011) and Pum binds to *bcd* and induces deadenylation of the mRNA in the early embryo (Gamberi et al. 2002).

However, the role of the poly(A) tail in translational control is more complex than a long tail being necessary and sufficient for translation (Cui et al. 2013, Proudfoot 2011, Weil 2015). Profiling of poly(A) tail lengths in different tissues (Subtelny et al. 2014) reveals a strong correlation between poly(A) tail length and translational efficiency in zebrafish and *Xenopus* embryos before gastrulation, but not after. There is also no correlation in non embryonic tissues, suggesting that poly(A) tail length and translation are not always coupled. Moreover, alternative polyadenylation (APA), can generate different 3'UTRs from the same transcripts (Di Giammartino et al. 2011) (Lianoglou et al. 2013). In yeast, APA generates transcripts with different 3' UTRs, affecting transcript stability, and interactions with different trans-acting factors (Gupta

et al. 2014). A similar mechanism may function in zebrafish and mouse (Ji et al. 2009, Spies et al. 2013, Ulitsky et al. 2012). However, it is unclear whether APA is a widespread mechanism for post-transcriptional control.

eIF4E mediated translational control

In *Xenopus* and *Drosophila* oocytes, translation is often repressed by proteins binding eIF4E (Figure 1-5 (B)). *Drosophila* Cup (Nakamura et al. 2004, Wilhelm 2003) and mammalian 4E-transporter (4E-T, Kamenska et al. 2014, Minshall et al. 2007) perform similar functions to *Xenopus* Maskin, but only share primary sequence homology in their eIF4E binding region (Nakamura et al. 2004). These proteins bind eIF4E, preventing eIF4G binding it at the 5' Cap. These eIF4E binding proteins (4E-BPs) are recruited to mRNA by RBPs and loaded onto the 3'UTR. eIF4E homology proteins (4E-HP) bind the mRNA directly at the 5' cap and outcompete eIF4E (Figure 1-5 (C), Richter & Lasko 2011). *caudal* mRNA translation is repressed in *Drosophila* embryos by binding of d4EHP, to the 5' cap and to Bcd protein, which is also bound to the Bicoid binding region (BBR) in the *caudal* 3' UTR, creating a closed loop and preventing eIF4E association with the 5' Cap (Cho et al. 2005).

Translational control by non-coding RNAs and P bodies

Non-coding RNAs also regulate mRNA (Bartel 2004). MicroRNAs (miRNAs), control translation at *Drosophila* synapses (Muddashetty et al. 2011), dendrites (Bicker et al. 2013), and the embryo (Pinder & Smibert 2013). Recent evidence suggests that RBPs like 4E-T may increase miRNA mediated silencing independently of their role in eIF4E binding (Kamenska et al. 2014), suggesting a network where key proteins control translation of numerous mRNAs by distinct mechanisms.

Processing bodies (P bodies) are non membrane bound, electron dense structures originally identified in *Drosophila* nurse cells (Wilsch-Bräuninger et al. 1997). P bodies contain non-translating mRNA, translational repressors, and mRNA decay machinery (Decker & Parker 2012, Parker & Sheth 2007, Teixeira & Parker 2007). Although well characterised in yeast, P bodies are also thought to be important for regulating transcripts in mammalian tissue (Beckham & Parker 2008, Minshall et al. 2009), and in development of the *Drosophila* oocyte and nervous system (Barbee et al. 2006, Snee & Macdonald 2009, Weil et al 2012b). At the oocyte DA corner, the core of P bodies is enriched for translational repressors including the DEAD box helicase, Maternal expression at 31B (Me31B), Bruno, and the decapping enzyme Dcp2, and is devoid of ribosomes. The P body edge is enriched for the translational activator and CPEB homolog Orb, and *grk* association with the edge and *bcd* with the core controls their respective translation and repression (Weil et al. 2012b).

Degradation

All mRNAs are eventually degraded, and the extent and timing of mRNA degradation can control protein expression. Degradation of unlocalised mRNA, and protection of localised mRNA from degradation, generates high concentrations of *nos* and *polar granule component* (*pgc*) mRNA at the posterior of the *Drosophila* oocyte (Bashirullah et al. 1999, Bergsten & Gavis 1999, Nelson et al. 2004, Zaessinger et al. 2006), and restricts *vasa* and *nos* mRNAs to the primordial germ cells of zebrafish embryos (Wolke et al. 2002, Yoon et al. 1997).

The maternal-to-zygotic transition (MZT), when the zygotic transcriptome is activated, requires the degradation of the maternal transcriptome (Baugh et al. 2003, De Renzis et al. 2007, Hamatani et al. 2004). In zebrafish and *Drosophila*, maternal transcript

clearance is regulated largely by miRNA-mediated deadenylation and short interfering RNA (siRNA) mediated degradation (Figure 1-6, (Bushati & Cohen 2008, Giraldez et al. 2006, Tadros & Lipshitz 2009). In yeast, cytoplasmic mRNA degradation occurs largely in association with P bodies (Figure 1-6, Aizer et al. 2008, Brengues 2005, Decker & Parker 2012), and they are thought to perform a similar role in other tissues. In the *Drosophila* oocyte, P bodies may function as sites of degradation of ectopically produced transcripts (Weil et al. 2012b).

mRNAs can be degraded by a number of mechanisms. Deadenylation by the Ccr4/Pop2/Not complex is followed by 3' to 5' exonucleolytic decay (Anderson & Parker 1998, Daugeron et al. 2001, Garneau et al. 2007, Parker & Song 2004, Thore et al. 2003, Tucker et al. 2001, Wang & Kiledjian 2001). In many eukaryotes, 3' to 5' degradation occurs through the multi-subunit exosome complex, which also has complex roles in a range of RNA processing steps (Hilleren & Parker 1999, Liu et al. 2006, Mitchell et al. 1997, Wang & Kiledjian 2001). The exosome functions both in the nucleus and the cytoplasm, and it's activity is regulated by the association of a host of trans-acting proteins (Chlebowski et al. 2013). However, the major degradation pathway is decapping by the Dcp1/Dcp2 enzymes followed by 5' to 3' degradation by the Xrn1 exonuclease (Decker & Parker 1993, Dunckley & Parker 1999, Hsu & Stevens 1993, Muhlrad et al. 1994, Muhlrad et al. 1995, Steiger et al. 2003, van Dijk et al. 2002).

There are also numerous quality control systems designed to detect and remove abberant transcripts, such as NMD of mRNAs with premature stop codons (Isken & Maquat 2007, Muhlrad & Parker 1994, Trcek et al. 2013); no-go decay (NGD) of mRNAs which stall in translation elongation (Doma & Parker 2006, Harigaya &

Parker 2010); and non-stop decay (NSD) of mRNAs without translation termination codons (Frischmeyer et al. 2002, van Hoof et al. 2002).

Degradation exists in an equilibrium with translation initiation, mediated by proteins which bind to and alter the 5' cap and 3' poly(A) tail. For example, the Dhh1/Rck DEAD-box helicase, and the Pat, Edc3, Scd6/Rap55 and Lsm107 complex, act to both block formation of the translation initiation complex and function in decapping prior to degradation (Decker & Parker 2012). The Ccr4/Pop2/Not deadenylase complex is inhibited by the poly(A) binding protein Pab1 (Tucker et al. 2002). Moreover, evidence that mRNA can be degraded during translation suggests that the removal of the translation machinery and the onset of degradation are not always sequential events (Hu et al. 2009).

Figure 1-6: Degradation

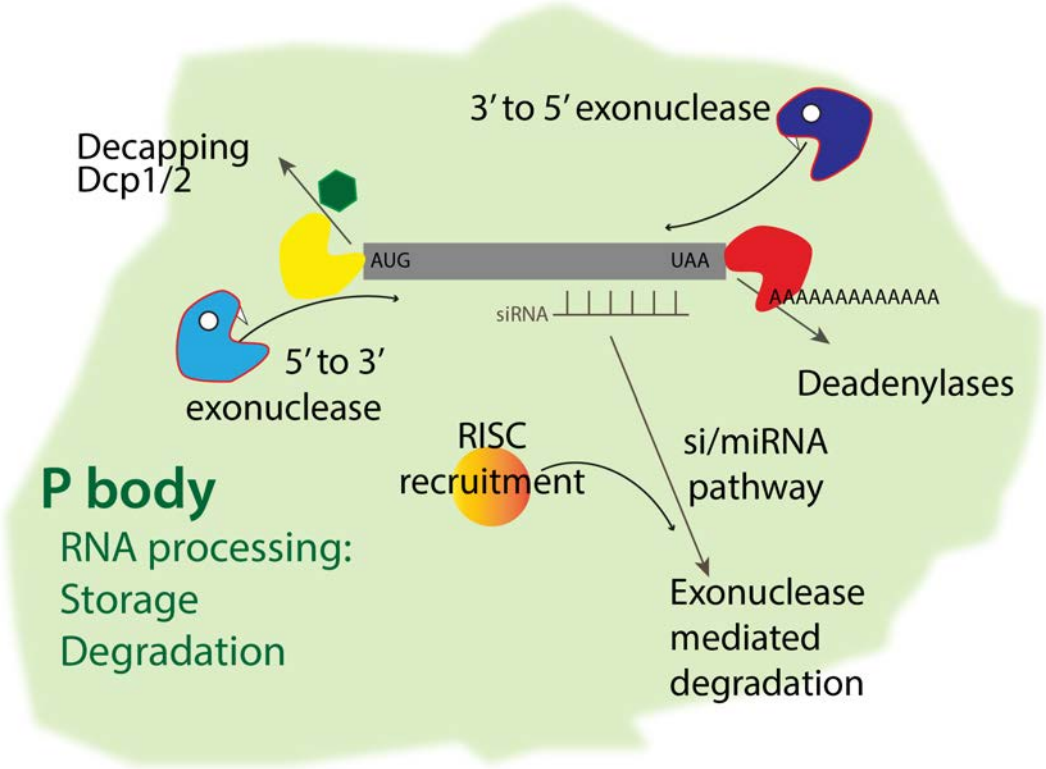

Figure 1-6:

Once translated, mRNA is degraded. Much of degradation occurs in P bodies, by 5' to 3' and 3' to 5' exonucleases, following decapping and deadenylation respectively. mRNA silencing and degradation can also be mediated by siRNA and miRNA pathways. AUG, start codon (coding sequence); Dcp1 and 2, mRNA-decapping enzyme subunits 1 and 2; P-body, processing body; RISC, RNA-induced silencing complex; siRNA, small interfering RNA; miRNA, micro-RNA; UAA, stop codon (coding sequence).

Localised mRNA translation in *Drosophila* oogenesis

The *Drosophila* oocyte is a widely used model for studying mRNA localisation (Weil 2014). The requirement of maternal mRNAs in symmetry breaking and oocyte patterning was first elucidated through analysis of embryonic patterning defects (Schupbach & Wieschaus 1986, Schupbach & Wieschaus 1991). This Thesis will discuss the function of a group of mRNAs known as axis determining transcripts, which pattern the oocyte; *grk*, *bcd*, *osk* and *nos*, focussing on *grk* mRNA.

Drosophila oogenesis

Female flies have two ovaries containing 16-20 ovarioles (King 1970, Spradling 1993). Every ovariole is a string of egg chambers, with the germline stem cells (GSCs) in the germarium at the anterior. Egg chambers bud off from the germarium and develop as they proceed to the posterior, where mature eggs are ready to be activated, fertilised and deposited (Figure 1-7, King 1970, Spradling 1993).

Each egg chamber comprises 16 germline cells. One cell, the oocyte, will form the embryo, and has a nucleus that is transcriptionally silent until after fertilisation (King & Burnett 1959). The 15 supporting nurse cells transcribe maternal mRNAs and other cytoplasmic components for transport into the oocyte. The germline cells in the egg chamber are linked by actin bridges (ring canals) arising from incomplete cytokenesis, and are surrounded by a single layer of 600 - 1000 somatic epithelial follicle cells. These are involved in cell signalling with the oocyte, and will secrete the eggshell. Egg chambers are connected to their older and younger siblings by specialised follicle cells called stalk cells, which are also involved in signalling between egg chambers (Horne-Badovinac & Bilder 2005).

Figure 1-7: The *Drosophila* ovary

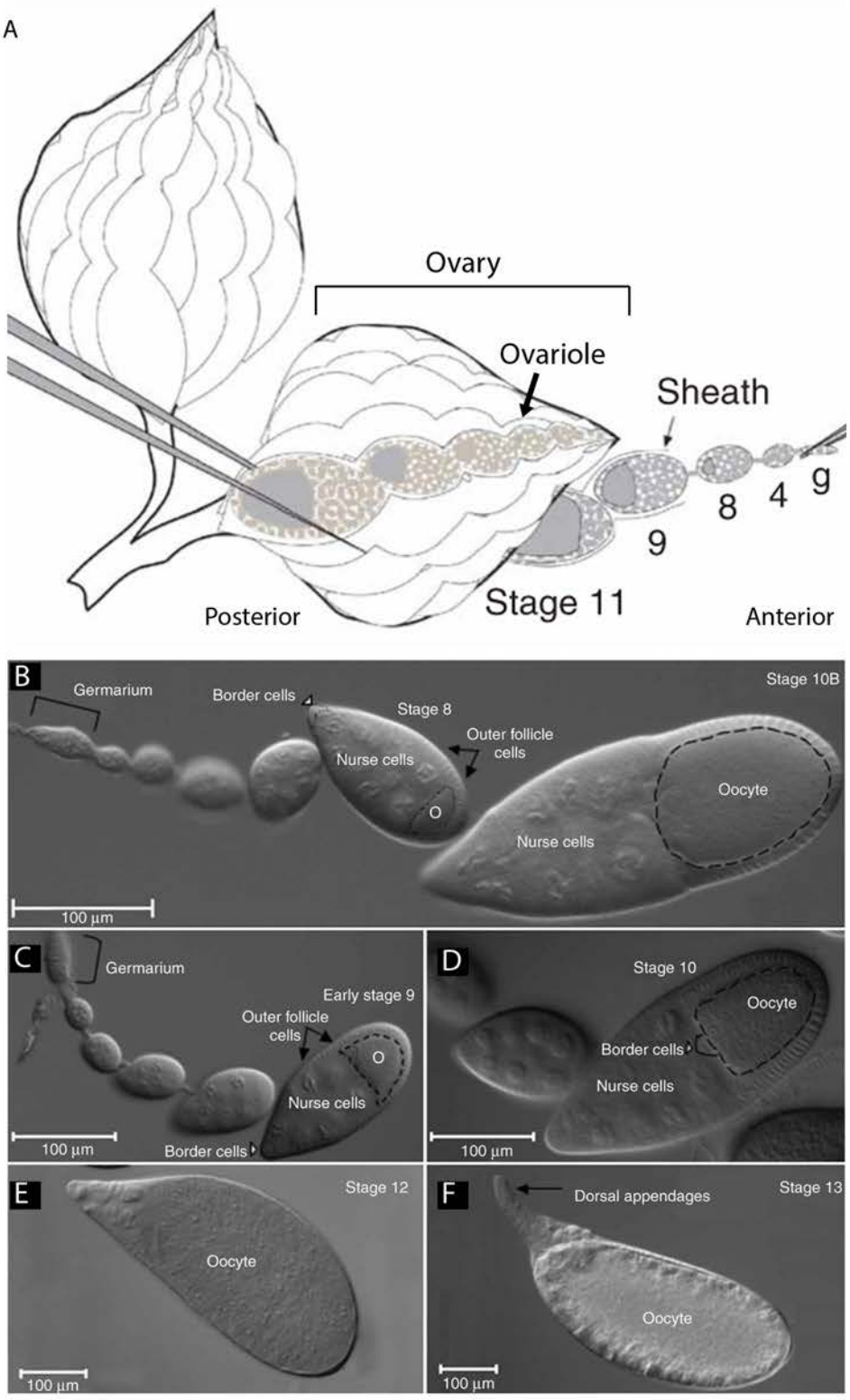

Figure 1-7: (Adapted from Prasad & Montell 2007).

(A): Schematic of the two *Drosophila* ovaries, each of which contains 16-20 ovarioles (coloured and shown being removed from the ovary), comprised of egg chambers increasing in maturity from the anterior to the posterior. (B-F): Nomarski images of dissected egg chambers, with the posterior oriented to the right. Arrows label follicle cells, arrowheads label border cells where possible, dashed black line marks the edge of the oocyte in stages 8-10. O, oocyte. Scale bars 100 μm

Early development and specification of the oocyte

The germarium comprises 4 regions. In the anterior of the germarium (region 1) GSCs divide asymmetrically, generating another stem cell and a daughter cytoblast, which differentiates. The daughter cell undergoes four rounds of mitotic division with incomplete cytokenesis, forming a cyst of 16 interconnected cells. The 16 cell cyst then moves into region 2a, where one cell is defined as the oocyte.

Of the 16 cells, 8 cells have one ring canal, four cells have two, two cells have three, and two cells have four ring canals (Figure 1-8, Huynh & St Johnston 2004). The two cells with four ring canals are pro-oocytes, one of which will become the oocyte. Each cyst contains a fusome, a branched, membranous structure (de Cuevas et al. 1996, Lin et al. 1994). This controls the orientation of the divisions within the cyst, and the future oocyte contains higher levels of fusome material than the other cells as the cyst moves into region 2a (de Cuevas & Spradling 1998, Huynh et al. 2001).

The fusome restricts meiosis to the oocyte (Bolívar et al. 2001, Huynh & St Johnston 2000), polarises microtubules, and directs the transport of mitochondria, centrioles, and mRNAs and proteins into both pro-oocytes, then just the oocyte (Bolívar et al. 2001, R. T. Cox & Spradling 2003, Grieder et al. 2000, McGrail & Hays 1997). These include BicD, Egl, Barentsz (Btz), Orb and Cup proteins, as well as *osk*, *BicD* and *orb* mRNAs (Bolívar et al. 2001, Ephrussi et al. 1991, Huynh et al. 2001, Huynh & St Johnston 2000, Lantz et al. 1994, Mach & Lehmann 1997, Navarro et al. 2004, Röper & Brown 2004, Suter et al. 1989, Swan et al. 1999, van Eeden 2001, Wharton & Struhl 1989).

Figure 1-8: Oocyte specification in the germarium

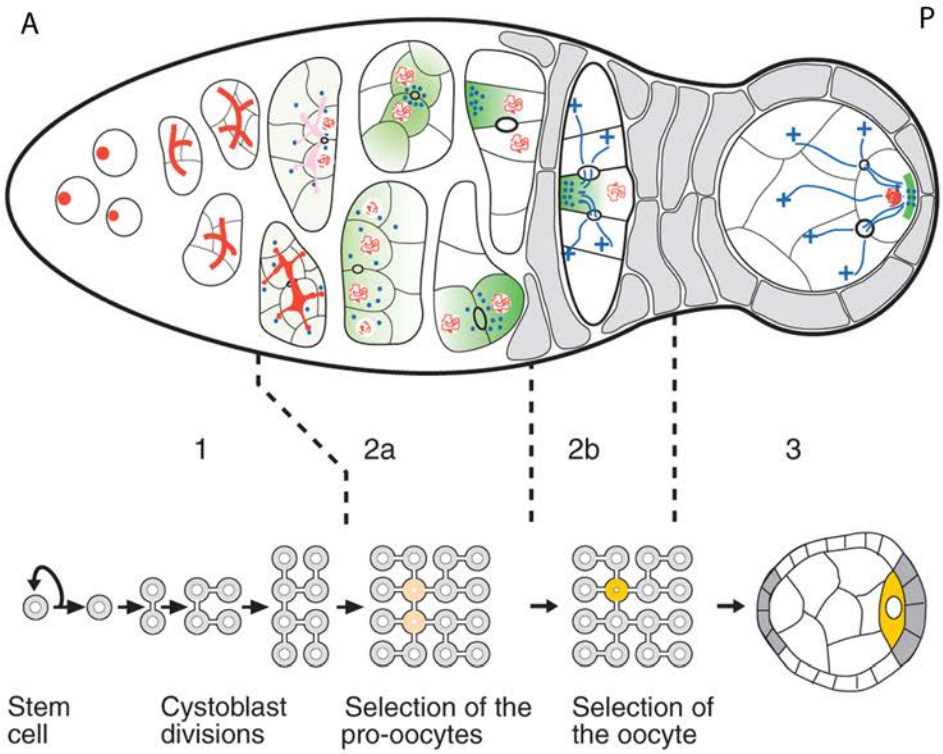

Figure 1-8: (Adapted from Huynh & St Johnston 2004).

Each egg chamber comprises 16 germline cells surrounded by a somatic follicle cell monolayer. The germarium, at the anterior of the ovariole, containes germline stem cells and its anteriormost point. These cells divide 4 times with incomplete cytokenesis to produce a 16 cell cyst, with all of the cells linked together by ring canals and the fusome (red structure). In region 2a, the synaptonemal complex (red lines) forms in the two cells with 4 ring canals (the pro-oocytes, yellow) as they enter meiosis. In region 2b, the oocyte is selected by the concerted action of the polarisation of microtubules, entry of oocyte specific proteins, mRNAs and mitochondria (green) and centrioles (blue circles) into the oocyte, and the restriction of entry into meiosis to the oocyte. The oocyte is the only cell to remain in meiosis. The follicle cells (grey) migrate around the germline cells.

(FIgure 1-8 continued)

As the cyst moves into region 3, the oocyte adheres to the posterior follicle cells and repolarises its microtubule cytoskeleton, with minus ends at the posterior of the oocyte and plus ends running through ring canals into the nurse cells. A, anterior; P, posterior.

As the cyst migrates into region 2b, the oocyte is specified and maintained by PAR-1, and is the only cell to remain in meiosis (Cox et al. 2001, Huynh et al. 2001). The follicle cells surround the cyst, and in region 3, the oocyte adheres via Cadherin signalling to the posterior follicle cells (Godt & Tepass 1998, González-Reyes & St Johnston 1998). The microtubule cytoskeleton is repolarised with plus ends in the nurse cells, and minus ends at the posterior of the oocyte. Specific cytoplasmic determinants are directed to the posterior on Dynein such as BicD, Orb, and the Balbiani body mitochondrial components (Cox & Spradling 2003, Pare & Suter 2000). Delta signalling from the germline specifies the anterior follicle cells as polar cells, which signal to the neighbouring egg chamber to form stalk cells between these egg chambers (Grammont & Irvine 2001, McGregor et al. 2002, Roth 2001).

Egg chamber development

Once the egg chamber buds off from the germarium it goes through 14 morphologically distinct stages of development (Figures 1-7 and 1-9, King 1970, Spradling 1993). The oocyte nucleus continues through meiotic prophase, and the nurse cell nuclei undergo several rounds of endoreplication and increase in size. The nurse cells selectively deliver mRNA, proteins, yolk, and organelles through ring canals into the oocyte, which increases in size. The follicle cells proliferate until the end of stage 6, separating into two competence domains. Terminal follicle cells at the anterior and posterior poles can respond to different signals to the mainbody follicle cells elsewhere (González-Reyes & St Johnston 1998).

At stage 6, the follicle cells stop proliferating and undergo three rounds of endoreplication and growth, controlled by Delta signalling in the germline, and Notch and Hippo pathway signalling in the follicle cells (Botchan & Levine 2004, Calvi &

Spradling 1999, Horne-Badovinac & Bilder 2005, Wu et al. 2008). Simultaneously, the symmetry of the oocyte is broken by Grk signalling, the posterior MTOC disassembles, and the microtubule cytoskeleton is re-organised (González-Reyes & St Johnston 1998). This was thought to give rise to a highly polarised microtubule array with microtubule minus ends at the oocyte anterior and plus ends at the posterior (Clark et al. 1994, Clark et al. 1997, Theurkauf et al. 1992), but recent evidence suggests that PAR-1 controls a biased random organisation of microtubules, with more plus ends at the posterior through higher levels of microtubule nucleation at the anterior (Parton et al. 2011). The oocyte nucleus is pushed by growing microtubules from the oocyte posterior to the DA corner (Januschke et al. 2002, Zhao et al. 2012).

At stage 7, the follicle cells secrete yolk into the oocyte. A group of anterior follicle cells (border cells) migrate to the anterior border of the nurse cells and the oocyte, and up to the dorsal corner near the nucleus (Montell 2003). At stage 10a the follicle cells around the oocyte are converted to columnar cells, and move to cover the oocyte. The follicle cells surrounding the nurse cells become squamous stretch cells. At stage 10b, a subset of columnar follicle cells become centripetal cells, and move between the nurse cells and the oocyte, surrounding the oocyte completely. These secrete specialised eggshell structures including the dorsal appendages, two flat paddles involved in gas exchange (Horne-Badovinac & Bilder 2005). The oocyte increases to half of the egg chamber volume to stage 10b, when the cytoskeleton is reorganised again. Microtubules begin “streaming” to mix the ooplasm, aiding the assembly of the germ plasm, the future germ line, at the posterior (Dahlgaard et al. 2007, Forrest & Gavis 2003, Gutzeit 1986, Serbus et al. 2005). Simultaneously, the nurse cells begin to unselectively transfer their contents into the oocyte, “nurse cell

dumping", followed by the apoptosis of the nurse cells (Spradling 1993) and clearing of the nurse cell nuclei (Kronja et al. 2014). By stage 14, the oocyte comprises the total volume of the egg chamber and the egg is ready for activation and laying.

The nurse cells

The nurse cells are essential for oogenesis. When they are not correctly oriented, or nurse cell nuclear organisation is disrupted, oogenesis arrests (Filardo & Ephrussi 2003, Lantz et al. 1994, Nakamura et al. 2001, Schupbach & Wieschaus 1991).

All mRNAs are transcribed in the nurse cell nuclei during oogenesis, including *grk*, *osk*, *bcd* and *nos.* When the nurse cells cannot transcribe mRNA the oocyte is incorrectly patterned (Caceres 2005), and in Dynein mutants where mRNAs and proteins are not trafficked into the oocyte, the oocyte is not specified (Mach & Lehmann 1997). Many trans-acting factors which are required for localisation and translational control of mRNAs are produced in the nurse cells, and the specific localisation of some proteins in the nurse cells is key for their function. The perinuclear nuage is a non membrane bound organelle around nurse cell nuclei (Snee & Macdonald 2004). The localisation of the DEAD box helicase Vasa, UAP56, Rhino, and PIWI interacting RNA (piRNA) proteins like Ago3 and Aub in the nuage is essential for piRNA-processing, oocyte, and pole cell development (Findley et al. 2003, Harris & Macdonald 2001, Liang et al. 1994, Schupbach & Wieschaus 1986, Zhang et al. 2012).

However, not all mRNAs are translated in the nurse cells. Notably, *grk*, *osk* and *bcd* mRNAs are translationally repressed until they reach the oocyte (Lehmann & Nüsslein-Volhard 1986, Markussen et al. 1995, Neuman-Silberberg & Schupbach

1993, Schupbach 1987, St Johnston et al. 1989). Presumably, ectopic translation of these mRNAs in the nurse cells would lead to severe patterning defects. Indeed, when determinants of oocyte fate are present in all germline cells in the germarium, oogenesis arrests (Lantz et al. 1994, Huynh & St Johnston 2000).

Although the nurse cells are essential, they are poorly understood, as most research has focussed on mRNA localisation and translational control in the oocyte. The mechanisms of mRNA and protein transport and translational control in the nurse cells are not well characterised. This is partly because many genes which affect nurse cell morphology result in arrest during early oogenesis. Moreover, factors identified with roles in the *grk*, *osk*, *bcd* and *nos* regulation were discovered because they are necessary to localise mRNA and generate protein in the oocyte. Although these phenotypes may be due to mRNA processing defects in the nurse cells, the effect is seen in the oocyte. The nurse cells are harder to study than the oocyte for many reasons; 1.) aligning egg chambers to study specific nurse cells is difficult, 2.) cytoplasmic components and organelles obscure fluorescent imaging, 3.) nurse cells are difficult to inject, 4.) they cannot be separated from the oocyte for biochemical analysis, and 5.) although some mRNAs are localised to distinct regions of the nurse cells (Jambor et al. 2015), most are localised only in the oocyte.

In this Thesis, I will examine how mRNAs and proteins are transported in the nurse cells, and how *grk* mRNA is translationally repressed in the nurse cells, but translationally activated in the oocyte. First, I will discuss the current models for localised translation of the axis determining transcripts during oogenesis.

Figure 1-9: mRNA localisation during *Drosophila* oogenesis

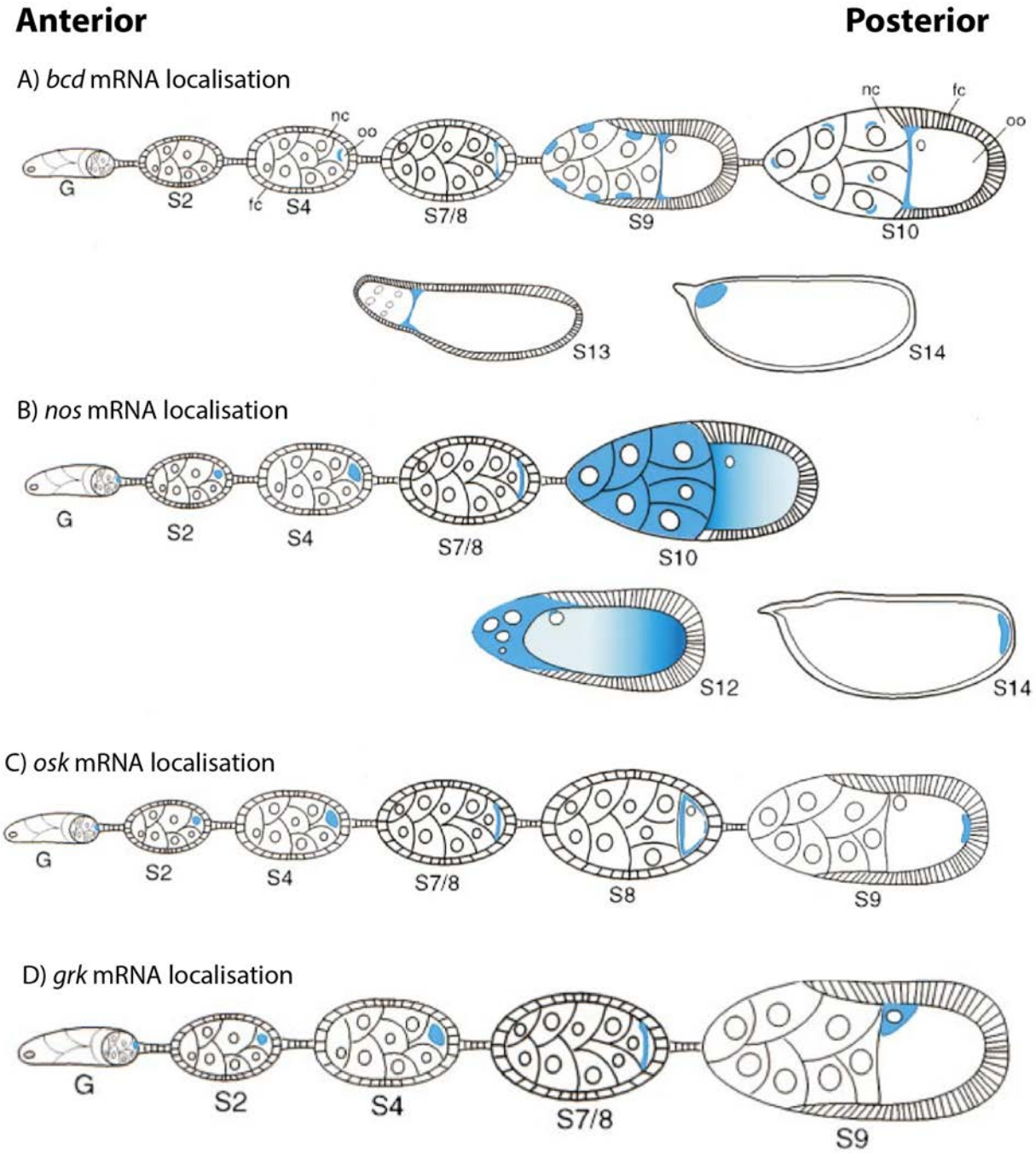

Figure 1-9: (Adapted from Lasko 1999).

(A): Some *bcd* mRNA accumulates in the oocyte posterior during mid-oogenesis, with the bulk of *bcd* localisation at the anterior occurring coincidentally with nurse cell dumping from stage 10 onwards, where it is required for head and thorax specification and patterning of the embryo.

(B): *nos* mRNA is present in the nurse cells during mid oogenesis and is transported into the oocyte with nurse cell dumping. It is anchored at the posterior in late stage oocytes where it is required for posterior patterning, and unlocalised *nos* is degraded.

(C): *osk* mRNA is present in the oocyte from stage 1, and localises transiently to the centre and anterior of the oocyte from stages 6-8 before being localised to the posterior cortex from stage 9 onwards, where it patterns the future germ line and posterior structures.

(D): *grk* mRNA accumulates in the oocyte in early stages and localises to the posterior side of the oocyte nucleus from stage 6 onwards, signalling to the follicle cells to rearrange the cytoskeleton. By stage 9 *grk* accumulates around the oocyte nucleus where it signals to the follicle cells to adopt a dorsal fate and patterns the dorsal appendages.

The numbers below each egg chamber indicate the stage of oogenesis. S, stage; G, germarium; nc, nurse cells; fc, follicle cells; oo, oocyte.

Localisation and translational control of *bcd* and *nos*

bcd and *nos* establish the anteroposterior axis. *bcd* is localised to the anterior of the oocyte and *nos* at the posterior during oogenesis, but neither is translated until egg activation in the early embryo (Figure 1-9 (A, B), Berleth et al. 1988, Lehmann & Nüsslein-Volhard 1991, St Johnston et al. 1989, C. Wang & Lehmann 1991). Here, Nos and Bcd proteins diffuse from the poles and pattern the embryo by regulating the transcription and translation of the gap genes *hunchback* and *caudal* (Jaeger 2011, Nüsslein-Volhard et al. 1987, St Johnston & Nüsslein-Volhard 1992). *bcd* and *nos* are required to generate head and thorax structures (Frohnhöfer et al. 1986) and abdominal segments respectively (Lehmann & Nüsslein-Volhard 1991, Wang & Lehmann 1991).

Some *bcd* mRNA localises at the oocyte anterior during mid-oogenesis (Berleth et al. 1988, Cha et al. 2001, St Johnston et al. 1989), but most enters at nurse cell dumping, where it localises to the anterior by Dynein-mediated transport to microtubule minus ends. Localisation is maintained by continuous active transport on microtubules in a process requiring Stau (Weil et al. 2006, Weil, et al. 2010b), but becomes stably associated with the actin cytoskeleton at the end of oogenesis until fertilisation (Weil et al. 2008). Localisation of *bcd* within the oocyte and embryo requires the *bicoid* localisation element (BLE) in the 3‘UTR (Macdonald et al. 1995, Macdonald & Kerr 1997, Macdonald & Kerr 1998, Snee et al. 2005).

During oogenesis, *bcd* translation is repressed by targeting to the translationally silent core of P bodies (Weil, et al. 2012b). At egg activation, *bcd* is released from P bodies as they dissociate. At this point, PAP-mediated poly(A) tail extension of *bcd* is required for translation (Juge et al. 2002, Lieberfarb et al. 1996, Sallés et al. 1994),

but this is sufficient to induce *bcd* translation only in the embryo, not the oocyte (Juge et al. 2002). *bcd* mRNA stability is also mediated by a 43 nucleotide sequence, the *bicoid* instability element (BIE, Surdej & Jacobs-Lorena 1998), and *bicoid* stability factor (BSF, Mancebo et al. 2001). In the embryo, *bcd* away from the anterior is translationally repressed by Pum, which interacts with Nanos response elements (NRE) in the *bcd* 3' UTR to deadenylate and destabilise the mRNA (Gamberi et al. 2002).

nos localises at the posterior pole at stage 10b (Gavis & Lehmann 1992, Wang & Lehmann 1991), and its diffusion in the ooplasm is aided by cytoplasmic streaming. Only *nos* which reaches the posterior is packaged into higher order *nos* RNPs, and is retained by Dynein and Kinesin and eventually anchored by Osk protein (Forrest & Gavis 2003, Little et al. 2015, Sinsimer et al. 2011, Sinsimer et al. 2013). Unlocalised *nos* is degraded, ensuring high levels of *nos* accumulates specifically at the posterior pole (Bashirullah et al. 1999, Bergsten & Gavis 1999). Correct localisation of *nos* at the posterior also requires multiple redundant localisation sequences within a 547 nucleotide region of the 3' UTR (Gavis, et al. 1996a).

nos translational repression is mediated by the 90 nucleotide TCE in the 3'UTR, which has a complex secondary structure (Crucs et al. 2000, Forrest et al. 2004) (Gavis, et al. 1996b). Distinct regions interact with specific repressor proteins at different stages of development. The hnRNP protein Glorund (Glo) binds TCE stem-loop III and represses *nos* translation during oogenesis (Kalifa et al. 2006), whereas Smaug binds to a Smaug recognition element (SRE) in stem loop II to repress *nos* translation during early embryogenesis (Smibert et al. 1996). Smaug recruits Cup to repress *nos* via a cap dependent mechanism (Nelson et al. 2004), and also acts with

piRNAs to recruit the the CCR4 deadenylase to deadenylate unlocalised *nos* (Jeske et al. 2011, Rouget et al. 2010, Semotok et al. 2005, Zaessinger et al. 2006). Smaug further recruits Argonaute via Ago1 and represses *nos* by an miRNA independent mechanism (Pinder & Smibert 2013). Although deadenylation of unlocalised *nos* is necessary to localise the mRNA at the germ plasm, whether translational activation is mediated primarily by poly(A) tail extension is unclear (Rangan et al. 2009). Much of the translationally repressed *nos* is associated with polysomes, indicating another possible mechanism of translational repression independent of Smaug-Cup mediated repression of translation initiation (Clark et al. 2000). Once localised, *nos* translational repression is relieved by Osk-mediated RNP remodelling, disrupting the Smaug-*nos* interaction (Zaessinger et al. 2006).

Localisation and translational control of *osk*

Osk protein accumulation is established by *osk* mRNA localisation at the posterior of the oocyte during mid-oogenesis (Ephrussi et al. 1991). *osk* localisation is necessary for the formation of the abdominal segments of the embryo and establishment of the germ plasm and the pole cells at the posterior (Ephrussi et al. 1991, Kim-Ha et al. 1991, Lehmann & Nüsslein-Volhard 1986). By stage 10 of oogenesis, localised *osk* (Figure 1-9 (C)) is translated into two isoforms, long Osk and short Osk. Long Osk anchors *osk* mRNA to the posterior cortex, and short Osk assembles the germ plasm (Markussen et al. 1995, Rongo et al. 1995, Vanzo & Ephrussi 2002). Levels of Short-Osk are controlled by Par-1, and GSK-3/Shaggy phosphorylation and ubiquitin ligase mediate degradation, ensuring germ plasm assembly is restricted the posterior pole of the oocyte (Morais-de-Sá et al. 2013). *osk* mRNA also has a noncoding function, and is involved in both karyosome formation and sequestering Bruno in germline tissue and away from the follicle cells (Jenny et al. 2006, Kanke et al. 2015).

Contrary to early models of *osk* localisation by diffusion and anchoring (Glotzer et al. 1997) or Kinesin moving *osk* away from all cortical regions except at the posterior (Cha et al. 2002), *osk* is actively transport to the plus ends of microtubules by Kinesin on a subtly biased microtubule network (Parton et al. 2011, Zimyanin et al. 2007) (Zimyanin et al. 2008). This process requires the EJC, Hrp48, Tropomyosin II, and Stau (Zimyanin et al. 2008). Both *osk* and *nos* localisation in late stage egg chambers is maintained by their continual trafficking at the posterior cortex by both Dynein and Kinesin (Sinsimer et al. 2013). The restriction of the motility of these transcripts requires the motor protein regulator Klarsicht (Klar) β, and the correct ratio of *osk* mRNA to Osk protein at the posterior cortex (Gaspar et al. 2014).

Localisation of *osk* relies on numerous cis-acting regions. The 67 nucleotide oocyte entry signal (OES) in the 3' UTR controls transport into the oocyte on Dynein (Jambor et al. 2014), while the 28 nucleotide spliced *oskar* localisation element (SOLE) in the coding region targets *osk* to the posterior of the oocyte on Kinesin (Ghosh et al. 2012, Kim-Ha et al. 1993, Simon et al. 2015). *osk* transcripts also interact with each other directly, and unspliced transcripts can localise to the posterior by hitchiking on processed *osk* mRNAs (Hachet & Ephrussi 2004) via stem loop interactions between 3' UTRs (Jambor et al. 2011).

osk translational control has been extensively studied, and has formed a paradigm for translational control of localised mRNAs during *Drosophila* oogenesis by binding of repressor proteins (Besse & Ephrussi 2008). Me31B is required for the translational silencing of *osk* mRNA in nurse cell granules (Nakamura et al. 2001), and *osk* translation in the oocyte is repressed by Bruno, which binds Bruno response elements (BREs, consensus U(G/A)U(A/G)U(G/A)U) in the 3' UTR (Kim-Ha et al.

1995, Reveal et al. 2010). Bruno acts with a Cup-eIF4E complex to inhibit small ribosomal subunit recruitment to the 5' Cap (Chekulaeva et al. 2006, Nakamura et al. 2004, Wilhelm 2003). It also induces, with polypyrimidine binding tract protein (PTB), the oligomerisation of *osk* into silencing particles containing Me31B and Cup (Besse et al. 2009, Chekulaeva et al. 2006). Interestingly, *osk* transcripts with BREs can confer the translational repression activity of these elements in *trans* to *osk* transcripts lacking BREs within the same RNP (Reveal et al. 2010).

Cup also binds eIF4E, preventing eIF4G binding (Kinkelin et al. 2012, Nakamura et al. 2004, Wilhelm 2003). Both Cup and Bic-C proteins further repress *osk* translation by recruiting the CCR4 deadenylase complex to the mRNA and reducing its poly(A) tail length (Chicoine et al. 2007, Igreja & Izaurralde 2011, Jeske et al. 2011, Saffman et al. 1998). Repression of *osk* translation in early oogenesis also requires numerous piRNA genes (Chen et al. 2007, Cook et al. 2004, Findley et al. 2003, Lim & Kai 2007, Pane et al. 2007, Tomari et al. 2004).

In the oocyte, *osk* translation is activated by disruption of Bruno repressive activity. The mechanism for this is unclear, but may involve Bruno dimerisation and phosphorylation by Protein Kinase A (PKA), and certain BREs which can act in both translational repression and translational activation (Kim et al. 2015, Reveal et al. 2010, Yoshida et al. 2004). *osk* translation also requires Vasa, and Tudor, Osk and Orb proteins (Chang et al. 1999, Lasko & Ashburner 1988, Markussen et al. 1995). Orb interacts with PAP and Wispy, both poly(A) polymerases, to extend the *osk* poly(A) tail to over 150 nucleotides (Benoit et al. 2008, Castagnetti & Ephrussi et al 2003, Juge et al. 2002). These data suggest that, Orb acts on *osk* in a similar manner to CPEB in *Xenopus*; to activate *osk* translation by poly(A) tail elongation.

However, despite deadenylation by CCR4 and further poly(A) tail shortening by PABP2 (Benoit et al. 2005, Chicoine et al. 2007, Igreja & Izaurralde 2011, Jeske et al. 2011, Saffman et al. 1998), *osk* has a relatively long poly(A) tail during transport, and a longer poly(A) tail is not sufficient to overcome repression by Bruno (Castagnetti & Ephrussi 2003). Moreover, BRE mediated repression does not regulate poly(A) tail length (Castagnetti & Ephrussi 2003, Lie & Macdonald 1999, Reveal et al. 2010). Although the model for *osk* translational control is being constantly reassessed (Kanke & Macdonald 2015), the evidence suggests that *osk* silencing is mediated primarily by repressor protein binding, rather than control of poly(A) tail length.

Translational activation of *osk* also requires Stau and Hrp48 interactions with the 5' and 3' UTRs of *osk* (Micklem 2000). More factors have been identified with potential roles in *osk* translational control which have not been characterised, including Apontic, Imp, Exu and Ypsilon Schachtel (YPS), and Sqd, (Goodrich et al. 2004, Lie & Macdonald 1999, Munro et al. 2006, Wilhelm et al. 2000).

Localisation and translational control of *grk*

grk encodes a TGF-α homolog (Neuman-Silberberg & Schupbach 1993, Schupbach 1987) which functions twice to establish polarity during oogenesis (Figure 1-9 (D), (Gonzalez-Reyes et al. 1995, Roth et al. 1995). First, it signals to posterior follicle cells at stage 6, inducing an epidermal growth factor receptor (EGFR) signalling response, causing the follicle cells to signal back to the germline and reorganise the cytoskeleton (González-Reyes & St Johnston 1998, Neuman-Silberberg & Schupbach 1993). The "back signal" is unknown, but may involve the Salvador Warts Hippo (SWH) signalling pathway, and requires the Merlin protein and Laminin A in the

follicle cells (Deng & Ruohola-Baker 2000, Frydman & Spradling 2001, MacDougall et al. 2001, Meignin et al. 2007, Polesello & Tapon 2007).

Second, *grk* mRNA localises at the oocyte DA corner at stage 9 in a cap around the oocyte nucleus (Jaramillo et al. 2008, MacDougall et al. 2003, Neuman-Silberberg & Schupbach 1993). Grk protein expression is restricted to this region by dual signalling of Gurken and Decapentaplegic, a TGF-β family member (Deng & Bownes 1997, Peri & Roth 2000). Grk specifies dorsal fates by activating Torpedo, the *Drosophila* EGFR homolog, in the dorsal follicle cells (Neuman-Silberberg & Schupbach 1993, Roth et al. 1995, Sapir et al. 1998, Schupbach 1987, Wasserman & Freeman 1998). This signalling forms two dorsal appendages because high levels of EGFR signalling activate Argos, a repressor which splits the peak of EGFR signalling in two (Dorman et al. 2004, Wasserman & Freeman 1998). Grk signalling in the dorsal follicle cells also inhibits the action of *pipe*, confining Dorsal protein localisation to the nucleus, and adoption of ventral cell fates to ventral follicle cells.

Localisation of *grk* mRNA at the oocyte DA corner is required for dorsoventral patterning. When Grk is not expressed, no appendages form, and when it is overexpressed or mislocalised along the anterior margin, ectopic appendages form (Kelley 1993, Neuman-Silberberg & Schupbach 1993, Neuman-Silberberg & Schupbach 1994). Other proteins and signalling cascades are involved in the formation of dorsal appendages, but how they relate to *grk* is unclear (Clouse et al. 2008, McDermott et al. 2012, Rittenhouse & Berg 1995, Tran & Berg 2003).

grk mRNA localises in the oocyte in two independent steps. *grk* moves first to the anterior margin, and then to the DA corner (MacDougall et al. 2003). Both steps

require microtubules and Dynein, and it is hypothesised that two distinct sets of microtubules mediate this transport (MacDougall et al. 2003). Correct localisation of *grk* also appears to require Kinesin (Januschke et al. 2002). Although other models of *grk* localisation exist, including multiple rounds of anterior transport followed by trapping at the DA corner (Lan et al. 2010), the model described above is the most widely accepted. However, it is unclear at this point where *grk* mRNA that localises to the DA corner originates; is this from the posterior population of *grk* at stage 6, or is this population degraded after translation, and localised *grk* in the oocyte at stage 9 originates solely from the nurse cells?

grk localisation at the DA corner requires the *grk* localisation signal (GLS), a 64 nucleotide sequence which is necessary and sufficient for localisation to the DA corner (Van De Bor et al. 2005). Several trans-acting factors bind the GLS and are required for *grk* localisation, including Sqd, BicC, Cup, Syncrip and Egl (Dienstbier et al. 2009, McDermott et al. 2012). Without these proteins, *grk* is mislocalised along the anterior of the oocyte, causing dorsal patterning defects in the egg (Clouse et al. 2008, Geng & Macdonald 2006, Goodrich et al. 2004, McDermott et al. 2012, Neuman-Silberberg & Schupbach 1993, Norvell et al. 1999). *grk* is anchored at the DA corner by Sqd, which switches Dyein from a motor to a static anchor (Delanoue et al. 2007, Jaramillo et al. 2008).

The prevailing model for *grk* translation control is that Sqd binds to the 3' UTR and recruits Bruno (Filardo & Ephrussi 2003, Norvell et al. 1999) Cup, Hrb27C and Ovarian tumour (Otu, Clouse et al. 2008, Goodrich et al. 2004), which coordinate to repress translation. *grk* translation is sensitive to the DNA repair pathway, and is not translated in *spindle*-class mutants where this pathway is disrupted. The *spindle*

genes are involved in repairing double strand breaks (DSBs), and when the *RAD51* homolog *spindle-B* (*spn-B*) is mutated, the accumulation of DSBs causes activation of a meiotic checkpoint. This inhibits the translation of *grk*, most likely because this phosphorylates of Vasa and prevents it from activating *grk* translation (Abdu et al. 2002, Ghabrial & Schupbach 1999, Johnstone & Lasko 2004, Styhler et al. 1998).

grk translation is promoted in *spn-B* egg chambers by inhibition of TOR activity when when the SH2B family adaptor gene *lnk* is mutated (Ferguson et al. 2012). This has led to speculation that *grk* translation can be modulated by insulin and TOR signalling via an IRES in the 5' UTR of *grk*, although this IRES has yet to be identified. Analysis of *spn-B* mutants revealed that the majority of untranslated *grk* mRNA is associated with large repressive RNP complexes, and the association with translationally repressed RNPs instead of polysomes requires Sqd (Li et al. 2014).

At the DA corner, *grk* translation requires PABP55B and Encore (Enc, Clouse et al. 2008, Hawkins et al. 1996, Hawkins et al. 1997, Van Buskirk et al. 2000). Here, *grk* docks and is translated at the edge of P bodies, where Orb, which is required for *grk* translation, is enriched (Chang et al. 2001, Weil, et al. 2012b). Moreover, both *grk* and Orb are detected in heavier, translationally competent complexes in biochemical analyses (Li et al. 2014). These data suggest a model where *grk* is translationally repressed in transit by binding of repressor proteins. This repression is lifted once *grk* is localised at the DA corner and docks at the edge of P bodies, most likely regulated by PABP55B, Enc, Vasa and Orb (Figure 1-10).

Figure 1-10: Translational control of *grk* mRNA

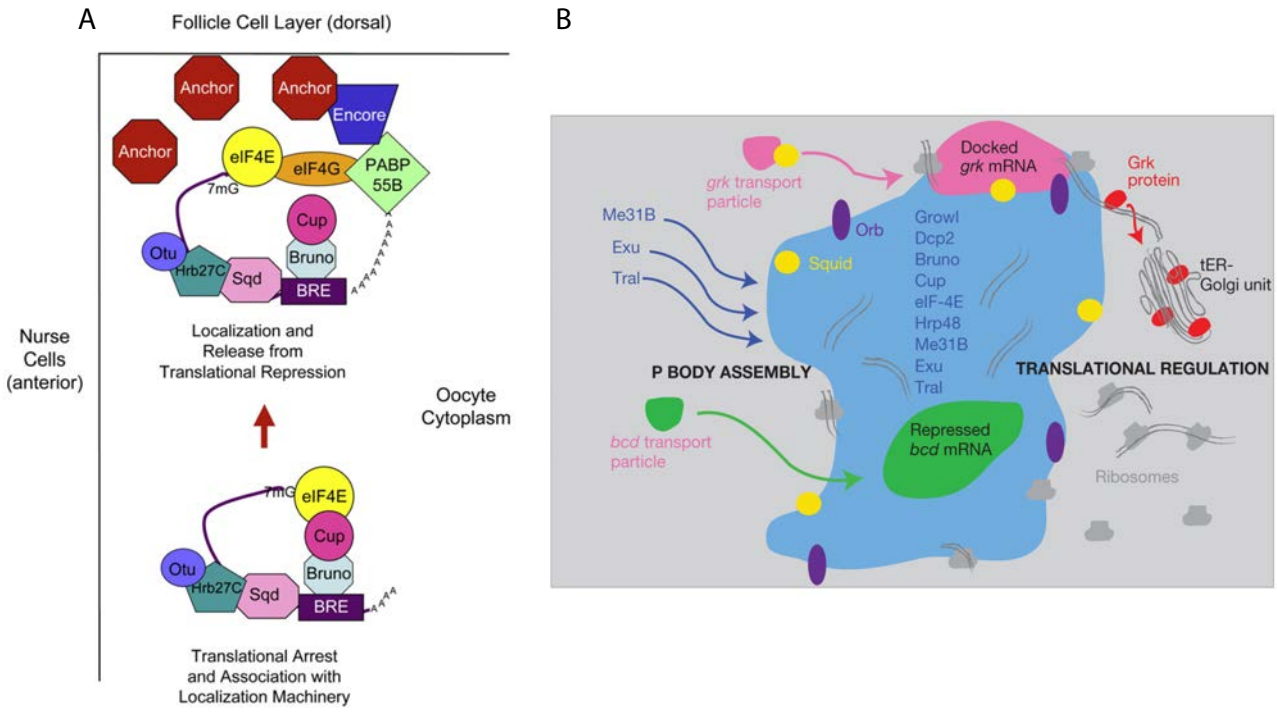

Figure 1-10: (Adapted from (Clouse et al. 2008, Weil, et al. 2012b) .

(A): Model from Clouse et al. 2008. Unlocalised *grk* mRNA is bound by Bruno at the BRE in the 3' UTR, which represses translation by generating a closed loop with Cup binding to eIF4E, and maintaining a short poly(A) tail. This translational repression is also mediated by Sqd, Otu, and Hrb27C. When localised (red arrow), *grk* mRNA is anchored at the dorsal anterior corner, and the binding of Encore and PABP55B to the translation initiation machinery displaces the Cup-Bruno complex, the poly(A) tail is extended, and *grk* mRNA is translated. (B): Model from Weil, et al. 2012b. P bodies (blue) are assembled at the DA corner and are enriched for translational repressors including Me31B and Bruno (list in blue inside P body). Sqd (yellow) anchors *grk* (pink) at the edge of P bodies, where Orb (purple) and ribosomes (grey) are also enriched. Orb activates translation of *grk* and Grk protein (red) is trafficked through the secretory pathway (tER-Golgi units in grey). Conversely, *bcd* (green) is targeted to the core of P bodies and is translationally repressed.

However, the role of Bruno in *grk* translational control is not clear. There is evidence that Bruno overexpression represses *grk* translation through a single BRE (Filardo & Ephrussi 2003, Kim-Ha et al. 1995, Norvell et al. 1999), but another lab did not reproduce this result (Snee et al. 2007). Furthermore, in various *arrest* mutant allelic combinations (*arrest* (*aret*) encodes the Bruno protein, Kim-Ha et al. 1995, Webster et al. 1997) Grk expression in the oocyte is normal (Yan & Macdonald 2004). This suggests that Bruno is not a key repressor of *grk* translation in the oocyte.

The role of Cup in *grk* translational control is also disputed. In *cup* mutant egg chambers Grk was found to be correctly (Nakamura et al. 2004) and incorrectly (Clouse et al. 2008) expressed by two different groups. In both *cup* and *sqd* mutant egg chambers, *grk* mRNA is mislocalised in addition to Grk protein being ectopically expressed (Clouse et al. 2008, Jaramillo et al. 2008). These two phenotypes are difficult to dissect, especially in light of the evidence that when *grk* mRNA is overexpressed it is localised and translated ectopically along the anterior margin (Weil et al. 2012b). This raises an important question: is the determining factor in restricting Grk expression to the DA corner the localisation of *grk* mRNA?

The function of the nurse cells in localised mRNA translation

grk, *bcd*, *osk* and *nos* processing in the nurse cells affects their localisation and translation. *osk* and *bcd* mRNA injected into the oocyte do not localise correctly (Cha et al. 2001, Glotzer et al. 1997), and although injected *grk* mRNA does localise, it is ectopically translated along the anterior margin (Weil et al. 2012b). Little is known about *nos* in the nurse cells, and will not be discussed.

Factors in the nurse cells required for localised translation of *grk*, *osk* and *bcd*

osk mRNA interacts with numerous proteins in the nurse cell nuclei. Deposition of the EJC, containing the proteins Mago Nashi (Micklem et al. 1997, Newmark et al. 1997), Y14 (Hachet & Ephrussi 2001) and the conserved helicase eIF4AIII (Palacios et al. 2004), on the mRNA during its splicing is required for localisation at the posterior pole (Hachet & Ephrussi 2004). *osk* also requires exposure to Hrp48 (Huynh et al. 2004) (Zimyanin et al. 2008) and Btz, a cytoplasmic component of the EJC (Palacios et al. 2004, van Eeden 2001, Wilhelm 2003). Assembly of a localisation-competent *osk* RNP requires stepwise addition of these components during *osk* nuclear export (Glotzer et al. 1997, Zimyanin et al. 2008).

bcd RNA injected into the oocyte does not localise, and is transported to the nearest cortical surface (Cha et al. 2001). However *bcd* which is injected into the nurse cells, then removed and reinjected into the oocyte localises correctly at the anterior, as *bcd* localisation requires exposure to Exuperentia (Exu) in the nurse cell cytoplasm (Cha et al. 2001). Similarly, the activity of the Sqd in the nurse cell nuclei is required for translational regulation of *grk* mRNA in the oocyte (Cáceres & Nilson 2009), and *grk* has been shown to be transcribed in nurse cell nuclei (Caceres 2005). This, combined with evidence that injected *grk* is ectopically translated (Weil et al. 2012b), suggests that *grk* mRNA requires exposure to proteins in the nurse cells.

mRNA and protein transport in the nurse cells

How mRNAs and proteins are transported in the nurse cells is not clear. They are thought to be trafficked into the oocyte during early oogenesis by Dynein, on a highly polarised network of microtubules with their minus ends arranged at the posterior of the oocyte and their plus ends in the nurse cells (Theurkauf & Hazelrigg 1998). *in*

vitro synthesised *grk* RNA injected into the nurse cells diffuses through ring canals and is localised correctly at the DA corner of the oocyte, in a process which requires Dynein, microtubules, BicD and Egl proteins (Clark et al. 2007). Similarly, *bcd* RNA injected into the nurse cells is transported to the anterior margin of the oocyte (Cha et al. 2001), Exu protein motility in the nurse cells requires Dynein and microtubules (Mische et al. 2007, Theurkauf & Hazelrigg 1998), and *osk* transport into the oocyte requires Dynein (Ephrussi et al. 1991, Jambor et al. 2014, Mach & Lehmann 1997, McGrail & Hays 1997, Suter & R. Steward 1991, Swan et al. 1999). The cytoskeletal organisation of the nurse cells has been explored, and suggests, contrary to earlier models, a random organisation of microtubules in the nurse cell cytoplasm, except at the ring canals where microtubules are more densely packed and highly polarised (Clark et al. 2007, Mische et al. 2007).

These data suggest that mRNA and proteins are transported into the oocyte on microtubules by Dynein. However, they do not address several points. First, experiments have relied on injection of *in vitro* synthesised RNA (Cha et al. 2001, Clark et al. 2007), which is not always correctly processed (Cha et al. 2001, Glotzer et al. 1997, Weil et al. 2012b). Second, the model of a highly polarised network of microtubules is not verified by visualisation of microtubules, and does not explain how mRNAs are transported into the oocyte once the microtubule cytoskeleton is reorganised after stage 6. Third, the speeds and directionality of proteins and mRNA in nurse cells do not suggest they are transported by a similar mechanism. Exu protein particles move in numerous directions in the nurse cell cytoplasm on microtubules, whereas injected *grk* moves directly towards ring canals (Clark et al. 2007), and the speeds of movement of *grk*, *osk*, and Exu are significantly different (Clark et al. 2007, Mhlanga et al. 2009, Theurkauf & Hazelrigg 1998).

Fourth, although the OES has been identified in *osk* (Jambor et al. 2014), the regions of the *grk* and *bcd* which mediate transport of these mRNAs into the oocyte are not defined. The existence of the OES and the requirement of BicD and Egl proteins for *osk* transport into the oocyte (Jambor et al. 2014, Mach & Lehmann 1997), McGrail & Hays 1997, Swan et al. 1999) suggests that not all mRNAs are transported on dyenin into the oocyte by default, but whether *grk* and *bcd* use a similar mechanism is unclear. Fifth, whether *grk*, *osk* and *bcd* mRNAs are transported in the same or distinct particles, and if they are transported with their trans-acting factors in the nurse cells, is not known. Finally, we do not understand how *grk, bcd* and *osk* are all transported into the oocyte in the same direction, but at the ring canals are transported to distinct regions of the oocyte.

Translational control in the nurse cells

How axis determining transcripts are translationally regulated in the nurse cells is less well understood than in the oocyte. *osk* is ectopically translated in the nurse cells of *me31B* mutant egg chambers (Nakamura et al. 2001), and when Osk::GFP is expressed which lacks a 3' UTR, or has with a 3' UTR with mutated BREs, the Osk::GFP protein is expressed in the nurse cells (Kim et al. 2015). However, this may be because this transgene is driven by strong *Gal4VP16* driver. When BREs are removed from the 3'UTR of endogenous *osk*, or *cup* or *Bic-C* are mutated, *osk* is prematurely translated in the oocyte, but not in the nurse cells (Kim-Ha et al. 1995, Nakamura et al. 2001, Nakamura et al. 2004, Saffman et al. 1998). Similarly, although BRE-like motifs repress expression of GFP reporter transgenes in the nurse cells (Reveal et al. 2011), translational repression of localised mRNAs by Bruno specifically in this tissue has not been demonstrated. Furthermore, the mechanism of *bcd* translational repression throughout oogenesis may be because it is targeted

inside P bodies at the anterior of the oocyte until activation, but how *bcd* is translationally repressed during nurse cell transit is not clear.

grk ectopic translation in nurse cells been reported in double mutant egg chambers for both *aret*, and *Star*^{1} (*S*^{1}). *S*^{1} encodes a transmembrane protein required for post-cleavage tracking and secretion of Grk to the follicle cells (Ghiglione et al. 2002). In double mutant egg chambers Grk protein is visible at boundaries in between the nurse cells (Yan & Macdonald 2004). However, in mutants for *aret* alone no Grk protein was expressed in the nurse cells. The authors hypothesise that in the absence of Bruno, excess *grk* is translated, but is normally trafficked into the oocyte by *S*^{1}. In *aret/S*^{1} double mutants this trafficking is disrupted, and Grk is not effectively moved into the oocyte, leading to Grk accumulation in the nurse cells. However, this model has not been tested, and the role of *S*^{1} is not clear - alternative explanations such as Grk protein moving into the nurse cells from the oocyte cannot be excluded. Similarly, in egg chambers where *Drosophila* Syncrip is overexpressed, Grk protein is ectopically translated in rings around nurse cell nuclei, but the reason for this ectopic expression is unclear (McDermott et al. 2012).

In mutants for *spoonbill* (*spoon*), which encodes a multifunctional RBP, *grk* mRNA and Grk protein are both present at reduced levels in the oocyte and are increased in the nurse cells (Motola & Neuman-Silberberg 2004). This suggests that the mRNA is not effectively trafficked into the oocyte, but how this mRNA is then translated into Grk protein prematurely in the nurse cells is not clear.

nos, unlike *grk*, *osk* and *bcd*, is translated in the nurse cell cytoplasm of early stage oocytes (Forrest et al. 2004). Nos protein and *nos* mRNA are then transferred into

the oocyte at nurse cell dumping. Unlocalised *nos* in the oocyte is repressed whilst localised *nos* at the posterior is translated, and Nos protein in the ooplasm which originates from the nurse cells is degraded at stage 13 (Forrest et al. 2004). How *nos* is translated in the nurse cells and then repressed when unlocalised in the oocyte is not known. The repression of *grk*, *osk* and *bcd* in the nurse cells, while *nos* is translationally active, suggests that *nos* mRNA is under a fundamentally different mechanism of translational regulation in the nurse cells.

Aims of this Thesis

To determine how mRNAs are differentially regulated in two interconnected tissues, and how they are translationally repressed during transport and translated once localised, I examined nurse cells with the aim of answering the following questions:

- **Are mRNAs and proteins transported within the nurse cells into the oocyte by the same, or distinct mechanisms?**
- **Do axis determining transcripts move with their trans-acting factors in the nurse cells, or are these added to the RNP in the oocyte?**
- **How are mRNAs translationally repressed in the nurse cells?**

In order to answer these questions, I used a combination of imaging and genetic approaches. Although biochemical analysis would provide useful insights, isolation of the nurse cells from the oocyte and follicle cells is difficult, as separation of the tissues leads to loss of cytoplasm and disruption of cellular processes (R. Parton, T. Weil, I. Palacios personal communication). The MS2 system is a non invasive technique which labels endogenously processed mRNA in live tissue (Bertrand et al. 1998), and has been used to study mRNAs in the oocyte (Forrest & Gavis 2003, Weil et al. 2006, Zimyanin et al. 2008, Weil et al. 2012b), but not in the nurse cells. This imaging assay would allow co-visualisation of mRNA and proteins, and could begin to answer some of the questions outlined above. Moreover, analysis of *grk* mRNA in fixed tissue using fluorescent *in-situ* hybridisation (FISH) has so far been unsuccessful (A. Clark Thesis; R. Parton, T. Weil, C. Rabouille personal communication). In this Thesis, I will explore the mechanisms of *grk* mRNA transport and translational control specifically in the nurse cells as follows:

Chapter 2

I detail the techniques and protocols used to throughout this Thesis.

Chapter 3

Can the MS2 system be used to visualise mRNA in nurse cells? Here I optimise a protocol for imaging *grk* and *osk* mRNA in live nurse cells for the first time, and use this to characterise the dynamics of mRNA transport in nurse cells. I show that mRNAs move significantly faster in the nurse cells than in the oocyte, and there appear to be differences in RNP packaging between the two tissues.

Chapter 4

Can single molecule FISH (sm-FISH) be used to detect *grk* mRNA in nurse cells? Here I optimise an sm-FISH protocol to detect *grk* in the nurse cells for the first time, which again suggests a difference in the number of *grk* molecules per RNP between the nurse cells and the oocyte.

Chapter 5

Do P bodies have a similar protein distribution in the nurse cells and the oocyte? Here I use live cell imaging, immunofluorescence, and analysis of immuno-electron microscopy (IEM) data collected by collaborators to characterise the protein composition, dynamics, and mechanism of transport of nurse cell P bodies. I show that P bodies in the nurse cells contain markedly less Orb protein than those in the oocyte, and that P body proteins in the nurse cells move significantly faster than those in the oocyte.

Chapter 6

Is *grk* translationally repressed in the nurse cells by known repressor proteins or targeting to P bodies? Here I use mutants and overexpression lines to test the role of several proteins, and live cell imaging and sm-FISH to examine *grk* and P bodies in the nurse cells. I show that *grk* translation is not prevented in the nurse cells by the activity of any one of these repressor proteins, or by the association of *grk* with P bodies.

Chapter 7

Is *grk* translation prevented in the nurse cells by low levels of its translational activator, Orb, in this tissue? Here use genetic peturbation, immunofluorescence and sm-FISH to show that the lower level of Orb in the nurse cells is a crucial factor in preventing *grk* translation in this tissue. I identify a novel mechanism contributing to the translational control of *grk*, through restricted spatial access to its translational activator, Orb.

Chapter 8

I discuss the wider implications and future directions of my research.

Chapter 9

I detail papers referenced throughout the Thesis.

Chapter 10

Appendices for additional detail. A USB drive is included on the back page of the Thesis, which contains supplementary movies and a high resolution PDF of the Thesis.

Chapter 2: Materials and methods

Table 2-1: The following definitions and abbreviations are used throughout:

Abbreviation/definition	Definition
Rinse	Solution added to sample and removed once the egg chambers have settled (30s-1 min)
Wash	Addition of solution to sample for an extended period of time (longer than 1 min)
Incubation	Addition of a solution containing an enzyme, antibody or probe, or washing at a temperature other than room temperature for longer than 1 min.
s	Second
min	Minute
h	Hour
PBST	Phosphate buffered saline with tween 20 (0.2%)
PBTX	Phosphate buffered saline with Triton-X (0.1%)

The lengths of specific washes and incubations are detailed in the relevant protocols. Unless otherwise stated, all washes in antibody staining or FISH protocols were performed on a rotating wheel.

Molecular Biology

Solutions and reagents

All solutions and buffers were prepared as described in “Molecular cloning - A laboratory manual” (Sambrook et al 1989), unless otherwise stated. Phosphate buffered saline (PBS), Tris-EDTA (TE), Tris-acetate-EDTA (TAE), Saline-sodium citrate (SSC), Super Optimal Broth with Catabolite repression (S.O.C) and Luri Betani (LB) media were prepared and autoclaved by the Department of Biochemistry media kitchens. The media kitchen also prepared LB-agar plates with antibiotics, and apple juice agar plates as below (Table 2-2)

Buffer	Recipe
1x PBS	For 1 litre: 10 phosphate buffered saline (Dulbecco A) tablets, 1L MiliQ water.
TE	10 mM Trisl-HCl (pH 7.5), 1mM EDTA (pH 8.0)
10x TAE	0.4M Tris base, 10mM EDTA (pH 8.0), 1.2% (v/v) glacial acetic acid
20x SSC	For 1 litre: 175.3g NaCl, 100.5g (Tri-sodium citrate ($2H_2O$) in 800ml distilled H_2O, balanced to pH 7.0 with HCl
S.O.C medium	For 1 litre: 20g Tryptone, 5g Yeast extract, 0.59g NaCl, 0.186g KCl, 2.03g $MgCl_2.6H_2O$, 2.46g $MgSO_4.7H_2O$, 180 ml of 20% glucose
LB bacterial media	For 1 litre: 10g Bacto tryptone (Difco), 5g Bacto yeast extract, 5g NaCl
LB-Agar	For 1 litre: 16g Bacto tryptone (Difco), 10g Bacto yeast extract, 5g NaCl
Apple juice Agar	For 1 litre: 250ml Apple Juice, 25g sucrose, 22g agar, 750ml water

RNA extraction

Total RNA extraction was performed using the illustra RNAspin Mini RNA Isolation Kit (GE healthcare). Centrifugation times and speeds are as directed by the protocol unless otherwise stated. Ovaries from 48 h fattened female flies were dissected and immediately flash frozen in liquid nitrogen. Ovaries were lysed in lysis buffer containing RNase inhibitor (RNAsin, Promega, 20-40 u/μl, 1:100) with a rotor-stator (VWR). The lysate was then filtered using RNAspin Mini Filter columns to reduce lysate viscosity and remove unhomogenised tissue. RNA binding conditions were adjusted by adding 3x the lysate volume of 70% ethanol to the lysate followed by vortexing, the sample was then applied to the RNAspin Mini Column. After RNA binding, the column silica membrane was desalted using Membrane Desalting Buffer. Sample were then treated with DNase (10μl reconstituted DNase with 90μl reaction buffer, 90μl of mix was then added directly to the column) and incubated for 15 min at room temperature. The columns were then washed with wash buffer RA2 and then wash buffer RA3 twice, before the RNA was eluted from the column in 50μl of RNase free H_2O (centrifuge for 2 min at 11,000 g, 4^0C). To attain higher RNA concentrations, the eluate was reapplied to the column and the centrifugation step was repeated. RNA concentration and purity was assessed using a nanodrop (ND-1000 Spectrophotometer).

Reverse-transcriptase (RT)-PCR

The reaction was carried out using the RevertAid First Strand cDNA synThesis kit (Thermo scientific), following the manufacturers protocol. Either oligo$(dT)_{12\text{-}18}$ (Invitrogen) or random hexamers (invitrogen) were used as primers depending on the experiment. For the DNA splint mediated poly(A) test assay (sPAT) random hexamers were used, for mapping the *grk* poly(A) site olgio$(dT)_{12\text{-}18}$ was used. To

eliminate secondary structures, samples were first incubated with with primers and dNTP (Invtrogen) for 5 min at 65^{0}C. Subsequently, samples were chilled on ice for 1 min, followed by the addition of RT buffer, RevertAid premium reverse transcriptase and Ribolock RNase inhibitor (Thermo Scientific). Samples were then incubated for 10 min at 25^{0}C (annealing), 50^{0}C for 30 min (Reverse Transcription), 85^{0}C for 5 min (enzyme inactivation). Singe stranded cDNA products were stored at -20^{0}C until use.

Nested PCR

4ul of sample from the RNA extraction protocol (> 500ng/μl in RNase free H_2O) was incubated with 50μM dNTPs (Invitrogen), 1.6μM forward primers (Appendix A, Eurofins genomics), 1.6μM reverse primer (RT anchor primer or anchor primer for sPAT, oligodT primer for 3' end mapping, Appendix A), 1x High Fidelity Phusion buffer (New England Biolabs), 0.1 units Phusion polymerase (New England Biolabs) and H_2O to achieve a final volume of 25μl. Incubations were: 2 min at 98^{0}C, then 25 cycles of; 25 s at 98^{0}C, 25 s at 16^{0}C, 30 s at 72^{0}C, 1 min 70^{0}C, held at 4^{0}C.

PCR with magnesium titration for poly(A) mapping

The protocol adapted from Davis & Ish-Horowicz 1991 was performed in collaboration with L. Yang (Davis lab). 10μg of total RNA was extracted using the Illustra RNAspin Mini RNA Isolation Kit (GE healthcare) as described above. Total RNA was used as the template for reverse transcription using oligo(dT)$_{12\text{-}18}$ as described above. Nested PCR was performed with different Mg concentrations (1 mM - 3.5 mM). 4μl cDNA was incubated with 1x Taq buffer (variable Mg concentration), 50μM dNTP (invitrogen), 1.6μM forward and reverse primer (Outer forward, *grk* outer; inner forward, *grk* inner; outer and inner reverse, oligodT$_{(12\text{-}18)}$, invitrogen), and Taq polymerase (0.625 units, New England Biolabs).

sPAT assay

Protocol adapted from Minasaki et al. 2014 and performed in collaboration with L. Yang. RNA was extracted from ovaries using the Illustra RNAspin Mini RNA Isolation Kit (GE healthcare) as described above. 10μg of the RNA was taken for poly(A) tail trimming as a control. The poly(A) tail was trimmed by incubating 10μg of RNA in 20mM Tris-HCl pH 7.8, 40mM KCl, 8mM MgCl2, 1mM DTT, 4μM oligo-DT 12-18 for one min at 95^{0}C followed by 25 min at 20^{0}C. 5 units RNaseH and 40 units Ribolock (RNase inhibitor) was added and the mixture incubated for a further 60 min at 37^{0}C. Trimmed RNA was re-purified using the Illustra RNAspin Mini RNA Isolation Kit omitting the DNAse digestion step (to avoid DNase contamination during splint annealing). The DNA splint (sequences in Appendix A) was annealed to both trimmed and untrimmed samples by incubating 15μl of each sample with 2μM DNA splint and 3μM RNA anchor. The incubation was as follows: 5 min at 75^{0}C, 5 min at 60^{0}C, 5 min at 42^{0}C, 5 min at 25^{0}C. For ligation of the RNA anchor, 10μl of the product from the annealing reaction was incubated with 50mM Tris-HCl pH 7.5, 2 mM MgCl2, 1mM DTT, 440 μM ATP, 10 units RNA ligase 2 and 40 units Ribolock (RNase inhibitor) at 15^{0}C for 16 h. RNA was extracted and DNA splint removed during the process using the Illustra RNAspin Mini RNA Isolation Kit. Samples were reverse transcribed using random hexamers and the RevertAid First Strand cDNA synThesis kit (Thermo Scientific) as described above. Nested PCR was performed as described above.

TAE agarose gel electrophoresis

Samples were mixed with 1x gel loading dye, blue (New England Biolabs) and loaded onto agarose gels. For both sPAT and *grk* poly(A) site mapping, 2.5% agarose gel (agarose MP, Roche) containing 0.5 μg/ml Ethidium Bromide (Sigma) was used. Electrophoresis was carried out in 1x TAE running buffer at a constant

voltage of 70 V, nucleic acids were visualised using an enclosed UV transilluminator with associated imaging software.

Gel extraction of DNA

DNA for sequencing of the *grk* 3'UTR was gel extracted using a silica membrane assembly in the QIAquick gel extraction kit (QIAGEN 28704) following the manufacturers protocol. Bands were cut out of the gel using a clean razor blade under a UV transilluminator.

Amplification and purification of plasmid DNA

Prior to transformation, 3' overhangs were added to the gel extraction product using the TOPO TA cloning kit for sequencing (Life technologies) according to the manufacturers protocol. 2μl of TOPO cloning product was added to chemically competent cells (Stellar *E.coli* HST08, Clontech and incubated for 10 min on ice. Bacteria were heat shocked for 30 s at 42^{0}C, before adding 250μl S.O.C to the samples and incubating for 45 min at 37^{0}C, at 300rpm on a thermomixer. Bacteria were spun down and resuspended in 50μl of the original S.O.C. 10μl of bacteria was plated onto 100μg/ml ampicillin/kanamycin plates and spread. Plates were incubated overnight at 37^{0}C and then incubated at 4^{0}C for the following day. Single resistant colonies were picked in the evening and added to 50μg/ml of ampicillin in 3ml of LB for incubation for 12-16 h at 37^{0}C. The plasmid was then isolated using the QIAprep Spin Miniprep kit (QIAGEN 27106) according to the manufacturers protocol.

DNA sequencing

DNA sequencing was performed by the Source Biosciences Sanger Sequencing Facility within the University of Oxford. Sequencing was performed by SpeedREAD

technology. 1μg of plasmid DNA was provided within a total volume of 10μl (100ng/μl). Both forward and reverse sequences were analysed for each sample.

DNA sequence analysis

Data from sequencing was analysed using *Drosophila melanogaster* nucleotide BLAST (http://blast.ncbi.nlm.nih.gov/Blast.cgi?PAGE_TYPE=BlastSearch&BLAST_SPEC=OGP__7227__9554) from the RefSeq RNA database optimised for somewhat similar sequences.

Preparation of DNA templates for *in-vitro* transcription

For standard transcription, 5-10μg plasmid cDNA (*grk66* was a gift from T. Schupbach) was digested using the appropriate restriction enzyme (New England Biolabs) and inserted into the pBluescript plasmid. Digests were visualised by TAE agarose gel electrophoresis and purified using the QIAquick PCR purification kit (QIAGEN 28104).

***in vitro* transcription of DIG *in situ* probes**

1ug linearised template DNA in the pBluescript plasmid was transcribed by incubating at 37^{0}C for two h in reaction mix as follows: 1x transcription buffer (dependent on the polymerase, 40 mM Tris-HCl, pH 8.0, 6mM $MgCl_2$, 10mM DTT and 2mM spermidine, Roche), matched to the polymerase depending on the promoter present (T7 for transcribing probe, T3 for transcribing sense), 10mM DIG UTP/rNTP mix (Roche), 20 units T7/T3 RNA polymerase (Roche), and 40 units RNase inhibitor (Promega). Template DNA was removed with 2 units Turbo DNase (Life technologies) for 10 min at 37^{0}C. Unincorporated nucleotides were removed using a Sephadex G50 RNA spin column (Roche) according to the manufacturers

instructions. RNA was precipitated by adding 2.5x volume of 100% ethanol (RNase free) and 1/5 volume Sodium Acetate (5M) and leaving overnight at -20^{0}C. RNA was then pelleted by spinning at 14,000 rpm for 30 mins at 4^{0}C. Salts were removed from the pellet by gentle rinsing with cold 70% ethanol which was removed immediately before being respun for 5 min at 14,000 rpm to remove residues. Pellets were air dried for at room temperature and then resuspended in 10 to 20μl of DEPC water. RNA concentration and purity was tested with a nanodrop. Samples from after transcription, after DNA template removal and after G50 column treatment were analysed using TAE agarose gel electrophoresis.

Stellaris probe design

Probes for sm-FISH were designed using the Biosearch Stellaris probe designer (https://www.biosearchtech.com/stellarisdesigner/), see Appendix B.

Generating *grk-MS2-24* constructs (B. Steinkraus)

The *grk-MS2-24* construct was generated by B. Steinkraus in the Fulga lab at the Weatherall Institute of Molecular Medicine, University of Oxford. NotI/EagI and BglII restriction enzyme sites were inserted into the 3'UTR of the *grk66* cDNA in a pBluescript plasmid at position 343, with an 8 nucleotide spacer between the two sites, by overlapping PCR for site directed mutagenesis. This position was used to insert the *MS2-12* sequence into the *grk* 3' UTR in the past (Jaramillo et al. 2008). The modified section of the 3' UTR was cloned into a TOPO vector and sequenced to verify the presence of NotI/EagI and BglII sites. This section was then cloned back into the *grk66* cDNA in the pBluescript vector by digestion with SwaI and BstZ17I and sequenced. The *grk66* cDNA with the modified 3'UTR was then cut out of the pBluescript by a partial digest with XhoI and EagI, and analysed using TAE agarose

gel electrophoresis. This fragment was ligated into an empty pCaSpEr4 vector for transgenics digested with XhoI and NotI. The pCR4-24XMS2SL plasmid (Addgene, R. Singer, (Lionnet et al. 2011) was then cloned into position 343 of the *grk* 3' UTR between the NotI and BgIII sites and sequenced.

Drosophila Methods

Fly husbandry

All stocks and crosses were raised on standard cornmeal agar medium at 25^{0}C *OrR* was used as the wild-type strain unless otherwise stated. Fly strains in Appendix C.

Heat shock treatment of FRT-FLP mosaic lines (Nakamura et al. 2001)

hsFLP/w ; gfp-vas FRT40A virgin females were crossed to either *hsFLP/w ; me31B$^{\Delta 1}$ FRT40A,* or *hsFLP/w ; me31B$^{\Delta 2}$ FRT40A* males. At early pupal stage vials were sealed with parafilm and placed in a water bath for two h at 37^{0}C. Vials were placed at room temperature for one h, and then incubated at 37^{0}C in the water bath for another two h. Vials were returned to 25^{0}C until eclosure.

Embryo injection (in collaboration with T. Weil)

grk-MS2-24 flies were generated by co-injecting 500ng/µl of the *grk-MS2-24* plasmid with 100ng/µl helper plasmid (transposase Δ2-3, Weil et al. 2006. Adult *yw* flies were raised in cages on apple juice agar plates with yeast paste. During injection sittings, embryos were collected every 45 min, washed into a sieve, dechorionated in 50% bleach for two min and then rinsed thoroughly with distilled water. Embryos were aligned on a slice of apple juice agar with a probe (Fine Science Tools), and transferred to a piece of double sided tape on a 22x50 1.5 thickness cover slip and dessicated in silica gel (pre-heated to 50^{0}C) for 10 min. Embryos were then

immediately covered in series 700 halocarbon oil and plasmids injected using femtotip needles (Eppendorf). Injected embryos were stored in a moist container at 25^{0}C until hatching, when larvae were transferred to vials with softened fly food. After eclosure flies were crossed to *yw* virgins/males respectively. Progeny were screened for eye colour and crossed to second and third chromosome balancer stocks to map the insertion, and then to balance the insertion. 11 stable lines were generated and were crossed to *Pnos-NLS-MCP-GFP* flies to test for fluorescence.

Ovary dissection for live imaging

For live imaging, adult female flies no less than 24 h after eclosure were fattened on dried active bakers yeast (Allinsons) for 48 h at 25^{0}C. Flies were dissected using tweezers (Fine Science Tools, Weil et al 2012a), and ovaries placed in series 95 halocarbon oil on standard no. 1.5 coverslips (Scientific Laboratory Supplies ltd). Individual ovarioles were teased out and aligned as previously described (Weil et al 2012a). Egg chambers were imaged until 40 min after dissection.

Eggshell preparation for scoring dorsal appendage morphology

Adult flies were raised in a cage on apple juice agar plates with yeast paste for two h at 25^{0}C. Eggs were washed with water in a sieve and then placed on a standard no. 1.5 coverslip (Scientific Laboratory Supplies ltd). Eggs were scored in water for dorsal phenotype defects in batches of 30 by two independent researchers (myself and R.M. Parton). Representative eggs from each genotype were then imaged under dark field on the DeltaVision CORE widefield deconvolution system (Applied Precision, a subsidiary of GE Healthcare).

Fixation for immunofluorescence

Adult females flies were fattened as described above. Flies were dissected into 4% paraformaldehyde in PBST (0.1%) (stock solution 16% paraformaldehyde methanol free ultra - pure EM grade, Polysciences) in a watch glass. Ovaries were splayed open using tweezers and probes (Fine Science Tools) but were not fully separated. Individual ovaries were transferred into an eppendorf and vortexed briefly following the addition of 800μl heptane. Ovaries were fixed for no more than 15 min in total, followed by 3 rinses and 3 washes of 10 min in PBST. Where necessary, egg chambers were incubated in GFP or RFP booster (1:200 Chromotek) in PBST for one hr at room temperature, followed by multiple washes in PBST.

Fixation and protein detection for cryo-EM (T.Weil, B.Herpers and C.Rabouille)

Egg chambers were fixed, frozen, stained and and sectioned for EM by T. Weil, B. Herpers and C. Rabouille at the Department of Cell Biology, UMC Utrecht, Netherlands. Protein detection was performed as described previously (Delanoue et al. 2007, Rabouille 1999, Slot & Geuze 2007, Weil et al. 2012b).

Antibody staining for immunofluorescence

Flies were fattened and egg chambers dissected and fixed as described above. Following PBST washes, ovaries were washed for 5 min in 0.01% PBTX and then rinsed in PBST. Ovaries were blocked in 4% bovine serum albumin (BSA) in PBST for 30 min. Primary antibody was added at the required concentration (Appendix D) in PBST for 2 h at room temperature, followed by 3 rinses and 3 washes of 20 min in PBST. Secondary antibody was added at 1:500 in PBST for one h at room temperature followed by 3 rinses and 3 washes of 20 min in PBST. Ovaries were mounted on 1mm superfrost microscope slides (VWR) in Prolong Gold antifade

reagent (Life technologies) and ovarioles separated fully during the mounting process. When preparing samples for structured illumination microscopy on the OMX V3 (GE Healthcare), all egg chambers older than stage 10 were removed to ensure the coverslip would be level. A 1.5 22x22 coverslip (High Precision Coverslips, guaranteed 0.17 mm thickness, GE Healthcare) was placed on top of the samples and left for 16 h (overnight) in a flat, dark place to cure. Slides were sealed the following morning with nail varnish. Antibodies in Appendix D.

FISH using digoxygenin probes

Females were fattened, dissected, fixed and PBTX permeabilised as described above. Ovaries were washed at 70^{o}C for 10 min in 50% PBST 50% Hyb (-) buffer (50% de-ionised formamide, 5x SSC, 0.1% Tween 20, balanced to pH 6.5 with concentrated HCl), followed by a 10 min wash in 100% Hyb (-). Ovaries were then pre-hybridised for 1 h 30 min at 70^{0}C in Hyb (+) buffer (50% de-ionised formamide, 5x SSC, 0.1% Tween 20, 100μg/ml *E.coli* tRNA, 100μg/ml heparin, balanced to pH 6.5 with concentrated HCl). DIG probe was opened by heating at 80^{0}C for 5 min and then flash cooled on ice. Probe was added to ovaries in Hyb (+) at 1:500 dilution at 70^{0}C overnight. Probe was removed by serial washes as follows: two 20 min washes in Hyb (-), one 20 min wash in 50% Hyb (-), 50% PBST, four 20 min washes in PBST. Ovaries were blocked in 4% BSA for 10 min before incubation at room temperature in Sheep anti-DIG (Fab fragments) at 1:400 dilution in PBST for two h. Primary antibody was washed off by 3 rinses in PBST and 2, 20 min washes in PBST. Ovaries were incubated in secondary antibody (1:400 Donkey anti-sheep Alexa 488 or Donkey anti-sheep Alexa 568) for two h at room temperature. Secondary antibody was washed off by 3 rinses in PBST and 2, 20 min washes in PBST. Ovaries were mounted in Prolong Gold as described above.

FISH using digoxygenin probes with Tyramide Signal Amplification (TSA)

FISH protocol carried out as described as above until the addition of primary antibodies. Ovaries were incubated in Mouse anti-DIG HRP conjugate (Horse Radish Peroxidase, PerkinElmer) diluted 1:1000 in PBST. This was washed off with 3 rinses and 3, 20 min washes in PBST. For the TSA detection, the Fluorescent Tyramide stock solution (Alexa Fluor 568 Tyramide, Life Technologies) was diluted 1:50 in Amplification Diluent for 4 min as per manufacturers instructions (Life Technologies). The Tyramide labelling reaction was stopped with two 5 min washes in PBST, before mounting in Prolong Gold as described above.

Stellaris sm-FISH protocol

Females were fattened, dissected, fixed and PBTX permeabilised as described above. For RNase treatment, egg chambers were incubated in 40μg/ml DNase free RNase (Roche) in PBST for 30 min at room temperature, and then washed extensively with PBST. Ovaries were washed in 50% PBST and 50% Hyb (-) buffer (10% de-ionised formamide, 2x SSC, 0.02% BSA, 2mM VRC) for 10 min, before being washed for 10 min in 100% Hyb (-). They were then pre-hybridised for 1 h in Hyb (+) buffer (10% de-ionised formamide, 2x SSC, 0.02% BSA, 2mM VRC, 10% Dextran Sulphate. Probe was hybridised with sample at 25nM in Hyb (+), overnight, at 37^{0}C, in the dark with gentle rocking. Probe (Stellaris, Biosearch Technologies) was removed by two washes of one h in wash buffer at 37^{0}C (15% de-ionised formamide, 2x SSC). Ovaries were mounted in Prolong Gold as previously described. Adaptations from the T. Trcek protocol (Trcek et al. 2011, Trcek et al. 2012, T. Trcek personal communication) included:

- Removal of steps specific to embryos including dechorionation, rehydration in methanol and proteinase K treatments.

- Lowering of formamide concentration to 10% w/v to preserve morphology.
- Addition of serial washes in 50% PBST and Hyb (-), Hyb (-), and Hyb (+).
- Aliquoting and freezing de-ionised formamide to prevent ionisation.
- Use of fresh (< 1 month old) SSC stock to improve detection.

Drug treatments for the cytoskeleton

Females were fattened for 24 h on yeast, followed by 16-24 h on standard fly food without yeast, and then 4-6 h on yeast with appropriate drug/ethanol mix. For colcemid treatment, yeast paste was prepared with Colcemid in 100% ethanol, final concentration of 20μg/ml.

Nutrient stress assay

Females were raised in cages on apple juice agar plates either with yeast paste ("fed" condition) or without yeast paste ("starved" condition) for 24 hours. Females from the "starved condition" were transferred to apple juice plates with yeast paste for "refeeding" for 12 h.

Microscopy and image analysis

Imaging parameters in Appendix E, image analysis protocols in Appendix F.

Widefield Imaging of fixed egg chambers

Imaging was performed on a DeltaVision CORE widefield deconvolution system (Applied Precision, a subsidiary of GE Healthcare) based upon an Olympus IX71 microscope, x20 0.75 NA dry or x100 1.4 oil NA objectives, a 16 bit Roper Cascade II camera and standard Chroma filter-sets.

3D Structured illumination microscopy (3D-SIM)

Structured illumination was performed on the OMX V3 (Applied Precision, a subsidiary of GE Healthcare) microscope in collaboration with R. Parton. Images were acquired using the sCmos camera (PCO AG), the 60 x 1.3 NA silicon oil immersion objective (Olympus). Images were checked for structured illumination suitability using Sim Check (Ball et al 2015 in review), and 3D-SIM data was then reconstructed using the proprietary algorithm from Applied Precision/GE Healthcare run in SoftWorx. Images were registered in Editor (J. Sedat UCSF) using a reference image of *Me31B::GFP* and Me31B antibody staining with Alexa 568.

Widefield live cell imaging

Imaging was performed on the DeltaVision CORE widefield deconvolution system described above. For imaging mRNA particles in the nurse cells, a focal plane close to the nurse cells/follicle cell boundary closest to the coverslip was chosen.

Live cell imaging on the OMX V3

For fast live imaging over multiple Z frames, the OMX V3 (Applied Precision, a subsidiary of GE Healthcare) microscope was used (Dobbie et al. 2011). The custom "Z sweep acquisition protocol" allows a series of acquisitions whilst the stage moves continuously in Z, and was established on the OMX V3 by Ian Dobbie and Micron Oxford in collaboration with Applied Precision.

Deconvolution

Where required, image sequences were deconvolved with the SoftWoRx Resolve 3D constrained iterative deconvolution algorithm from Sedat/Agard (Applied Precision).

This re-assigns out of focus light to its point of origin and improves signal to noise ratio (Parton & Davis 2006).

Further image processing

Where required, images were further processed with SoftWorx (Applied Precision) including maximum intensity projection of multiple Z stacks. Images were contrasted using SoftWoRx Resolve 3D. Where contrast was adjusted, contrast settings were identical for all images being compared unless stated otherwise. Unless otherwise stated, all images of whole egg chambers are oriented with the posterior to the right, and the dorsal to the top.

Ultra thin cryo Immuno-electron microscopy (IEM, T.Weil, B.Herpers and C.Rabouille)

Cryo immuno-electron micrsocopy work was performed by T. Weil, B. Herpers and C.Rabouille at the Department of Cell Biology, UMC Utrecht, Netherlands. Samples were imaged using a Jeol EX1200 Electron Microscope (Delanoue et al. 2007, Rabouille 1999, Slot & Geuze 2007, Weil et al. 2012b). Analysis of P body boundaries was determined by C. Rabouille manually on the basis of electron density (Weil, et al. 2012b).

Chapter 3: Characterisation of mRNA dynamics in the nurse cells

Introduction

A key question in the field of mRNA localisation is how transcripts with a common origin are transported to distinct subcellular locations. In the *Drosophila* egg chamber, how *grk*, *osk*, and *bcd* are trafficked through ring canals into the oocyte at similar times, but then differentially localised, has not been resolved. The mechanism of transport and localisation of these mRNAs in the oocyte has been well studied, but little is known about mRNA transport in nurse cells. Injection of *bcd* and *grk* (Cha et al. 2001, A. Clark et al. 2007), FISH analysis of *osk* (Jambor et al. 2014) and tracking of fluorescently labelled proteins (Mische et al. 2007, Theurkauf & Hazelrigg 1998) suggests that mRNAs are transported towards ring canals by Dynein on microtubules. However, some data are not explained by this model (Chapter 1).

Correct assembly of *grk*, *osk* and *bcd* RNPs in the nurse cells is essential for their localisation and translational regulation, but endogenous mRNA dynamics or interactions with trans-acting factors in the nurse cells has not been studied. An understanding of the composition of nurse cell RNPs, and how these differ from RNPs in the oocyte, is key to elucidating how these mRNAs are localised and translationally controlled in each tissue. In this chapter, I will use the MS2 system to characterise the dynamics of mRNA in live nurse cells.

Visualising mRNA in live tissues

Visualising mRNA in live tissues is a powerful assay for studying mRNA localisation and translational control. Characterisation of mRNA speeds, directionality, and

mechanisms of transport with tracking algorithms, pharmacological reagents and mutant analysis has been key in elucidating the mechanisms of localised mRNA translation in many organisms (Buxbaum et al. 2015, Weil et al. 2010a).

Initial experiments relied on injection of *in-vitro* transcribed fluorescently labelled mRNA, used in *Xenopus* oocytes (Yisraeli & Melton 1988, Yisraeli et al. 1990), *Drosophila* embryos (Bullock & Ish-Horowicz 2001, Lall et al. 1999, Vendra et al. 2007, Wilkie & Davis 2001), and mouse oligodendrocytes (Ainger et al. 1993). This assay provides a means to quickly and easily examine how transcripts are transported and localised, including; *grk* transport on microtubules by Dyenin in the oocyte (MacDougall et al. 2003) and the nurse cells (Clark et al. 2007) and anchoring by Sqd at the DA corner (Delanoue et al. 2007); *bcd* localisation on microtubules in the nurse cells (Cha et al. 2001); and dissecting cis-acting elements responsible for mRNA localisation in the *Drosophila* embryo (Bullock & Ish-Horowicz 2001).

However, the levels of injected mRNA are not the same as the endogenous transcript, and the mRNA is not subject to normal processing in the nuclei, so in some cases RNP assembly is not correct. Although *grk* mRNA injected into the oocyte localises correctly (MacDougall et al. 2003), *bcd* must be injected into the nurse cells (Cha et al. 2001), and injected *osk* does not localise correctly as it is not exposed to the nurse cell nuclei (Glotzer et al. 1997). Furthermore, there is evidence that injected *grk* in the oocyte is not correctly translationally controlled (Weil et al. 2012b). Despite these issues, and the potential damage caused by injection, this assay has lead to major insights in mRNA localisation and translational regulation.

Molecular beacons, hairpin-loop RNA probes which fluoresce only when bound to their target sequence, can also label mRNA when injected (Bratu 2006, Tyagi & Kramer 1996). However, attempts to label *grk* with beacons have been unsuccessful (A. Clark, Thesis), and conclusions drawn from imaging of *osk* mRNA using beacons has not been widely accepted (Mhlanga et al. 2009). Recently promising dyes have been developed which bind either specific proteins like a SNAP tag (Carrocci & Hoskins 2014), or to RNA aptamers such as Spinach and RNA-Mango (Dolgosheina et al. 2014, Paige et al. 2011).

Some mRNAs can be tracked using a fluorescently tagged RBP as a proxy, for example Exu for *bcd* and Stau for *osk* (Alami et al. 2014, Köhrmann et al. 1999, Martin & St Johnston 2003, Tiruchinapalli et al. 2003, Wang & Hazelrigg 1994, Zimyanin et al. 2008). However, many RBPs associate with multiple transcripts, and not all mRNA molecules are in a complex with their trans-acting factors. In the *Drosophila* oocyte, it is unclear whether there are any RBPs which associate permanently and exclusively with a single mRNA.

The MS2 system

mRNAs can be directly labelled with the MS2 system (Figure 3-1), which comprises: 1.) expression of an mRNA with multiple MS2 bacteriophage stem loops in the 3' or 5' UTR, driven by its endogenous promoter, and 2.) expression of the MS2 Coat Protein (MCP) conjugated to a fluorescent protein (MCP-FP). When co-expressed, MCP binds essentially irreversibly to the MS2 loops (dissociation constant of 5nm, (LeCuyer et al. 1996), and decorates the mRNA with the fluorescent protein (Bertrand et al. 1998). The system can be refined by expressing the MCP-FP construct in

Figure 3-1: Labelling mRNA with the MS2 system

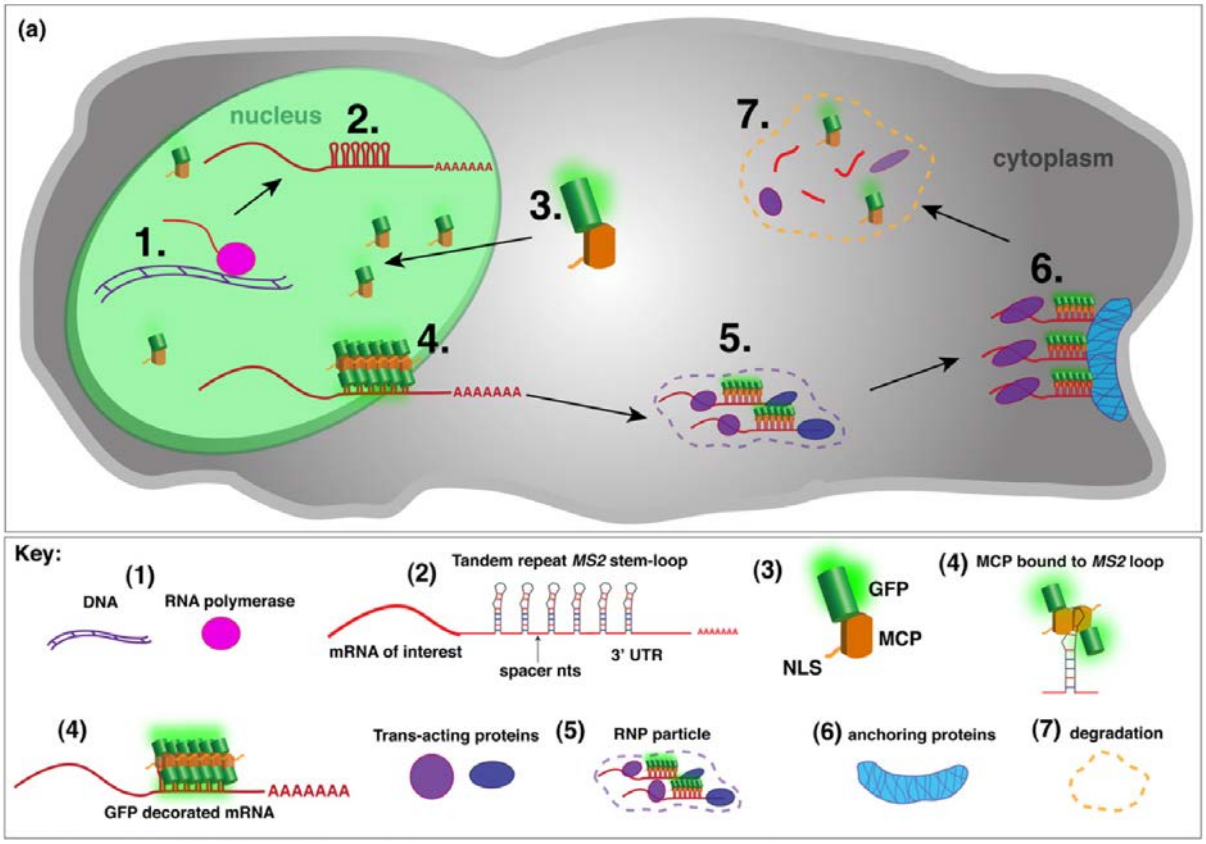

Figure 3-1: (Adapted from Weil, et al. 2010a).

A transgene encoding the gene of interest is transcribed in the nucleus (1), and the mRNA contains multiple copies of the MS2 stem loop separated by spacer regions, normally in the 3' UTR (2). The MCP protein conjugated to a fluorophore, in this case GFP, is translated in the cytoplasm and is targeted to the nucleus by an NLS (3). Here, *MCP-GFP* binds the MS2 stem loops as a dimer, and decorates the mRNA with fluorescent protein (4). This mRNA is labelled throughout its life cycle, and once exported forms an RNP with other trans-acting proteins (5), is transported to its final destination and anchored (6) and is eventually degraded (7). See key for explanation of symbols.

specific tissues, and attaching an NLS so that unbound MCP-FP is sequestered in the nucleus, reducing cytoplasmic background fluorescence.

Most MS2 labelled mRNAs, including *bcd*, *nos*, *osk* and *grk*, rescue mutants, and are localised and translated correctly, suggesting they are endogenously processed (Bertrand et al. 1998, Forrest & Gavis 2003, Jaramillo et al. 2008, Weil et al. 2006, Zimyanin et al. 2008). Moreover, this system requires no injection, allowing non-invasive imaging of transcripts expressed at near wild-type levels. It does not require fixing, so mRNA can be visualised in live tissues, and it can be combined with fluorescently labelled proteins to covisualise mRNA and trans-acting factors.

However, there is no consensus on where the MS2 loops should be placed, and MCP-FP protein often leaks out of nuclei and aggregates in the cytoplasm (Weil et al. 2010a). Recent evidence also suggests that MCP binding to MS2 loops can interfere with 5' to 3' degradation in yeast, causing an accumulation of potentially misleading fluorescently labelled mRNA 3' decay fragments (Garcia & Parker 2015). Moreover, the MS2 system requires making transgenic animals, which is time consuming, and makes labelling mRNA in mutant backgrounds laborious compared to injecting fluorescent RNA. Finally, the MS2 labelled mRNA is normally expressed as well as the endogenous gene, and interactions between the labelled and endogenous population could obscure results, such as *osk* dimerisation and hitchiking (Jambor et al. 2011). However, this can be addressed by knocking in the MS2 loops directly to the gene of interest, tagging all mRNA with the fluorophore (Lionnet et al. 2011).

These disadvantages aside, the MS2 system has been extensively used to label mRNA in yeast (Bertrand et al. 1998), *Xenopus* (Gagnon et al. 2013), mice (Park &

Singer 2014), tissue culture cell lines (Halstead et al. 2015) and plants (Hamada et al. 2003). Recently, homologous systems using hairpin-coat proteins have been developed, including PP7 and PP7 Coat Protein (PCP) labelling (Chao et al. 2008), which can be used with MS2 labelling for numerous imaging and biochemical applications (Buxbaum et al. 2015).

The MS2 system has been used to study *grk* (Jaramillo et al. 2008), *bcd* (Weil et al. 2006, Weil et al. 2008), *osk* (Zimyanin et al. 2008) and *nos* (Forrest & Gavis 2003) localisation, and the translational regulation of *grk* and *bcd* (Weil, Parton, Herpers, et al. 2012b). However, it has not been used to visualise mRNA in the nurse cells, and the composition of *grk*, *osk* and *bcd* RNPs in the nurse cells, how these change in the oocyte, and which factors are required for correct localisation and translational regulation in each tissue, is unclear.

Aims of this chapter and experimental rationale

In this chapter I test whether the MS2 system can be used to visualise localised mRNAs in the nurse cells. Specific questions include:

- **Can MS2-labelled *grk* and *osk* mRNA be visualised in the nurse cells?**
- **Do *grk* and *osk* move at similar speeds in the nurse cells and the oocyte?**
- **Can recent advances of the MS2 system be applied to increase detection of *grk* in the nurse cells?**

To answer these questions, I worked with microscopists and image analysts in the Davis lab and Micron Oxford to optimise imaging protocols on both conventional widefield and the OMX microscopes to deal with the following issues:

First, *grk* particles in the nurse cells are likely to be small, faint, and at a lower density than in the oocyte. Visualising small, dynamic MS2 labelled mRNA particles has been difficult using confocal microscopes which lack the speed to track dynamic particles, (Parton et al. 2010, Weil et al. 2010a). I used the widefield DeltaVision CORE microscope with CCD detectors (Parton et al. 2010), which have been used to visualise mRNA in the oocyte (Weil et al. 2012, Zimyanin et al. 2008), and allows post deconvolution processing, (Parton & Davis 2006). I imaged at high exposures (300ms) at 3 fps to try and visualise faint and fast moving particles.

Second, most *grk* has been trafficked out of the nurse cells by stage 9. I imaged stage 6-8 egg chambers, where more *grk* is likely to be in the nurse cells. I imaged the nurse cells nearest to the oocyte, as mRNA from all nurse cells must enter the oocyte through ring canals here, so there is likely to be a higher density of mRNA near the ring canals before they diffuse through them (Clark et al. 2007).

Third, fluorescence from the follicle cells obscures particles in the nurse cells. To minimise MCP-FP expression in follicle cells, I drove expression of *MCP-GFP* (Green fluorescent protein) and *MCP-mCherry* (monomeric Cherry) with a germline specific promoter, *Pnos*. I also imaged at a shallow focal plane just beneath the follicle cells to minimise light scattering through the tissue. Finally, cytoplasmic MCP-FP assemblies hinder mRNA visualisation (Weil et al. 2010a). I imaged flies expressing two copies of the *grk-MS2-12* construct recombined on the same chromosome, and one copy of the MCP-FP. This should ensure that the majority of the MCP-FP is bound by *grk-MS2*, and minimise free MCP-FP.

Results

Localised mRNAs can be visualised in the nurse cells with the MS2 system

The MS2 system has been used to study *grk* regulation in the oocyte (Jaramillo et al. 2008, Weil et al. 2012b), but not to visualise *grk* mRNA in live nurse cells. To test whether *grk* mRNA can be visualised in the nurse cells with the MS2 system, I imaged egg chambers expressing *grk-MS2-12* and *Pnos-MCP-GFP* (*grk*GFP*). *grk* particles are visible at the oocyte DA corner as previously reported (Jaramillo et al. 2008). I also observe small (200-500nm), bright (>1.5x cytoplasmic background) spherical puncta in the nurse cell cytoplasm (Figure 3-2 (A), supplementary movie 3-1) of all egg chambers imaged (n=89, Table 3-1). Most of these particles are half as bright as those in the oocyte (Figure 3-3, supplementary movie 3-2), but otherwise share similar characteristics.

To test whether these particles are *grk* RNPs rather than MCP-FP assemblies, I imaged egg chambers expressing two copies of *Pnos-MCP-GFP* without *grk-MS2*. No particles are visible in the oocyte, and the GFP fluorescence in nurse cell nuclei is higher than in *grk*GFP* egg chambers, most likely because less MCP-GFP is drawn out of the nucleus by *grk-MS2*. No bright puncta are visible in any egg chambers (n=110). In 62% of egg chambers, large (>500nm) assemblies are visible, which have an irregular shape, are not significantly brighter than the cytoplasmic background, and move with the bulk cytoplasmic flow (Figure 3-2 (B, C) supplementary movie 3-3). I conclude that these assemblies are MCP-GFP. In egg chambers expressing only one copy of *Pnos-MCP-GFP* (n=145), fewer egg chambers (44%) contained large assemblies. With one and two copies of *Pnos-MCP-GFP*, a large number of egg chambers (38% and 55%) do not contain any particles.

Figure 3-2: *grk* mRNA particles are visible in the nurse cell cytoplasm of *grk*GFP, but not* MCP-GFP *egg chambers*

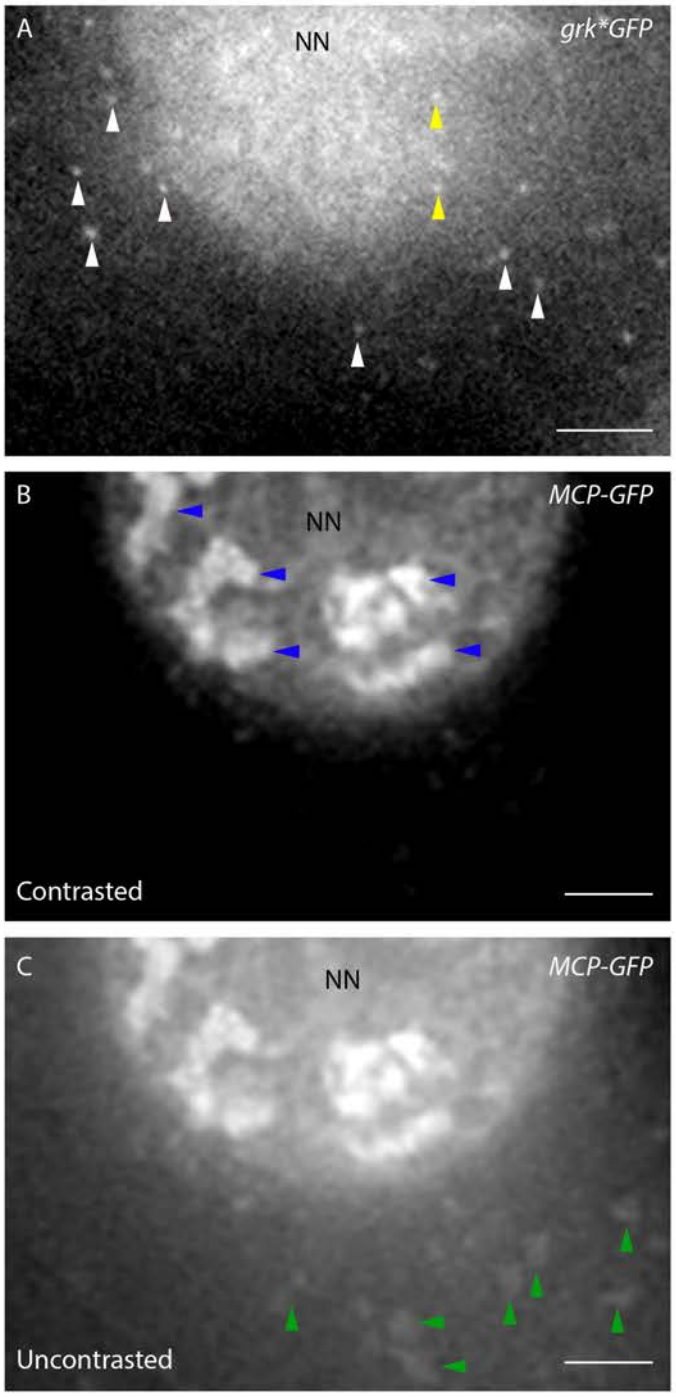

Figure 3-2:

(A): In all *grk*GFP* egg chambers (n=89), small, bright, spherical puncta are visible in the nurse cell cytoplasm (white arrowheads). Some are visible in the nurse cell nuclei (yellow arrowheads), but are harder to distinguish from nuclear fluorescent

(Figure 3-2 continued):

background. (B-C): In egg chambers expressing only two copies of *MCP-GFP*, these puncta are never visible (n=110). Regions of the nurse cell nuclei are much brighter in these egg chambers (blue arrowheads). Images in (A) and (B) are equally contrasted. Image (C) is the same egg chamber as (B) but contrasted to show large, fluorescent assemblies in the nurse cell cytoplasm (green arrowheads) which are present in 62% of egg chambers. All images collected at 100x magnification and deconvolved. NN, nurse cell nuclei. Scale bars 5 μm.

Figure 3-3: *grk* mRNA particles are brighter and at a higher density in the oocyte than in the nurse cells

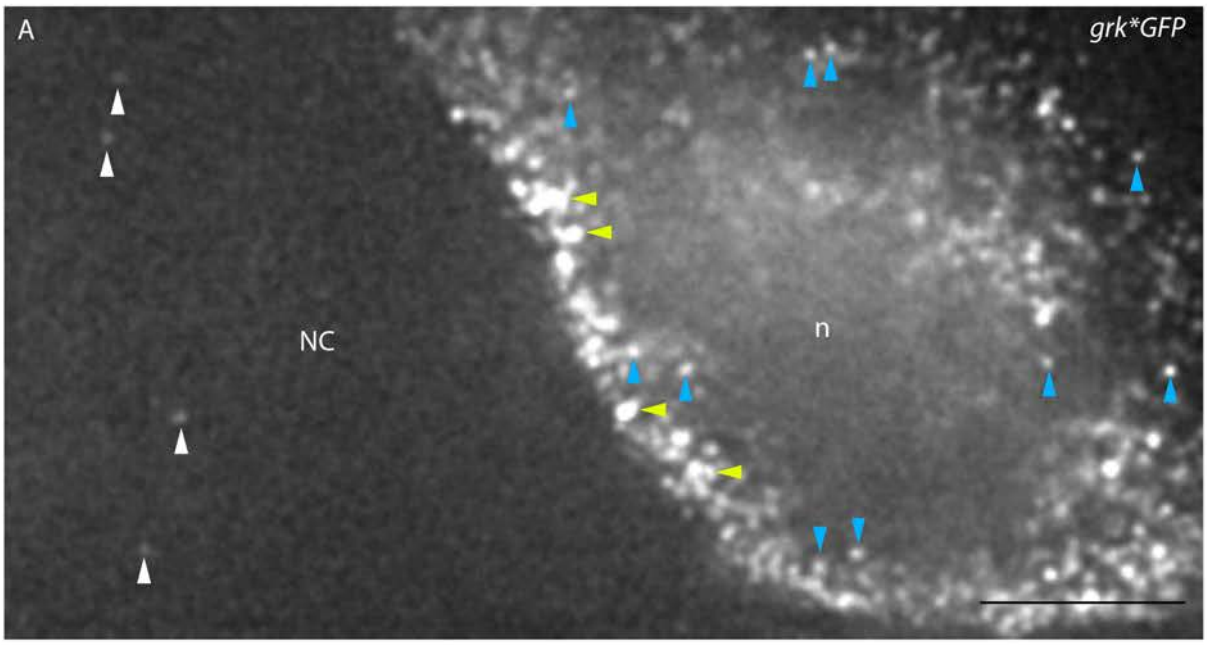

Figure 3-3:

(A): In *grk*GFP* egg chambers, individual RNA particles in the oocyte (blue arrowheads) are significantly (50-100%) brighter than individual particles in the nurse cells (white arrowheads). The density of particles is also much higher in the oocyte, and some particles cluster together (yellow arrowheads). Image is deconvolved and is a 1 μm maximum intensity projection. NN, nurse cell nuclei; n, oocyte nucleus. Scale bar 5 μm.

Proteins are often tagged with GFP or YFP, so covisualisation of mRNA and proteins requires mRNA labelled with a red fluorophore. mCherry (Shaner et al. 2004) has been used to label *grk* in the oocyte (Hayashi et al. 2014, Weil et al. 2012b), but is less bright than GFP, and readily forms aggregates (R. Parton and T. Weil, personal communication). To test whether *grk* can be visualised with mCherry in the nurse cells, I imaged egg chambers expressing *grk-MS2-12* and *Pnos-MCP-mCherry* (*grk*mCherry*). Similar puncta are visible in the nurse cell cytoplasm (Figure 3-4 (A), supplementary movie 3-4), in the majority (98%) of egg chambers (n=42, Table 3-1). However, they are less bright and bleach faster than *grk*GFP* particles, and fewer can be seen in each egg chamber (57% contain >10 visible particles, compared to 89% of *grk*GFP* egg chambers).

To test whether these particles are *grk* RNPs, not MCP-mCherry assemblies, I imaged egg chambers expressing *Pnos-MCP-mCherry* without *grk-MS2-12*. In 85% of these egg chambers (n=114) assemblies are visible in the nurse cell cytoplasm (Figure 3-4 (B, C), supplementary movie 3-5). In rare cases (11% of egg chambers), small, fast moving puncta are visible which are comparable to those seen in *grk*mCherry* egg chambers. Normally only one of these particles is seen per egg chamber. There are more large assemblies visible in the nurse cells of egg chambers expressing *Pnos-MCP-mCherry* than *Pnos-MCP-GFP*, and in *grk*mCherry* egg chambers, large assemblies are often seen in addition to small puncta. Similar aggregation issues have been reported with RFP (Brechbiel & Gavis 2008).

osk mRNA is translationally regulated in the nurse cells by being packaged into translationally silent multimers (Chekulaeva et al. 2006), and is thought to be trafficked into the oocyte on microtubules by Dynein (Jambor et al. 2014).

Figure 3-4: *grk* mRNA particles are visible in the nurse cell cytoplasm of *grk*mCherry*, but not *MCP-mCherry* egg chambers

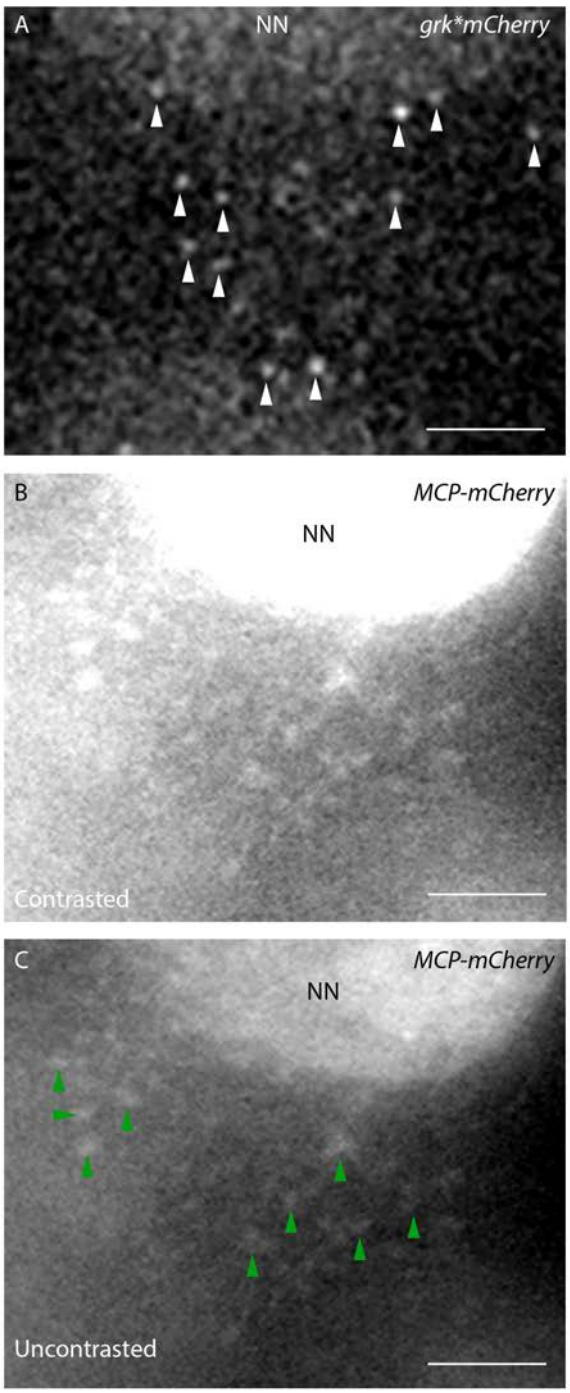

Figure 3-4:

(A): In 98% of *grk*mCherry* egg chambers (n=42), small, bright, spherical puncta are visible in the nurse cell cytoplasm (white arrowheads). (B-C): In 89% of egg chambers expressing only *MCP-mCherry*, these puncta are not visible (n=114). The nurse cell nuclei are significantly brighter in these egg chambers.

(Figure 3-4 continued:)

Images in (A) and (B) are equally contrasted. Image (C) is the same egg chamber as (B) but contrasted to show large, fluorescent assemblies in the nurse cell cytoplasm (green arrowheads) which are present in 85% of egg chambers. All images collected at 100x magnification and deconvolved. NN, nurse cell nuclei. Scale bars 5 μm.

However, *osk* dynamics have not been characterised in the nurse cells using the MS2 system. To test whether this imaging protocol can also be used to visualise *osk* mRNA, I imaged egg chambers co-expressing *osk-MS2-10* and *Pnos-MCP-GFP* (*osk*GFP*). In all egg chambers (n=86, table 3-1), small bright particles are visible in the nurse cell cytoplasm (Figure 3-5 (A), supplementary movie 3-6), which are not seen in *Pnos-MCP-GFP* egg chambers (Figure 3-5 (B), supplementary movie 3-3).

To test whether *osk* can be visualised with mCherry, to allow for covisualisation with GFP tagged proteins, I imaged egg chambers expressing *osk-MS2-10* and *Pnos-MCP-mCherry* (*osk*mCherry*). Puncta are visible in the nurse cell cytoplasm of 98% of egg chambers (n=55), and although these are less bright than GFP labelled *osk*, they are easily distinguishable from assemblies of MCP-mCherry (Figure 3-6, supplementary movie 3-7). *osk* particles are less bright than *grk* particles labelled with GFP and mCherry. *osk* particles are a similar size to *grk* particles (300-500nm), which is unexpected, as data from molecular beacons indicate that *osk* is present in large multimers in the nurse cells (Mhlanga et al. 2009).

Conclusion: *grk* and *osk* RNPs can be visualised in the nurse cell cytoplasm with both GFP and mCherry fluorophores. MCP-FP leaks out of the nurse cell nuclei and form fluorescent cytoplasmic assemblies, but these are easily distinguishable from mRNA particles. MCP-mCherry forms more assemblies than MCP-GFP. Individual *grk* particles in the oocyte are brighter than those in the nurse cells, suggesting there may be more mRNA molecules in *grk* RNPs in the oocyte.

Figure 3-5: *osk* mRNA particles are visible in the nurse cell cytoplasm of *osk*GFP*, but not *MCP-GFP* egg chambers

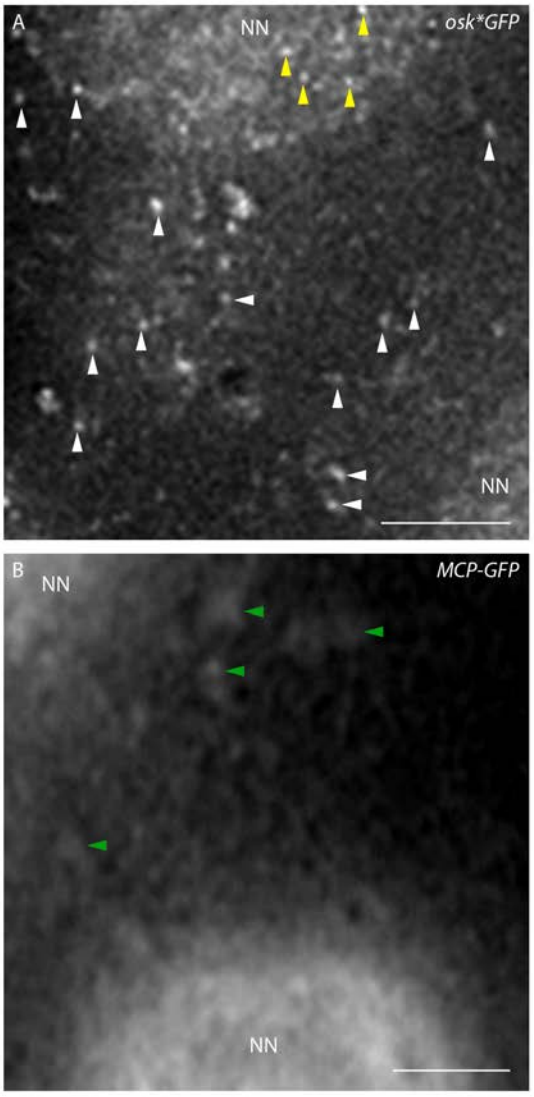

Figure 3-5:

(A): In all *osk*GFP* egg chambers (n=86), small, bright, spherical puncta are visible in the nurse cell cytoplasm (white arrowheads). Some are visible in the nurse cell nuclei (yellow arrowheads), but are harder to distinguish from nuclear fluorescent background. (B): In egg chambers expressing only two copies of *MCP-GFP*, these puncta are not seen (n=110), and 62% of egg chambers contain large, fluorescent assemblies in the nurse cell cytoplasm (green arrowheads). All images collected at 100x magnification and deconvolved. NN, nurse cell nuclei. Scale bars 5 μm.

Figure 3-6: *osk* mRNA particles are visible in the nurse cell cytoplasm of *osk*mCherry*, but not *MCP-mCherry* egg chambers

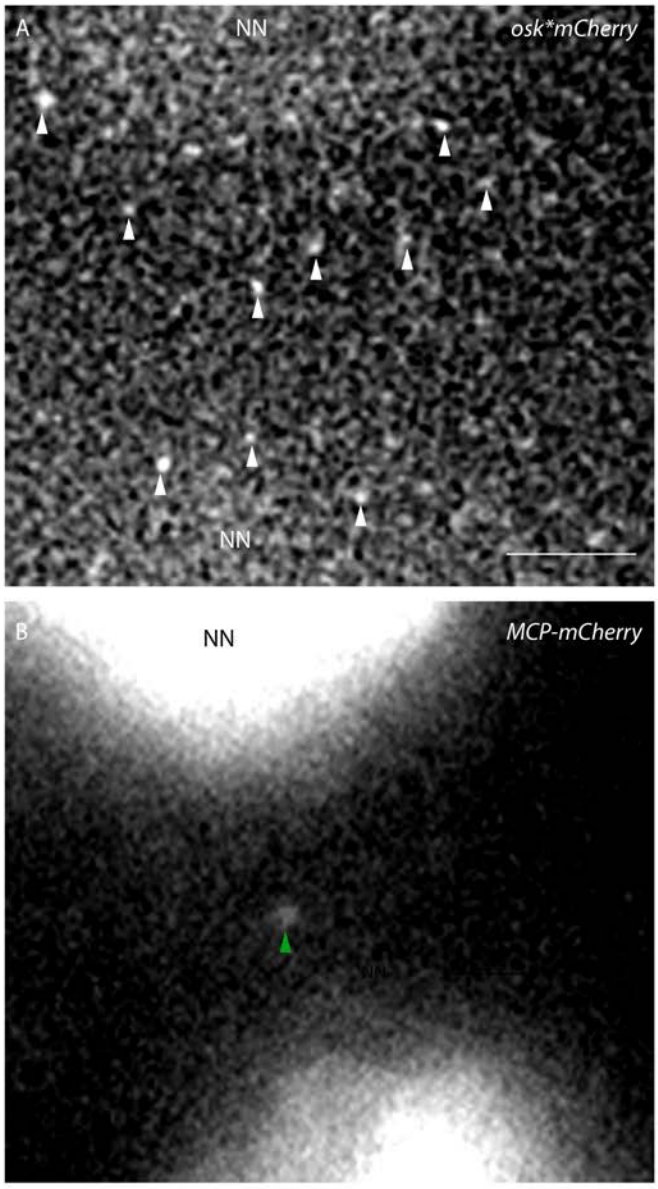

Figure 3-6:

(A): In 98% of *osk*mCherry* egg chambers (n=55), small, bright, spherical puncta are visible in the nurse cell cytoplasm (white arrowheads). (B): In 89% of egg chambers expressing only *MCP-mCherry*, these puncta are not visible (n=114). The nurse cell nuclei are significantly brighter in these egg chambers, and large, fluorescent assemblies (green arrowheads) are present in the nurse cell cytoplasm in 85% of egg chambers. All images collected at 100x magnification and deconvolved. NN, nurse cell nuclei. Scale bars 5 μm (A), 10 μm (B).

Dynamics of *grk* and *osk* in the nurse cells

The dynamics of *grk* and *osk* have been characterised in the oocyte using the MS2 system (Weil et al. 2012b, Zimyanin et al. 2008), and these mRNAs are actively transported on microtubules by Dynein and Kinesin respectively. To examine whether these mRNAs are transported in a similar manner in the nurse cells, I analysed time-lapse movies of *grk*GFP* and *osk*GFP*, where particles are easier to visualise than in *grk*mCherry* or *osk*mCherry* egg chambers. I separated particles into three classes, “actively transported”, “paused” and “static” (Appendix F, Figure 3-7, supplementary movies 3-1 and 3-6). Interestingly, few particles of *grk* (29%) and *osk* (24%) are actively transported (Table 3-2), and more particles are paused (50% and 40% respectively) than are static or actively transported. A larger proportion of *osk* particles (36%) are static compared to *grk* (21%).

To test whether *grk* and *osk* in the nurse cells move at speeds indicative of active transport like in the oocyte (Weil et al. 2012b, Zimyanin et al. 2008), I tracked motile particles in *grk*GFP* and *osk*GFP* egg chambers (see Appendix F). Both paused and actively transported *grk* (0.931 μm/s average) and *osk* particles (0.92 μm/s average) move significantly faster in the nurse cells than in the oocyte (0.49 μm/s and 0.47 μm/s respectively), and move at speeds indicative of active transport (Table 3-3). *grk* and *osk* particles in the nurse cells move at similar velocities, and the velocity of all *grk* particles tracked in the nurse cells is similar to that of *in-vitro* transcribed *grk* injected into the nurse cells (Clark et al. 2007). No run length data are available for *grk* in the oocyte, but actively transported *osk* particles undergo runs of similar length to those in the oocyte. There is no statistically significant difference between the run lengths of actively transported *grk* and *osk*, or paused *grk* and *osk* particles.

Figure 3-7: Dynamics of *grk* and *osk* in the nurse cells

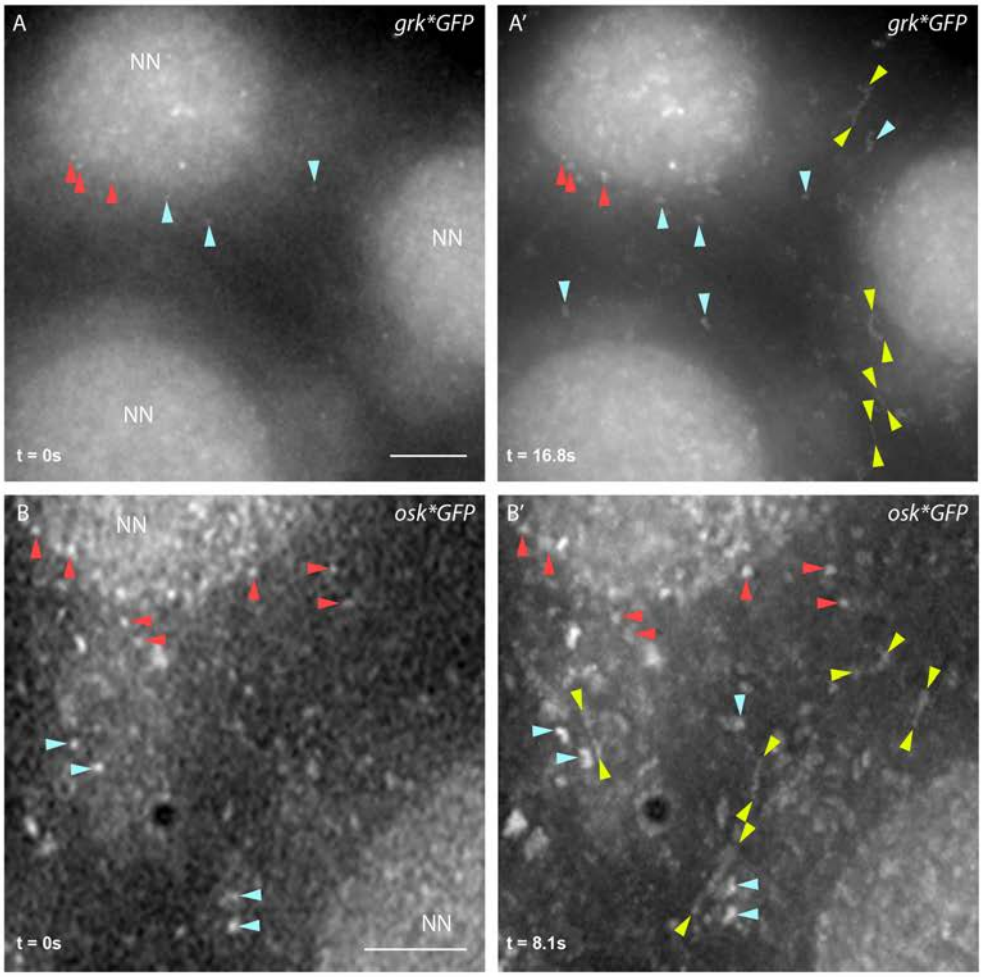

Figure 3-7:

(A-B'): Live cell imaging of *grk*GFP* and *osk*GFP* egg chambers. (A): *grk*GFP* egg chamber at t = 0s (A) and t = 16.8s (A') with trail image of 50 frames superimposed (movie collected at 3fps). (B): *osk*GFP* egg chamber at t = 0s (B) and t = 8.1s (B') with trail image of 24 frames superimposed (movie collected at 3fps). Moving particles appear as a set of dots. Yellow arrowheads indicate RNA particles undergoing long runs and mark the first and last visible point in the time sequence. Blue arrowheads indicate paused particles which move in a restricted fashion, and red arrowheads indicate static particles. Image series collected at 100x magnification and deconvolved. NN, nurse cells nuclei. Scale bars 5 μm.

In the oocyte, *osk* moves on a biased network of microtubules, which requires computational analysis to be detected (Parton et al. 2011, Zimyanin et al. 2008). Conversely, *grk* particles injected into the nurse cells near the ring canals move in directed paths towards ring canals (Clark et al. 2007). However, my data do not show an obvious directionality of either *grk* or *osk* particles towards the ring canals.

Conclusion: All classes of *grk* and *osk* move significantly faster in the nurse cells than in the oocyte, but *grk* and *osk* have similar dynamics in the nurse cells. There is no obvious bias in particle transport towards the ring canals.

grk particles can be visualised using the OMX

Accurate tracking of small, faint, motile particles requires high temporal resolution, and is enhanced by imaging over multiple Z planes. This captures particles changing focal planes, and allows for higher quality deconvolution. However, imaging using the DeltaVision microscope at high exposures is limited to 3fps in one Z plane. To try and improve the quality of the data and more accurately track *grk* and *osk* particles, potentially allowing automated tracking, I imaged *grk*GFP* egg chambers on the OMX V3, a microscope designed to be able to perform both 3D-SIM and fast multi-colour widefield imaging. This microscope is designed to image significantly faster with lower exposures than the DeltaVision CORE system, and also has a “Z sweep” function (established by Micron Oxford and Applied Precision), which allows a series of rapid acquisitions whilst the stage moves continuously in Z.

Using this imaging protocol, particles are visible in the nurse cell cytoplasm with a much greater signal to noise ratio than on the DeltaVision, and these particles can be visualised undergoing long runs (Figure 3-8, supplementary movie 3-8). However, the

GFP fluorescence bleaches very quickly, meaning a maximum of 50 frames of usable data can be acquired from each egg chamber. The OMX can also image in red and green channels simultaneously, which allows greater accuracy tracking of motile particles in both channels compared to the DeltaVision. To test whether the OMX could be used to visualised *grk* labelled with a red fluorophore, with the aim of covisualising *grk* and trans-acting factors labelled with GFP or YFP, I imaged *grk*mCherry* egg chambers on the OMX. Using a number of imaging protocols, *grk*mCherry* particles consistently bleach within 30 frames (Figure 3-9, supplementary movie 3-9).

Conclusion: The OMX can be used to visualise *grk*GFP* and *grk*mCherry* particles with significantly higher contrast and temporal resolution than on DeltaVision systems, but fluorescent RNPs are bleached rapidly by this imaging protocol.

Attempts to improve imaging of *grk*GFP* with new constructs

Insights from imaging mRNA in live nurse cells, including analysing particle directionality and covisualising mRNA and fluorescently tagged trans-acting factors, would benefit from brighter and more photostable *grk* particles. A construct containing 24 MS2 loops (instead of the 12 used so far) has been used in mice, and these loops are also predicted to be bound by MCP with higher occupancy (Lionnet et al. 2011). To test whether imaging of *grk* could be improved by using this construct, I generated transgenic flies expressing *grk-MS2-24* (in collaboration with T. Weil, constructs generated by B. Steinkraus, Chapter 2). In egg chambers expressing both *grk-MS2-24* and *Pnos-MCP-GFP* (*grk*GFP-24*), puncta are visible in the nurse cell nuclei with the same characteristics of those in *grk*GFP* egg chambers, but some of which are up twice as bright (Figure 3-10 (A-D), supplementary movie 3-10).

Figure 3-8: *grk* dynamics in the nurse cells visualised on the OMX

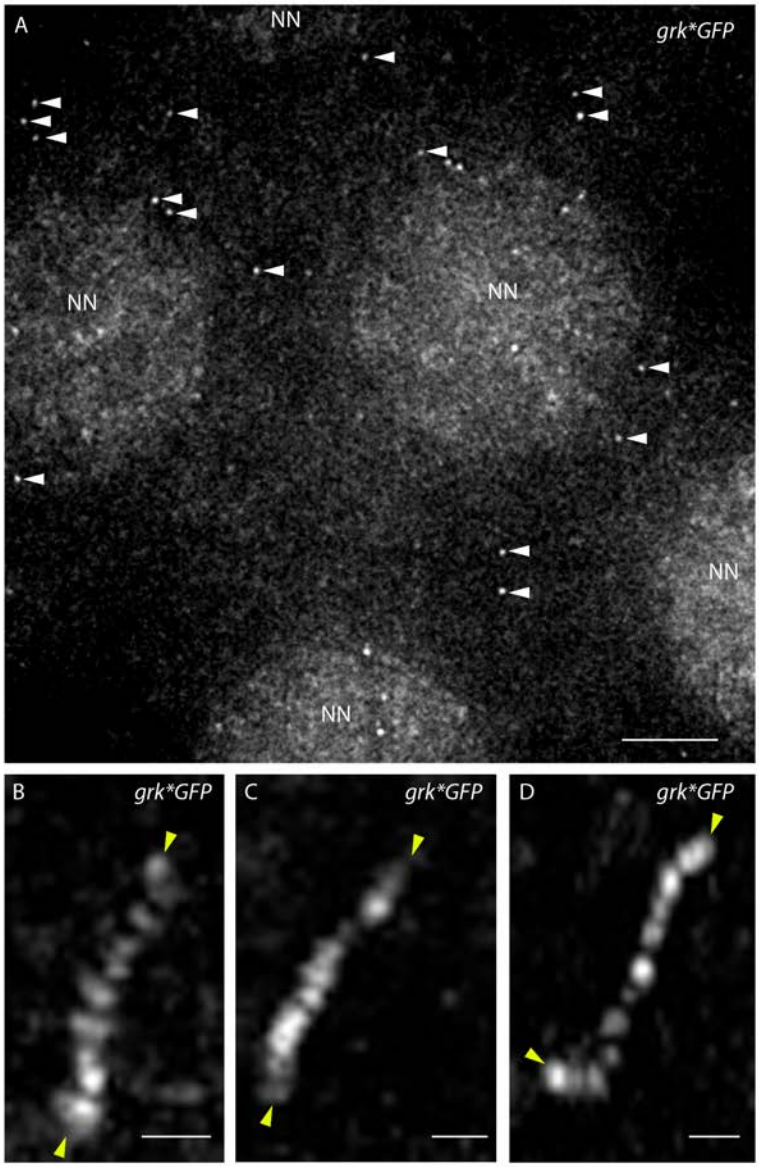

Figure 3-8:

(A-D): *grk*GFP* particles imaged on the OMX V3. (A) Particles are visible in the nurse cell cytoplasm (white arrowheads) with a high signal-to-noise ratio. (B-D) individual particles can be visualised undergoing long directed runs. Trail images of (B): 15 frames superimposed from t=0s to t=1s, (C): 20 frames superimposed from t=0s to t=1.4s, (D): 15 frames superimposed from t=0s to t=1s . Yellow arrowheads mark the first and last visible points in the time sequence. All Image series collected at 60x magnification, deconvolved, and are 1 μm maximum intensity projections. Images collected at 15fps. NN, nurse cells nuclei. Scale bar 5 μm (A), 500 nm (B-D).

Figure 3-9: *grk*mCherry* fluorescence bleaches quickly on the OMX

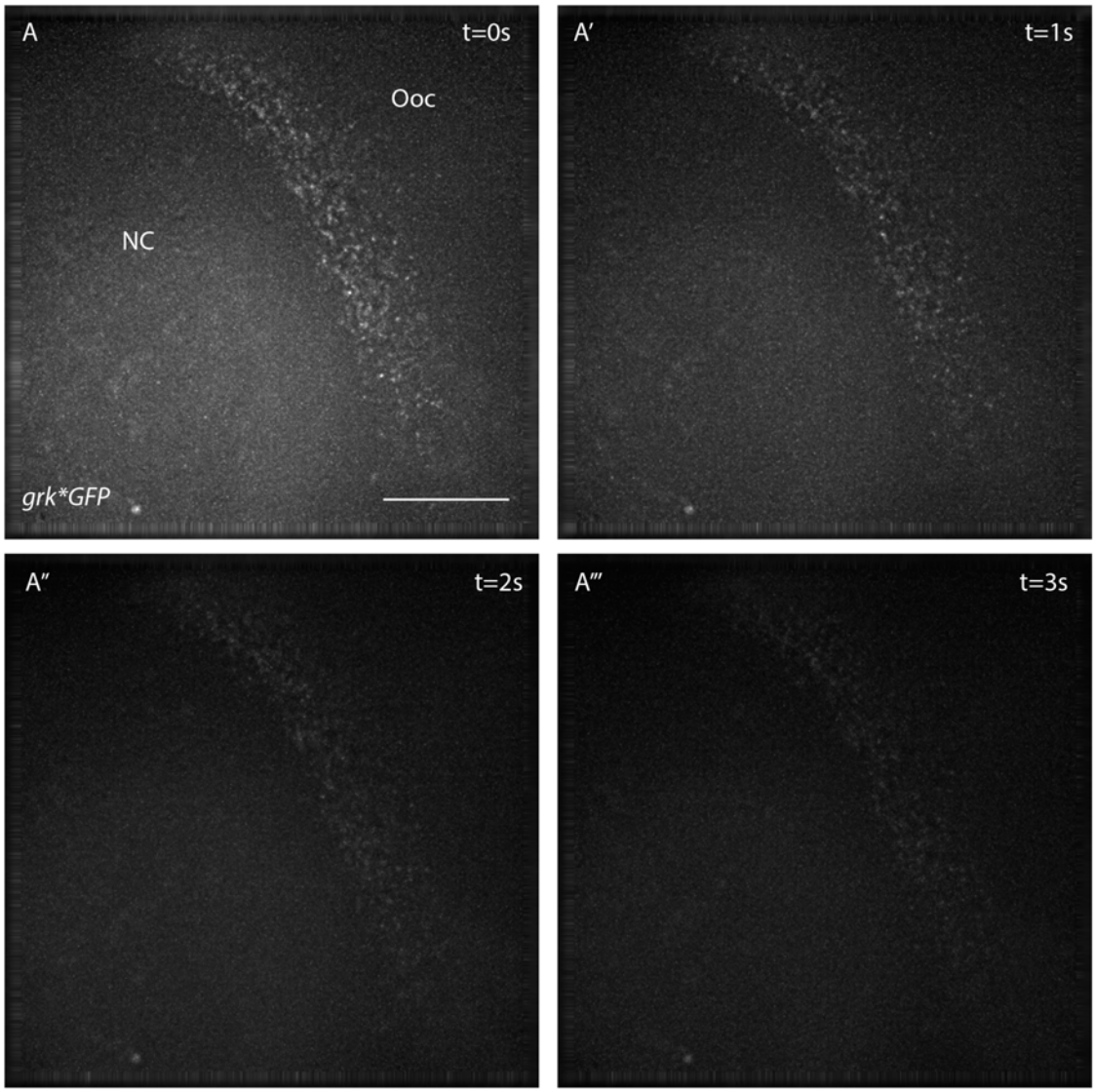

Figure 3-9:

(A-A‴) *grk*mCherry* egg chamber imaged on the OMX V3. mCherry fluorescence bleaches and particles are no longer visible within 3 seconds. All images collected at 60x magnification, deconvolved, and are 1 μm maximum intensity projections. Images collected at 5fps. NN, nurse cells nuclei. Scale bars 10 μm.

The density of these particles in the nurse cell nuclei is also significantly higher than in *grk*GFP* egg chambers (0.16 particles/μm ^{2} compared to 0.03 particles/μm ^{2}, n=30 nuclei for each condition and n=779 and 119 particles respectively, P = 0.0001 compared by a two-tailed t test, Figure 3-10 (C, D), supplementary movie 3-11). In *grk*GFP-24* egg chambers, some particles are localised to the DA corner of the oocyte, but far fewer than in *grk*GFP* egg chambers (Figure 3-10 (E, F), supplementary movies 3-12 and 3-13). These data suggest that although *grk* particles can localise, most are trapped in the nurse cell nuclei and are not exported.

Dimerisation of MCP is necessary for MS2 loop binding (Chao et al. 2008), and pre-dimerised tandem dimer MCP (tdMCP) offers significant advantages in brightness and stability in mammalian tissue culture cells (Wu et al. 2012). To test whether this MCP could be used to improve imaging in the egg chamber, I imaged flies co-expressing *grk-MS2-12* with *Pnos-tdMCP-GFP* (*grk*tdGFP*). Particles of *grk* are not visible in the nurse cells, and particles in the oocyte are less bright than comparable particles in *grk*GFP* (Figure 3-11 (A, A'), supplementary movie 3-14). Moreover, in egg chambers expressing *Pnos-tdMCP-GFP* alone, there is an increase in the number of MCP assemblies (Figure 3-11 (B, B'), supplementary movie 3-15).

Conclusion: *grk*GFP-24* particles are brighter than those in *grk*GFP*, but the majority are not exported from the nurse cell nuclei and potentially cannot be used to study *grk* localisation. Although they have tremendous potential, tdMCP proteins do not improve imaging of *grk* particles in the nurse cells or the oocyte. Without further assessment and improvement, neither construct was used further in this Thesis.

Figure 3-10: The majority of *grk*GFP-24* particles are retained in the nurse cell nuclei

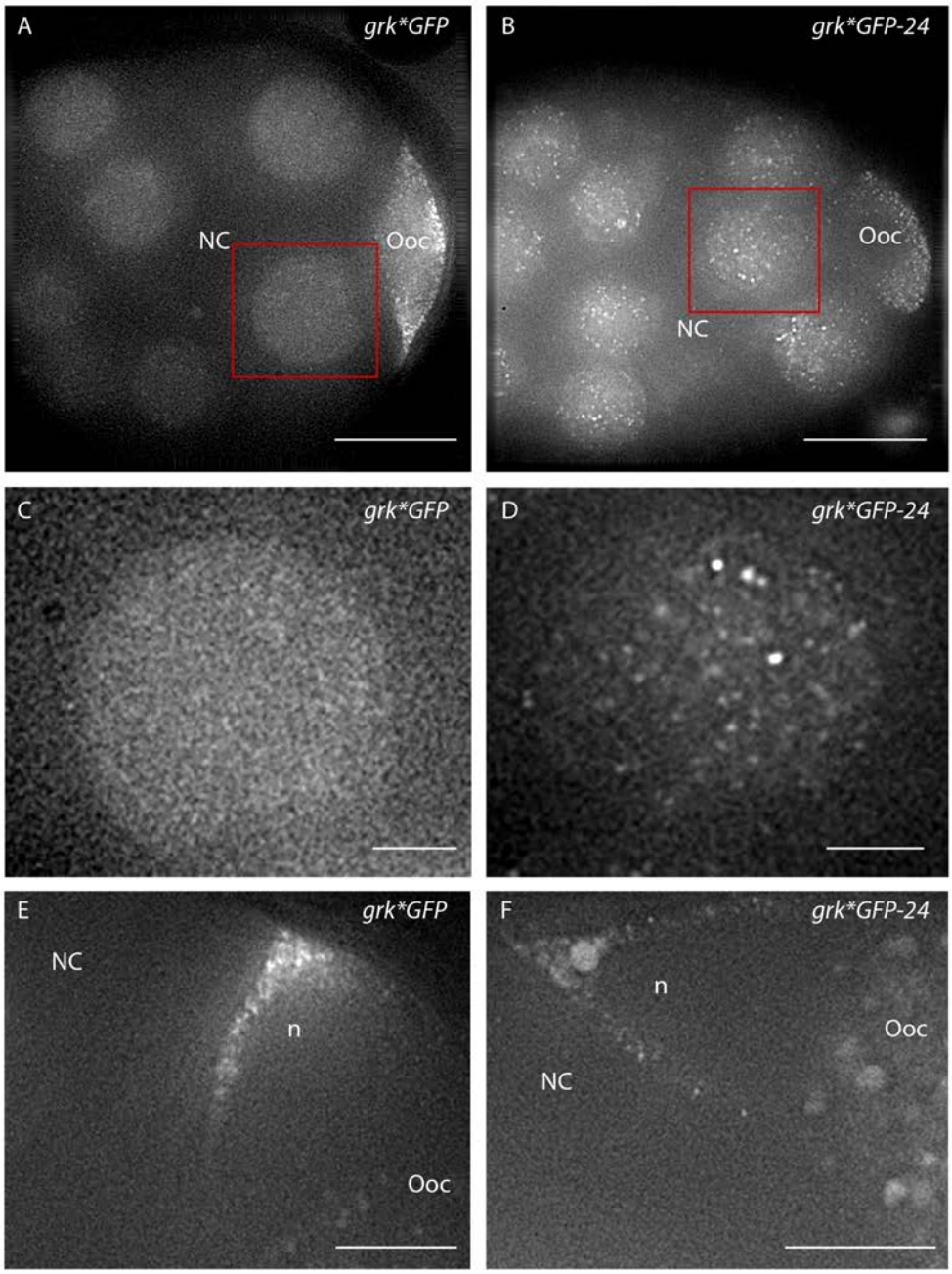

Figure 3-10:

(A-F): Still from time lapse imaging of live *grk*GFP* or *grk*GFP-24* egg chambers, constructs for the latter generated by B. Steinkraus. (A) In *grk*GFP* egg chambers, particles are difficult to visualise in the nurse cell nuclei. (B) However, in *grk*GFP-24* egg chambers they are readily visible. (C-D) are close-ups of boxed regions in A and B respectively. (D) Many more particles of *grk* are visible in *grk*GFP-24* nuclei than *grk*GFP* nuclei (C). (E) In *grk*GFP* egg chambers particles localise to the DA corner

(Figure 3-10 continued)

of the oocyte, whereas far fewer do so in *grk*GFP-24* egg chambers (F). All images acquired on 100x magnification, and deconvolved. NC, nurse cells; NN, nurse cells nuclei; Ooc, oocyte; n, oocyte nucleus. Scale bars 20 μm (A,B) 5 μm (C,D) 10 μm (E,F).

Figure 3-11: *td-MCP-GFP* does not improve imaging of MS2 tagged *grk* mRNA

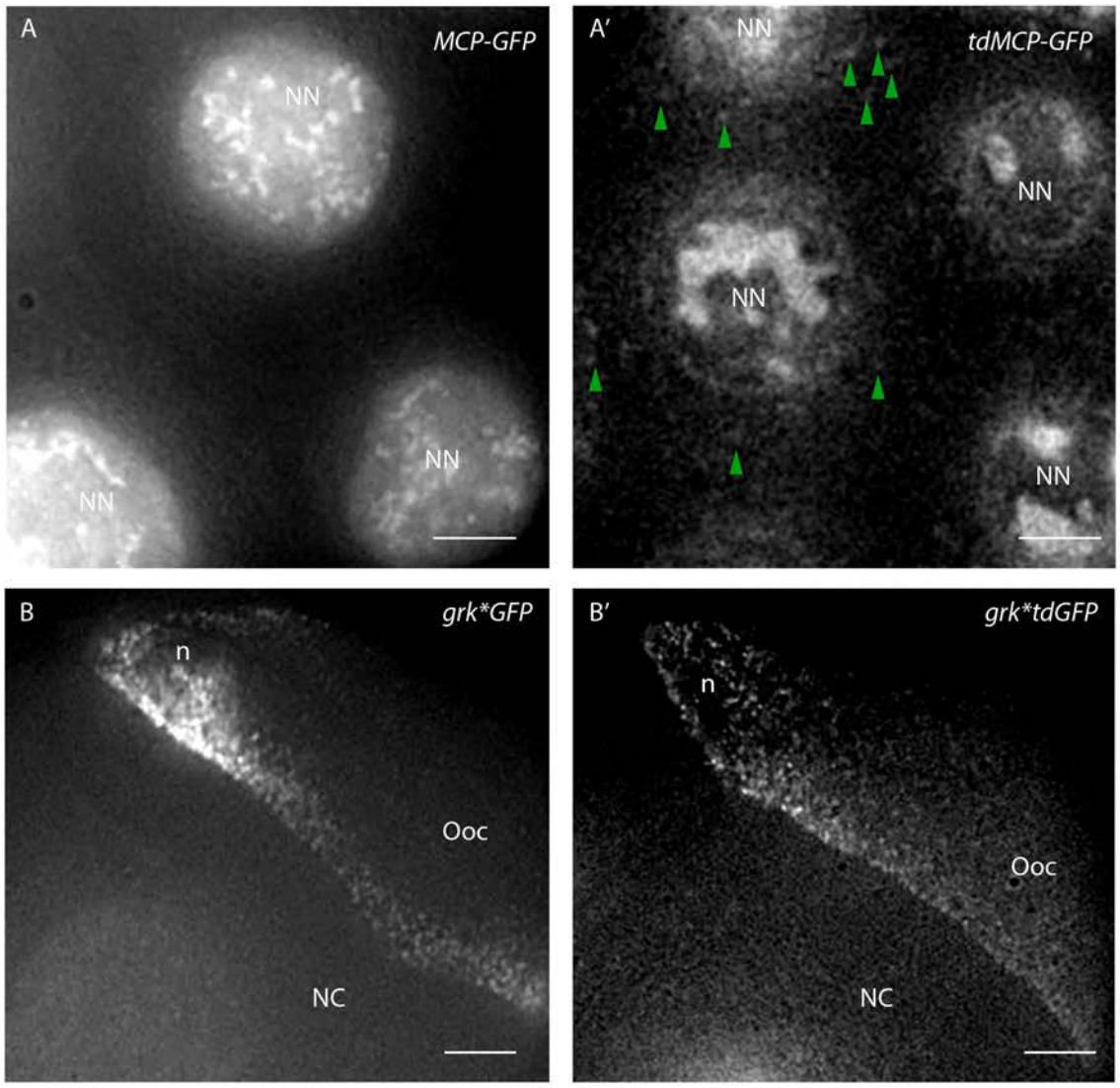

Figure 3-11:

(A') In *tdMCP-GFP* egg chambers, the nurse cell nuclei are less bright than those in *MCP-GFP* egg chambers (A), and more assemblies are present in the nurse cell cytoplasm (green arrowheads). (B') Puncta are not visible in the nurse cell cytoplasm of *grk*tdGFP* egg chambers, and particles in the oocyte are less bright than in *grk*GFP* egg chambers (B). All images acquired on 100x magnification, and deconvolved. NC, nurse cells; NN, nurse cell nuclei; Ooc, oocyte; n, oocyte nucleus. Scale bars 5 μm.

Discussion

Here, for the first time, I have used the MS2 system to visualise *grk* and *osk* RNPs in the nurse cells. I have characterised the dynamics of these mRNAs in the nurse cells, and have shown they move significantly faster than in the oocyte. Although flies expressing *bcd-MS2* and *Pnos-MCP-GFP* were not available, the imaging protocol I have developed can now be used to further investigate how localised mRNAs are transported in the nurse cells, whether mRNAs associate with their trans-acting factors in the nurse cells, and how RNPs are remodelled as mRNAs move from the nurse cells into the oocyte.

grk and *osk* particles in the nurse cells are different to those in the oocyte

I have detected a population of small, bright puncta in the nurse cells of *grk*GFP*, *grk*mCherry*, *osk*GFP* and *osk*mCherry* egg chambers (Figures 3-2 to 3-6), which are less bright than those seen in the oocyte but are similar in terms of size, shape and speed. These particles are not visible in egg chambers expressing *MCP-GFP* or *MCP-mCherry* alone. Although *grk-MS2* is expressed in addition to the endogenous gene, the fact that the MS2 system has been used for over 15 years to label mRNA, and this *grk-MS2-12* transgene has been used to study *grk* localisation and translational control in the oocyte (Jaramillo et al. 2008, Weil et al. 2012b) leads me to conclude that these particles behave in a comparable manner to endogeous *grk*, and can be used to study *grk* transport and translational regulation in the nurse cells.

Single mRNA particles detected by sm-FISH are smaller than the resolution of conventional light microscopy (<200nm), and it seems unlikely that the particles I observe here are single molecules of *grk* or *osk*. More likely, these are RNPs of several mRNA particles and trans-acting proteins. Interestingly, individual particles of

grk in the nurse cells are less bright than those in the oocyte (Figure 3-3). As the number of GFP molecules decorating a single MS2-labelled mRNA should remain constant throughout the life of the mRNA, this suggests that *grk* particles may be assembled in higher order complexes in the oocyte.

osk particles are a similar size to *grk* particles in the nurse cells, and do not appear in much larger silencing particles as previously hypothesised (Chekulaeva et al. 2006, Mhlanga et al. 2009). Either *osk* is not packaged into higher order complexes in the nurse cells, or MS2-labelled mRNA is specifically excluded from these complexes. However, *osk-MS2* is not ectopically translated in the nurse cells of *osk*GFP* or *osk*mCherry* egg chambers, suggesting *osk-MS2* is correctly translationally regulated. This agrees with recent sm-FISH data indicating that *osk* is packaged into multimers only as it enters the oocyte (Little et al. 2015), and suggests that perhaps packaging into large silencing complexes is not the key mechanism of *osk* translational repression in the nurse cells. For *grk* and *osk*, the number of mRNAs per particle could be investigated using step-photobleaching to estimate the number of GFP molecules in each RNP (Cherny et al. 2010), to determine if there is a difference between *grk* and *osk* packaging in the nurse cells, and between *grk* packaging in the nurse cells and the oocyte. This could also be examined using sm-FISH techniques with complementary RT-qPCR as previously described (Little et al. 2015), which will be explored in Chapter 4.

Both *grk* and *osk* move significantly faster in the nurse cells than in the oocyte. A small proportion (29% and 24%) of particles undergo directed runs and move at speeds indicative of active transport (Figure 3-7, Tables 3-2, 3-3). These particles move at similar speeds to each other, suggesting they are transported by the same

mechanism, and perhaps even in the same particles. Indeed, it is hypothesised that all mRNAs and proteins are transported into the oocyte by Dynein (Bullock & Ish-Horowicz 2001, Cha et al. 2001, Clark et al. 2007, Ephrussi et al. 1991, Jambor et al. 2014, Mische et al. 2007, Theurkauf & Hazelrigg 1998), and this could potentially occur in the same RNP, and the mRNAs then packaged into distinct particles upon entry into the oocyte. The mechanism of *grk* and *osk* transport could be elucidated with motor mutants (Clark et al. 2007, MacDougall et al. 2003) and pharmacological interventions (Firestone et al. 2013, Weil et al. 2006). Covisualisation of both *grk* labelled with the MS2 system and *osk* labelled with the PP7 system (Chao et al. 2008) and two different fluorophores, could allow simultaneous tracking of both transcripts to determine if they are transported in the same RNPs.

How *grk*, *osk*, and *bcd* are transported in the oocyte has been well studied (MacDougall et al. 2003, Weil et al. 2006, Zimyanin et al. 2008). However how they are transported through the nurse cells in the same direction (potentially along the same cytoskeletal tracks by the same motors) and are then targeted to different destinations when they enter the oocyte, is unclear. The higher velocities of mRNA particles in the nurse cells could shed light on changes in RNP particle composition, and associations with motors or cytoskeletal components between the two tissues. Although this difference in speed could be due to differences in cytoplasmic viscosity, or density of yolk granules and organelles between the two tissues, it could also be due to fundamental differences in the mechanism of transport. *in-vitro* analysis to test whether there are differences in the number and efficiency of motors recruited to mRNAs in the nurse cells and the oocyte (Amrute-Nayak & Bullock 2012, Soundararajan & Bullock 2014) could answer this question.

However, most particles of both *grk* and *osk* are static or paused, and more *osk* particles are static than *grk* particles. These particles could be anchored on the perinuclear nuage, a site of mRNA processing (Zhang et al. 2012), or may be associated with P bodies in the nurse cells as they are in the oocyte (Weil et al. 2012b, Chapter 6), and covisualisation of these mRNAs with protein components of these bodies could test this hypothesis.

Nurse cell mRNA particles do not move with an obvious directional bias towards the ring canals, and whether they move in a biased random walk, similar to *osk* transport in the oocyte (Parton et al. 2011, Zimyanin et al. 2008), could be investigated with computational tracking of particles, combined with analysis of the cytoskeletal components on which they are transported. This assay could also be used to covisualise *grk* and *osk* with the cytoskeleton, and determine if different RNAs, or different classes of particle, associate with distinct subsets of microtubules, as previously suggested (MacDougall et al. 2003).

Improving imaging of MS2 labelled mRNA in the nurse cells

I have attempted to improve detection of *grk* and *osk* particles through new imaging tehcniques and constructs. The OMX V3 improves visualisation of dynamic particles (Figure 3-8), and obtaining data with higher signal to noise ratios could allow for automated tracking of particles to assess speeds and directionality more objectively and accurately (Jaqaman et al. 2008). However, rapid MCP-FP bleaching limits the utility of this approach (Figure 3-9). Simultaneous imaging in two channels on the OMX would allow for more accurate covisualisation of mRNA and proteins, and optimisation of an imaging protocol using lower exposures and laser power, combined with post-acquisition denoising (Carlton et al. 2010, Yang et al. 2010) could

allow these particles to be imaged for longer using this system. Other microscopes could also be considered, such as two-photon systems, which use red-shifted excitation light to reduce photon scattering, and allow high temporal resolution imaging of mRNA particles in thick tissues (Sinsimer et al. 2013).

In *grk*GFP-24* egg chambers, some particles localise correctly in the oocyte, but the majority are trapped in the nurse cell nuclei, suggesting they are not exported from the nucleus (Figure 3-10). No problems have been reported with the MS2-24 construct in mammalian tissue culture cells (Lionnet et al. 2011), but a recent publication using this construct to image mRNA in mammalian cell lines did use it to label *osk* in oocytes, suggesting others may have experienced problems with this construct in *Drosophila* (Halstead et al. 2015).

As the MS2-24 loops were cloned into the same region as the MS2-12 loops in *grk-MS2-12*, both are inserted into the same *grk66* plasmid, and constructs were sequenced throughout cloning, it seems unlikely that the construct itself is faulty. It is possible that when all 24 loops are bound by MCP-GFP, either the resulting RNP is too large for nuclear export, or the strength of the 48 NLS's overpowers the nuclear export machinery. If this is the case, *grk-MS2-24* particles should be exported from the nucleus when MCP-GFP is not expressed, and could be detected using sm-FISH probes designed against the MS2-24 stem loops. If these unbound particles are still unable to be exported from the nucleus, this suggests that mRNA with 24 MS2 loops is too large to be exported. In this instance, an MS2-18 construct could be tested to determine whether it suffers from similar drawbacks.

tdMCP proteins have also been used successfully in mammalian cell lines (Wu et al. 2012), but in the egg chamber decrease the ability to image *grk* mRNA. Further communication with both the lab that produced the construct (Singer) and the lab that produced the flies (Ish-Horowicz) is required to resolve this problem. For example, it could be that the expression of these constructs was driven at a higher level in the egg chamber than in the mammalian cells, causing the increase in assembly formation. Differences in tdMCP-FP folding between the two tissues could also lead to differences in brightness.

Different approaches could be used to image mRNAs in the nurse cells. Fluorescent dyes like Alexa-fluors are brighter and more photo-stable than fluorescent proteins (Parton et al. 2010). Injection of *in-vitro* synthesised MCP conjugated to a fluorescent dye into egg chambers expressing MS2 tagged mRNA could improve mRNA labelling. A split YFP system could also be tested. Here, mRNA with both MS2 and PP7 loops is co-expressed with both MCP and PCP, each fused to one half of a split YFP. Each half of the split YFP only fluoresces when brought into close proximity with one another upon binding to the MS2/PP7 loops. This could increase the signal-to-noise ratio of the mRNA particles (Wu et al. 2014). Similarly, although mCherry is brighter and more photostable than RFP, other fluorophores could also be considered including tdTomato, mKate2 and mKatushka, and monomeric Kusabira Orange 2 (mKO2, Grünwald & Singer 2010, Karasawa et al. 2004, Sakaue-Sawano et al. 2008, Shaner et al. 2004, Shcherbo et al. 2007, Shcherbo et al. 2009).

Imaging of mRNA and it's processing in the nurse cell nuclei could be facilitated using an MCP-FP with a nuclear import/export signal rather than an NLS, which would draw unbound MCP-FP into the cytoplasm. The nuclear export, transcription

and translation of mRNA could likewise be visualised by labelling the same mRNA with two different fluorophores with the MS2 and PP7 system simultaneously (Halstead et al. 2015, Hocine et al. 2013).

Final conclusions

Here I have characterised the dynamics of *grk* and *osk,* and have potentially uncovered differences in RNP composition between the nurse cells and the oocyte. This is the first time endogenously processed localised mRNAs have been visualised in the nurse cells. This assay could help to elucidate the mechanisms of mRNA transport and the cytoskeletal organisation in the nurse cells, and also allows covisualisation of mRNA and fluorescently labelled trans-acting proteins, which I will use in Chapters 5 and 6. With advanced imaging techniques such as super-registration microscopy (Grünwald & Singer 2010), it may soon be possible to image the interactions between localised mRNAs and trans-acting factors throughout the life of the mRNA. This could elucidate where RNPs are assembled, how they are remodelled during the life of the mRNA, the proteins required for this remodelling, and where trans-acting factors are required for correct localised mRNA translation.

Although live imaging of the mRNA in the nurse cells opens numerous possibilities, some questions require examination of mRNA in fixed material. *grk* has been difficult to visualise in fixed nurse cells, and in Chapter 4 I will attempt to do so with sm-FISH.

Tables and statistics

Genotype (n egg chamber)	% > 10 RNA particles	% 1-9 RNA particles	% only large assemblies	% no particles
*grk*GFP* (53)	89	11	0	0
Pnos-MCP-GFP (110)	0	0	62	38
Pnos-MCP-GFP/+ (145)	1	0	44	55
*grk*mCherry* (42)	57	41	2	0
Pnos-MCP-mCherry (114)	1	10	85	4
*osk*GFP* (77)	86	14	0	0
*osk*mCherry* (55)	83	15	2	0

Table 3-1: Quantitation of particles in *grk* and *osk-MS2* and MCP control egg chambers.

Egg chambers were scored as detailed in Appendix F. A far greater percentage of *grk*GFP, grk*mCherry*, *osk*GFP* and *osk*mCherry* egg chambers contain RNA particles than *MCP-GFP* or *MCP-mCherry* controls. For both *grk* and *osk*, GFP labelled mRNA is easier to visualise than *mCherry* labelled mRNA.

Genotype (n particles)	% Active transport	% Paused	% Static
*grk*GFP* (340)	29	50	21
*osk*GFP* (387)	24	40	36

Table 3-2: Classes of *grk* and *osk* particles in the nurse cells.

Egg chambers were scored as detailed in Appendix F. For both *grk* and *osk*, a surprisingly low proportion of particles are actively transported, with the majority being paused. More *osk* particles are static than *grk* particles.

Particle class (n)	Velocity (μm/s)	Run length (μm)
Total *grk* nurse cell(91)	0.931 ± 0.05	1.546 ± 0.30
Total *osk* nurse cell (90)	0.920 ± 0.05	1.324 ± 0.16
AT *grk* nurse cell (33)	1.163 ± 0.08	2.785 ± 0.66
AT *osk* nurse cell (33)	1.118 ± 0.10	2.245 ± 0.38
Paused *grk* nurse cell (58)	0.798 ± 0.60	0.840 ± 0.06
Paused *osk* nurse cell (57)	0.806 ± 0.04	0.790 ± 0.04
*grk*GFP* oocyte[1] (37)	0.490 ± 0.23	N/A
Injected *grk* nurse cells[2] (231)	0.980 ± 0.01	N/A
*osk*GFP* oocyte[3] (272)	0.470 ± 0.01	2.430 ± (0.07)

Table 3-3: Dynamics of *grk* and *osk* in the nurse cells.

Average velocities and run lengths of *grk* and *osk* mRNA in the nurse cells and selected sub-classes of these particles. Velocities in μm/s ± s.e.m, run lengths in μm ± s.e.m. Speeds from the oocytes and injected *grk* in the nurse cells were performed by: [1] Weil, et al. 2012b, [2] Clark et al. 2007, [3] Zimyanin et al. 2008. Run lengths were not recorded as part of the analysis performed by Weil et al and Clark et al, and raw data for run lengths was not availble from V. Zimyanin for statistical analysis. My *grk*GFP* data from the nurse cells was statistically compared to *grk*GFP* data from the oocyte (Weil et al. 2012b) because particles were imaged on the same microscope, with the same settings, and analysed the same way. Imaging and image analysis performed by A. Clark for injected *grk* in nurse cells was different, and so was not used for statistical analysis. AT, actively transported.

P values from Student's t-tests (two tails), P = <0.001

Velocity statistics:

AT *grk* nurse cell vs *grk*GFP* oocyte: significant, P = 0.0002

Paused *grk* nurse cell vs *grk*GFP* oocyte: significant, P = 0.0001

Total *grk* nurse cell vs *grk*GFP* oocyte: significant, P = 0.0001

AT *grk* nurse cell vs paused *grk* nurse cell: significant, P = 0.0001

AT *osk* nurse cell vs *osk*GFP* oocyte: significant, P = 0.0001

Paused *osk* nurse cell vs *osk*GFP* oocyte: significant, P = 0.0001

Total *osk* nurse cell vs *osk*GFP* oocyte: significant, P = 0.0001

AT *osk* nurse cell vs paused *osk* nurse cell: not significant, P = 0.006

AT *grk* nurse cell vs AT *osk* nurse cell: not significant, P = 0.485

Paused *grk* nurse cell vs paused *osk* nurse cell: not significant, P = 0.913

Total *grk* nurse cell vs total *osk* nurse cell: not significant, P = 0.771

Run length statistics

AT *grk* nurse cell vs paused *grk* nurse cell: significant, P = 0.0001

AT *osk* nurse cell vs paused *osk* nurse cell: significant, P = 0.0001

AT *grk* nurse cell vs AT *osk* nurse cell: not significant, P = 0.480

Paused *grk* nurse cell vs paused *osk* nurse cell: not significant, P = 0.458

Total *grk* nurse cell vs total *osk* nurse cell: not significant: P = 0.465

Chapter 4: Detecting *grk* mRNA in the nurse cells with fluorescent *in-situ* hybridisation

Introduction

in-situ hybridisation (ISH) techniques are well established, assays for labelling mRNAs in fixed tissues, and offer many advantages over other labelling methods. First, ISH labels endogenous transcripts, without the need to overexpress or inject RNA. Second, new FISH labelling techniques allow single transcript detection (Buxbaum et al. 2015). Third, many cellular structures such as cytoskeletal components, nuclei, or the nuclear envelope, can be covisualised alongside ISH with additional reagents such as antibody stainings in fixed tissue. Fourth, synthesising ISH probes is straightforward, fast, and different probes can be used to simultaneously detect multiple mRNAs (Little et al. 2015), since probes are very specific and generate only low levels of background signal. Similarly, covisualising mRNA and proteins is often easier using ISH in conjunction with antibody staining, rather than fluorescent protein traps or P-element insertions, and P-elements often result in overexpression of the protein (Spradling et al 1995, Bellen et al 2004). Finally, introducing both components of the MS2 system into different genetic backgrounds can be challenging, and FISH is a more straightforward alternative.

ISH and FISH to label mRNA in fixed tissues

ISH techniques employ hybridisation of a DNA or RNA probe with complementary (antisense) sequence to the mRNA of interest. Initial experiments used radioactively labelled probes detected by silver staining (Akam 1983), but later used alkaline-phosphatase-coupled antibodies that detect Digoxigenin (DIG) labelled probes (Edgar et al. 1987). These were adapted to allow fluorescent labelling of mRNA (DIG-

FISH) by first binding a primary antibody to the DIG labelled probe, then attaching a secondary antibody conjugated to a fluorescent dye (Lawrence & H 1986, Wilkie et al. 1999). Alterations to this protocol, including TSA, which uses horseradish peroxidase (HRP) to deposit fluorescently labelled Tyramide derivatives at the location of the probe, can increase brightness and contrast (Raap & Van de Corput 1995, Speel et al. 1997, Wilkie et al. 1999).

Most recently, sm-FISH techniques have been developed to allow labelling of single mRNA molecules. These use a mixture of short (20 nucleotide) probes each designed to hybridise with specific parts of the transcript, and to avoid regions of secondary structure that are unsuitable for hybridisation. Each probe is conjugated directly to a fluorescent dye molecule, so that each mRNA molecule is labelled with multiple fluorophores (Battich et al. 2013, Femino et al. 1998, Little et al. 2011) (Levsky et al. 2002, Raj et al. 2006, Raj et al. 2008, Shaffer et al. 2013).

Histochemical staining methods depend on the production of a coloured or fluorescent precipitate, catalysed by an enzyme such as alkaline phosphatase or horse radish peroxidase. Such precipitates can sometimes diffuse away from the site of their production, and are not quantitative, as their production is not linear with the levels of the molecules detected. In contrast, the oligo array that is deployed in sm-FISH leads to a linear increase in the level of fluorescence with the concentration of the RNA detected. Furthermore, the large number of distinct probes used reduces background signal, since multiple probes must bind in order to allow detection. In conventional FISH protocols using RNA probes, the large probe size (200-1,000s of nucleotides) requires pre-hybridisation of the tissue at high temperatures (70^0C) and formamide concentrations (50%) to denature secondary structures in the target

mRNA. The smaller probes used in sm-FISH methods remove these requirements. Combined with the fact that smaller probes can penetrate tissues more easily and thus require less permeabilisation, sm-FISH protocols are less damaging to tissue morphology and fluorescent proteins expressed within the tissue.

sm-FISH techniques have been used in yeast (Trcek et al. 2011, Trcek et al. 2012), mammalian tissues (Trcek et al. 2013), *C.elegans* (Garcia et al. 2014. Raj et al. 2008), the developing nervous system (Buxbaum et al. 2014), the *Drosophila* embryo (Little et al. 2011) and imaginal discs (Raj et al. 2008) and have recently been optimised to allow high-throughput, quantitative analysis of FISH data to determine absolute mRNA levels (Battich et al. 2013, Jakt et al. 2013, Shaffer et al. 2013).

Although FISH with DIG probes has been used to study localised mRNAs in the *Drosophila* oocyte (Clark et al. 2007, Delanoue et al. 2007, Jambor et al. 2014, McDermott et al. 2012, Weil et al. 2012b), and can detect *bcd* and *osk* in the nurse cells (Ephrussi et al. 1991, Jambor et al. 2014, St Johnston et al. 1989) *grk* has not been successfully detected in the nurse cells (A. Clark Thesis, C. Rabouille, T. Weil, R. Parton personal communication). Attempts to label *grk* in nurse cells using large nascent transcripts (with lines expressing *grk-X44* and $grk_{genomic}$*-lacZ* constructs lacking a poly(A) signal, (Wilkie et al. 1999), and fragmentation of RNA probes, were unsuccessful (A. Clark Thesis).

sm-FISH techniques have been used to detect *osk*, *nos*, *pgc* and *cyclin B* (*cycB*) transcripts in the nurse cells (Little et al. 2015), but there are no reports of *grk* detection in the nurse cells using this technique. Whilst the research in this chapter

was being undertaken, no protocol for performing sm-FISH in oocytes existed, although one was published during the writing of this Thesis (Little et al. 2015).

Although *grk* was thought to be transcribed in the oocyte nucleus (Saunders & Cohen 1999), *grk* transcription is now known to be required only in the nurse cell nuclei (Caceres 2005). Detection of *grk* in fixed nurse cells would allow us to investigate the interactions between *grk*, it's trans-acting factors, and cellular components in different mutant backgrounds, and could help answer key questions about *grk* RNP formation and remodelling throughout it's life cycle.

Aims of this chapter and experimental rationale

In this chapter I test whether conventional and sm-FISH methods can be used to detect *grk* mRNA in the nurse cells. Specific questions include:

- **Can improvements in imaging allow visualisation of DIG FISH labelled *grk* in the nurse cells?**
- **Can sm-FISH probes detect *grk* in the nurse cells?**
- **Is there a difference in the number of *grk* transcripts in RNPs in the oocyte and the nurse cells?**
- **Can the puncta visualised by MS2 in living cells be detected as *grk* RNPs using sm-FISH?**

To answer these questions, I used DIG-FISH protocols adapted from R.Parton, which label *grk* in the oocyte (A. Clark et al. 2007, Delanoue et al. 2007, McDermott et al. 2012, Weil et al. 2012b). Although *grk* particles were not detected in the nurse cells using this method (A. Clark Thesis), I aimed to test whether the DeltaVision widefield

deconvolution microscope could be used to detect any particles in the nurse cells. This microscope is more sensitive than the spinning disc or confocal microscopes, and the imaging protocol I developed in Chapter 3 was able to visualise faint MS2 particles not previously seen using this system. I then adapted sm-FISH protocols from T. Trcek (Lehmann Lab), which are highly successful at labelling localised mRNAs in the *Drosophila* embryo (Little et al. 2011), for use in the oocyte.

Results

DIG-FISH protocols detect *grk* mRNA in the oocyte, but not in the nurse cells

I used my imaging protocol (Chapter 3) to test whether *grk* mRNA could be detected in the nurse cells with conventional FISH protocols. I stained wild-type egg chambers using antisense *grk* DIG probes. *grk* is visible in the oocyte in a cap around the DA corner, and is absent from egg chambers stained with control sense probes. However, with multiple dyes, fixation and tissue permeabilisation protocols, imaging parameters and contrasting conditions, no nurse cell signal is detected (Figure 4-1).

To test whether *grk* can be detected in the nurse cells by amplifying the fluorescent signal, I performed *grk* FISH with TSA staining. Labelling of *grk* in the oocyte is brighter than without TSA, but no nurse cell particles are visible (Figure 4-2).

Conclusion: DIG-FISH cannot detect *grk* in the nurse cells. This may be due to differences in labelling efficiency between the oocyte and the nurse cells, or fewer *grk* transcripts per RNP in the nurse cells than in the oocyte (see discussion).

sm-FISH techniques detect *grk* particles in the nurse cells

To test whether sm-FISH techniques can label *grk* in fixed tissues, I adapted a protocol for sm-FISH in *Drosophila* embryos (T. Trcek) for use in the oocyte (Chapter 2). In egg chambers stained for with *grk* sm-FISH probes, *grk* mRNA is strongly labelled at the oocyte DA corner (Figure 4-3 (A)). When the contrast on these images is increased, puncta are visible in the nurse cell nuclei and cytoplasm (Figure 4-3 (B)). In agreement with my MS2 data (Figure 3-4), these particles are less bright than oocyte particles, and the particle density is lower than at the DA corner (Figure 4-3). Puncta are not visible in either tissue when sm-FISH is performed with sense probes

Figure 4-1: DIG-FISH probes detect *grk* mRNA in the oocyte, but not in the nurse cells

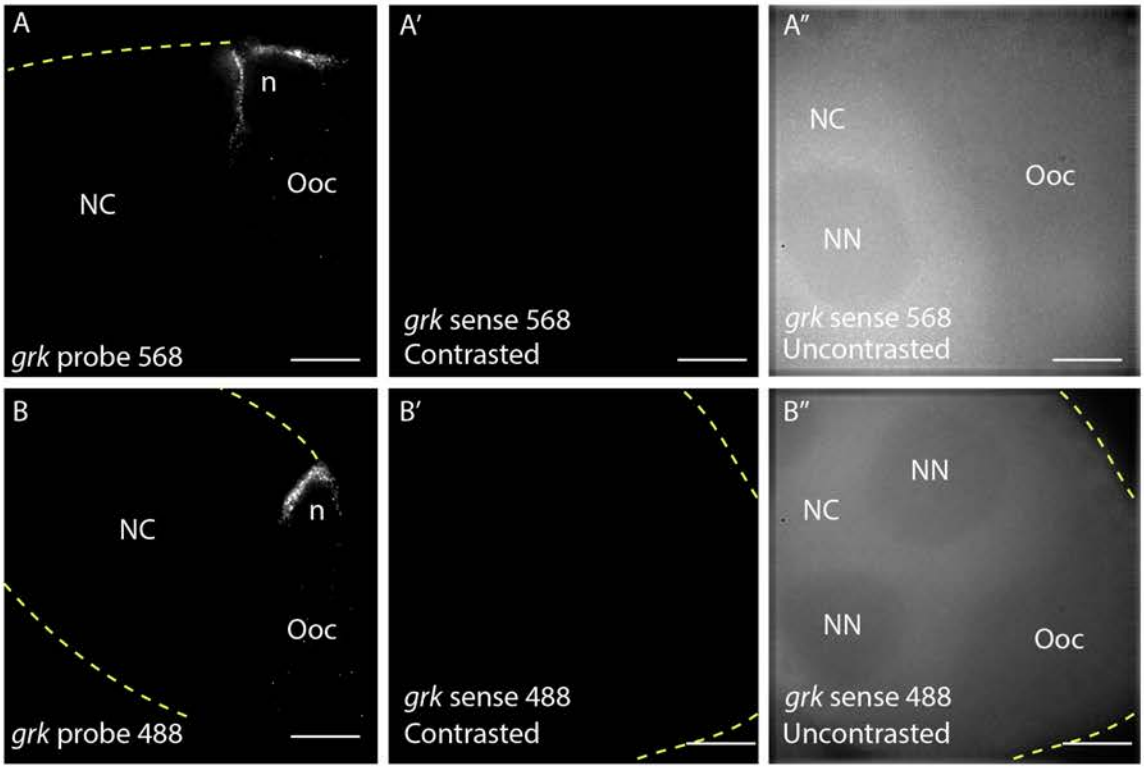

Figure 4-1:

(A-B"): DIG-FISH staining on wild-type egg chambers. *grk* is detected in the oocyte but not the nurse cells of egg chambers stained with DIG-FISH antisense *grk* probes labelled with (A) red (Alexa568) or (B) green (Alexa488) fluorescent dyes. Signal in the nurse cells was not detected under any contrasting conditions. (A'-A", B'-B"): No signal is detected in egg chambers stained with *grk* sense control probes. Images in (A') and (B') are equally contrased with images in (A) and (B), images in (A") and (C") are uncontrasted to show the egg chamber orientation. Dotted yellow lines indicate the edge of the egg chamber where applicable. All images acquired on 100x magnification, and deconvolved. NC, nurse cells; NN, nurse cell nuclei; Ooc, oocyte; n, oocyte nucleus. Scale bars 15 μm.

Figure 4-2: TSA protocols do not detect *grk* mRNA in the nurse cells

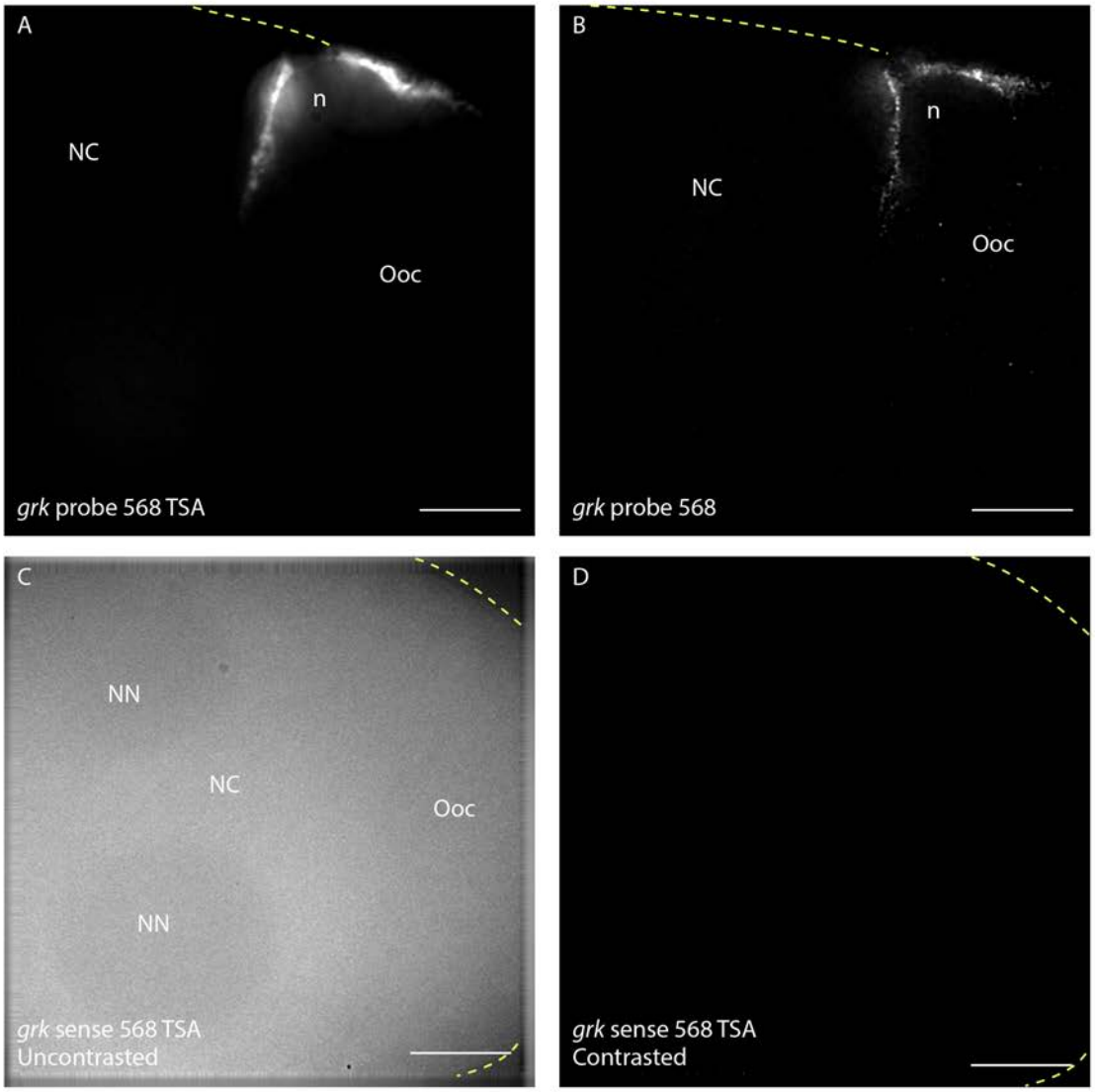

Figure 4-2:

(A-D) DIG-FISH staining on wild type egg chambers. (A): When DIG-FISH is performed with TSA staining, the *grk* signal in the oocyte is increased compared to un-amplified DIG-FISH (B), but no particles are seen in the nurse cells under multiple imaging and contrasting conditions. (C, D): No signal is detected in egg chambers stained with *grk* sense control probes with TSA staining. Image in (C) is uncontrasted to show the egg chamber orientation, image in (D) is equally contrasted with images in (A) and (B). Dotted yellow lines indicate the edge of the egg chamber where applicable. All images acquired on 100x magnification, and deconvolved. NC, nurse cells; NN, nurse cell nuclei; Ooc, oocyte; n, oocyte nucleus. Scale bars 15 μm.

against *grk*, or a "scrambled" *grk* sequence where the nucleotides in the *grk* antisense probe are randomly rearranged (Figure 4-4). When egg chambers are RNase treated before probing with *grk* antisense probes, no puncta are detected (Figure 4-4 (C, G)). This suggests these puncta are *grk* RNPs.

To further confirm that the nurse cell puncta are *grk* RNPs, I performed sm-FISH with *grk* intron probes. These have been used in other systems (Dimitrova et al. 2014) and should label only nascent, unspliced transcripts in the nuclei, not mature cytoplasmic mRNA. However, no signal above background is visible with intron probes designed against *grk* or sense control probes (Figure 4-5). This is most likely due to the short and A-T rich nature of *grk* introns, which causes the probe designer (Biosearch) to generate less than the minimum 23 probes. Interestingly, *grk* DIG-FISH intron probes have been previously reported to not label *grk* nascent transcripts (A. Clark Thesis). To further test the identity of nurse cell puncta as *grk* mRNA particles, I performed sm-FISH on *grk* mutant egg chambers. grk^{2B6} mutants are putative *grk* RNA nulls (Neuman-Silberberg & Schupbach 1993, Neuman-Silberberg & Schupbach 1996, Thio et al. 2000), however the Davis lab stock of these flies has accumulated lethal mutations and cannot be used. I crossed grk^{2B6} to grk^{2E12} mutants, which are protein nulls, and have been reported to be mRNA nulls (A. Clark Thesis, Herpers & Rabouille 2004, Neuman-Silberberg & Schupbach 1993). However, *grk* probes still detect puncta in the oocyte and the nurse cells (Figure 4-6).

Conclusion: Puncta are visible in the nurse cells of egg chambers stained with *grk* sm-FISH probes. Although intron probes and *grk* RNA nulls could not be used to further verify the identity of these puncta, the fact that they are not present in sense probe or RNase treated controls suggests that these are *grk* RNPs.

Figure 4-3: sm-FISH with *grk* probes detects particles in the nurse cells

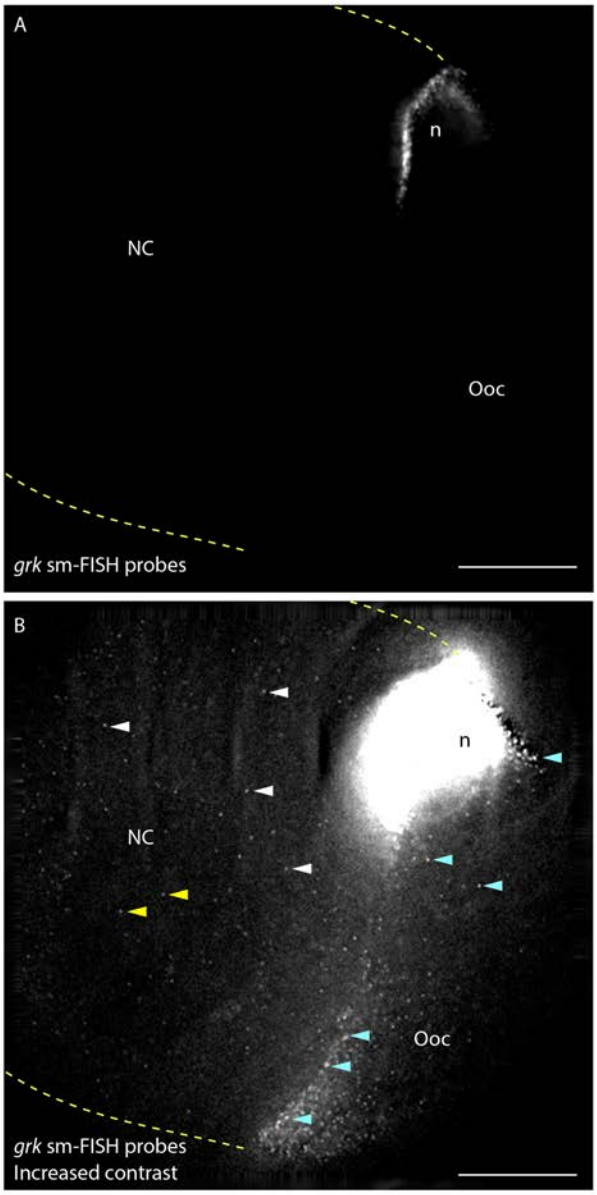

Figure 4-3:

(A-B): sm-FISH staining on wild-type egg chambers with *grk* probes. (A) sm-FISH probes for *grk* label localised *grk* at the oocyte DA corner. (B) When the contrast is increased, particles are also visible in the nurse cells (white arrowheads), and nurse cell nuclei (yellow arrowheads) which have a high signal to noise ratio. These particles are less bright than particles in the oocyte (blue arrowhead). Dotted yellow lines indicate the edge of the egg chamber where applicable. All images acquired on 100x magnification, and deconvolved. NC, nurse cells; NN, nurse cell nuclei; Ooc, oocyte; n, oocyte nucleus. Scale bars 15 μm.

Figure 4-4: sm-FISH detects *grk* particles in the nurse cells

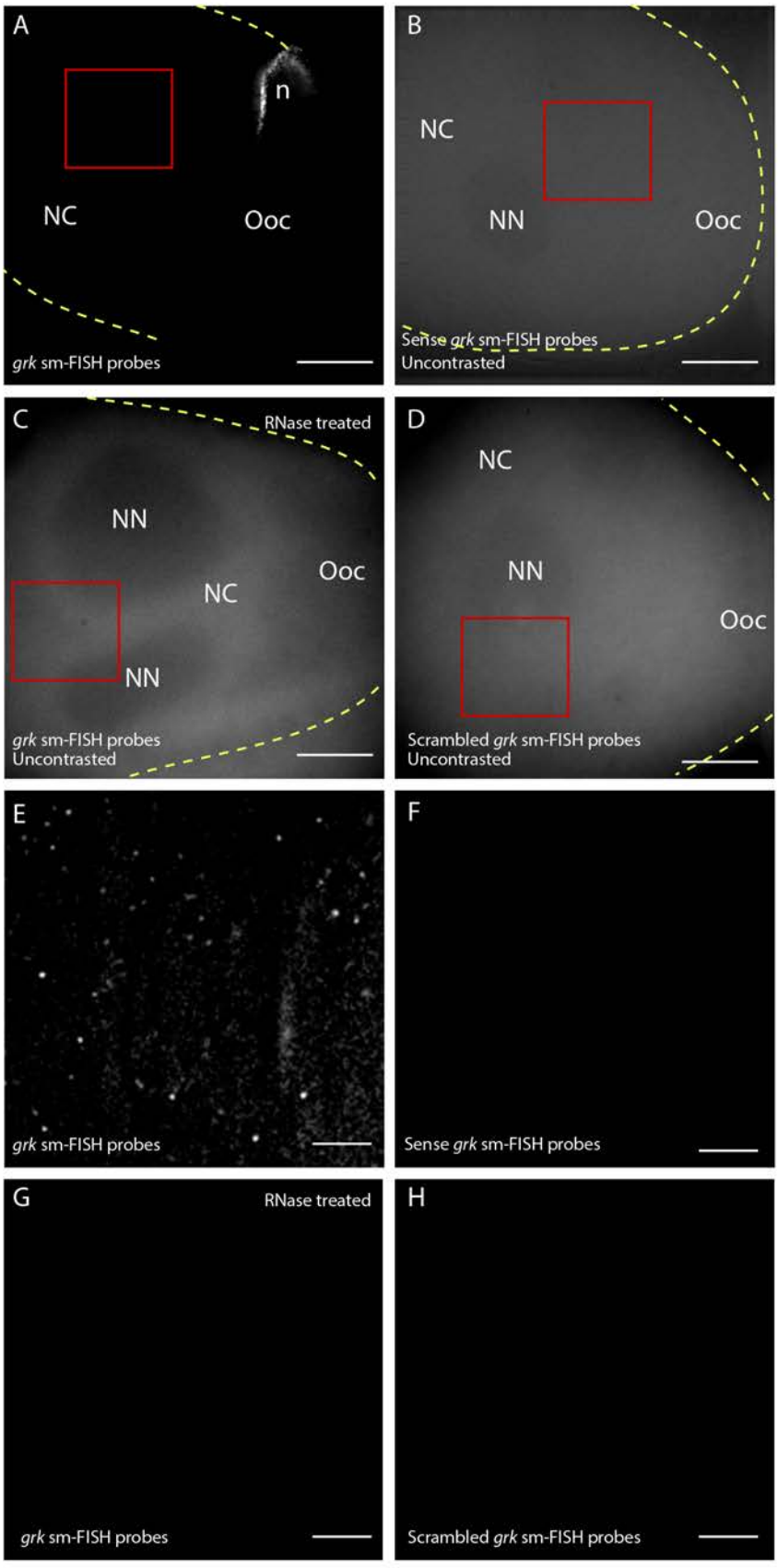

Figure 4-4:

(A-H): sm-FISH staining on wild-type egg chambers. (A): sm-FISH probes against *grk* label localised *grk* at the oocyte DA corner. (B-D): Egg chambers stained with sense control probes (B), *grk* antisense probes after RNase treatment (C) or a scrambled *grk* probe (D) do not. Images in (B-D) are uncontrasted to show the egg chamber. When contrasted equally to (A), the images are black. (E-H):Puncta in the nurse cells detected by sm-FISH probes against *grk* (E) are not visible in the nurse cells of egg chambers stained with sense control probes (F), *grk* antisense probes after RNase treatment (G) or a scrambled *grk* probe (H). Images in (E-H) are close ups of boxed areas in (A-D), and are all contrasted equally. Dotted yellow lines indicate the edge of the egg chamber where applicable. All images acquired on 100x magnification, and deconvolved. NC, nurse cells; NN, nurse cell nuclei; Ooc, oocyte; n, oocyte nucleus. Scale bars 15 μm (A-D), 5 μm (E-H).

Figure 4-5: sm-FISH intron probes do not detect nascent *grk* transcripts

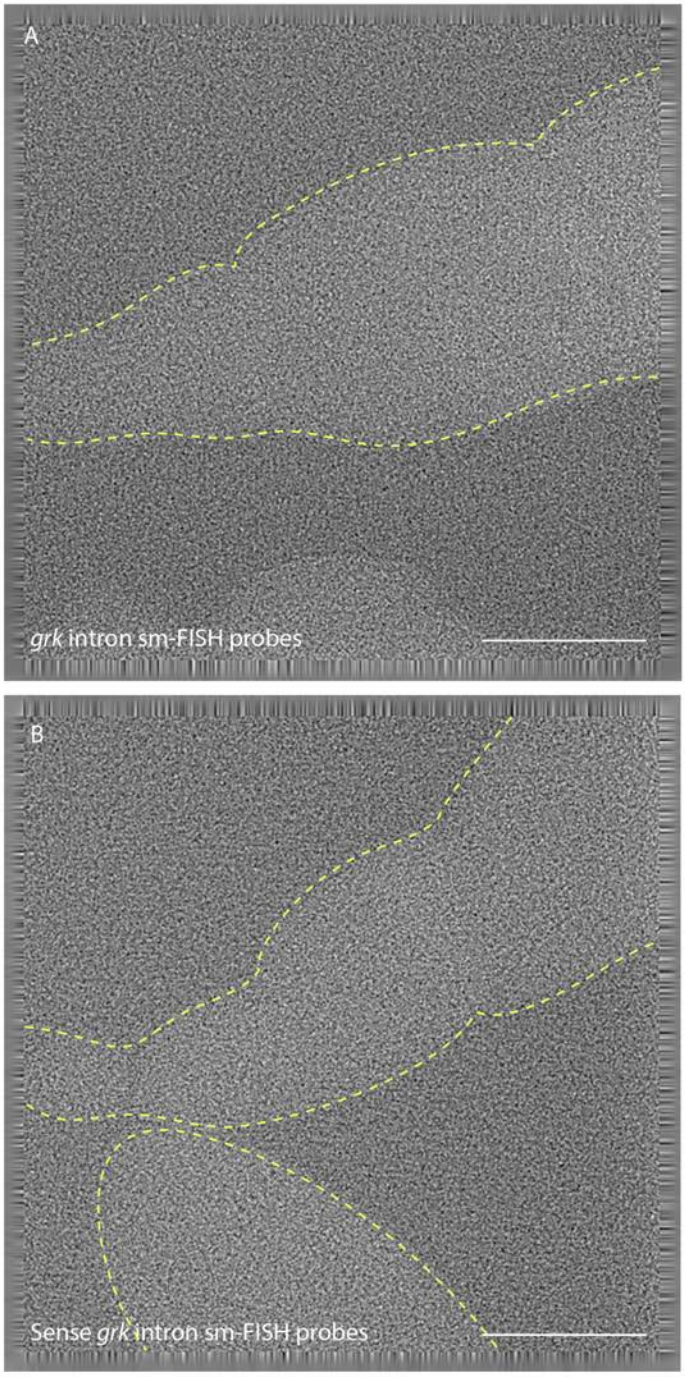

Figure 4-5:

(A-B): sm-FISH staining on wild-type egg chambers with *grk* intron probes. No signal is visible above background in egg chambers stained for with sm-FISH probes against *grk* introns (A) or sense control probes (B). Images acquired on 20x magnification, and deconvolved. Dotted yellow lines indicate the edge of the egg chamber where applicable. Scale bars 100 μm.

Figure 4-6: *grk*$^{2E12/2B6}$ mutants are not RNA nulls

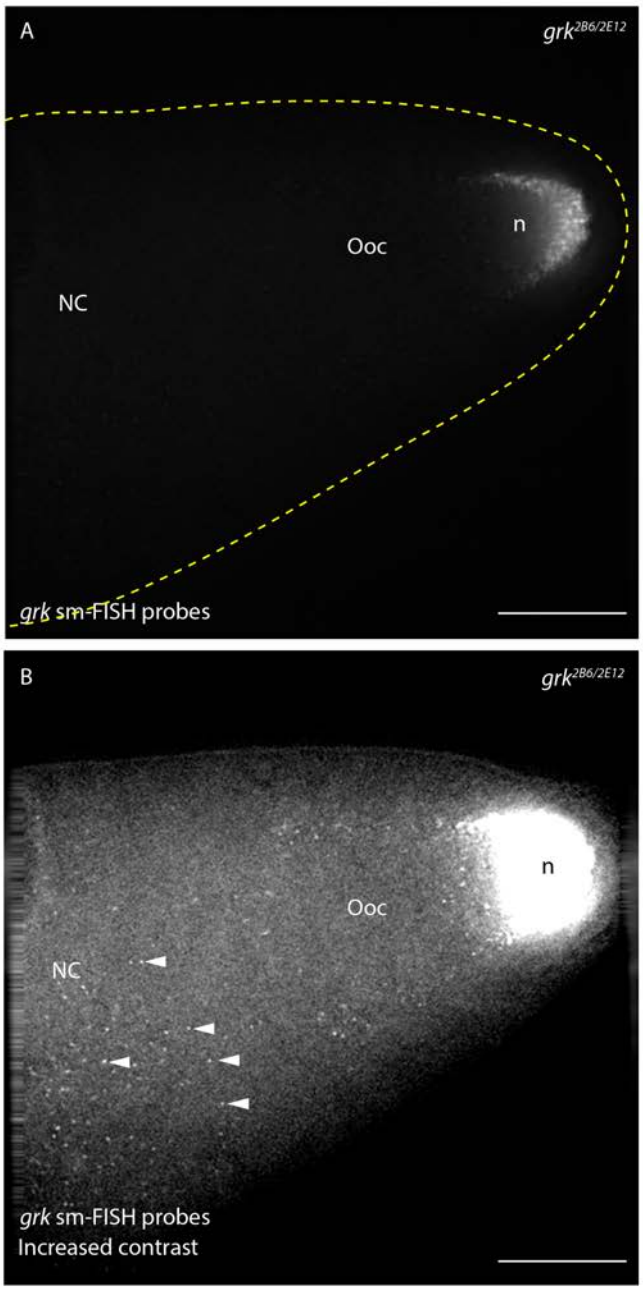

Figure 4-6:

(A-B): sm-FISH staining on *grk* mutant egg chambers. (A): In *grk*$^{2B6/2E12}$ mutants, particles of *grk* mRNA are still detected by *grk* sm-FISH probes in the oocyte, and particles are visible in the nurse cells (white arrowheads) when the contrast is increased (B). In these egg chambers, the oocyte nucleus and *grk* mRNA are localised to the posterior of the oocyte as previously reported (Neuman Silberberg & Schupbach 1993). All images acquired on 100x magnification and deconvolved. NC, nurse cells; Ooc, oocyte; n, oocyte nucleus. Scale bars 15 μm.

Using FISH to detect MS2 labelled *grk* in fixed tissues

In Chapter 3 I visualised puncta in *grk*GFP* and *grk*mCherry* but not *MCP-GFP* or *MCP-mCherry* expressing egg chambers. Although the MS2 system has been used to study mRNA localisation for over 15 years, and the *grk-MS2-12* construct can rescue *grk* mutants (Jaramillo et al. 2008), I sought to further verify the identity of these MS2 puncta as *grk* RNPs using FISH. To test whether FISH probes could label GFP tagged *grk-MS2* in the nurse cells, I performed FISH with DIG probes on *grk*GFP* egg chambers. GFP fluorescence is bleached in both the oocyte and the nurse cells (Figure 4-7 (A-A")). With sm-FISH *grk* probes, FISH fluorescence colocalises with GFP labelled *grk* in the oocyte, but GFP labelled puncta are still not visible in the nurse cells (Figure 4-7 (B-B")).

This result suggests that *grk*GFP* particles are not visible when fixed, which would eliminate the MS2 system as an assay to visualise *grk* and proteins or cellular components labelled with antibodies in fixed tissue. To try and improve the preservation of these particles, I fixed *grk*GFP* and *grk*mCherry* egg chambers without subsequent FISH processing. In both cases, puncta in the nurse cells are significantly harder to visualise than in live egg chambers (Figure 4-8 (A, B)). In the oocyte, the brightness and stability of *grk*GFP* and *grk*mCherry* can be increased using llama antibodies conjugated to an ATTO448 or ATTO594 dye, directed against GFP or RFP (Weil et al. 2012b). To test if these "Boosters" can be used to preserve MS2 labelled mRNA during fixation, I stained *grk*GFP* and *grk*mCherry* egg chambers with GFP or RFP booster respectively after fixation (RFP booster recognises *grk*mCherry*, (Weil et al. 2012b). This increased the number of particles visible in fixed egg chambers and their brightness (Figure 4-8 (A', B')). To test whether boosting can maintain *grk*GFP* puncta in the nurse cells throughout FISH

Figure 4-7: FISH protocols affect *grk*GFP* fluorescence to varying degrees

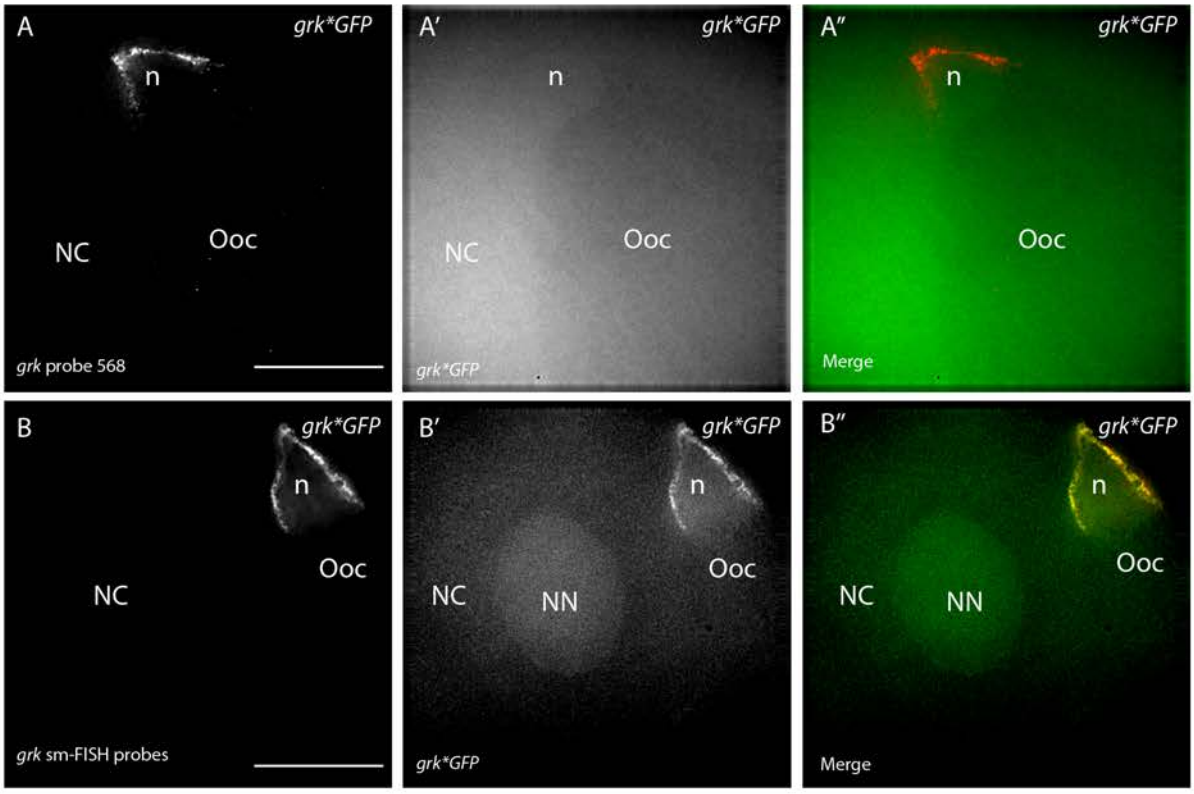

Figure 4-7:

(A-A"): DIG-FISH *grk* staining on *grk*GFP* egg chambers. Probes detect *grk* in the oocyte (A), but *grk* particles labelled with GFP are lost in both the oocyte and the nurse cells (A', A"). (B-B"): sm-FISH staining on *grk*GFP* egg chambers. When egg chambers are stained with *grk* sm-FISH probes, *grk* can be detected in the oocyte by the probes (B) and GFP fluorescence is visible (B'), but GFP labelled *grk* puncta in the nurse cells are lost (B', B"). sm-FISH labelled *grk* puncta in the nurse cells are still visible if the contrast is increased as in Figure 4-3, but are not shown here. All images acquired on 100x magnification and deconvolved. NC, nurse cells; Ooc, oocyte; n, oocyte nucleus; NN, nurse cell nuclei. Scale bars 15 μm.

Figure 4-8: Visualisation of *grk*GFP* and *grk*mCherry* nurse cell particles in fixed egg chambers

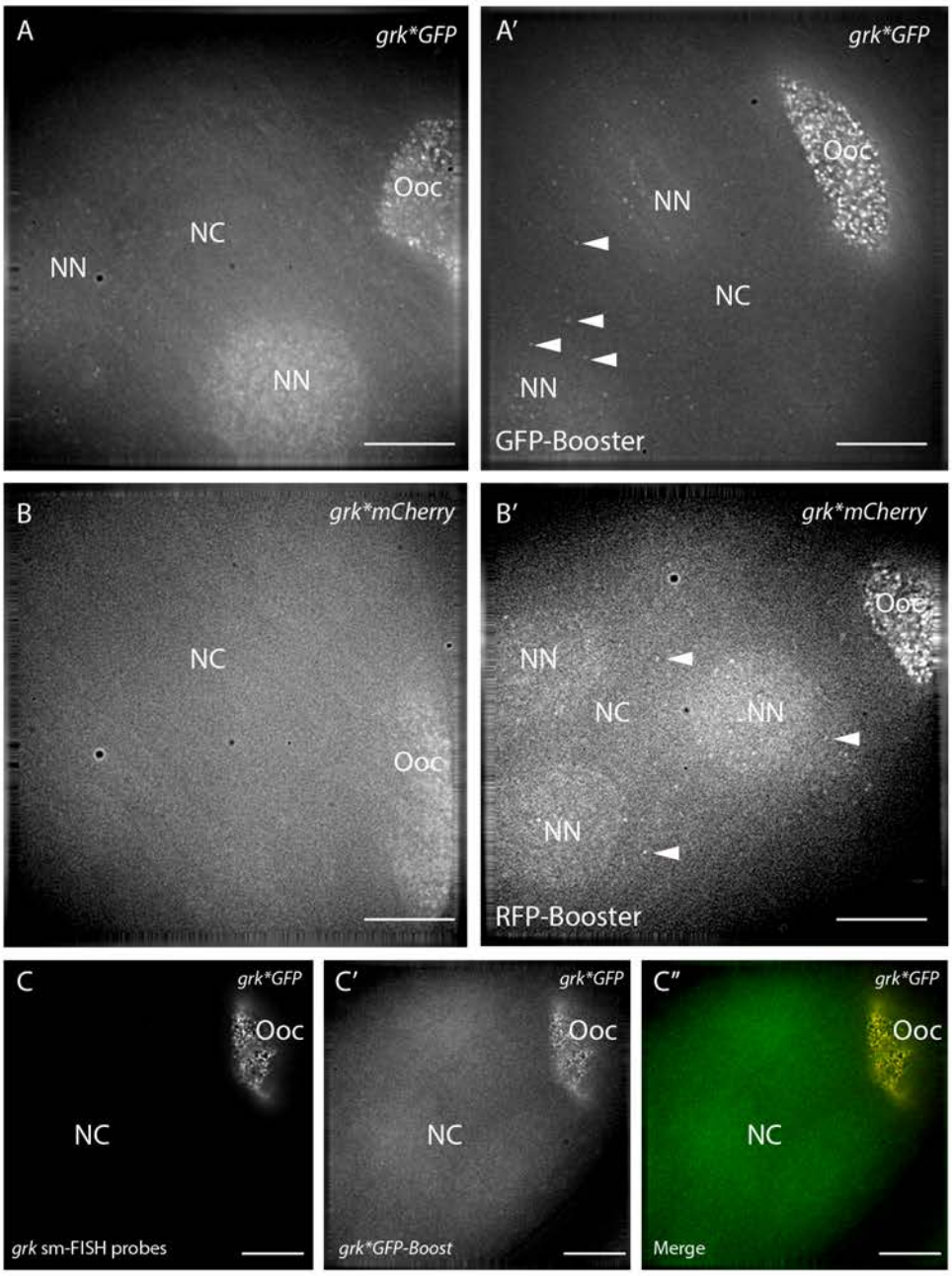

Figure 4-8:

(A, B): Fixed *grk*GFP* and *grk*mCherry* egg chambers. (A', B'): Fixed *grk*GFP* and *grk*mCherry* egg chambers with GFP or RFP booster. (A-A'): Particles of *grk* are significantly harder to visualise in the nurse cells of fixed *grk*GFP* egg chambers (A), but detection is aided by using GFP-Booster (A'). (B-B'): In fixed *grk*mCherry* egg chambers, *grk* particles are difficult to visualise in both the oocyte and the nurse cells (B). This is improved by RFP booster, but these particles are still very low signal-to-noise (B'). (C-C'') sm-FISH on *grk*GFP* GFP-boosted egg chambers. GFP labelled puncta in the nurse cells are still undetectable after boosting (C'). All images acquired on 100x magnification and deconvolved. NC, nurse cells; Ooc, oocyte; n, oocyte nucleus; NN, nurse cell nuclei. Scale bars 15 μm.

protocols, I stained with GFP booster before performing sm-FISH with *grk* probes on *grk*GFP* egg chambers. However, GFP labelled puncta are still not visible in the nurse cells of these egg chambers (Figure 4-8 (C-C")).

Fixation of *grk*GFP* particles seems to be incompatible with FISH protocols. In other systems, FISH probes have been used against MS2 sites to verify that MS2 puncta are the mRNA of interest (Lionnet et al. 2011). To test whether these probes could label *grk*GFP* puncta, I designed sm-FISH probes against the spacers in between MS2 stem loops in the *grk-MS2-12* 3' UTR, and performed sm-FISH with these probes in *grk*GFP* and *grk-MS2-12* egg chambers. In both genotypes, the probe detects *grk* in the DA corner of the oocyte. This signal colocalises with GFP fluorescence in *grk*GFP* egg chambers, and is lost in sense or RNase treated egg chambers (Figure 4-9 (A-A", B-B")).

MS2 probes also detect puncta in the nurse cells, similar to those detected by *grk* probes (Figure 4-9 (C)). These particles are not visible when a sense control probe is used, or egg chambers are RNase treated prior to probe hybridisation (Figure 4-9 (C', C")). Puncta are also not detected in the oocyte or nurse cells of *OrR* egg chambers probed for with the MS2 antisense probe (data not shown). To test whether the MS2 probe is labelling *grk-MS2-12* RNPs, I performed sm-FISH with *grk* probes labelled with a red fluorophore (Cal Fluor 590) and MS2 probes labelled with a far-red fluorophore (Qasar 670) on *grk-MS2-12* egg chambers. In these egg chambers, the majority of MS2 labelled puncta colocalise with *grk* labelled puncta (Figure 4-10 (B-B")). Some particles are only labelled with MS2, presumably because the *grk* probes do not hybridise to 100% of the mRNA. Many *grk* labelled puncta are not also

labelled with the MS2 probe, as endogenous *grk* without the MS2 loops is still transcribed in these egg chambers, and is detected by only the *grk* probe.

Conclusion: *grk* mRNA particles in the nurse cells labelled with the MS2 system are bleached during FISH protocols, and cannot be maintained by boosting. However, colocalisation of *grk* and MS2 probe labelled puncta verifies that particles in the nurse cells labelled with the MS2 system are *grk* RNPs.

Figure 4-9: MS2 probes label *grk-MS2* puncta in the nurse cells

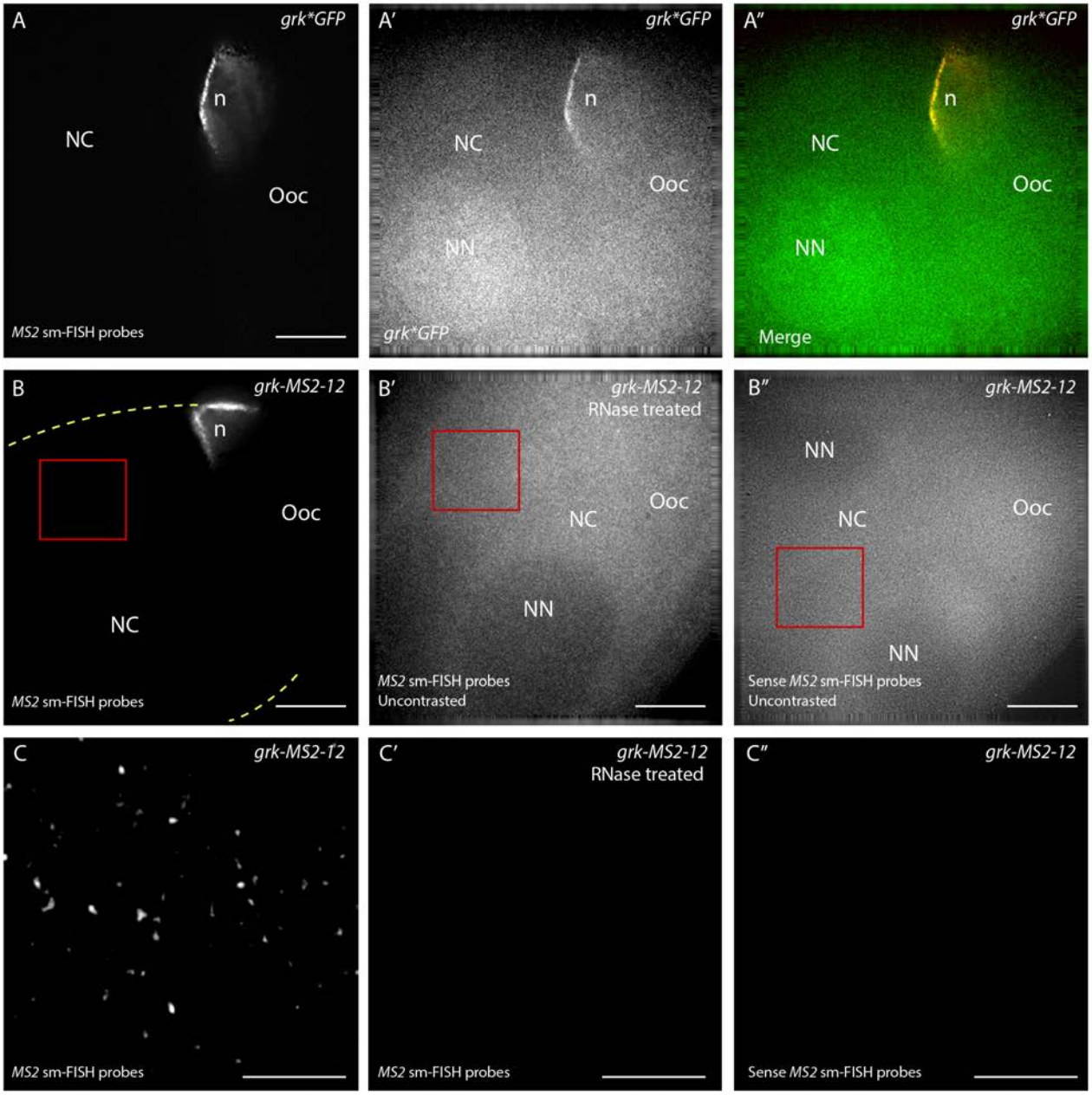

Figure 4-9:

(A-C") sm-FISH staining with probes against MS2 loops. (A-A"): sm-FISH staining of *grk*GFP* egg chambers. These probes label localised *grk-MS2* at the oocyte DA corner of *grk*GFP* egg chambers (A-A") and *grk-MS2-12* egg chambers (B). (B'-B") In egg chambers stained for with sm-FISH MS2 probes after treatment with RNase (B') or egg chambers stained for with sense control probes (B") no signal is visible. Images in (B') and (B") are contrasted to show the egg chamber, and are black if

(Figure 4-9 continued)

contrasted equally to (B). (C-C'): Close ups of red boxed regions in (B-B'). When the contrast is increased, puncta are detected in the nurse cells detected by sm-FISH probes against MS2 (C), but not RNase treated (C') or sense probed (C'') controls. Images in (C-C'') are all contrasted equally. All images acquired on 100x magnification, and deconvolved. Dotted yellow lines indicate the edge of the egg chamber where applicable. NC, nurse cells; NN, nurse cell nuclei; Ooc, oocyte; n, oocyte nucleus. Scale bars 15 μm (A, B), 5 μm (C).

Figure 4-10: MS2 puncta in the nurse cells are *grk* RNPs

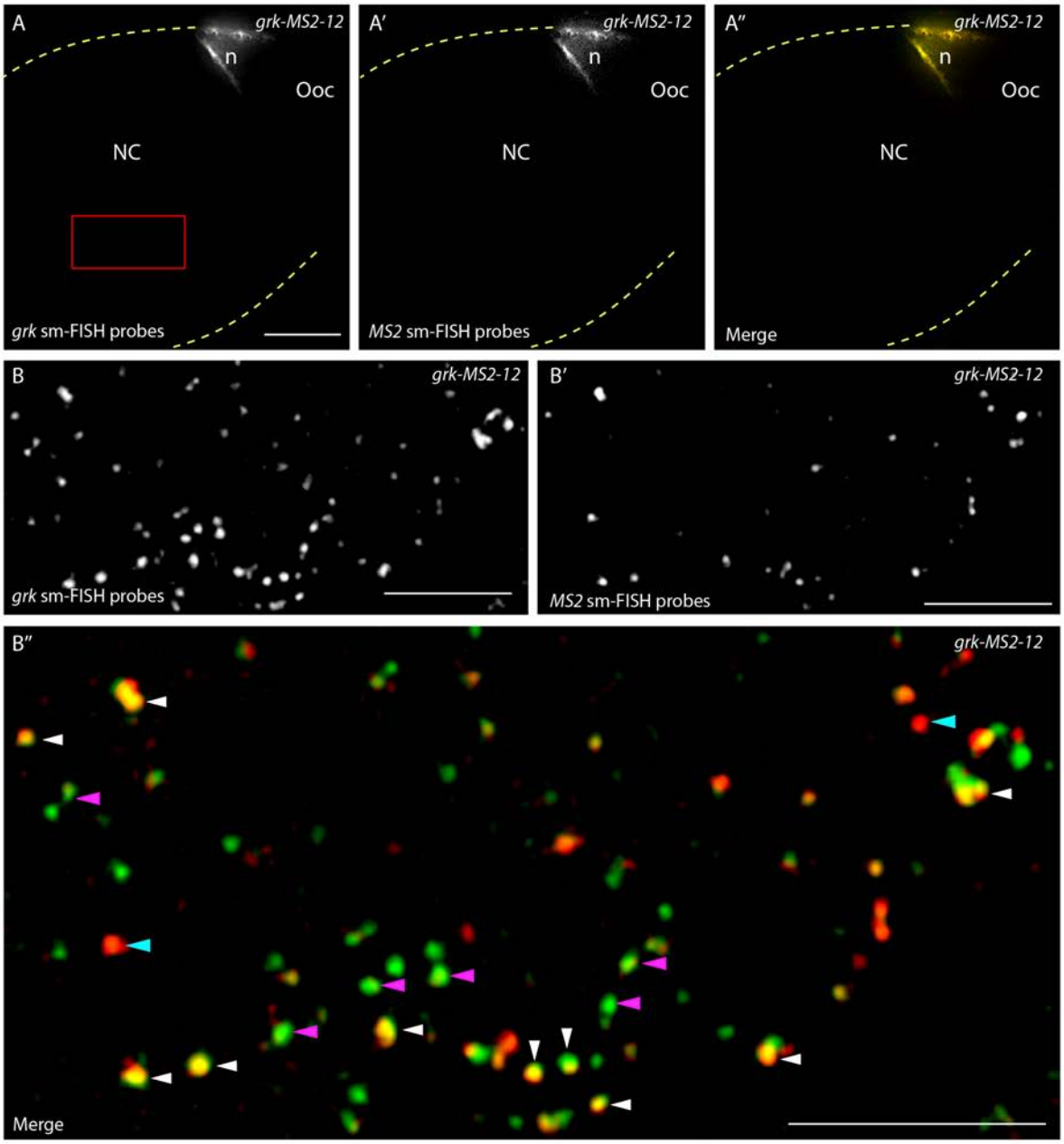

Figure 4-10:

(A-B'') sm-FISH staining with probes against MS2 loops and *grk* mRNA on *grk*-MS2-12 egg chambers. Throughout, the sm-FISH grk probes (Cal Fluor 590) are coloured green and the MS2 loop probes (Qasar 670) are coloured red.

(A-A'') Both probes label localised *grk* mRNA (presumably both endogenous and MS2 tagged mRNA) at the DA corner of the oocyte.

(Figure 4-10 continued)

(B-B”): Close ups of red boxed region in (A). (B”): In the nurse cell cytoplasm, the majority of MS2 labelled particles (red) are also labelled with the *grk* probe (green, particles with both stains are yellow, labelled with white arrowheads). However, there are many particles labelled only with the *grk* probe and not the MS2 probe (particles are green, labelled with magenta arrowheads), which represent the endogenous, non-MS2 tagged *grk* mRNA. Although there are some MS2 particles not labelled with the *grk* probe (red particles, labelled with cyan arrowheads), this is presumably because the probes do not detect 100% of the mRNA. All images acquired on 100x magnification and deconvolved. Images in B-B” are 1 *μ*m maximum intensity projections. Dotted yellow lines indicate the edge of the egg chamber. NC, nurse cells; NN, nurse cell nuclei; Ooc, oocyte; n, oocyte nucleus. Scale bars 15 *μ*m (A-A”), 5 *μ*m (B-B”).

Discussion

Here I have adapted an sm-FISH protocol for use in egg chambers to detect *grk* transcripts in nurse cells. I have visualised *grk* by FISH in fixed nurse cells for the first time. The absence of puncta in sense probe and RNase treated egg chambers suggests that these puncta are *grk* RNPs. *grk* labelling with this technique indicates that *grk* is packaged into higher order complexes in the oocyte than in the nurse cells. I have also used this protocol to label MS2 particles in *grk-MS2-12* egg chambers, which demonstrate that these are *grk* mRNA particles, validating the use of the MS2 system to label and study *grk* mRNA in the nurse cells.

Differences in effectiveness of FISH techniques in the nurse cells

Previous attempts to label *grk* mRNA in the nurse cells with DIG-FISH probes have been unsuccessful, although this technique can label *bcd* and *osk* in the nurse cells (Ephrussi et al. 1991, Jambor et al. 2014, St Johnston et al. 1989). I found that although DIG probes could detect *grk* only in the oocyte (Figure 4-1), sm-FISH was able to detect transcripts in both tissues (Figure 4-3).

The discrepancy between the nurse cells and the oocyte, and between these techniques, could be due to many factors. MS2 and sm-FISH data both indicate that *grk* particles are less bright in the nurse cells than in the oocyte (Figure 3-4, Figure 4-3). This suggests that *grk* may be transported as single molecules or low copy number particles in the nurse cells, but packaged in higher order complexes in the oocyte. Indeed, *nos* and *osk* RNPs contain one or two copies of the mRNA in the nurse cells, but in the oocyte contain up to 250 mRNA molecules per granule (Little et al. 2015). The presence of *grk* at low copy numbers could render *grk* transcripts in

the nurse cells undetectable by DIG-FISH, whereas sm-FISH is able to detect single transcripts and hence label these lower-order complexes.

sm-FISH has been used to determine the number of transcripts in *osk* and *nos* RNPs, how their packaging changes as they are trafficked into the oocyte, the assembly of germ plasm granules, and the importance of segregating different mRNAs to different granules for germline development (Little et al. 2015). This technique could also elucidate how and where *grk* RNPs are assembled and remodelled throughout the life of the mRNA, and whether other localised mRNAs are packaged with *grk* during it's transport. Colocalisation analysis with FISH probes to label other localised mRNAs, and FISH particle counting with RT-qPCR analysis, combined with step-bleaching techniques, could answer these questions.

Interestingly, successful DIG-FISH detection of *osk* and *bcd* in the nurse cells suggests that either these mRNAs are packaged into multimers in the nurse cells, - which is not suggested by my MS2 data (Chapter 3) - or that probes against *osk* and *bcd* are better able to penetrate tissue than those designed against *grk*. Alternatively there could be more *bcd* and *osk* in the nurse cells than *grk*. Indeed, my MS2 data indicate a higher density of *osk* particles in the nurse cells than *grk* particles (Supplementary movies 3-1 and 3-6). The labelling efficiency of the probes may well be the same, but the relative abundance of *osk* and *bcd* could make labelling these mRNAs in the nurse cells easier.

Moreover, differences in the tissue itself could render the nurse cells sub-optimal for DIG-FISH labelling. FISH protocols are not necessarily transferable between tissues. For example, protocols which label mRNA in the *Drosophila* larval brain are not

successful in the *Drosophila* larval NMJ, and mRNA detection by FISH in these tissue has required extensive modification of existing protocols (L. Yang and J. Titlow personal communication). Probes may be less able to penetrate the nurse cells and the overlying follicle cells, which have different characterstics to those overlying the oocyte in mid-oogenesis (Horne-Badovinac & Bilder 2005). However, I attempted the DIG-FISH protocol with increased permeabilisation, with no effect.

T. Weil, B. Herpers and C. Rabouille detected *grk* at the DA corner of the oocyte with ISH-IEM, but were unable to use this technique to detect *grk* in the nurse cells. ISH-IEM is performed on ultra-thin frozen sections (60nm), where the probe does not need to pass through 20μm of tissue (Herpers et al. 2010). However, with ISH-IEM it is difficult to simultaneously preserve the ultrastructure of the sample and permeabilise the tissue to allow probe penetration, and the detection efficiency is low (1-5%, Herpers & Rabouille 2004). The inability of this technique to label *grk* in the nurse cells suggests that some intrinsic property of the nurse cell cytoplasm makes FISH labelling difficult. However, *osk* mRNA is readily detected by IEM in nurse cells (T. Weil, C. Rabouille personal communication), so potentially the lower levels or packaging of *grk* in the nurse cells make detection of this mRNA in particular challenging. Although these hypotheses could be examined further, the success of sm-FISH at labelling *grk* in the nurse cells suggests that these issues are specific to DIG probes, and should not hinder any future sm-FISH experiments in this tissue.

FISH treatment of MS2 labelled egg chambers

In Chapter 3 I visualised *grk* particles labelled with the MS2 system in live nurse cells. Although the MS2 system has been used to label mRNA in multiple tissues for over 15 years, and the *grk-MS2-12* construct I used in chapter 3 rescues *grk* mutant s

(Jaramillo et al. 2008), FISH has never been used to verify the identity of these particles as *grk*. MS2 probes colocalise with *grk* probes (Figure 4-10), which confirms that the particles I visualise in the nurse cells are *grk* RNPs.

Interestingly, fixation of *grk*GFP* or *grk*mCherry* egg chambers significantly reduces the ability to visualise *grk-MS2* particles in the nurse cells (Figure 4-8), sm-FISH protocols destroyed the fluorescence of these particles, and the DIG-FISH protocol also ablated *grk*GFP* fluorescence in the oocyte (Figure 4-7). This difficulty in fixing *grk*GFP* particles could again be explained by low *grk* copy number in the nurse cells. If there are less *grk* mRNA molecules per granule in the nurse cells than in the oocyte, there will also be fewer GFP molecules per granule. These molecules, which are likely to be bleached or denatured by the formamide and high temperatures of FISH protocol, would be lost from the nurse cells but remain visible in the oocyte. Under the much higher formamide and much higher temperature of the DIG-FISH protocol, however, GFP in the oocyte is also bleached. This is not the case in other systems (Lionnet et al. 2011). Further work on alternative FISH protocols and improving *grk-MS2* labelling would be required to covisualise MS2 tagged mRNA and FISH labelled mRNA in fixed nurse cells.

Final conclusions

Here I have detected *grk* in fixed tissues using sm-FISH. MS2 and FISH approaches can be used to elucidate the mechanism of *grk* transport in the nurse cells, examine the assembly and remodelling of the *grk* RNP throughout the life of the mRNA, and investigate changes in trans-acting factors associated with *grk* in mutants of key regulatory proteins. In Chapter 5, I will explore the distribution and dynamics of the protein components of P bodies and key trans-acting factors of *grk* in the nurse cells.

Chapter 5: P body protein distribution and dynamics in the nurse cells

Introduction

P bodies are non membrane bound, electron dense structures with conserved roles in RNA processing (Decker & Parker 2012, Wilsch-Bräuninger et al. 1997). P bodies are sites of *grk* and *bcd* translation regulation in the *Drosophila* oocyte (Weil et al. 2012b), but whether or not P bodies are involved in the translational control of localised mRNAs in the nurse cells has not been established. In this chapter I will characterise the composition and dynamics of P bodies in the nurse cells.

P body structure and function

P bodies are important sites of mRNA degradation, and contain factors such as decapping enzymes, 4E-BPs, and DEAD box helicases involved in translational repression (Decker & Parker 2012, Parker & Sheth 2007, Teixeira et al. 2005). There is emerging evidence that P bodies regulate mRNA quality control, including mediating NMD (Sheth & Parker 2006). Under conditions of stress, specific mRNAs can escape P bodies and be translated to mount a stress response (Bhattacharyya et al. 2006, Halstead et al. 2015).

The protein complement of P bodies overlaps with that of other cytoplasmic bodies including stress granules, transport particles, P-granules, and neuronal RNA granules (Kiebler & Bassell 2006). These bodies are distinguished based on the presence of specific factors, their function, where they are located, and when they assemble. For example, the Ccr4/Pop2/Not deadenylation complex and Dcp1/2 decapping enzymes are primarily found in P bodies (Cougot et al. 2004, Sheth & Parker 2003),

components of the translation initiation machinery are predominantly enriched in stress granules, (Buchan et al. 2011, Groušl et al. 2009, Kedersha & P. Anderson 2002, Kimball et al. 2003, Low et al. 2005), and Argonaute proteins, the Dhh1 helicase and the Xrn1 5' to 3' exoncuclease are found in both bodies (Kedersha et al. 2005, Sen & Blau 2005, Sheth & Parker 2003, Wilczynska et al. 2005).

However, there is no consensus on what constitutes a P body, and the continuum of structure, protein composition, and function between P bodies and stress granules often makes these bodies hard to distinguish. Although stress granules form primarily under conditions of physiological stress (Buchan et al. 2011), they also assemble when translation is inhibited by other means (Buchan & Parker 2009). Moreover P bodies have functions in unstressed cells, but more form in response to stress (Kedersha et al. 2005, Teixeira et al. 2005).

Moreover, the role and necessity of P bodies is further complicated by evidence that mRNA processing, such as degradation and translational repression, can occur independently of P bodies in yeast and mammals (Buchan et al. 2008, Chu & Rana 2006, Decker et al. 2007, Kwon et al. 2007). Indeed, Dynein hypomorphic mutant *Drosophila* oocytes almost completely lack P bodies in the oocyte, and yet still develop through oogenesis (Delanoue et al. 2007).

P body assembly

How these bodies assemble is an important question, as they are involved in many aspects of mRNA regulation. P bodies are dynamic structures that require a pool of non-translating mRNAs (Liu et al. 2005, Pillai et al. 2005, Teixeira et al. 2005), and are in a state of continual flux, with proteins continuously leaving and joining (Aizer et

al. 2008, Weil et al. 2012b). Insights from yeast and mammalian tissues have established the following model for P body assembly. Translationally repressive RNPs assemble and are bound by pre-existing complexes of P body factors, such as a the Dcp1/2, Edc3 and Dhh1 translational repression complex, and the Pat1/ Lsm1-7/Xrn1 decapping and exonuclease complex (Bouveret et al. 2000, Fenger-Grøn et al. 2005, Gavin et al. 2006, Teixeira & Parker 2007, Tharun et al. 2000, Tharun & Parker 2001). These proteins then interact with each other and form closed loops of mRNA, before forming aggregates via their glutamine (Q) and asparagine (N) rich domains (Gilks et al. 2004, Kedersha et al. 1999, Mazzoni et al. 2007, Nissan et al. 2010, Pilkington & Parker 2008, Reijns et al. 2008).

mRNAs do not remain within one body, however, and move between polysomes, P bodies and stress granules in the “mRNA cycle”. This involves remodelling of the RNP complex, facilitated by helicases, moving transcripts between bodies as they are translated, stored and translationally repressed, and degraded (Decker & Parker 2012). Moreover, the assembly of some cytoplasmic bodies is dependent upon the presence of other bodies; stress granule assembly during glucose deprivation in yeast requires P bodies, but not vice versa (Buchan et al. 2008). The protein remodelling steps and cues in the mRNA cycle have not been elucidated, and how RNPs initially aggregate is unknown.

There are also increasing efforts to understand the physical properties of P bodies. As non-membrane bound structures, it is unclear how they maintain a distinct protein composition from the rest of the cytoplasm. P-granules in *C.elegans,* which are similar to P bodies, are liquid or gel like compartments driven to phase-seperate from the cytoplasm by numerous, weak, multivalent interactions between components

within the P-granule (Brangwynne et al. 2009, Hyman et al. 2014, Li et al. 2012a, Toretsky & Wright 2014, Updike & Strome 2010, Weber & Brangwynne 2012, Wolf et al. 1983). They do not move as intact bodies, but rather dissassemble and reassemble after the individual components have been transported (Brangwynne 2013). Whether P bodies in other organisms exist in a similar hydrogel state has been explored, but not fully characterised (Han et al. 2012, Wippich et al. 2013).

It also appears that repetitive, low complexity, intrinsically disordered protein (IDP) domains which lack a fixed, ordered tertiary structure and form a range of conformational states, are important in P body formation (Castello et al. 2012, Dyson & Wright 2005, Han et al. 2012, Kato et al. 2012, Tompa & Csermely 2004). These regions are structurally versatile and important for intracellular phase transitions and RNA binding (Peng et al. 2014). IDPs have a role in the assembly of P-granules in *C.elegans* (Wang et al. 2014), the decapping complex (Jonas & Izaurralde 2013), and nuage phase separation in HeLa cells (Nott et al. 2015). When hydrogels are chemically induced, they contain similar mRNAs to those in neuronal RNA granules (Han et al. 2012). These mRNAs are released by phosphorylation, suggesting that the mRNA complement of P bodies may be controlled by a similar mechanism (Han et al. 2012, Toretsky & Wright 2014).

The role of P bodies during *Drosophila* oogenesis

P bodies at the DA corner of the *Drosophila* oocyte are important sites of translational regulation. The P body core is enriched for translational repressors including Me31B, Bruno and Dcp2, and is devoid of ribosomes, and the P body edge is enriched for the translational activator Orb (Weil et al. 2012b). *grk* mRNA docks with the edge of the P body and is translated, whereas translationally repressed *bcd* is maintained in the

P body core throughout oogenesis (Weil et al. 2012b). How these mRNAs interact with distinct regions of the pre-assembled P body, and how the proteins are arranged in such a manner to generate two specific regions, is unclear.

P body assembly in *Drosophila* is also poorly understood. Sponge bodies which are thought to anchor *grk* at the DA corner require Dynein, which is present in non-membrane bound electron dense transport particles containing *grk* in transit (Delanoue et al. 2007), and is required for P body assembly in response to starvation (Burn et al. 2015). Sqd is also necessary for the conversion of transport particles into sponge bodies at the oocyte DA corner (Delanoue et al. 2007). However, the key players in the mRNA cycle in *Drosophila*, if it exists, have not been identified.

Cytoplasmic bodies may also have a role in stress and starvation responses in *Drosophila*. YPS and *osk-MS2* aggregate in cytoplasmic foci in the nurse cells under nutrient stress, which is rescued by refeeding or exogenous insulin supplementation (Shimada et al. 2011). Insulin activity seems to modulate both the cytoskeleton and P body formation in the egg chamber, and formation of these P bodies is correlated with survival (Burn et al. 2015). The importance of the insulin signalling pathway in *Drosophila* oogenesis has been well studied, and is also involved in mRNA translation (Ferguson et al. 2012), GSC development (Hsu et al. 2008), and lipid droplet accumulation in the nurse cells (Vereshchagina & Wilson 2006) (Vereshchagina et al. 2008). Interestingly, in the oocyte, injected or overexpressed *grk* mRNA accumulates inside P bodies (Weil et al. 2012b). Whether P bodies in the nurse cells respond to stress and store mRNAs in a similar manner to stress bodies in yeast, and then release this mRNA under different conditions, has not been tested.

Although several oocyte P body proteins have been characterised (Lin et al. 2008, Weil et al. 2012b), the composition and function of nurse cell P bodies is poorly understood. Electron dense bodies exist in the nurse cells (Wilsch-Bräuninger et al. 1997), and YPS colocalises with P body markers under nutrient stress (Shimada et al. 2011). Nurse cell P bodies have been analysed using confocal microscopy to identify colocalising proteins in the nurse cell cytoplasm, and how these associations altered under stress conditions (Snee & Macdonald 2009). However, this study did not examine the distribution of many *Drosophila* P body protein homologs, the structure of these bodies, their dynamics, or their function. Moreover, some of the findings of this study have recently been challenged (Weil et al. 2012b).

Aims of this chapter and experimental rationale

Oocyte P bodies are sites of *grk* and *bcd* translational control, but whether nurse cell P bodies have a similar structure, protein complement, dynamics, or function, is unclear. In this chapter I characterise nurse cell P bodies. Specific questions include:

- **Which proteins are present in nurse cell P bodies?**
- **How dynamic are P bodies and other trans-acting factors in the nurse cells?**
- **How do P bodies and *grk* mRNA in the nurse cells change under nutrient stress?**

To answer these questions, I examined IEM of ultra-thin frozen sections of the nurse cells, stained with antibodies against P body proteins. The sample preparation and imaging was performed by T. Weil, B. Herpers and C. Rabouille, and I analysed the images for differences in protein distribution compared to the oocyte. I then analysed the distribution of proteins of interest in nurse cell P bodies using

immunofluorescence with antibodies against P body proteins. Combining these methods enabled me to specifically analyse the nurse cells. I also used widefield imaging and the OMX microscope to characterise P body dynamics. In chapter 3 I demonstrated the capability of these methods to visualise mRNA particles in the nurse cells, which should also allow characterisation of P body dynamics.

Results

The protein complement of nurse cell P bodies is similar to those in the oocyte

To examine the protein complement of nurse cell P bodies, I analysed IEM data of nurse cells collected by T. Weil, B. Herpers and C. Rabouille, previously used to visualise oocyte P bodies (Weil et al. 2012b). Like at the oocyte DA corner, non membrane bound bodies are visible which contain interdigitated electron light and electron dense material, characteristic of P bodies (Delanoue et al. 2007, Weil et al. 2012b). Me31B and Bruno are enriched, and ribosomes excluded from the core of these bodies (Figure 5-1).

Although IEM permits ultrastructural analysis, it gives a two dimensional view of ultrathin 60nm sections, and has limited sensitivity (Herpers & Rabouille 2004). To further examine the protein composition of nurse cell P bodies, I analysed fixed egg chambers stained with antibodies for P body components by immunofluorescence. Proteins which colocalise with Me31B, the Dhh1/Rck/p54 *Drosophila* homolog and a canonical P body marker, in the oocyte (Weil et al. 2012b) also colocalise with Me31B in the nurse cells, including Tral, eIF4E, Growl, Cup, and YPS (Figure 5-2).

Sqd is enriched at the edge of oocyte P bodies, and is required for *grk* anchoring at sponge bodies in the DA corner (Delanoue et al. 2007, Weil et al. 2012b). To test whether Sqd is present in nurse cell P bodies, I analysed IEM data collected by T. Weil, B. Herpers and C. Rabouille. Using a GFP antibody in *Sqd::GFP* egg chambers, Sqd is visible in nurse cell P bodies (Figure 5-3 (A)). However, when examining the same *Sqd::GFP* line with widefield microsopy, no cytoplasmic bodies are visible (Figure 5-3 (B)), and antibody staining with a Sqd antibody does not detect

Figure 5-1: Nurse cell P bodies visualised by IEM have a similar protein complement to those in the oocyte

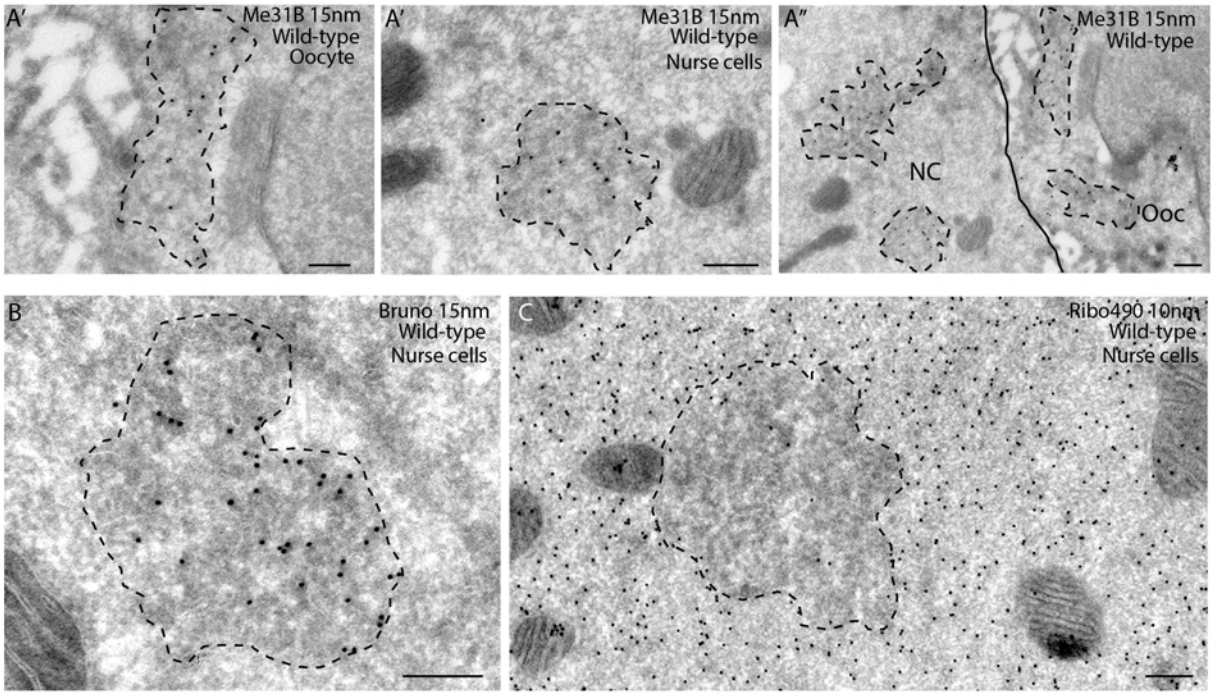

Figure 5-1:

(A-C): Protein detection by IEM on ultra-thin sections of wild-type egg chambers, carried out by T. Weil, B. Herpers and C. Rabouille. (A-A'): Me31B is enriched in the core of P bodies in the oocyte (A), and the nurse cells (A'). P bodies in both tissues display similar structure of interdigitated electron-light and electron-dense material, and contain Me31B. (B): Bruno is enriched in the core of nurse cell P bodies as it is in the oocyte. (C): Ribosomes are excluded from the core of P bodies and do not appear to be enriched at the P body edge, as seen in the oocyte. Solid black line marks the boundary between the nurse cells and the oocyte where applicable. Dashed black lines mark the edge of P bodies as determined by C. Rabouille based on electron density. Scale bars 200 nm

Figure 5-2: Nurse cell P bodies visualised by immunofluorescence have a similar protein complement to those in the oocyte

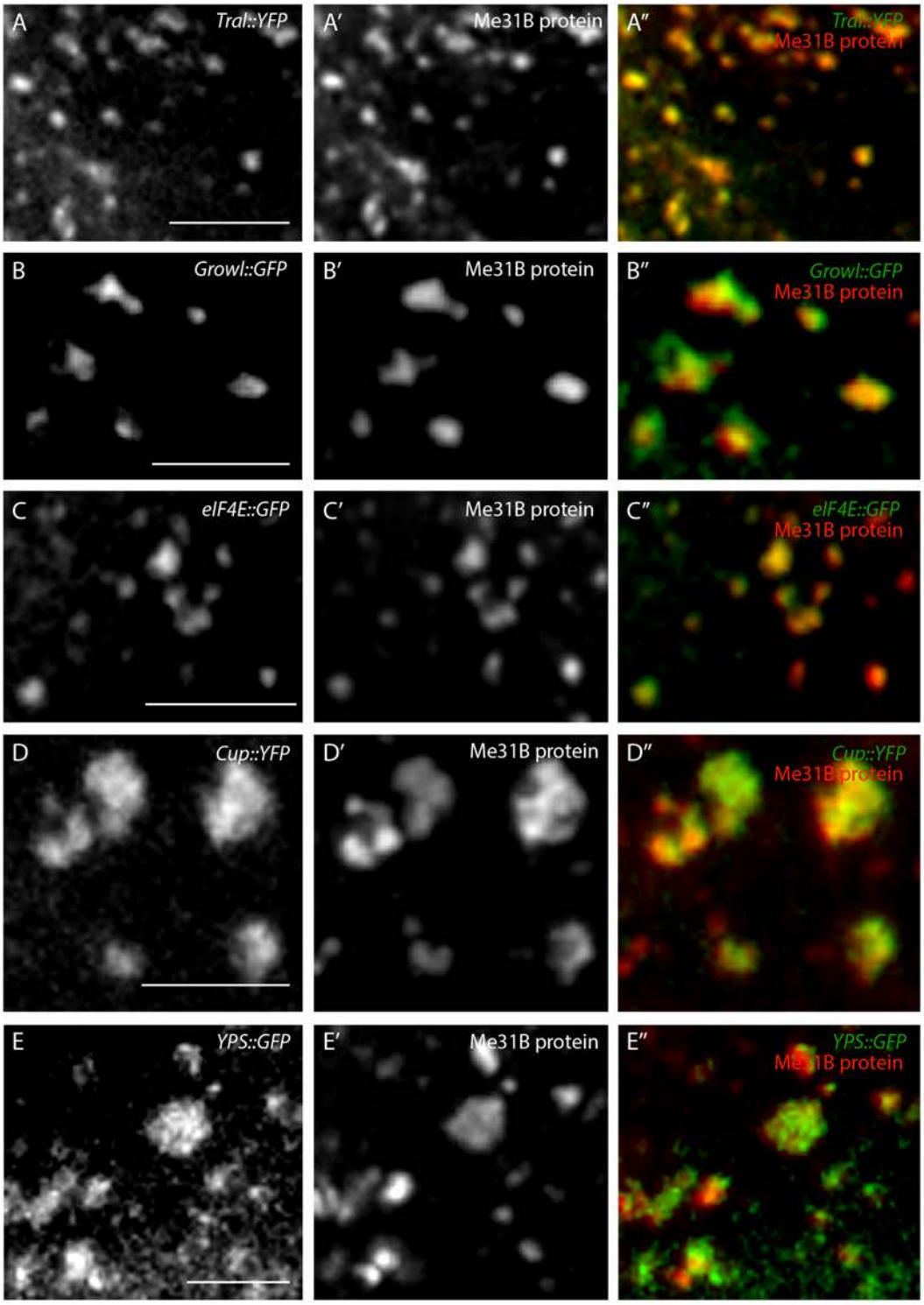

Figure 5-2:

(A-E): Protein detection by immufluorescence on whole egg chambers. Tral (A), Growl (B), eIF4E (C), Cup (D), and YPS (E) labelled with fluorescent protein traps colocalise extensively with Me31B antibody staining in the nurse cell cytoplasm. Some bodies are brighter in one channel, and the protein trap always has a lower signal to noise ratio than the antibody staining, sometimes making a direct comparison difficult. All images acquired at 100x magnification, deconvolved, and are 2 μm maximum intensity projections. Images were aligned using Me31B antibody staining (with Alexa 568 secondary) on *Me31B::GFP* egg chambers as a reference image. Scale bars: 5 μm (A, C), 2.5 μm (B, D, E)

Figure 5-3: Sqd is detected in nurse cell P bodies by IEM but not immunofluorescence

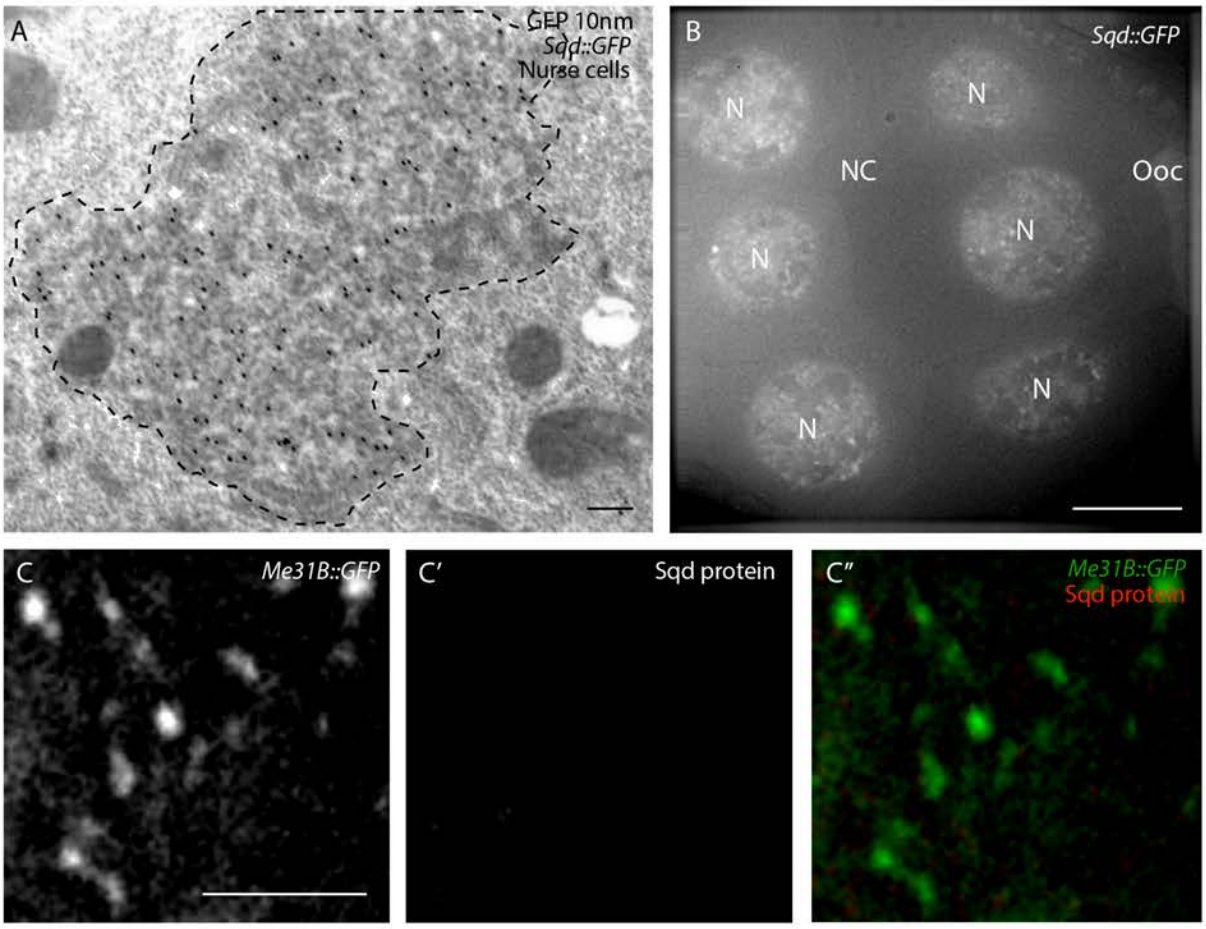

Figure 5-3:

(A): Protein detection by IEM on ultra-thin sections of nurse cells, carried out by T. Weil, B. Herpers and C. Rabouille. Sqd GFP is detected with a GFP antibody in nurse cell P bodies. (B): Widefield imaging of *Sqd::GFP* flies detects Sqd in the nurse cell nuclei and in a diffuse cytoplasmic background. (C-C"): Egg chamber expressing *Me31B::GFP* stained with Sqd protein. P bodies labelled with Me31B are clearly visible (C), but the Sqd antibody detects no signal above background in the nurse cell cytoplasm (C'). Dashed black lines in (A) mark the edge of P bodies as determined by C. Rabouille based on electron density. Images in (B) and (C-C") collected at 100x magnification and are deconvolved. NC, nurse cells; Ooc, oocyte; N, nurse cell nuclei. Scale bars 200nm (A), 15 μm (B), 5 μm (C).

cytoplasmic bodies (Figure 5-3 (C-C")). This discrepancy is most likely due to penetrance issues (T. Schupbach personal communication).

Conclusion: Nurse cell P bodies have a similar protein complement to those in the oocyte, with translational repressor proteins enriched and ribosomes excluded from the core. Based on IEM data, Sqd is also present in nurse cell P bodies.

Orb is expressed at much lower levels in the nurse cells than in the oocyte

At the oocyte DA corner, the edge of P bodies is enriched for the translational activator Orb. Strikingly, in the nurse cells significant levels of Orb protein were not detected by IEM in P bodies or the cytoplasm (Figure 5-4 (A-A')). C. Rabouille determined the density of Orb to be 18x higher in the oocyte than in the nurse cells. To verify this difference, I visualised Orb using immunofluorescence with an Orb antibody. Whereas the fluorescence intensity of *Me31B::GFP* is comparable between the two tissues, Orb is highly expressed along the oocyte cortex, but is present at lower levels in the nurse cells (Figure 5-4 (B-B")). The nurse cells nearest the oocyte contain the most Orb protein, with lower expression in the nurse cells further away from the oocyte (most anterior) as previously reported (Lantz et al. 1994).

Conclusion: Orb is expressed at markedly lower levels in the nurse cells than in the oocyte.

Characterisation of P body dynamics in the nurse cells

At the oocyte DA corner, small particles of Me31B are dynamic and are in flux with larger static P bodies, and *grk* and *bcd* mRNA move significantly faster than Me31B

Figure 5-4: Orb is expressed at much lower levels in the nurse cells than in the oocyte

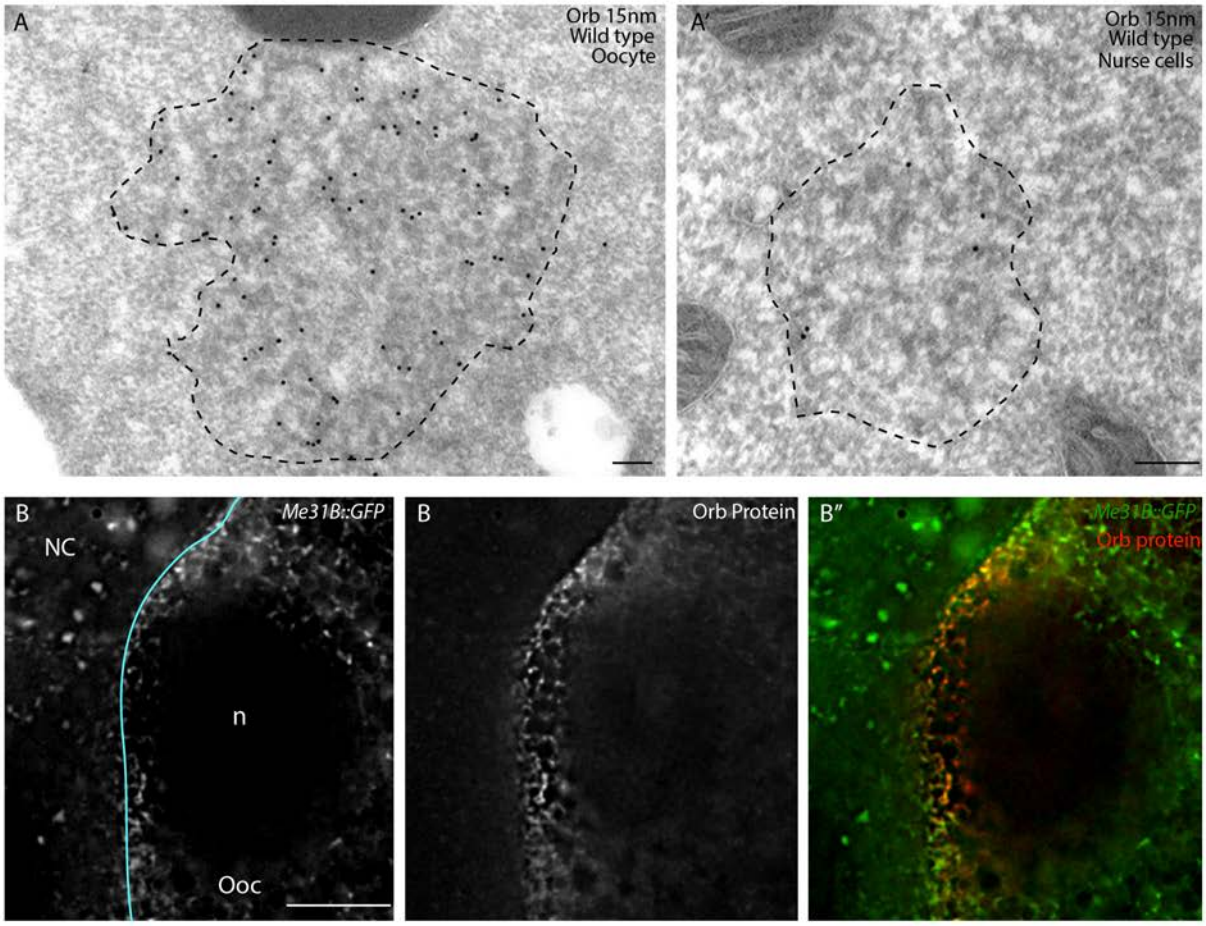

Figure 5-4:

(A-A'): Protein detection by IEM on ultra-thin sections of nurse cells, carried out by T. Weil, B. Herpers and C. Rabouille. Orb protein is present in P bodies in the oocyte (A), but levels of Orb in nurse cell P bodies and the nurse cell cytoplasm are significantly lower (A'). Images in (A) and (A') are from the same egg chamber. (B-B''): Widefield images of the nurse cell-oocyte boundary at the DA corner of an egg chamber expressing *Me31B::GFP*, stained with Orb protein. Levels of *Me31B::GFP* are comparable between the two tissues (B), whereas Orb is present at high levels in the oocyte around the oocyte nucleus, but at significantly lower levels in the nurse cells (B', B''). Dashed black lines in (A-A') mark the edge of P bodies as determined by C. Rabouille based on electron density. Solid cyan line in (B) marks the boundary

(Figure 5-4 continued)

between the nurse cells and the oocyte. Images in (B-B") imaged at 100x magnification and deconvolved. NC nurse cells, nurse cells; Ooc, oocyte; n, oocyte nucleus. Scale bars 200 nm (A-A'), 10 μm (B).

(Weil, Parton, Herpers, et al. 2012b). In the nurse cells, both *grk* and *osk* move significantly faster than in the oocyte (Chapter 3). To examine if the dynamics of P body components is similar between the nurse cells and the oocyte, I visualised *Me31B::GFP* in living nurse cells. Multiple classes of Me31B particles are visible including large, bright assemblies (>1 μm) and small faint particles (<500 nm, Figure 5-5, supplementary movie 5-1). Unlike *grk* and *osk* mRNA particles, the majority (56%) of Me31B particles (n=89) move in a fashion indicative of active transport, and fewer particles are paused (23%) or static (11%). Larger static assemblies make up a small proportion of the total Me31B (10%) (Figure 5-5, Table 5-1).

Nurse cell Me31B particles move significantly faster than those in the oocyte, (0.68 μm/s compared to 0.23 μm/s), suggesting these particles are actively transported (Weil, Parton, Herpers, et al. 2012b) Table 5-2). Unlike for *grk* and *osk*, there is not a significant difference in the speeds of actively transported (0.699 μm/s) and paused (0.648 μm/s) Me31B particles, although actively transported particles undergo significantly longer runs than paused particles (2.975 μm compared to 0.806 μm, Table 5-2). Actively transported Me31B particles also move more slowly than actively transported *grk* and *osk* in the nurse cells (*grk* and *osk* move at over 1.1 μm/s, Me31B particles only at 0.699 μm/s), moving at speeds which are similar to paused *grk* and *osk* particles (0.65 μm/sec to 0.8 μm/sec, Table 5-3). There is no significant difference between the run lengths of actively transported *grk*, *osk* and Me31B, or paused *grk*, *osk* and Me31B (Table 5-3).

Like *grk* and *osk* mRNAs, no consistent directionality of Me31B particles is observed. However, large assemblies of Me31B, and Growl could be visualised moving through ring canals (Figure 5-6, supplementary movies 5-2 and 5-3). These bodies move at

Figure 5-5: Me31B particle dynamics in the nurse cells

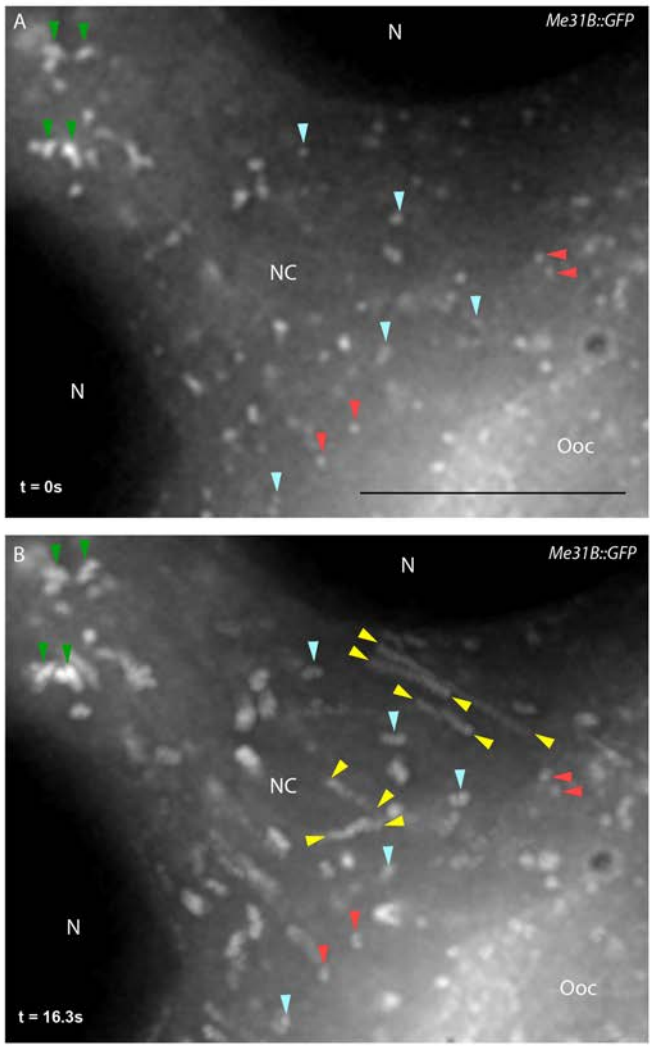

Figure 5-5:

(A-B): Live cell imaging of *Me31B::GFP* egg chambers. (A): Image of representative egg chamber at t = 0s and (B) trail image of 49 frames superimposed (from t = 0s to t = 16.3s, movie collected at 3fps). Moving particles appear as a set of dots. Yellow arrowheads indicate Me31B particles undergoing long runs and mark the first and last visible point in the time sequence. Blue arrowheads indicate paused particles which move in a restricted fashion. Red arrowheads indicate static particles, green arrowheads indicate large assemblies of Me31B which are largely static. Images were acquired at 100x magnification, and image series is deconvolved. NC, nurse cells; Ooc, oocyte; N, nurse cell nuclei. Scale bar 15 μm.

Figure 5-6: P body transport through ring canals

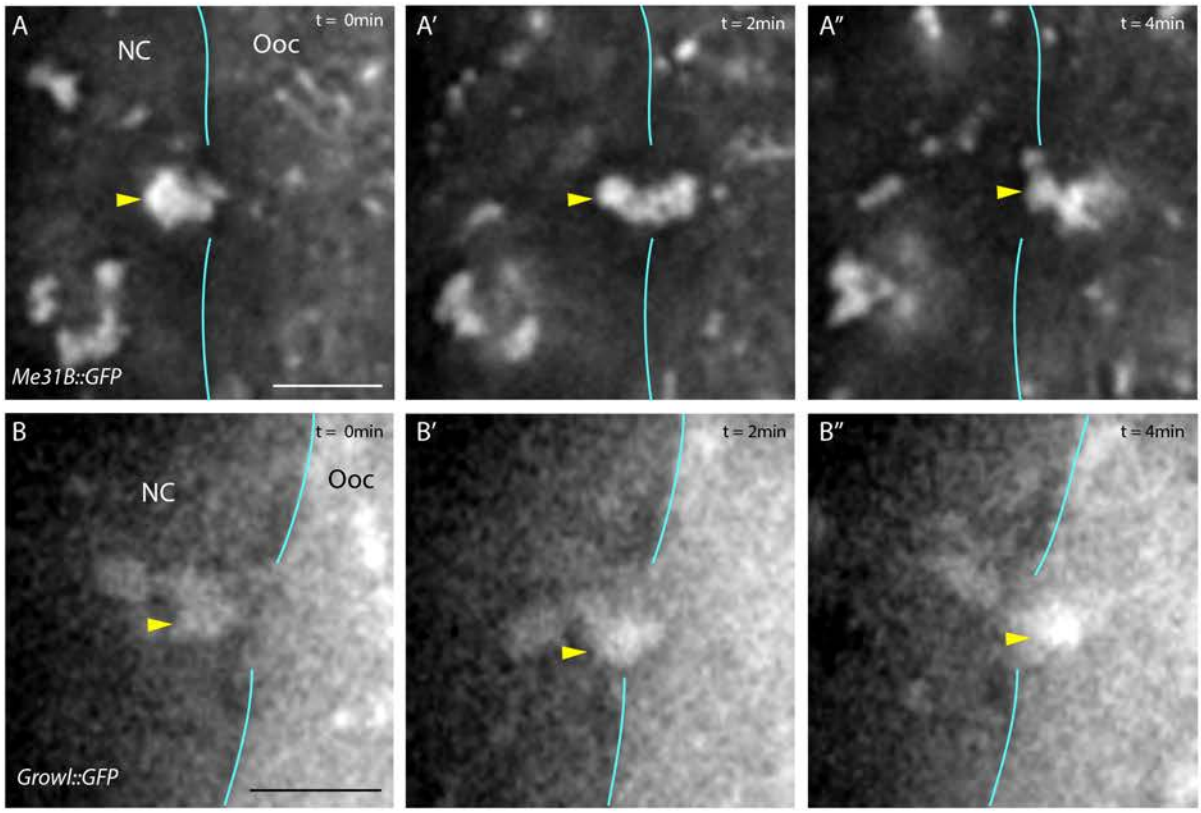

Figure 5-6:

(A-B): Live cell imaging of *Me31B::GFP* (A) and *Growl::GFP* (B) egg chambers. Large assemblies are visible moving through ring canals. Yellow arrowheads indicate large assemblies, cyan lines mark the boundary between the nurse cells and the oocyte. The break in the line represents the ring canal. Images acquired at 100x magnification, image series is deconvolved, images collected at 1 frame every 30s. NC, nurse cells; Ooc, oocyte. Scale bars 5 μm.

speeds of roughly 1 μm/min, indicative of diffusion. Smaller, more motile particles cannot not be visualised moving through ring canals.

To test whether small Me31B particles could be tracked with higher temporal resolution, and visualised moving through ring canals, I imaged *Me31B::GFP* egg chambers on the OMX V3 using the Z sweep function. All classes of Me31B are visible in the nurse cells, and small, motile particles can be tracked over long runs (Figure 5-7, supplementary movie 5-4). Although *Me31B::GFP* is much brighter and more resistant to bleaching than *grk*GFP* or *grk*mCherry*, particles could not be visualised moving through ring canals. Small particles may move through ring canals via diffusion or a dense microtubule network (Clark et al. 2007, Mische et al. 2007), and most likely pass into different Z planes as they do so, making tracking difficult. Alternatively, small nurse cells particles may join larger assemblies at the ring canals before being trafficked into the oocyte.

To elucidate how Me31B, and potentially P bodies, are transported in the nurse cells, I treated *Me31B::GFP* egg chambers with cytoskeleton depolymerising drugs. In flies fed on Colcemid, which depolymerises microtubules (Clark et al. 2007) (Weil et al. 2006), Me31B particles are all static (Figure 5-8 (B-B'), supplementary movie 5-5). Conversely, when flies are fed yeast with the equivalent proportion of ethanol, Me31B particles move normally (Figure 5-8 (A-A'), supplementary movie 5-6).

Conclusion: Me31B particles move faster in nurse cells than in the oocyte. A higher proportion of Me31B particles are actively transported than *grk*, or *osk*, but they move more slowly than these RNPs. There is no difference between the run length of actively transported Me31B and *grk* or *osk*, suggesting they are transported on the

Figure 5-7: Me31B in the nurse cells visualised on the OMX

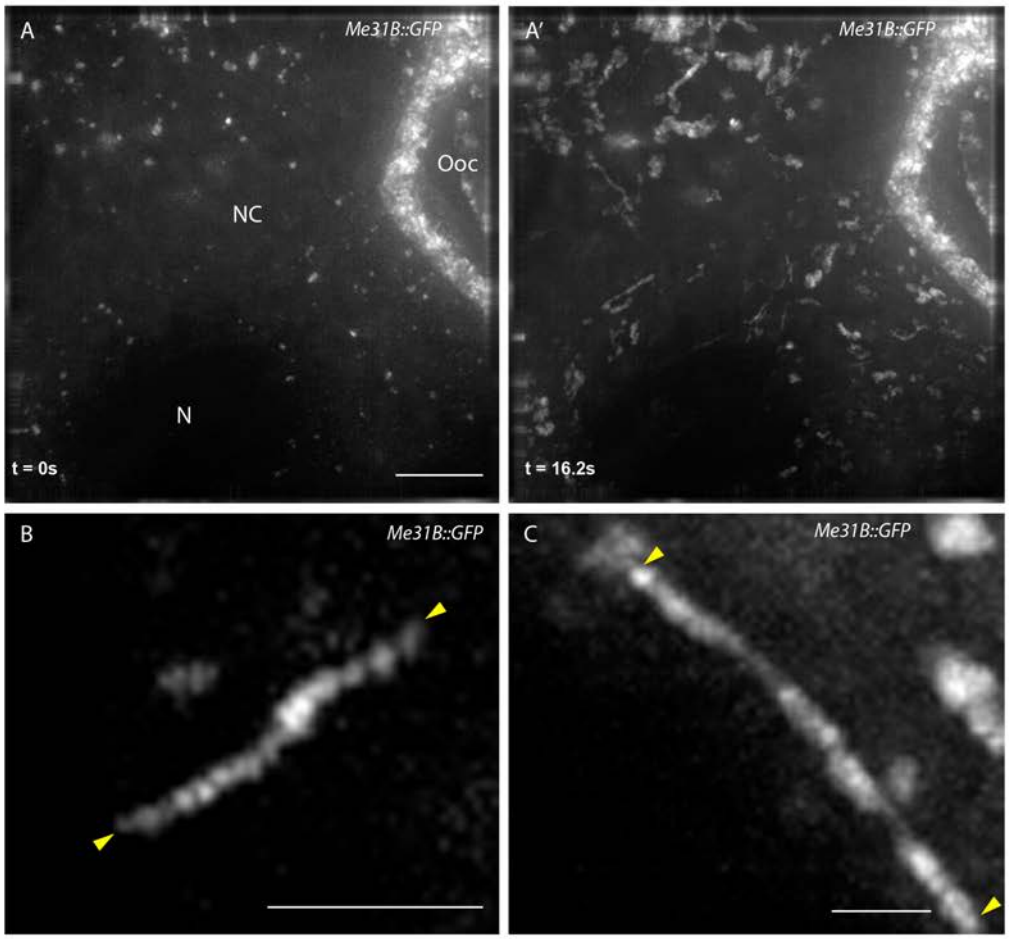

Figure 5-7:

(A-C): Live cell imaging of *Me31B::GFP* egg chambers on the OMX. (A): Image of representative egg chamber at t = 0s and (A') trail image of 113 frames superimposed (from t = 0s to t = 16.2s, movie collected at 7fps). Moving particles appear as a set of dots. All classes of Me31B particle are detected by the OMX. (B,C): Trail images of runs of individual Me31B particles from the egg chamber in (A). Yellow arrowheads mark the first and last visible point in the time sequence. (B): Trail image of 21 frames superimposed between t=0s and t=3s. (C): Trail image of 35 frames superimposed between t=0s and t=5s. All image series collected at 60x magnification and deconvolved. Images in (A) are 4 μm maximum intensity projections NC, nurse cells; Ooc, oocyte; N, nurse cell nuclei. Scale bars 2 μm (A) 2 μm (B, C).

Figure 5-8: Me31B motility in the nurse cells requires microtubules

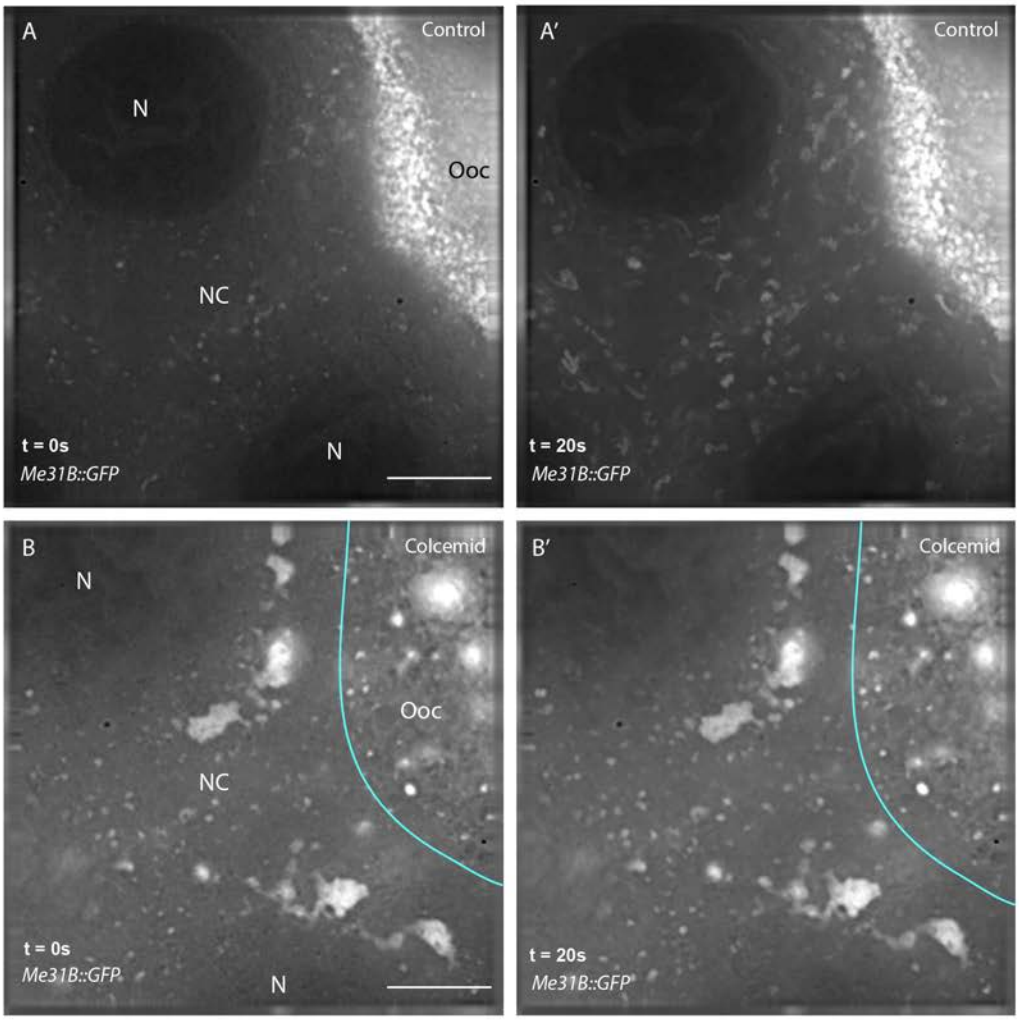

Figure 5-8:

(A-B'): Live cell imaging of Me31B::GFP egg chambers. (A) and (B) are images at t=0s, (A') and (B') are trail images of 140 frames superimposed (from t=0s to t=20s, images collected at 7fps). (A-A'): In egg chambers from females fed on yeast with ethanol as a control, Me31B particle motility in the nurse cells is normal. (B-B'): In egg chambers from females fed on yeast containing 20μg/ml Colcemid, particle motility is completely abolished and all particles are static in the nurse cells and the oocyte. All images acquired at 100x magnification, image series are deconvolved. Cyan line marks the boundary between the oocyte and the nurse cells in (B). NC, nurse cells; Ooc, oocyte; N, nurse cell nuclei. Scale bars 15 μm.

same cytoskeletal components, but may be moved by different numbers of motors. Transport of these small particles requires microtubules, whereas large P bodies appear to diffuse through ring canals.

P bodies are enlarged in response to nutrient stress

Nutrient stress increases the number and size of YPS bodies, which are thought to also contain *osk* mRNA in the nurse cells (Shimada et al. 2011). Recent evidence suggests that MS2 labelled *osk*, *bcd* and *grk* are enriched in P bodies in starved egg chambers (Burn et al. 2015), and in the oocyte, injected or overexpressed *grk* accumulates inside P bodies (Weil et al. 2012b). To test whether P bodies labelled with Me31B also respond to nutrient stress, I examined egg chambers from *Me31B::GFP* females deprived of yeast. P body number, size, and fluorescence intensity all appear to increase compared to egg chambers from fed control females, and P bodies in egg chambers from starved females are less dynamic (Figure 5-9 (A-A', B-B'), supplementary movies 5-7 and 5-8). After feeding on yeast for 12 hours, P bodies return to normal size, intensity and dynamics (Figure 5-9 (C-C'), supplementary movie 5-9).

To test whether *grk* accumulates in these P bodies, I examined egg chambers from starved females co-expressing *Me31B::GFP* and *grk*mCherry*. P bodies contain high levels of mCherry fluorescence throughout the egg chamber (Figure 5-10 (A-A'', B-B'')). To test whether this fluorescence was *grk* mRNA or MCP-mCherry, I examined egg chambers from starved females co-expressing *Me31B::GFP* and *MCP-mCherry*. P bodies contain high levels of mCherry fluorescence, indistinguishable from that seen in *grk*mCherry* flies (Figure 5-10 (C-C'', D-D'')).

Figure 5-9: P bodies assemble under nutrient stress

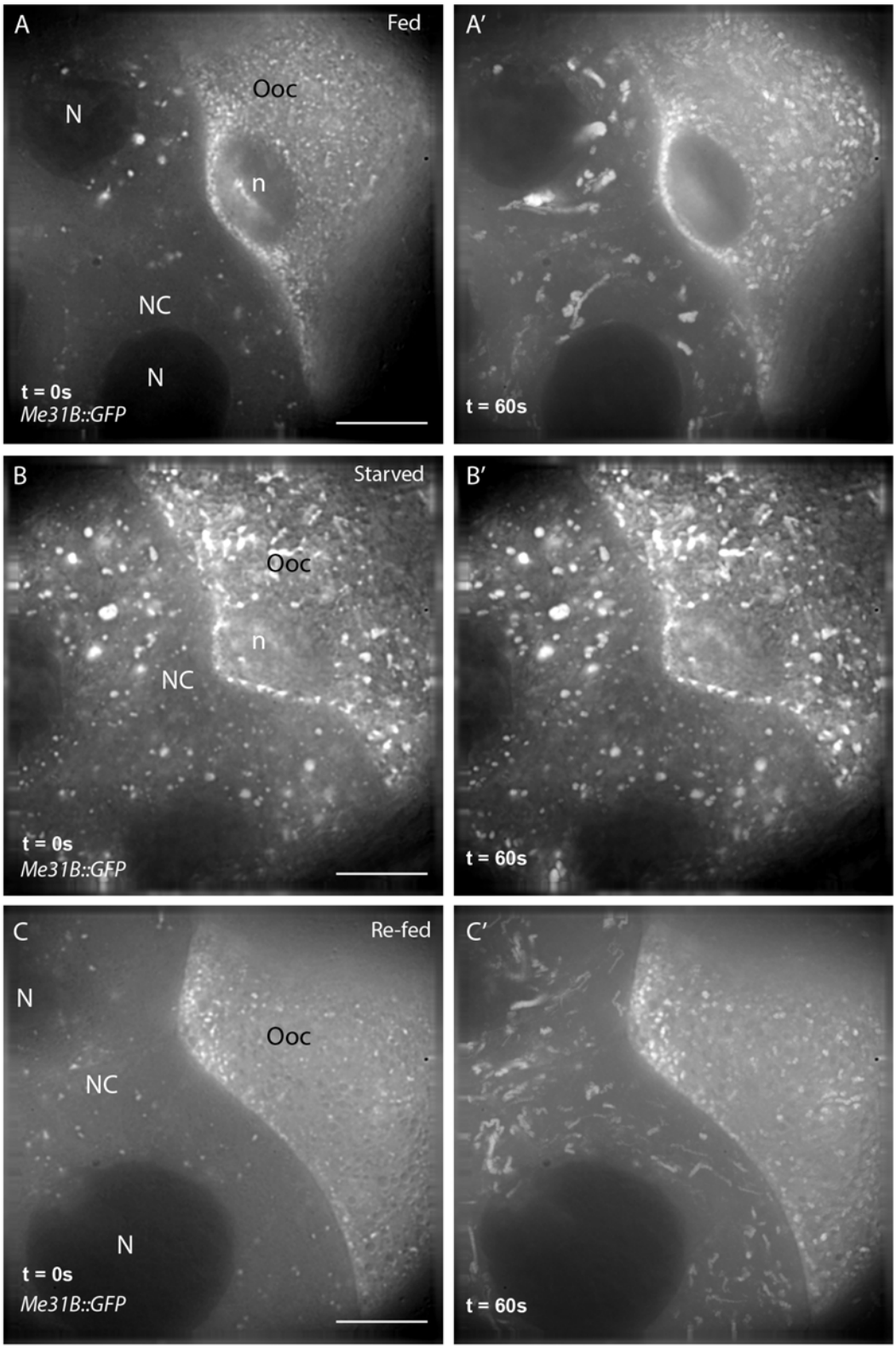

Figure 5-9:

(A-C"): Live cell imaging of *Me31B::GFP* egg chambers. (A), (B) and (C) are images at t=0s, (A'), (B') and (C') are trail images of 180 frames superimposed (from t=0 min to t=1 min, images collected at 3fps). (A-A'): In egg chambers from females fed on yeast for 24 hr, Me31B particle motility in the nurse cells is normal. (B-B'): When switched to an environment without yeast, Me31B bodies increase in size, number, and brightness, and particle motility is completely abolished. (C-C'): When females are re-fed on yeast for 12 hours, Me31B bodies revert to their normal characteristics and dynamics. All images acquired at 100x magnification, image series are deconvolved. NC, nurse cells; Ooc, oocyte; N, nurse cell nuclei; n, oocyte nucleus. Scale bars 15 μm.

Figure 5-10: The MS2 system cannot be used to visualise mRNA under nutrient stress

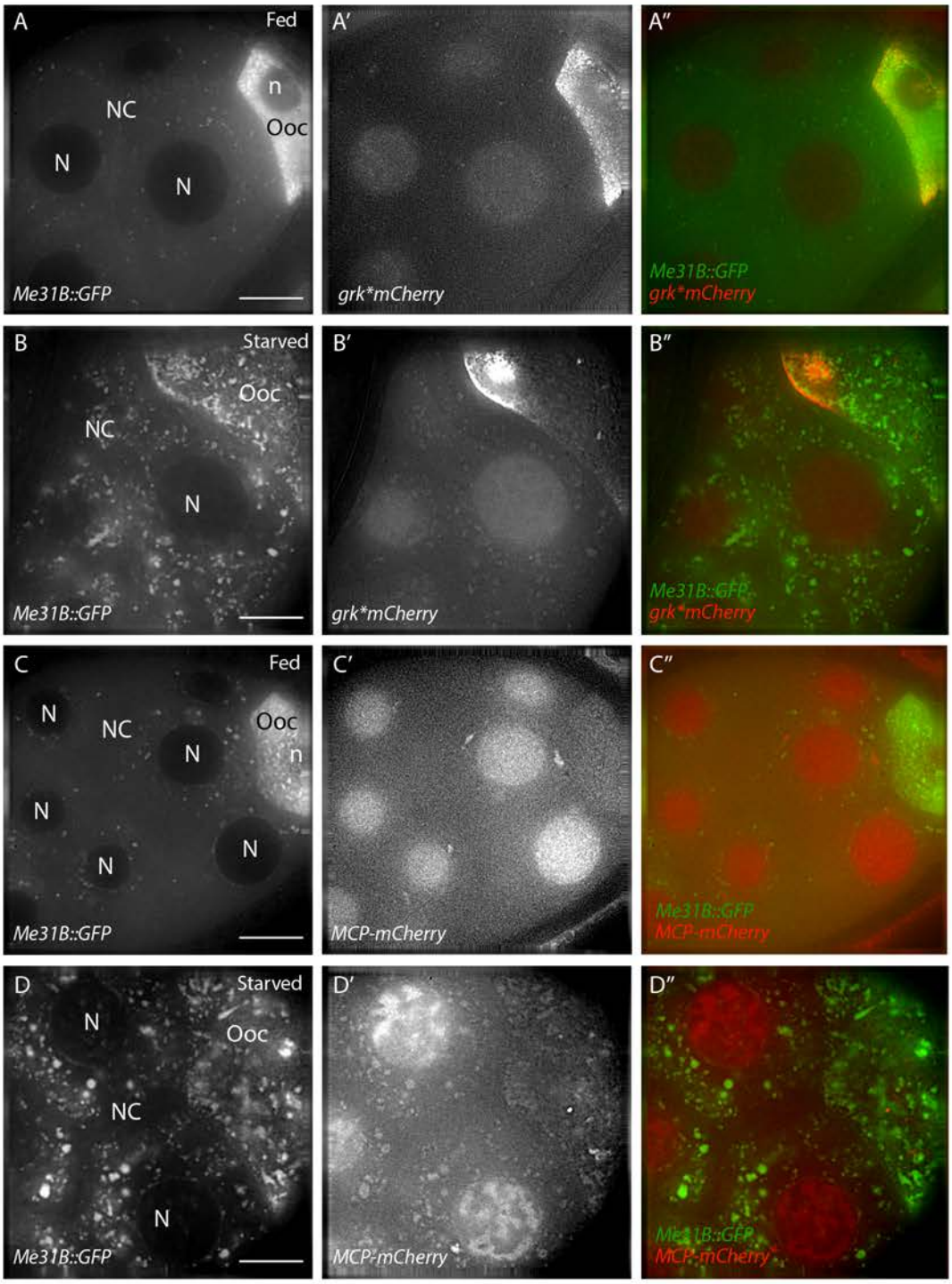

Figure 5-10:

(A-D”): Live cell imaging of egg chambers expressing *Me31B::GFP* and *grk*mCherry* (A-A”, B-B”) or Pnos-*MCP-mCherry* (C-C”, D-D”). In both genotypes, mCherry fluorescence is visible colocalising with Me31B bodies under nutrient stress (B-B”, D-D”) but not in fed conditions (A-A”, C-C”). The *Me31B::GFP* protein trap is much brighter than *grk*mCherry* or *Pnos-MCP-mCherry*, and so mCherry fluorescence is difficult to see in merged images (A”, B”, C”, D”). Images acquired at 100x magnification and deconvolved. NC, nurse cells; Ooc, oocyte; n, oocyte nucleus; N, nurse cell nuclei. Scale bars 15 μm.

Conclusion: Contrary to previous reports (Burn et al. 2015, Shimada et al. 2011), the MS2 system cannot be used to examine changes in the interactions between mRNA and P bodies under stress in nurse cells, as unbound MCP-FP aggregates in P bodies under nutrient stress.

A subset of trans-acting proteins are dynamic in nurse cells

To test whether other trans-acting factors of *grk* are dynamic in the nurse cell cytoplasm, I examined a number of fluorescently labelled protein lines. Particles of key trans-acting factors required for *grk* localisation, including Sqd, Heph, Bic-D and UAP56 (Mach & Lehmann 1997, McDermott et al. 2012, McDermott & Davis 2013, Meignin & Davis 2008, Norvell et al. 1999) were not visible in the nurse cell cytoplasm (Figure 5-11). However, particles of Vasa and Btz are visible in the nurse cells, and unlike *grk*, *osk* or Me31B, multiple particles undergo long runs along the same path in folds in the nurse cell nuclear envelope (Figure 5-12, supplementary movies 5-10 and 5-11).

Conclusion: Many trans-acting factors of *grk* do not appear to form particles in the nurse cell cytoplasm. Vasa and Btz move in a different fashion in the nurse cells to *grk* and *osk* mRNA or Me31B, suggesting a different mechanism of transport.

Figure 5-11: Particles of key trans-acting factors of *grk* are not visible in the nurse cell cytoplasm

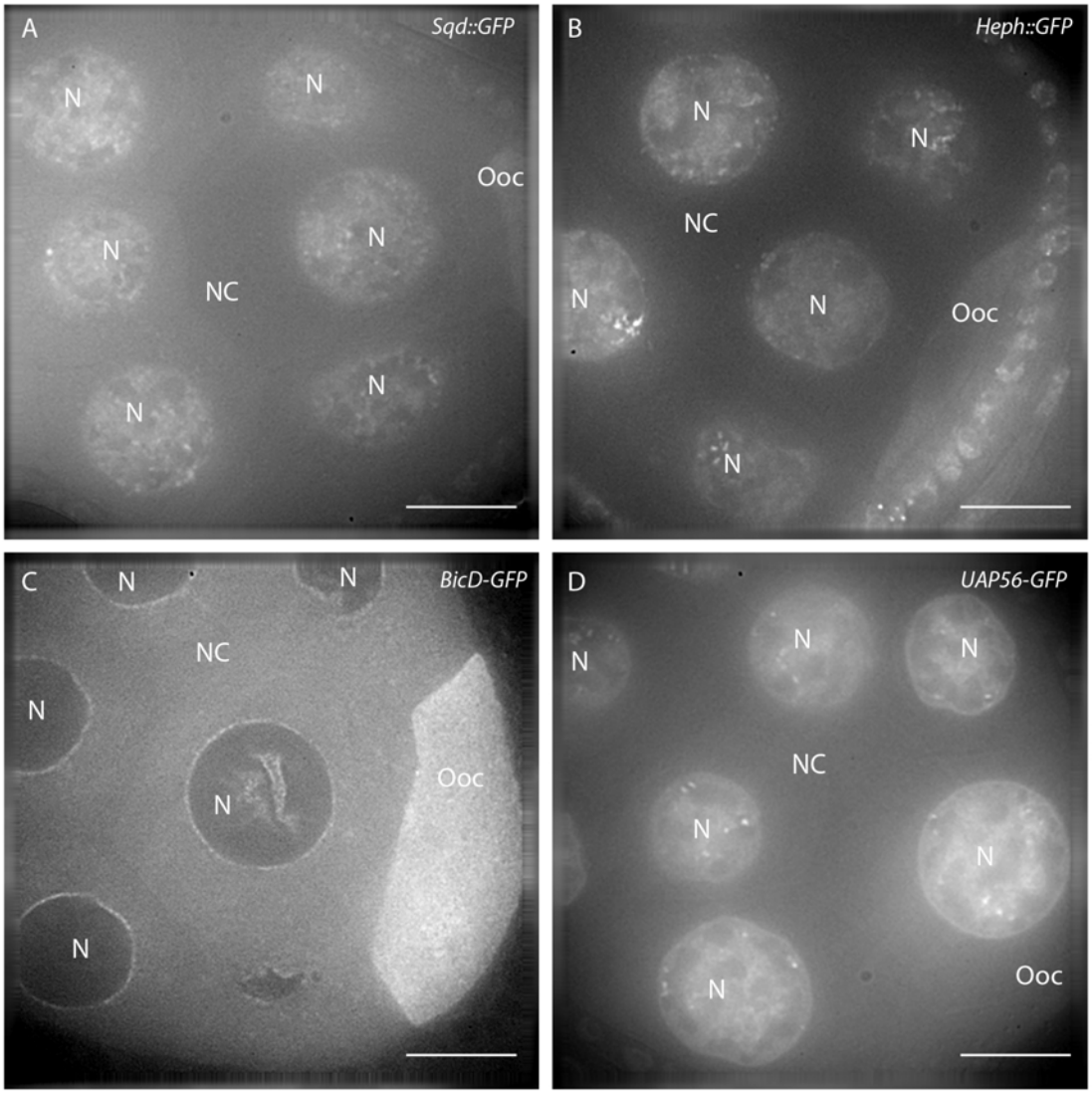

Figure 5-11:

(A-D): Fluorescent protein traps. Particles of Sqd (A), Heph (B), BicD (C) and UAP56 (D) are not visible in the nurse cell cytoplasm. Sqd (A), Heph (B) and UAP56 (D) are highly expressed in the nurse cell nuclei, whereas Bic-D (C) is highly expressed in the oocyte and in rings around the nurse cell nuclei. All images acquired at 100x magnification and deconvolved. NC, nurse cells; Ooc, oocyte; N, nurse cell nuclei. Scale bars 15 μm.

Figure 5-12: Vasa and Btz particles are highly dynamic in the nurse cells

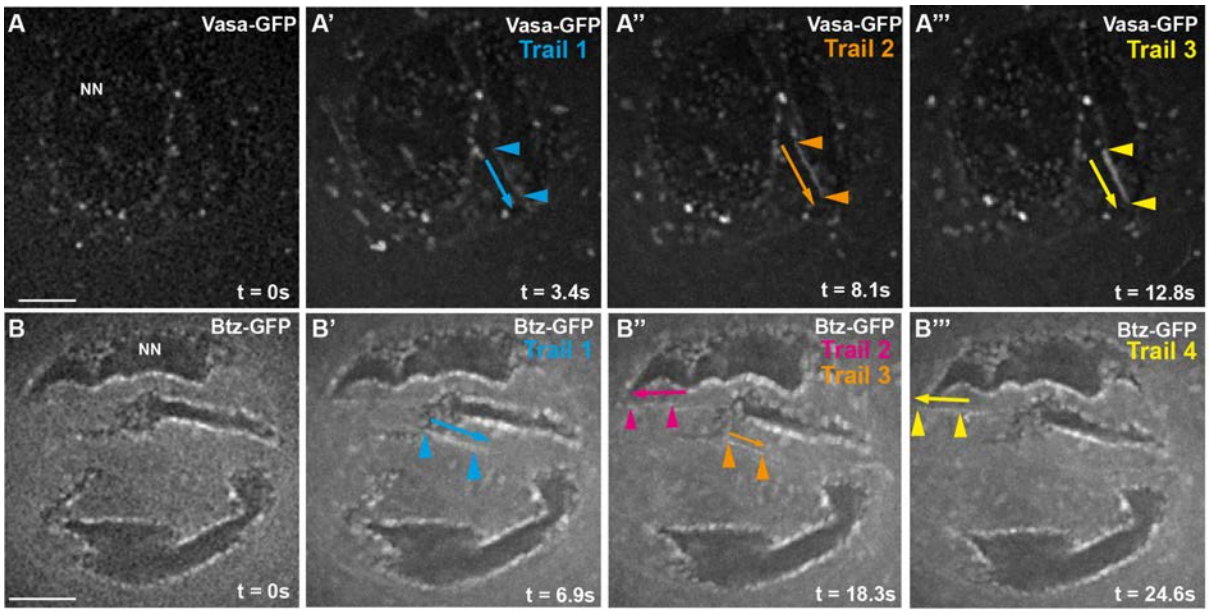

Figure 5-12:

(A-B'''): Live cell imaging of egg chambers expressing *vasa-GFP* (A-A''') or *Btz-GFP* (B-B'''). (A-A'''): Superimposed trail images showing multiple Vasa particles moving along the same track. Trail 1 (blue): 27 frames (t=0s to t=3.4s), trail 2 (orange): 36 frames (t=3.4s to t=8.1s), trail 3 (yellow): 36 frames (t = 8.1s to t = 12.8s). Images collected at 9 fps (B-B'''): Trail images showing multiple Btz particles moving along the same track. Trail 1 (blue): 24 frames (t=0s to t=6.9s), trail 2 (pink) and trail 3 (orange): 27 frames (t=10.5s to t=18.3s), trail 4 (yellow): 16 frames (t=19.8s to t=24.6s). Images collected at 4 fps, 100x magnification, image series are deconvolved. NN, nurse cell nucleus. Scale bars 5 μm.

Discussion

The protein complement of nurse cell P bodies is similar to those in the oocyte, but nurse cell P bodies contain less Orb

Here, I show that P bodies in the nurse cells are enriched for many of the same proteins as those in the oocyte, including translational repressors, and are devoid of ribosomes (Figure 5-1 to 5-3). However, the level of Orb protein in both nurse cell P bodies and the cytoplasm is lower than in the oocyte (Figure 5-4). Although it has been previously suggested that Orb is at lower levels in nurse cell P bodies (Snee & Macdonald 2009), the data I present here examine the ultrastructural characteristics and protein distribution of nurse cell P bodies, which has not been reported.

Why is Orb protein expression lower in the nurse cells? Orb protein translationally activates *orb* mRNA (Tan et al. 2001), and this autoregulatory loop is repressed in the nurse cells by Cup (Wong & Schedl 2011). Whether Orb protein expression can be increased in the nurse cells by disrupting this regulation will be explored in Chapter 7.

Orb is a translational activator of *grk*, *osk*, *K10* and *orb* mRNAs (Chang et al. 1999, Chang et al. 2001, Tan et al. 2001). *Xenopus* CPEB1, which is homologous to Orb, translationally activates some mRNAs but also binds and translationally represses mRNAs in immature oocytes via cooperation with Maskin. The reduced levels of Orb in the nurse cells suggest that: 1.) Low levels of Orb protein translationally repress mRNA, whereas high levels activate it, or 2.) In the egg chamber, Orb functions only to translationally activate, not repress, mRNAs. Both models are inconsistent with the role of CPEB in *Xenopus*, and will be explored further in Chapter 7.

Sqd protein was detected in nurse cell P bodies by IEM, but not immunofluorescence. This could be a penetrance issue, as when performing immunofluorescence on whole egg chambers, the nurse cell cytoplasm is beneath 20 μm of follicle cells, whereas ultrathin sections are 60 nm thick (Herpers et al. 2010) (Weil et al. 2012b). The Sqd antibody has also been previously reported to require heavy permeabilisation for immunofluorescence (T. Schupbach personal communication). However, IEM of *Sqd::GFP* with an anti-GFP antibody detects Sqd in nurse cells, but imaging of live and fixed *Sqd::GFP* flies cannot detect these bodies (Figure 5-3). This discrepancy should be further explored with different fixation, permeabilisation and staining parameters, as Sqd is thought to regulate *grk* anchoring in P bodies, and P body integrity (Delanoue et al. 2007, Weil et al. 2012b). Understanding the role of Sqd in P bodies and *grk* regulation is crucial.

P body dynamics in the nurse cells

I show that in nurse cells, Me31B, a P body marker, is present in large static bodies and small, dynamic particles, the motility of which requires microtubules (Figures 5-5 to 5-8). Like *grk* and *osk*, Me31B particles in the nurse cells move significantly faster than those in the oocyte. Together, these data suggest that transport of all particles in the nurse cells may be faster than in the oocyte, perhaps due to differences in cytoplasmic viscosity, density of yolk granules or organelles, or motor processivity (Amrute-Nayak & Bullock 2012, Soundararajan & Bullock 2014).

In contrast to *grk* and *osk*, most Me31B particles appear to be actively transported, but these particles move more slowly than the mRNAs. The similarity between the run lengths of actively transported Me31B and *grk* or *osk*, suggests they may move on the same cytoskeletal components. Me31B particles still move at speeds

indicative of active transport by motor proteins but move more slowly than *grk* and *osk*. Me31B, *grk* and *osk* particles are a similar size, suggesting the difference is not simply due to the size of the particle being transported. This discrepancy could be because of differences in the number or efficiency of motor proteins involved (Amrute-Nayak & Bullock 2012, Soundararajan & Bullock 2014).

Covisualisation of these particles with the cytoskeleton would provide insights into whether the mRNA and the proteins are moving on the same microtubules. Differences in speed could be examined by testing which motors are involved in the movement of *grk*, *osk* and Me31B particles with mutants (Clark et al. 2007, MacDougall et al. 2003) and pharmacological interventions (Firestone et al. 2013), as well as *in-vitro* analysis of the number and activity of motors recruited to these particles (Amrute-Nayak & Bullock 2012, Soundararajan & Bullock 2014). The higher proportion of actively transported Me31B particles compared to *grk* or *osk* could also be due to motor recruitment, and could be assessed with similar assays. Visualisation of Me31B, *grk* and *osk* on the OMX could assess the directionality of these particles, and they could be covisualised with fluorescently labelled cytoskeletal components (Parton et al. 2011) to characterise the polarity of nurse cell microtubules and how mRNAs and protein cofactors are transported into the oocyte.

Interestingly, it is unclear that these small particles are truly P bodies. By immunofluorescence, both small particles and large bodies of Me31B colocalise with other P body proteins (Figure 5-2). However, in the oocyte, transport particles containing *grk*, which are also non membrane bound and electron dense, contain different proteins to static sponge bodies at the DA corner (Delanoue et al. 2007). Further analysis of IEM data could test whether these dynamic particles are truly P

bodies, transport particles, or simply P body components moving to a new location, as the “liquid droplet” theory of P body motility hypothesis (Brangwynne 2013).

Dynamics of other trans-acting factors in the nurse cells

Unexpectedly, particles of UAP56, Bic-D, Sqd and Heph proteins are not seen in the nurse cell cytoplasm (Figure 5-11). These proteins are required for *grk* localisation and translational control (Mach & Lehmann 1997, McDermott et al. 2012, McDermott & Davis 2013, Meignin & Davis 2008, Norvell et al. 1999), and would be expected to move with the mRNA in the nurse cells. Indeed, Sqd and Heph bind the GLS in biochemical assays (McDermott et al. 2012). It is possible that my imaging methods cannot detect these proteins in the nurse cells. However, my systematic imaging approach visualises very faint mRNA particles in the nurse cells (Chapter 3). I imaged these egg chambers under many parameters, and worked closely with microscopists and image analysts in the Davis lab and Micron Oxford.

Alternatively, these proteins may not form microscopically visible particles. They may move with *grk* as single copies, or only associate with it when they are enriched at the oocyte DA corner. However, it is unlikely that *grk* is transported with no protein co-factors. It is possible that another, unknown factor, is bound to *grk* throughout its transport and excludes the trans-acting factors I have studied here, until *grk* reaches the DA corner. Generation of more fluorescently labelled proteins including Egl, Syncrip, Bruno, and Dynein, could answer this question.

Unlike other factors, Btz and Vas particles move in a unidirectional, highly processive fashion along the same tracks around nurse cell nuclei, which is strikingly different to how *grk*, *osk* and Me31B particles move (Figure 5-12). Vasa is enriched in the

perinuclear nuage (Zhang et al. 2012), and Btz is a cytoplasmic component of the EJC (Palacios et al. 2004, van Eeden 2001), suggesting that mRNA processing components may be enriched at the edge of the nurse cell nuclei by a distinct mechanism of transport. Further tracking of these particles, as well as testing which motors and cytoskeletal components are involved in their transport, could reveal why these proteins move differently to *grk*, *osk* and Me31B.

Btz and Vasa are required for regulation of *osk* and *grk* respectively (Johnstone & Lasko 2004, Styhler et al. 1998, van Eeden 2001). The association between *grk* and Vasa will be explored in chapter 6, but covisualisation of *osk* and Btz could reveal whether or not they move together. Btz would be expected to move with *osk* in the nurse cell cytoplasm. However, the difference in motility of *osk* and Btz suggests that not all mRNA particles are transported with the protein. Whether a subset of *osk* moves with Btz, and whether these mRNAs are regulated differently, could be tested with covisualisation of these components in live nurse cells.

Nurse cell P bodies in the stress response

osk, *grk* and *bcd* are thought to be targeted to nurse cell P bodies under nutrient stress (Burn et al. 2015, Shimada et al. 2011), and excess *grk* mRNA is targeted to the interior of oocyte P bodies (Weil et al. 2012b). Me31B body number and size increases under starvation, which disassemble when refed (Figure 5-9). However, both P bodies and stress granule formation increases under nutrient stress (Buchan et al. 2011, Kedersha et al. 2005, Teixeira et al. 2005), and in yeast Dhh1, the Me31B homolog (de Valoir et al. 1991, Nakamura et al. 2001), is found in both P bodies and stress granules. An analysis of the protein composition of these bodies using

antibody staining for P body and stress granule specific components is necessary before further conclusions about the function of these bodies can be drawn.

I aimed to test whether localised RNAs are stored in nurse cell P bodies during starvation, and released in nutrient rich conditions. However, unbound MCP-mCherry is enriched in P bodies under starvation, meaning the MS2 system cannot be used to study localised mRNAs in this context. sm-FISH of *grk* in the nurse cells could be used to study changes in *grk* association with P bodies under stress.

P body formation in the egg chamber

P bodies are crucial for translational regulation of *grk* and *bcd* mRNA in the oocyte (Weil et al. 2012b). However, how P bodies assemble during oogenesis is unclear. In the oocyte, smaller Me31B particles are in constant flux with larger static bodies (Weil et al. 2012b). Whether large nurse cell P bodies are maintained by constant turnover of small Me31B particles could be assessed with more detailed tracking of these particles. This could be combined with mutants and pharmacological reagents to examine the role of Dynein and microtubules in P body assembly. Dynein is required for P body integrity (Delanoue et al. 2007) and microtubules and Dyenin are involved in P body formation under stress conditions (Burn et al. 2015, Shimada et al. 2011). If Dynein is also involved in the transport of P body components, dissecting its function in these processes, could be difficult. Sqd is also necessary for the conversion of transport particles into sponge bodies at the oocyte DA corner (Delanoue et al. 2007), and examining nurse cell P bodies in *sqd*^{1} mutants could test whether Sqd also functions to maintain these bodies.

In other systems, the steps of the mRNA cycle, the mechanism of P body assembly, and the sequences which confer gel-like properties of P bodies have been explored (Brangwynne 2013, Decker & Parker 2012, Han et al. 2012, Kato et al. 2012). A similar understanding of the mechanism of P body assembly in *Drosophila* is lacking. Analysis of intrinsically disordered regions in *Drosophila* P body proteins, whether they have a role in P body formation, and biochemical analysis of the complexes formed by these proteins, is necessary to understand P body function in *Drosophila*.

Final conclusions

Here I have characterised the protein composition and dynamics of nurse cell P bodies. I have demonstrated that nurse cell P bodies differ from those in the oocyte as they contain lower levels of Orb protein, but the core of nurse cell P bodies appears to be a translationally silent environment similar to those in the oocyte. I have shown that Me31B, a canonical P body marker, is highly dynamic in the nurse cells, and that P bodies in the egg chamber are altered under nutrient stress. In the next two chapters I will examine the role of P bodies in translational regulation of *grk* in the nurse cells.

Tables and statistics

Genotype (n particles)	% Active transport	% Paused	% Static	% Large bodies
*grk*GFP* (340)	29	50	21	0
*osk*GFP* (387)	24	40	36	0
Me31B::GFP (89)	56	23	11	10

Table 5-1: Classes of Me31B particles in the nurse cells

Percentage of Me31B particles which were classed as actively transported, paused, static, or as large bodies, as detailed in Appendix F. The same analysis for *grk* and *osk* from Chapter 3 is provided for reference. Far more Me31B particles are actively transported than either *grk* or *osk*, and far fewer are paused or static.

Particle class (n)	Velocity (μm/s)	Run length (μm)
Total Me31B nurse cell (70)	0.684 ± 0.04	2.355 ± 0.25
Total Me31B oocyte (30)	0.230 ± 0.31	Not available
AT Me31B nurse cell (50)	0.699 ± 0.06	2.975 ± 0.31
Paused Me31B nurse cell (20)	0.648 ± 0.09	0.806 ± 0.08
Large bodies nurse cell (10)	0.205 ± 0.04	2.172 ± 0.59

Table 5-2: Dynamics of Me31B in the nurse cells

Average velocities and run lengths of Me31B in the nurse cells and oocyte, and selected sub-classes of Me31B in the nurse cells. Velocities in μm/s ± s.e.m, run lengths in μm ± s.e.m. The velocity and run length of large bodies was not compared to the other sub-classes due to low n numbers. Static particles do not move and are not included in this analysis. Run lengths in the oocyte were not collected in previous analyses (Weil et al. 2012b).

P values from Student's t-tests (two tails), P = <0.001.

Velocity statistics:

AT Me31B nurse cell vs total Me31B oocyte: significant, P = 0.0001

Paused Me31B nurse cell vs total Me31B oocyte: significant, P = 0.0001

Total Me31B nurse cell vs total Me31B oocyte: significant, P = 0.0001

AT Me31B nurse cell vs paused Me31B nurse cell: not significant, P = 0.601

Run length statistics:

AT Me31B nurse cell vs paused Me31B nurse cell: significant, P = 0.0001

Particle class (n)	Velocity (μm/s)	Run length (μm)
Total nurse cell Me31B (70)	0.684 ± 0.04	2.355 ± 0.25
Total nurse cell *grk* (91)	0.931 ± 0.05	1.546 ± 0.30
Total nurse cell *osk* (90)	0.920 ± 0.05	1.324 ± 0.16
AT Me31B nurse cell (50)	0.699 ± 0.06	2.975 ± 0.31
AT *grk* nurse cell (33)	1.163 ± 0.08	2.785 ± 0.66
AT *osk* nurse cell (33)	1.118 ± 0.10	2.245 ± 0.38
Paused Me31B nurse cell (20)	0.648 ± 0.09	0.806 ± 0.08
Paused *grk* nurse cell (58)	0.798 ± 0.6	0.840 ± 0.06
Paused *osk* nurse cell (57)	0.806 ± 0.04	0.790 ± 0.04

Table 5-3: Comparison of Me31B, *grk* and *osk* dynamics in the nurse cells

Average velocities and run lengths of Me31B, *grk* and *osk* in the nurse cells, and selected sub-classes of these particles in the nurse cells. Velocities in μm/sec ± s.e.m, run lengths in μm ± s.e.m. Static particles do not move and are not included in this analysis. Statistical comparisons between *grk* and *osk* data from chapter 3 is presented in table 3-3, and is not included in this table.

P values from Student's t-tests (two tails), P = <0.001.

Velocity statistics:

AT *grk* nurse cell vs AT Me31B nurse cell: significant, P = 0.0001

Paused *grk* nurse cell vs paused Me31B nurse cell: not significant, P = 0.141

Total *grk* nurse cell vs total Me31B nurse cell: significant, P = 0.0002

AT *osk* nurse cell vs AT Me31B nurse cell: significant, P = 0.0001

Paused *osk* nurse cell vs paused Me31B nurse cell: not significant, P = 0.101

Total *osk* nurse cell vs total Me31B nurse cell: significant, P = 0.0001

Run length statistics:

AT *grk* nurse cell vs AT Me31B nurse cell: not significant, P = 0.795

Paused *grk* nurse cell vs paused Me31B nurse cell: not significant, P = 0.726

Total *grk* nurse cell vs total Me31B nurse cell: significant, P = 0.0001

AT *osk* nurse cell vs AT Me31B nurse cell: not significant, P = 0.139

Paused *osk* nurse cell vs paused Me31B nurse cell: not significant, P = 0.850

Total *osk* nurse cell vs total Me31B nurse cell: significant, P = 0.0001

NB: The significant difference in run length between total nurse cell Me31B and total nurse cell *grk* and *osk* is most likely due to the higher proportion of nurse cell Me31B particles which are actively transported, as AT and paused *grk* and *osk* particles move over similar run lengths to AT and paused Me31B particles.

Chapter 6: *grk* mRNA translational control in nurse cells

Introduction

mRNA translational regulation is essential for targeted protein expression. The localisation and translational regulation of *grk* mRNA in both the nurse cells and the oocyte is essential for establishing the dorsoventral axis in *Drosophila* oogenesis. Previous work by a number of labs suggests a suite of repressor proteins including Sqd, Bruno, Cup, Hrb27C and Otu (Clouse et al. 2008, Filardo & Ephrussi 2003, Goodrich et al. 2004, Norvell et al. 1999) regulate *grk* translation. However, the prevailing model of regulation during transport does not explain how *grk* mRNA is translationally repressed whilst being transported in the nurse cells. To answer this question, one approach is to investigate proteins involved in translational regulation of *bcd* and *osk* mRNA, and those with putative roles in *grk* translational control.

Putative repressors of *grk* translation

me31B encodes a DEAD-box helicase, which is expressed in the core of P bodies in nurse cells and the oocyte, where *bcd* is targeted and is translationally repressed (Nakamura et al. 2001, Weil et al. 2012b). Me31B is required for the translational silencing of *osk* and *BicD* in the nurse cells (Nakamura et al. 2001). Me31B binds to *grk* (McDermott et al. 2012), and when excess *grk* mRNA is introduced in the oocyte, *grk* is directed to the P body core. These data suggest that Me31B may repress *grk* translation in the nurse cells, as it does for *osk*.

Bruno is an RNA binding protein which binds BREs in the *osk* 3' UTR, repressing *osk* by two mechanisms. It acts with PTB to induce the formation of silencing *osk*

oligomers (Besse et al. 2009, Chekulaeva et al. 2006) and recruits Cup, which binds to eIF4E and prevents translation initiation (Nakamura et al. 2004, Wilhelm 2003). The dosage of the *aret* gene affects dorsal-ventral polarity (Filardo & Ephrussi 2003), and Bruno can bind to the *grk* 3' UTR (Filardo & Ephrussi 2003, Kim-Ha et al. 1995, Norvell et al. 1999). Overexpression of Bruno may prevent *grk* translation, but this is disputed (Filardo & Ephrussi 2003, Snee et al. 2007). Like Me31B, Bruno is enriched in the translationally silent core of P bodies at both the oocyte DA corner (Weil et al. 2012b), and in the nurse cells (this work). Furthermore, *grk* is ectopically translated in the nurse cells of *aret* and S^{1} double mutants (Yan & Macdonald 2004), suggesting Bruno may regulate *grk* translation in some cases.

sqd is required for correct dorsal-ventral patterning (Kelley 1993), and encodes three hnRNP protein isoforms, SqdA, B and S, which have non-equivalent roles in *grk* localisation (Norvell et al. 1999). When all germ line isoforms of Sqd are mutated in sqd^{1} mutant egg chambers, *grk* mRNA and Grk protein are mislocalised along the oocyte anterior (Jaramillo et al. 2008, Norvell et al. 1999). Biochemical analysis indicates that Sqd interacts with Bruno, Cup and *grk* (Clouse et al. 2008, Norvell et al. 1999), and mediates the association of *grk* mRNA with translationally repressed RNPs (Li et al. 2014). When half of the nurse cells are unable to produce Sqd (but the oocyte is wild-type), *grk* is localised correctly but is translated ectopically along the anterior margin (Cáceres & Nilson 2009). These data suggest that exposure to Sqd is required in the nurse cells for *grk* translational regulation in the oocyte.

However, in sqd^{1} mutants, *grk* transport from the anterior margin to the DA corner is disrupted (MacDougall et al. 2003), and mislocalised *grk* mRNA at the anterior margin is dynamic, not anchored as it is at the DA corner (Jaramillo et al. 2008). This

anchoring of *grk* at the DA corner requires Sqd, where it converts Dynein from a motor into a static anchor (Delanoue et al. 2007). Sqd is also enriched at the edge of P bodies in the DA corner of the oocyte and has been suggested to act here to anchor *grk* (Weil et al. 2012b). It is difficult to separate the role of Sqd in both *grk* localisation and translational control, and no evidence has been presented for Sqd as a repressor of *grk* during nurse cell transport.

The activity of the *K10* gene, which encodes a protein with a helix-loop-helix DNA binding domain, is required for dorsoventral patterning (Wieschaus et al. 1978). However, some report that in *K10* mutants *grk* is mislocalised along the anterior margin (Neuman-Silberberg & Schupbach 1993, Roth & Schupbach 1994), others argue that *grk* localisation is normal, but that Grk protein is expressed ectopically along the anterior margin (Saunders & Cohen 1999). This suggests a possible role for *K10* in *grk* translational regulation.

The fly homolog of the mammalian SYNCRIP/hnRNPQ, *Drosophila* Syncrip, is involved in mRNA localisation in oogenesis and the nervous system (Halstead et al. 2014, McDermott et al. 2012, McDermott et al. 2014). Both Syncrip mutants and flies overexpressing Syncrip cause mislocalisation of *grk* mRNA and Grk protein expression throughout the oocyte, and dorsoventral patterning defects (McDermott et al. 2012). Interestingly, when Syncrip is overexpressed, Grk protein is visible in rings around the nurse cell nuclei (McDermott et al. 2012). Although these data suggest that Syncrip does not translationally repress *grk*, these lines may reveal changes in the expression or localisation of other proteins regulating *grk* translation.

More generally, it appears that in the oocyte *grk* is translationally repressed by saturable repression machinery. When *grk* is overexpressed, *grk* mRNA and protein are mislocalised along the oocyte anterior, causing dorsoventral patterning defects (Bökel et al. 2006, Weil et al. 2012b). Similarly, when *osk* is overexpressed, Osk protein is expressed in large assemblies in the nurse cells (Snee & Macdonald 2004). If there is *grk* translational repression machinery in the nurse cells, one would expect *grk* overexpression to cause ectopic Grk protein expression in this tissue.

Alternative mechanisms of *grk* translational control

At the oocyte DA corner, differential association with P bodies mediates the repression of *bcd* and the translation of *grk* (Weil et al. 2012b). *grk* could be translationally repressed by being transported in the core of nurse cell P bodies, similar to “transport particles” in the oocyte which contain *grk* (Delanoue et al. 2007).

Many of the factors involved in *osk*, and possibly *grk*, translational control are highly conserved and have been studied biochemically in *Xenopus* oocytes, where cytoplasmically polyadenylated mRNAs are maintained in a translationally silent state by binding of inactive forms of translational activator proteins (Richter & Lasko 2011). Unphosphorylated CPEB bound to Maskin mediates translational repression of mRNAs in immature oocytes, but at fertilisation translationally activates these mRNAs. *grk* mRNA could be repressed by a similar mechanism. The conserved DEAD-box helicase Vasa interacts with eIF5B and is required for the translation of *grk* (Johnstone & Lasko 2004, Styhler et al. 1998). If *grk* is packaged with inactive forms of its translational activators in nurse cells, one would expect Vasa and *grk* to move together in the nurse cells. The role of Orb, which is expressed at low levels in the nurse cells (Chapter 5), will be tested in Chapter 7.

These proteins are candidates for translational repressors of *grk*. Cup is a putative repressor of *grk*, and will be examined in Chapter 7 alongside Orb. There are other proteins with roles in *grk* localisation which are possible, if unlikely, candidates for *grk* repressors in the nurse cells. These include Imp, (Geng & Macdonald 2006), and Heph (McDermott & Davis 2013), and were not tested due to time constraints and availability of fly lines. Moreover, no data shows *grk* translation in the nurse cells of these mutant egg chambers (Geng & Macdonald 2006, McDermott & Davis 2013).

I did not test the role of *spindle*-class genes such as *spnB*, or *lnk* gene activity. These genes have been extensively characterised by the Schupbach lab, and they do not appear to repress *grk* translation, but activate it. Moreover, these genes act only when the meiotic DNA damage checkpoint is activated, suggesting they do not represent the canonical mechanism of *grk* translational control (Abdu et al. 2002, Ghabrial & Schupbach 1999, Li et al. 2014). Similarly, I have not test mutants for positive regulators of *grk*, including Vasa and Encore. I did not have time or reagents to examine *spoon* mutants, where Grk protein is expressed in the nurse cells (Motola & Neuman-Silberberg 2004). Moreover, this seems more likely to be a failure of *grk* mRNA trafficking into the oocyte, rather than just translational repression.

Aims of this chapter and experimental rationale

In this chapter I test whether the most likely candidate translational repressor proteins regulate *grk* translation during its transport in the nurse cells. Specific questions include:

- **Is *grk* translated in the nurse cells when its putative repressors are mutated?**
- **Does overexpression of *grk* cause Grk protein expression in the nurse cells?**
- **Is *grk* associated with P bodies in nurse cells?**
- **Does *grk* move within the P body core in nurse cells?**
- **Does *grk* move with Vasa in nurse cells?**

To determine whether the proteins tested regulate *grk* translation in the nurse cells, I examined fixed mutant egg chambers with immunofluorescence using a Grk protein antibody. It is not currently possible to isolate nurse cell material specifically for biochemical analysis, so biochemical quantitation of protein levels was not feasible. To test whether *grk* is maintained in a translationally silent state by transport within the core of nurse cell P bodies, I co-visualised *grk* mRNA labelled with sm-FISH and the MS2 system with *Me31B::GFP*. The DeltaVision widefield microscope allows visualisation of endogenously processed *grk* mRNA in the nurse cells (Chapter 3), and has been used to covisualise mRNA and P bodies in oocytes (Weil et al. 2012b).

Results

In *me31B* mutant egg chambers Grk is absent from the nurse cells

To test whether Me31B translationally represses *grk* in the nurse cells, I examined the distribution of Grk protein in *me31B* mutant egg chambers. Egg chambers which completely lack *me31B* die during oogenesis, so I used *me31B* germline clones (Nakamura et al. 2001). Flies where the *me31B* mutant locus is flanked with FRT40A sites are then crossed to *hsFLP/w;gfp FRT40A* flies. Heat shocking the progeny of this cross induces mitotic recombination by activating hsFLP recombinase expression, and recombination between the FRT sites on the *me31B* mutant and *vasa-GFP* loci causes some egg chambers to inherit two copies of the *me31B* mutation and no copies of *vasa-GFP*. *me31B* mutant egg chambers are distinguished from wild-type egg chambers in the same ovariole as they lack *vasa-GFP* staining.

To verify that these germline clones are functional, I stained for Me31B in *hsFLP/w; me31B$^{\Delta 1}$ FRT40A/vas-gfp FRT40A* egg chambers (Nakamura et al. 2001). In egg chambers not expressing *vasa-GFP*, there is also no Me31B staining (Figure 6-1). Wild-type egg chambers within the same ovariole express both *vasa-GFP* and Me31B. In *me31B* null egg chambers, Osk protein is ectopically expressed in the nurse cells (Nakamura et al. 2001). To test whether *grk* is also ectopically translated in the nurse cells of these mutants, I stained for Grk protein in *me31B* null egg chambers. Grk protein is restricted to the oocyte with no nurse cell staining (Figure 6-2, n=30). Because these mutant egg chambers degenerate during early oogenesis, mutant egg chambers were normally stage 6 or earlier. This is before *grk* is completely localised at the DA corner, but *grk* is still translated in the oocyte.

Conclusion: Me31B alone does not repress *grk* translation in the nurse cells.

Figure 6-1: *me31B* germline clones which do not express *vasa-GFP* are *me31B* null mutants

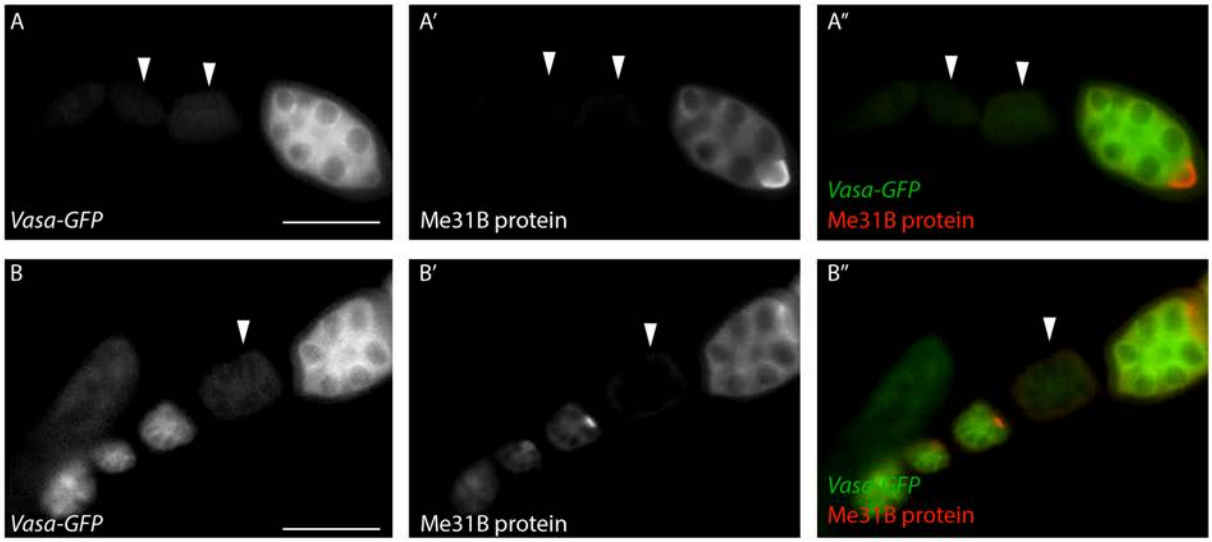

Figure 6-1:

(A-B"): Heat-shocked *me31B* germline clones, *vasa-GFP* (green), stained with anti-Me31B (red). White arrowheads mark *me31B* null egg chambers which do not express *vasa-GFP* or Me31B protein. Images acquired at 20x magnification. Scale bars 50 μm.

Figure 6-2: Grk expression is restricted to the oocyte in *me31B* mutant egg chambers

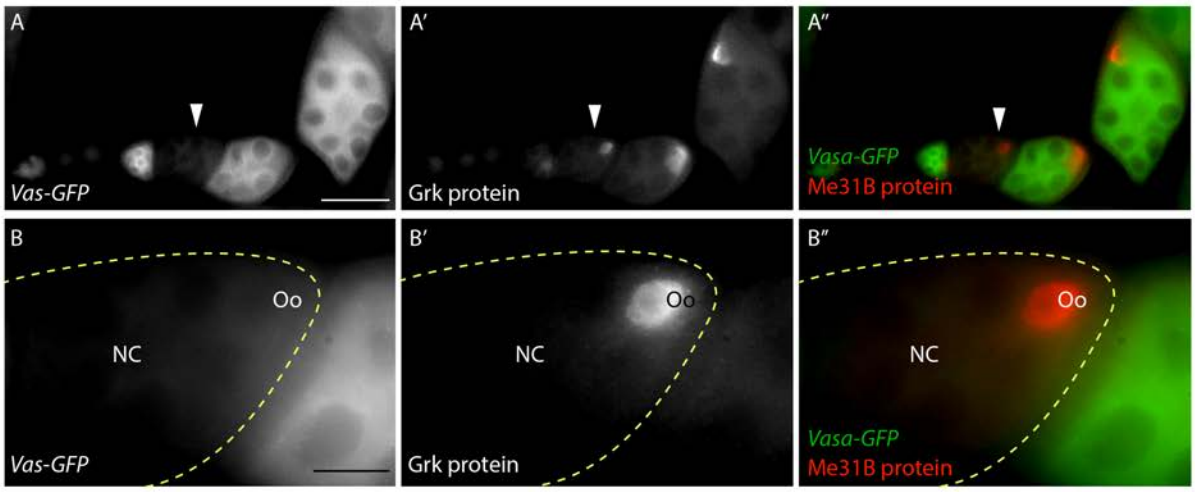

Figure 6-2:

(A-B”): Heat-shocked *me31B* germline clones, *vasa-GFP* (green), stained with anti-Grk (red). (B-B”); 100x magnification close up of egg chamber labelled with white arrowhead in (A): In *me31B* mutant egg chambers, Grk protein expression is restricted to the oocyte and absent from the nurse cells. White arrowheads mark *me31B* mutant egg chambers, dotted yellow line indicates the edge of the egg chamber. Images in (A-A”) acquired at 20x magnification, images in (B-B”) acquired at 100x magnification. NC, Nurse cells; Oo, oocyte. Scale bars 50 μm (A-A”), 15 μm (B-B”).

In *aret* mutant egg chambers Grk is absent from the nurse cells

Bruno translationally regulates *osk* via multiple mechanisms (Chekulaeva et al. 2006, Nakamura et al. 2004, Wilhelm 2003), and may repress *grk* translation in the oocyte (Filardo & Ephrussi 2003). To test whether Bruno represses *grk* translation in nurse cells, I visualised Grk protein in *aret* allelic combinations. $aret^{PD41}$ and a deficiency is the weakest combination, followed by $aret^{PD41/PA62}$ and $aret^{PD41/QB72}$ is the strongest allelic combination (Schupbach & Wieschaus 1991, Yan & Macdonald 2004). In all mutants, no Grk protein was detected in the nurse cells (Figure 6-3, n=60 per combination). Grk expression in the oocyte is restricted to the DA corner around the oocyte nucleus as in wild-type egg chambers, and mutant eggs had normal dorsal appendages, indicative of wild-type Grk expression.

To test whether Bruno can repress *grk* translation in the oocyte, I visualised Grk protein in *TubulinGal4VP16/UAS-bru* egg chambers (Filardo & Ephrussi 2003). Grk protein is expressed at the DA corner with no reduction compared to wild-type egg chambers (Figure 6-4 A-A')). These flies laid eggs with wild-type dorsal appendages, not ventralised as previously reported (Filardo & Ephrussi 2003).

Due to these inconsistencies, I tested by immunofluorescence whether these flies were actually overexpressing Bruno. However, Bruno antibody staining did not yield useful results, most likely because it failed to penetrate the tissue. Despite multiple attempts, the antibody was detected only in the follicle cells, not the germ line tissues where Bruno is expressed (Figure 6-4 (B-B')). I did not test the *UAS-bru* lines any further. Although it is possible that these flies have since stopped expressing the *UAS-bru* transgene, I did not see a phenotype for *grk* translational control as previously reported (Filardo & Ephrussi 2003).

Figure 6-3: Grk expression is restricted to the oocyte in *aret* mutant egg chambers

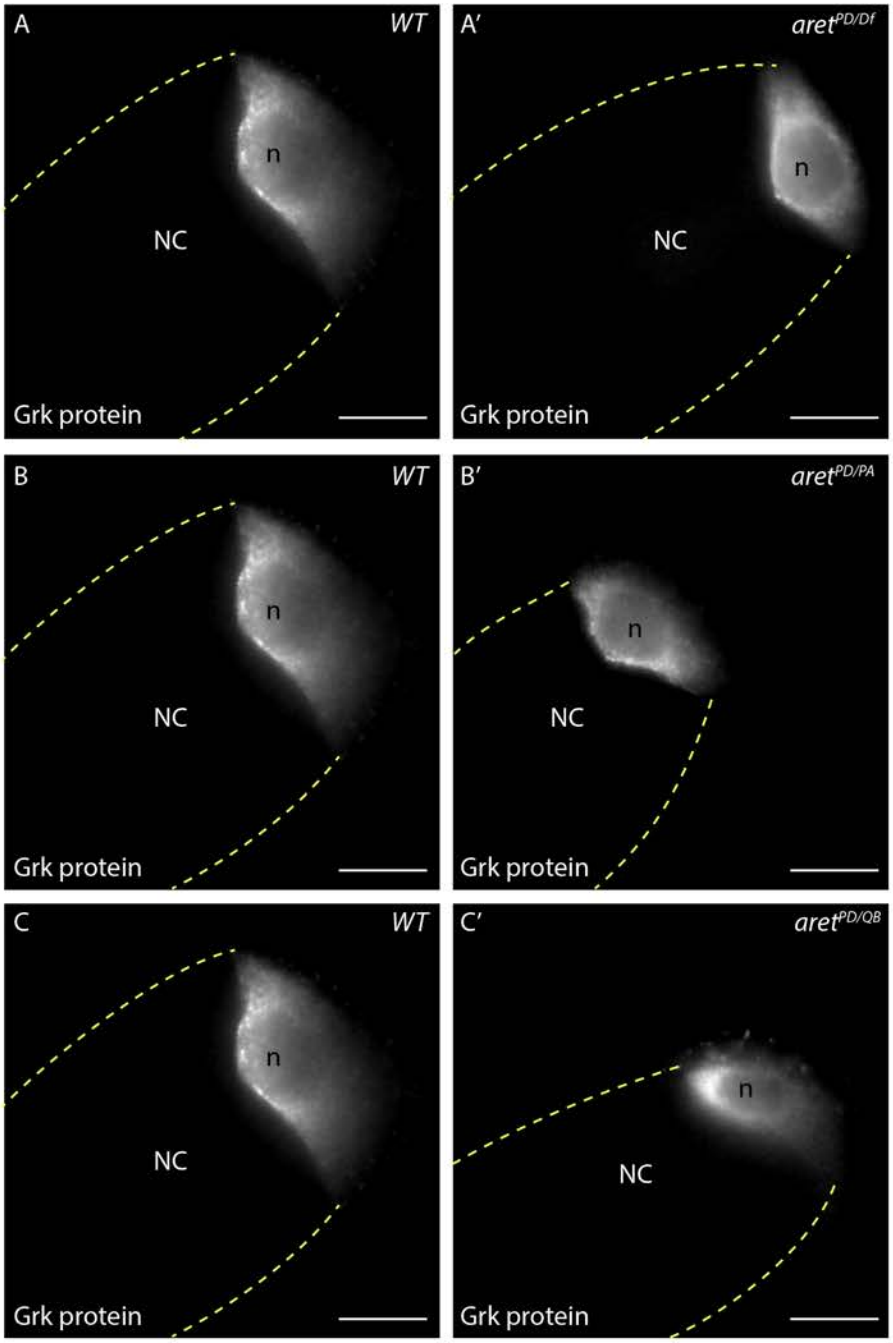

Figure 6-3:

(A-C'): Egg chambers stained for with anti-Grk. (A, B, C):In wild-type (*WT*) egg chambers Grk protein expression is restricted to the oocyte and absent from the nurse cells. This pattern of expression is also seen in weak (A'), medium (B') and strong (C') *aret* allelic combinations. Dotted yellow lines indicate the edge of the egg chamber. All images acquired at 100x magnification. NC, nurse cells; n, oocyte nucleus. Scale bars 15 μm.

Figure 6-4: In *UAS-bru* egg chambers, Grk expression in the oocyte is normal. Bruno antibody staining is not successful in fixed egg chambers

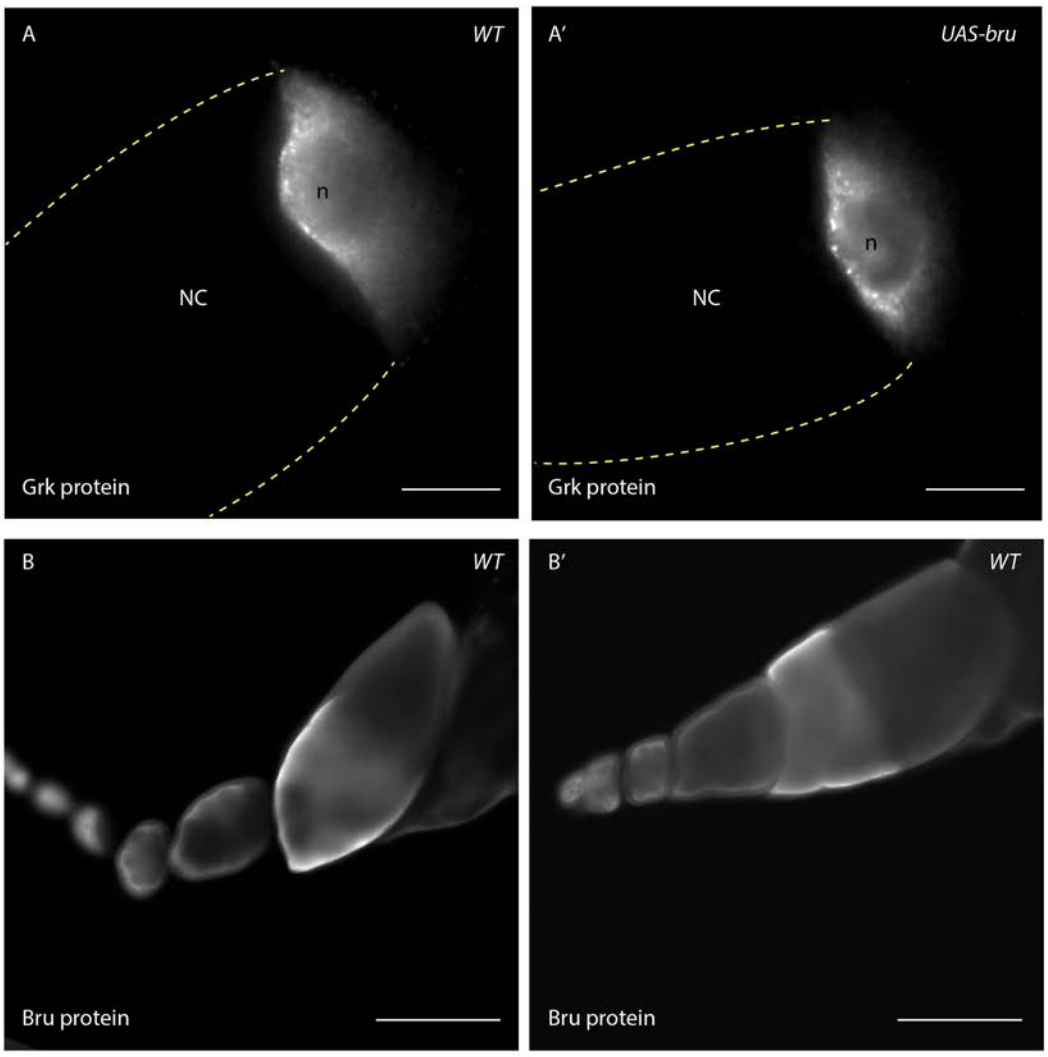

Figure 6-4:

(A-A'): Egg chambers stained for with anti-Grk. (A): In *WT* egg chambers Grk protein expression is restricted to the oocyte and enriched around the oocyte nucleus. (A'): This pattern of expression is also seen in *UAS-bru* egg chambers. (B-B'): Wild-type egg chambers stained for with Anti-Bru. Fluorescence is seen in the follicle cells and at low levels in the oocyte and nurse cells, suggesting poor antibody penetrance into the tissue. Dotted yellow lines indicate the edge of the egg chamber. Images in (A-A') acquired at 100x magnification, images in (B-B') acquired at 20x magnification. NC, nurse cells; n, oocyte nucleus. Scale bars 15 μm (A), 100 μm (B) .

Conclusion: Bruno alone is not required for translational repression of *grk* in the nurse cells, and the role of Bruno in *grk* translational control in the oocyte is still unclear and should be studied further.

In *sqd*^{1} mutant egg chambers Grk is absent from the nurse cells

Sqd is required for correct *grk* localisation in the oocyte (Delanoue et al. 2007) (Jaramillo et al. 2008, MacDougall et al. 2003), and is thought to translationally repress *grk* during its transport (Clouse et al. 2008, Goodrich et al. 2004, Li et al. 2014, Norvell et al. 1999). *grk*RFP* is mislocalised in *sqd*^{1} mutant egg chambers (Jaramillo et al. 2008), and *grk* RNA injected into *sqd*^{1} egg chambers does not localise correctly (MacDougall et al. 2003). However, endogenous (non-injected and non-MS2 labelled) *grk* mRNA has not been shown to be mislocalised in these egg chambers. To test whether Sqd is important for endogenous *grk* localisation, I performed sm-FISH on *sqd*^{1} mutant egg chambers, which has not previously been used to address this question. In these mutants *grk* is mislocalised along the whole anterior margin (Figure 6-5 (A-A', B-B')).

I then tested whether or not Sqd is involved in translational repression in the nurse cells by examining Grk protein distribution in *sqd*^{1} egg chambers. Grk protein is ectopically expressed along the anterior margin of the oocyte as previously reported (Norvell et al. 1999). However, there is no ectopic Grk expression in the nurse cells of these egg chambers (Figure 6-5 (C-C'), n=60).

Conclusion: Sqd is required for *grk* localisation in the oocyte, but not for translational repression of *grk* in the nurse cells.

Figure 6-5: In *sqd*[1] egg chambers, *grk* mRNA and Grk protein are mislocalised in the oocyte, but Grk is not expressed in the nurse cells

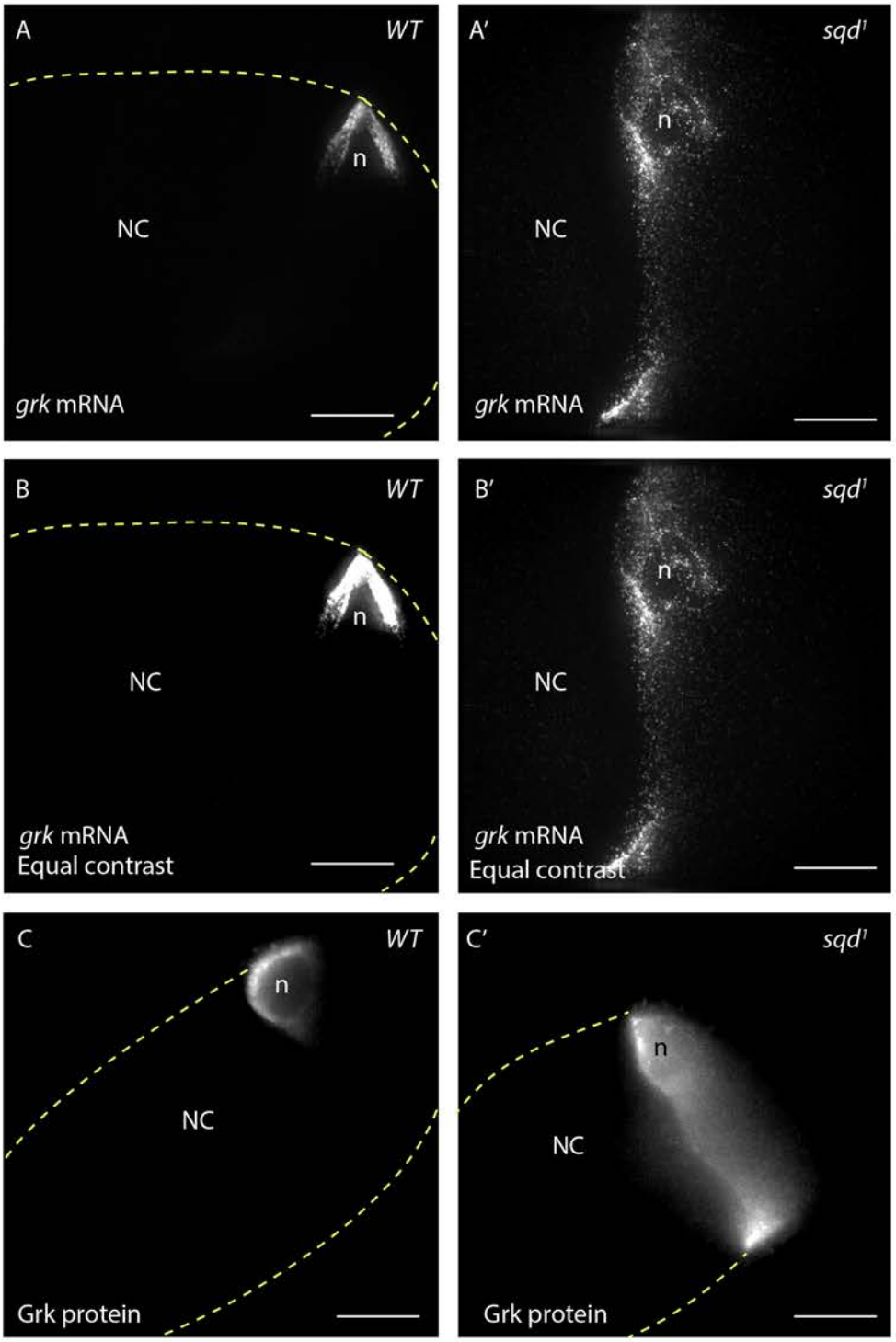

Figure 6-5:

(A-B'): Egg chambers labelled with *grk* sm-FISH probes (Cal Fluor 590). (A): In *WT* egg chambers *grk* is localised to the DA corner of the oocyte. (A'): In *sqd*^{1} egg chambers *grk* is mislocalised along the anterior margin. Images in (A) and (A') are contrasted for best display. (B) and (B') are the same images contrasted equally; note the higher fluorescence intensity of the signal at the DA corner in (B) compared to (B'), indicating a redistribution of *grk* rather than an increase in mRNA levels. (C-C'): Egg chambers stained for with anti-Grk. In *sqd*^{1} egg chambers Grk is expressed along the anterior margin, but not in the nurse cells (C'). Dotted yellow lines indicate the edge of the egg chamber. NC, nurse cells; n, oocyte nucleus. All images acquired at 100x magnification. Images in (A-B') are 8 μm maximum intensity projections and are deconvolved. Scale bars 15 μm.

In *K10¹* mutant egg chambers Grk is absent from the nurse cells

K10 is required for correct dorsoventral patterning (Neuman-Silberberg & Schupbach 1993). In *K10¹* mutants Grk protein is expressed along the anterior margin, but reports disagree on whether *grk* mRNA is mislocalised in these egg chambers (Neuman-Silberberg & Schupbach 1993, Roth & Schupbach 1994, Saunders &. Cohen 1999). To test whether *K10* is required for *grk* localisation, I performed sm-FISH. In *K10¹* mutant egg chambers (Wieschaus et al. 1978), *grk* is mislocalised along the anterior margin (Figure 6-6 A-A')). This suggests that *K10* is required for *grk* localisation as previously reported by the Schupbach lab (Neuman-Silberberg & Schupbach 1993, Roth & Schupbach 1994).

To test whether *K10* is required for the translational repression of *grk* mRNA in the nurse cells, I visualised Grk protein in *K10¹* mutant egg chambers. Grk protein is expressed along the anterior margin, but is absent from the nurse cells (Figure 6-6 (B-B'), n=30).

Conclusion: *K10* is required for *grk* localisation in the oocyte, but not *grk* translational repression in the nurse cells.

Syncrip overexpression does not affect *grk* translation in the nurse cells

Drosophila Syncrip is involved in the localisation and translational control of *grk* in the oocyte, and overexpression of Syncrip isoform F tagged with GFP causes Grk protein expression in rings around nurse cell nuclei (McDermott et al. 2012). To test whether Syncrip has a role in the translational repression of *grk* in the nurse cells, I examined the distribution of Grk protein in *TubulinGal4VP16/UASp-SypFGFP2* egg chambers (McDermott et al. 2012). These flies lay eggs with ectopic dorsal

Figure 6-6: In *K10¹* egg chambers, *grk* mRNA and Grk protein are mislocalised in the oocyte, but Grk is not expressed in the nurse cells

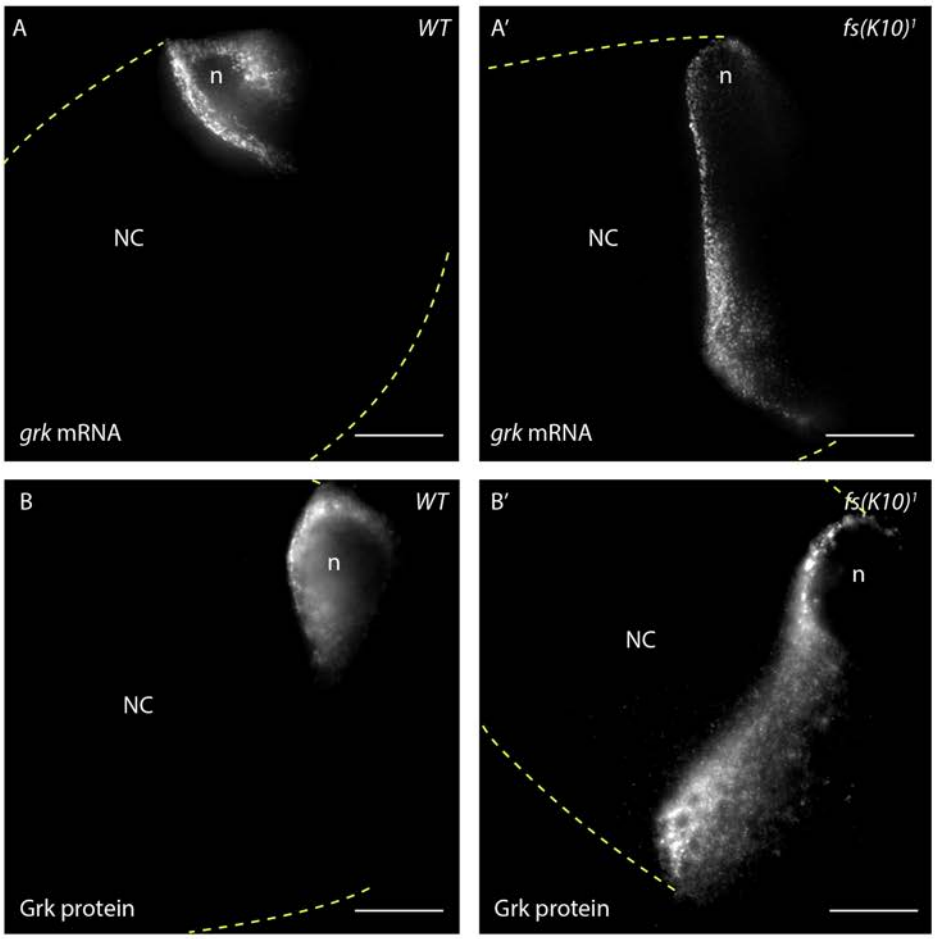

Figure 6-6:

(A-A'): Egg chambers labelled with *grk* FISH probes. (A): In *WT* egg chambers *grk* mRNA is restricted to the DA corner of the oocyte. (A'): In *K10¹* egg chambers *grk* is mislocalised along the anterior margin. Images in are contrasted equally; note the higher fluorescence intensity of the signal at the DA corner in (A) compared to (A'), indicating a redistribution of *grk* rather than an increase in mRNA levels. (B-B'): Egg chambers stained for with anti-Grk. (B'): In *K10¹* egg chambers Grk is expressed along the anterior margin, but not in the nurse cells. Dotted yellow lines indicate the edge of the egg chamber. All images acquired at 100x magnification. Images in (A-A') are 6 *μ*m maximum intensity projections and are deconvolved. NC, nurse cells; n, oocyte nucleus. Scale bars 15 *μ*m.

appendages, indicative of upregulated Grk signalling as previously reported (McDermott et al. 2012). However, rings of Grk around the nurse cell nuclei are not visible (Figure 6-7). The GFP fluorescence in the nurse cell nuclei indicates that the SypGFP is being overexpressed (Syncrip isoform F has an NLS and is expressed predominantly in nuclei, Figure 6-7). To try and reproduce the phenotype seen by McDermott et al, I repeated these experiments under different conditions including increased tissue permeabilisation, setting the cross at different temperatures, and repeating the cross in both directions. Grk protein is never visible in the nurse cells.

Although it is possible that my antibody staining is not detecting Grk in the nurse cells, this is unlikely as published data indicates that Grk in the nurse cells should be detectable (McDermott et al. 2012), and my imaging protocols are able to detect faint mRNA particles, and Grk protein which is expressed in the nurse cells (Chapter 7). It is also possible that these flies are no longer correctly expressing SypGFP, however the presence of GFP in nurse cell nuclei and the ectopic dorsal appendage phenotype of these egg chambers suggests this is not the case.

Conclusion: Syp overexpression does not alter *grk* translation in the nurse cells.

grk overexpression does not cause ectopic Grk expression in nurse cells

To test if a saturable repressor protein represses *grk* translation in the nurse cells, I visualised Grk protein in *TubulinGal4VP16/UAS-grk* egg chambers (Bökel et al. 2006). As previously reported Grk protein is ectopically expressed along the anterior margin of these egg chambers (Weil et al. 2012b). However, there is no Grk protein visible in the nurse cells (Figure 6-8). These data suggest that although in the oocyte

Figure 6-7: When Syncrip is overexpressed, rings of Grk protein are not visible around nurse cell nuclei

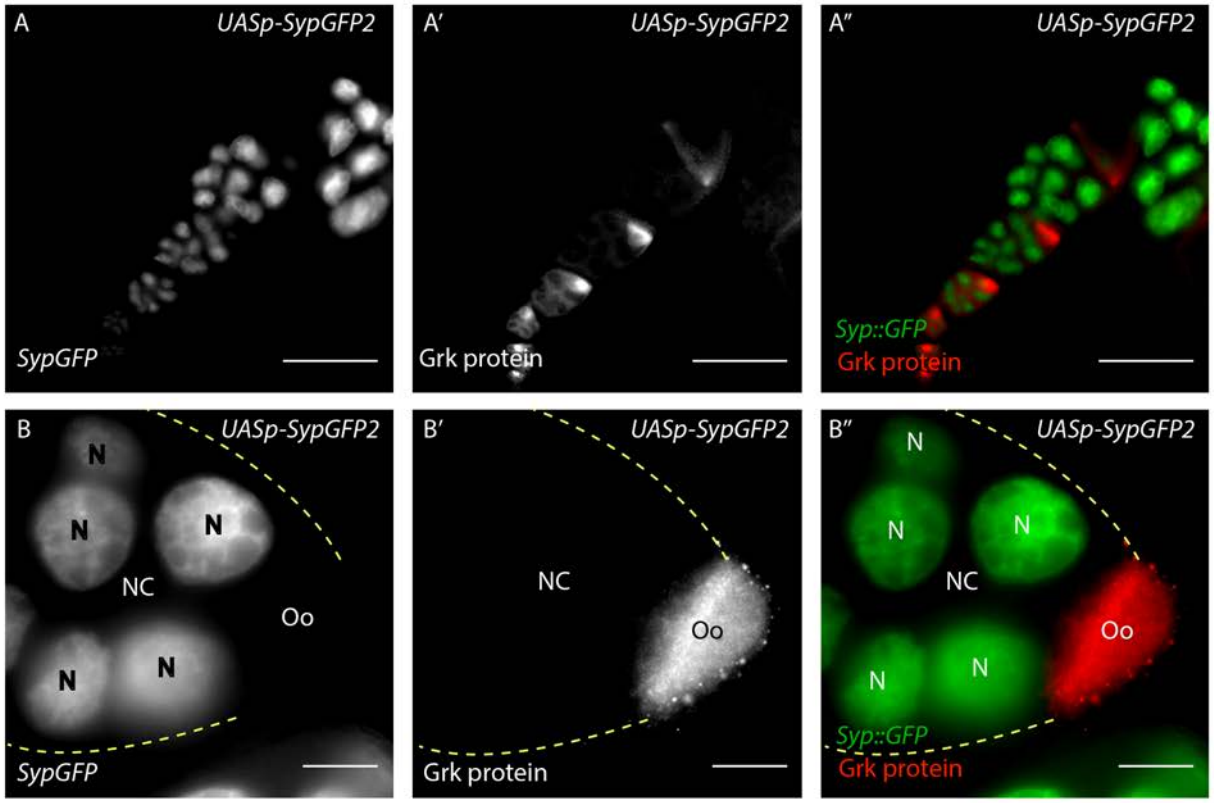

Figure 6-7:

(A-B"): Egg chambers expressing *UASp-SypGFP2* driven by *TubulinGal4VP16* labelled with anti-Grk. Contrary to previous reports, Grk protein expression is restricted to the oocyte in these egg chambers. Nuclei expressing GFP indicate the *UAS* construct is being driven. Dotted yellow lines indicate the edge of the egg chamber. Images in (A-A") acquired at 20x magnification, images in (B-B") acquired at 100x magnification. NC, nurse cells; N, nurse cell nuclei. Scale bars 100 μm (A-A"), 15 μm (B-B").

Figure 6-8: When *grk* is overexpressed, Grk protein is not expressed in the nurse cells

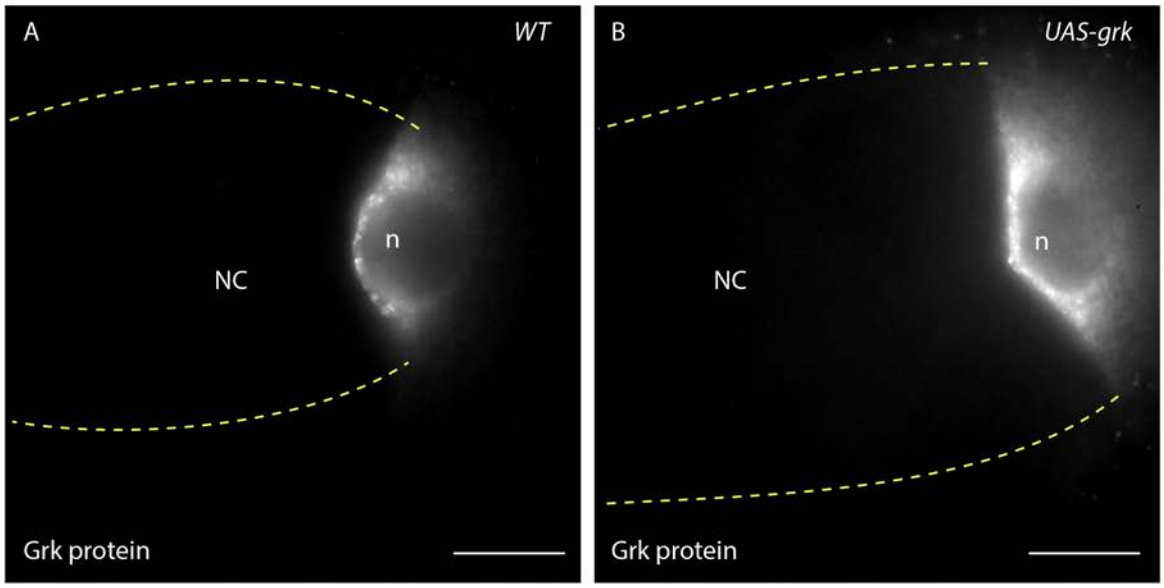

Figure 6-8:

(A-B): Egg chambers labelled with anti-Grk. (A): In wild-type egg chambers Grk expression is restricted to the DA corner of the oocyte and is absent from the nurse cells. (B): Egg chambers expressing *UASp-grk* driven by *TubulinGal4VP16* show a similar Grk expression pattern. Although Grk expression is upregulated in the oocyte, there is no Grk protein visible in the nurse cells. Dotted yellow lines indicate the edge of the egg chamber. Images acquired at 100x magnification. NC, nurse cells; n, oocyte nucleus. Scale bars 15 μm.

there appears to be repression machinery which can be saturated with excess *grk*, this is not the case in the nurse cells.

Conclusion: There is not a saturable repressor of *grk* translation in the nurse cells.

grk does not colocalise or move with P bodies in the nurse cells

In the oocyte, *bcd* mRNA is translationally repressed by targeting to the translationally silent P body core (Weil et al. 2012b). To test whether *grk* is translationally repressed in the nurse cells by being associated with the translationally silent P body core, I performed sm-FISH for *grk* on *Me31B::GFP* egg chambers. Only 16% of *grk* particles colocalise with P bodies (Figure 6-9, n=297 particles from 30 egg chambers).

To test whether *grk* is translationally repressed by being transported within the translationally silent P body core, I covisualised *grk*mCherry* and fluorescent protein traps of P body proteins (Appendix F). *grk* moves independently of Me31B, Tral, Growl, eIF4E, Cup, and YPS in 93-98% of cases (Table 6-1, Figures 6-10 to 6-12).

At the DA corner of the oocyte, 41% of *grk* particles (n=50) dock at the edge of P bodies, where *grk* is translated (Weil et al. 2012b). To test whether *grk* docks at the edge of P bodies in nurse cells, I further analysed the live cell imaging data of *grk* and P body proteins in the nurse cell cytoplasm. A lower percentage of *grk* particles dock at or move away from P bodies than in the oocyte, with a majority of particles not interacting with P bodies in any way (Table 6-2). These results indicate that *grk* particles rarely dock at the edge of P bodies.

Conclusion: *grk* is not repressed by being transported within the translationally silent core of nurse cell P bodies, and *grk* does not interact with the edge of P bodies as it does at the DA corner of the oocyte where it is translated.

***grk* does not move with Vasa in the nurse cells**

To test whether *grk* moves with inactive forms of its translational activators in the nurse cells, I covisualised *grk* mRNA with *vasa-GFP*, which is required for *grk* translation (Johnstone & Lasko 2004, Styhler et al. 1998). 100% of *grk* particles imaged (n=55) do not move with Vasa in the nurse cell cytoplasm, and no *grk* particles dock at, move from or move through Vasa particles (Figure 6-13).

Conclusion: Vasa is not packaged into the *grk* RNP in the nurse cells.

Figure 6-9: *grk* mRNA is not associated with nurse cell P bodies

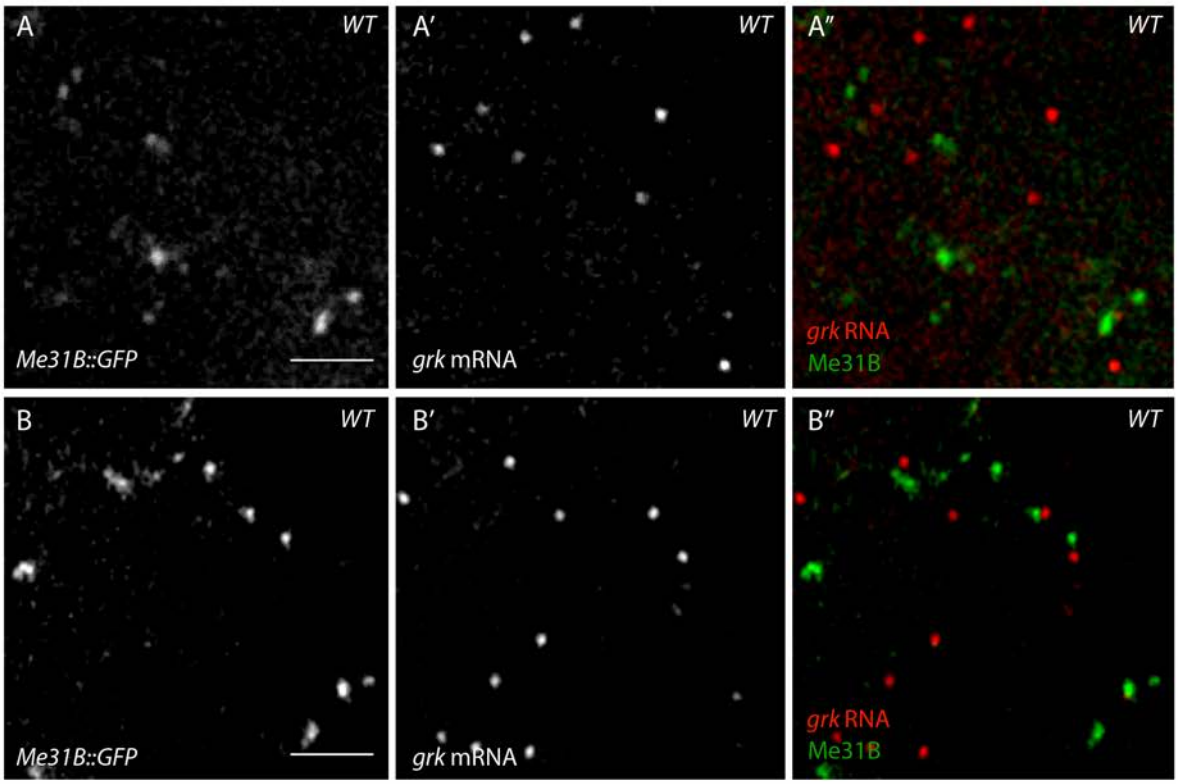

Figure 6-9:

(A-B"): Wild-type egg chambers expressing *Me31B::GFP* stained with *grk* sm-FISH probes. *grk* foci in the nurse cell cytoplasm (red) rarely colocalise with P bodies labelled with *Me31B::GFP* (green), with only 16% of *grk* particles associated with the edge of P bodies (n=297). Images acquired at 100x magnification and deconvolved. Scale bars 2 *μ*m.

Figure 6-10: *grk* mRNA does not move with Me31B or Tral in nurse cells

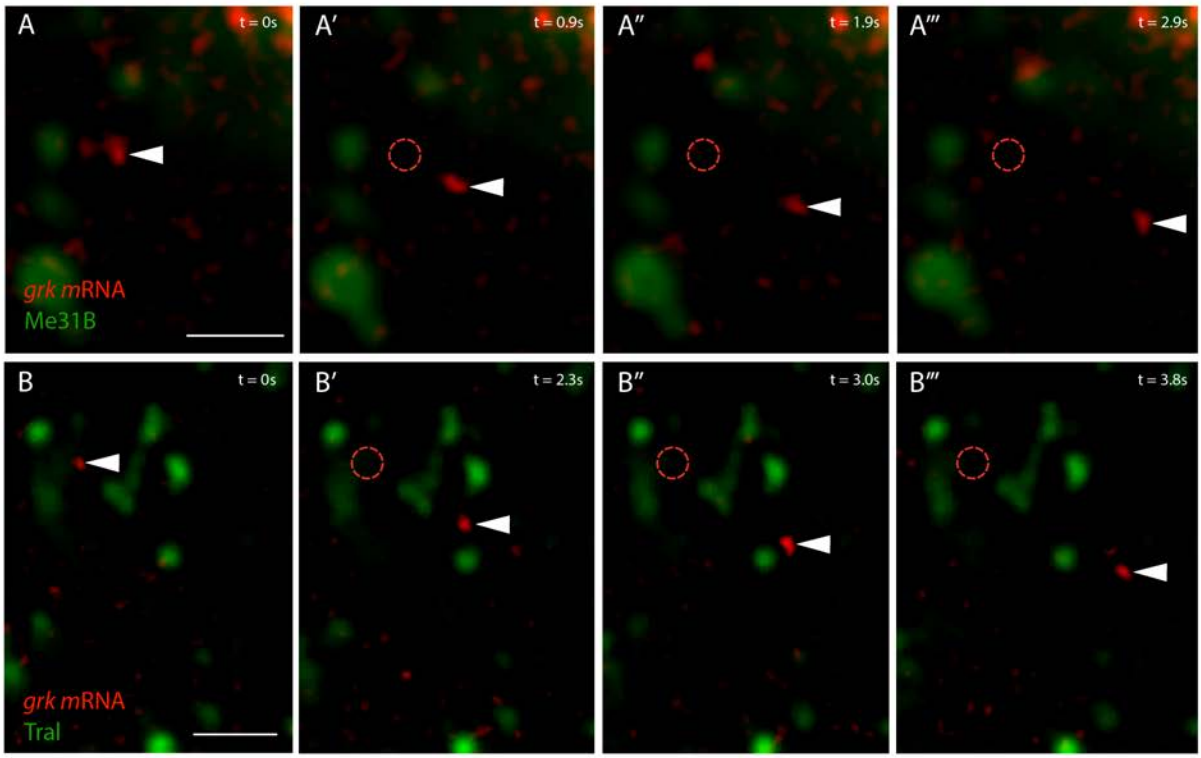

Figure 6-10:

(A-A'''): Stills from time lapse imaging of live egg chambers expressing *Me31B::GFP* and *grk*mCherry*. The *grk* particle (white arrowhead) moves independently of Me31B labelled P bodies (green) in 96% of cases (n=89). (B-B'''): Stills from time lapse imaging of live egg chambers expressing *Tral::YFP* and *grk*mCherry*. The *grk* particle (white arrowhead) moves independently of Tral labelled P bodies (green) in 98% of cases (n=98). Red dashed circle indicates starting point of *grk* particle at t=0s. Images acquired at 100x magnification and deconvolved. Scale bars 2 μm.

Figure 6-11: *grk* mRNA does not move with Growl or eIF4E in nurse cells

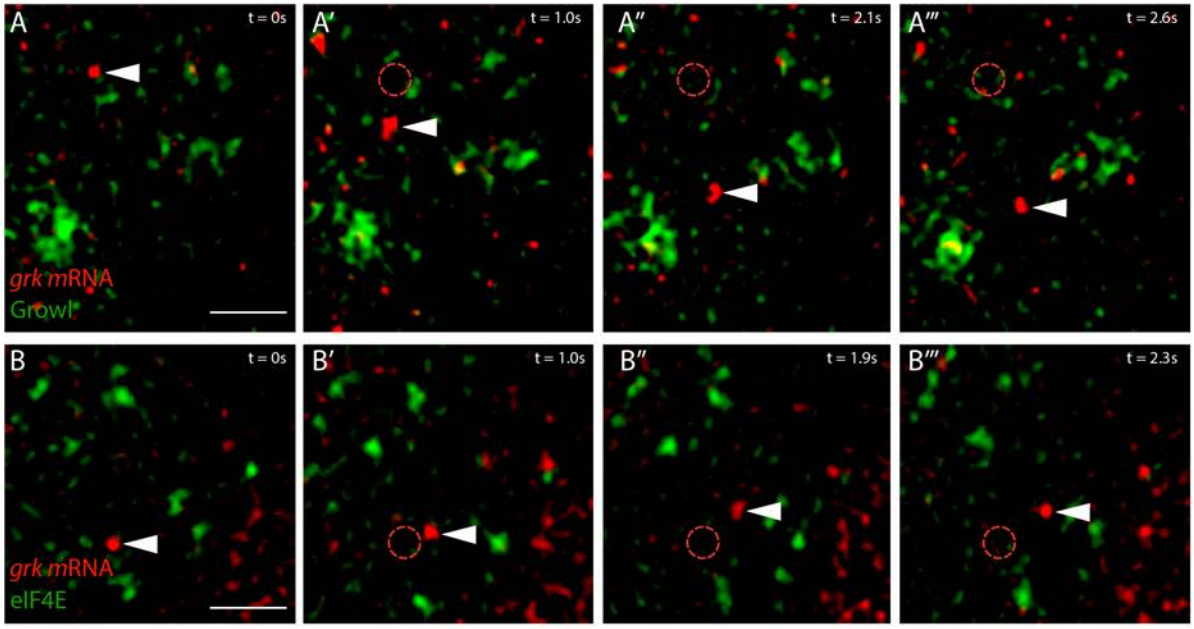

Figure 6-11:

(A-A‴): Stills from time lapse imaging of live egg chambers expressing *Growl::GFP* and *grk*mCherry*. The *grk* particle (white arrowhead) moves independently of Growl labelled P bodies (green) in 93% of cases (n=68). (B-B‴): Stills from time lapse imaging of live egg chambers expressing *eIF4E::GFP* and *grk*mCherry*. The *grk* particle (white arrowhead) moves independently of eIF4E labelled P bodies (green) in 97% of cases (n=70). Red dashed circle indicates starting point of *grk* particle at t=0s. Images acquired at 100x magnification and deconvolved. Scale bars 2 μm.

Figure 6-12: *grk* mRNA does not move with Cup or YPS in nurse cells

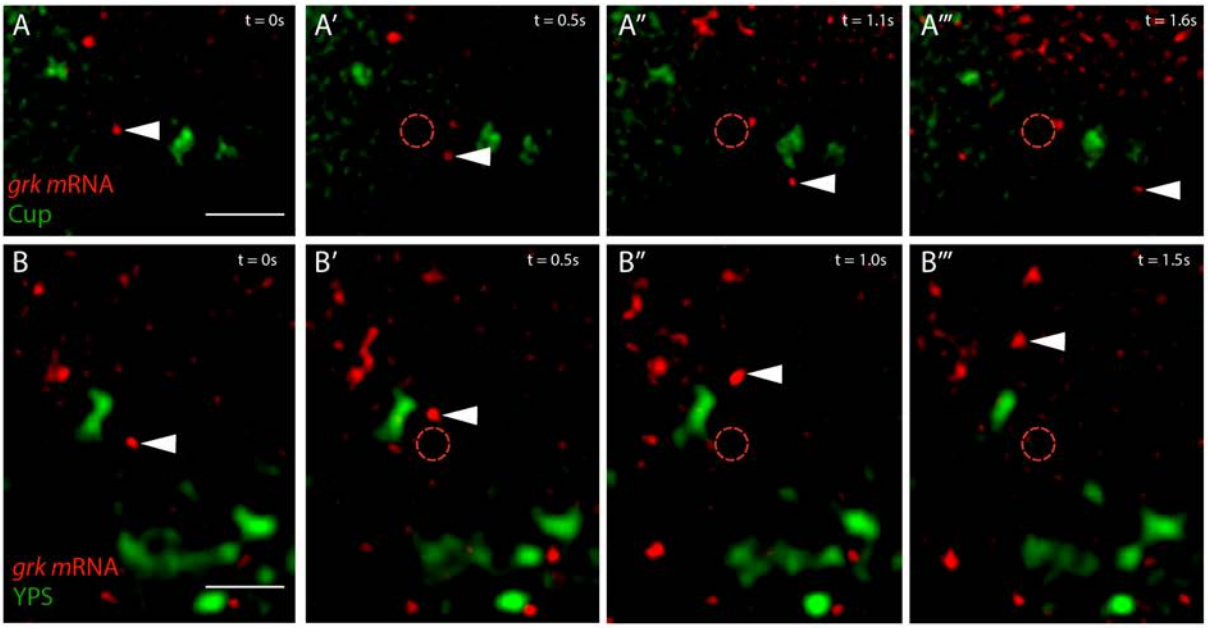

Figure 6-12:

(A-A‴): Stills from time lapse imaging of live egg chambers expressing *Cup::YFP* and *grk*mCherry*. The *grk* particle (white arrowhead) moves independently of Cup labelled P bodies (green) in 93% of cases (n=84). (B-B‴): Stills from time lapse imaging of live egg chambers expressing *YPS::GFP* and *grk*mCherry*. The *grk* particle (white arrowhead) moves independently of YPS labelled P bodies (green) in 97% of cases (n=67). Red dashed circle indicates starting point of *grk* particle at t=0s. Images acquired at 100x magnification and deconvolved. Scale bars 2 μm.

Figure 6-13: *grk* mRNA does not move with Vasa in nurse cells

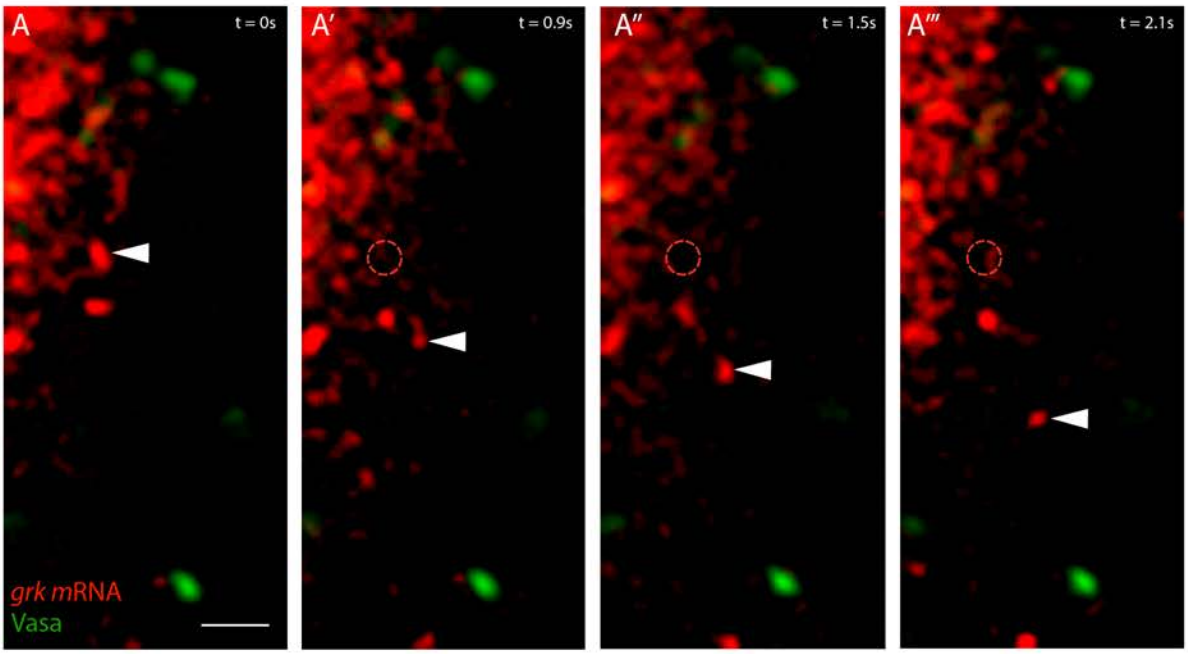

Figure 6-13:

(A-A‴): Stills from time lapse imaging of live egg chambers expressing *vasa-GFP* and *grk*mCherry*. The *grk* particle (white arrowhead) moves independently of Vasa (green) in 100% of cases (n=55). Fluorescence in the top left of each panel is from MCP-mCherry fluorescence in a nurse cell nucleus. Red dashed circle indicates starting point of *grk* particle at t=0s. Images acquired at 100x magnification and deconvolved. Scale bars 2 μm.

Discussion

Translational regulation of *grk* mRNA in the nurse cells

In this Chapter I show that, unlike *osk* mRNA, *grk* translational silencing in nurse cells does not require the action of a number of canonical repressor proteins. I demonstrate that *grk* is not associated or transported with the translationally silent core of nurse cell P bodies. Based on the following evidence, I propose that *grk* is not translationally repressed in the nurse cells by a known single translational repressor protein, or by P body proteins in the nurse cells.

First, *grk* is not translated in the nurse cells when candidate translational repressors are mutated (Figures 6-1 to 6-7). Second, overexpression of *grk* does not cause expression of Grk in the nurse cells as it does in the oocyte (Figure 6-8). This suggests there is no saturable repression machinery in the nurse cells for *grk*. Third, *grk* does not move, or interact with P bodies at frequencies similar to those previously recorded at the DA corner, and *grk* is not enriched in the core of P bodies as *bcd* is at the DA corner (Figures 6-9 to 6-12, (Weil et al. 2012b). This argues that *grk* is translationally repressed by an unidentified repressor, by multiple repressor proteins, or by a different mechanism to *osk* in the nurse cells. I further interpret these data to suggest that *grk* does not interact with P bodies in the nurse cells. This argues that either *grk* lacks the requisite signals to be targeted to P bodies in the nurse cells, or the nurse cell P bodies are not competent to interact with *grk*.

grk does not require single candidate translational repressors for silencing in the nurse cells.

These data differ from research on *osk* mRNA. My findings indicate that *grk* translation is not regulated by repressor proteins in the same manner as *osk* is, but

do not rule out multiple proteins acting in concert, or proteins which I did not test. The inability to reproduce a result with Syncrip overexpression flies where *grk* is translated in nurse cells is unusual, especially as the dorsal appendage phenotype and GFP expression was observed as expected (McDermott et al. 2012). These lines should be sequenced, and if necessary, remade, to try and reproduce this result.

My analysis of mutants was restricted to a single repressor proteins. It is possible that *grk* is repressed by a suite of proteins as previously suggested (Clouse et al. 2008), and that there is sufficient redundancy to compensate for the loss of one repressor. Indeed, Grk expression in nurse cells has been reported when both *aret* and S^{1} were mutated (Yan & Macdonald 2004), and multiple proteins regulate the translation of *osk* and *nos* mRNA (Chekulaeva et al. 2006, Besse et al. 2009, Crucs et al. 2000, Forrest et al. 2004, Nakamura et al. 2001, Nakamura et al. 2004). Visualisaton of Grk protein in double mutants for combinations of *me31B*, *aret*, *sqd* and *K10* could test this mechanism. These are challenging experiments due to the complex genetics required. However, this approach should be seriously considered. Similarly, some of these mutants are not nulls, and weak allelic combinations were used to allow the egg chambers to develop to mid-oogenesis. Stronger mutations for some of these proteins should be examined, if possible.

Moreover, my data do not show that *grk* does not interact with proteins like Sqd or Bruno in the nurse cell nuclei, nurse cell cytoplasm, or the oocyte; just that individually they are not required for it's translational repression in the nurse cells. Indeed, Sqd is required in the nurse cell nuclei for *grk* translational control in the oocyte, so it is likely they do interact in nuclei (Cáceres & Nilson 2009). And finally, I examined egg chambers during mid-oogenesis. It is possible that different repressors

act on *grk* at different times as well as in different tissues. Thorough biochemical and imaging analysis of the interactions between *grk* and these candidate proteins throughout oogenesis could dissect any differences in time as well as space.

It is possible that in these mutants, Grk protein is produced but is targeted for degradation, as Short-Osk protein is in the oocyte (Morais-de-Sá et al. 2013). However, ectopic Grk protein is expressed in the oocyte in many of these mutants, which would suggest that if such a degradation pathway for Grk existed, it operated specifically in nurse cells. Moreover, published visualisation of Grk protein in the nurse cells (Yan & Macdonald 2004) suggests that Grk protein is not immediately cleared from the nurse cells, and should be visible if expressed in this tissue.

While I was able to image well established P body proteins, all possible P body component or candidate translational repressor proteins were not covisualised with *grk*. This was in part due to time and availability of protein traps. Specifically, K10, Bruno, and Syncip protein trap lines were not available. When imaging *Sqd::GFP* egg chambers, no particles were visible in the cytoplasm, only a uniform cytoplasmic background and high nuclear signal (Chapter 5). Covisualisation of *grk* with more fluorescent proteins could further test the association of *grk* with nurse cell P bodies.

Vasa and *grk* RNP assembly

Another possible explanation of how *grk* is repressed in P bodies is by restricted temporal access to translational activators such as CPEB and Gld2 poly(A) polymerase (Richter & Lasko 2011). Before fertilisation in *Xenopus*, CPEB represses translation with Maskin, and only activates translation following its phosphorylation (Ivshina et al. 2014). Such temporal control of the binding and activity of activator

proteins could explain how *grk* is translationally regulated. Vasa is required for *grk* translation (Johnstone & Lasko 2004, Styhler et al. 1998). There are two models for when Vasa associates with *grk*: 1). Vasa is packaged with grk after nuclear export, but is maintained in an inactive form. This could be mediated by inhibitory proteins circularising the mRNA, as is seen in *Xenopus* oocytes, or 2.) Vasa is not incorporated into the *grk* RNP until *grk* is localised at the DA corner. My imaging data support the second model: that *grk* is not packaged and transported with Vasa in the nurse cells, and that Vasa binds localised *grk* only at the DA corner. It is still possible that *grk* is packaged with inactive forms of other translational activators, which are then activated once localised.

Additionally, my FISH data (Chapter 4) indicate that *grk* mRNA is present in the nurse cells for much of oogenesis. *grk* is thought to be transcribed in nurse cell nuclei and transported in the oocyte whilst *grk* is translated at the posterior of the oocyte at stage 5, and also as it is translated at the oocyte DA corner at stage 9. If *grk* translation were controlled by temporal activity of translational activators, this would need to be oocyte specific, and there is no obvious external signal, like fertilisation, to act as a trigger. This suggests that, unlike mRNAs in *Xenopus* oogenesis, *grk* mRNA in the nurse cells travels independently of its translational activators, and only associates with them in the oocyte. Based on these data I favour a model where *grk* is translationally repressed in nurse cells by another mechanism.

Similarly, my data showing that ectopic Grk protein is not expressed in the oocyte when a number of translational repressor proteins are mutated, begs the question of how *grk* translational is regulated in the oocyte. I will address these points in Chapters 7 and 8.

grk association with P bodies and translational regulation in the oocyte

The finding that *grk* is not associated with nurse cell P bodies, but at the DA corner docks at the edge of P bodies (Weil et al. 2012b) raises an important question about how the interaction between P bodies and mRNA is controlled. This interaction could be meditated by distinct cis-acting elements within the mRNAs, like the GLS, BLE, OES or SOLE which direct *grk*, *bcd* and *osk* localisation (Ghosh et al. 2012, Jambor et al. 2014, Macdonald & Kerr 1997, Macdonald & Kerr 1998, Snee et al. 2005, Van De Bor et al. 2005). Specific cis-acting regions within localised mRNAs could interact with IDPs within P bodies to target different mRNAs to different regions of the P body as previously shown (Weil et al. 2012b). Alternatively, this interaction could be controlled largely by trans-acting proteins transported with specific mRNAs to limit P body interactions to certain transcripts. Proteins could also be present in P bodies at distinct subcellular locations to mediate spatial control of mRNA - P body interactions. For example, I have shown that Orb is significantly reduced in nurse cell P bodies compared to those in the oocyte. These hypotheses will be investigated in Chapter 7.

Discussion of technical approaches used in this chapter

Although my results show that no Grk is detected in the nurse cells of the mutants I examined, they do not exclude alternative explanations. It could be argued that Grk may be expressed in the nurse cells in mutants of repressor proteins, but below the detection limits of the microscopes used. To ensure my results are accurate, I imaged fixed samples with multiple imaging parameters, objectives and mounting media. I varied my image processing methods including multiple parameters for deconvolution, Z stack intensity projections and contrasting. I worked closely with microscopists and image analysts in the Davis lab and Micron Oxford. Moreover, the widefield imaging system I use is able to detect faint *grk-MS2* and *osk-MS2* particles

in the nurse cells (Chapter 3). When Grk is ectopically translated in the oocyte, this is readily visible. While my systematic imaging approach suggests that there is no Grk in the nurse cells of these egg chambers, it remains a possibility that Grk is expressed below the imaging threshold of the technology available today.

If such low levels of Grk are being expressed, presumably only a fraction of *grk* mRNA in the nurse cells is being translated in these mutants, indicating the proteins mutated are not key repressors *grk* mRNA translation during transport. Biochemical analysis of protein levels in nurse cell extracts could provide greater sensitivity. However, nurse cell specific biochemical analysis would require careful removal of the nurse cells from the oocyte, ensuring that significant quantities of nurse cell cytoplasm are not lost. Obtaining sufficient material for biochemical analysis without inducing a stress response by this route is difficult to conceive.

Similarly, live cell imaging has a detection threshold. As each *grk-MS2* particle is decorated with multiple fluorophores, and each protein particle in a protein trap is labelled with only one fluorophore, it is possible that I am not visualising small P bodies or single Vasa protein particles travelling with *grk* mRNA. Moreover it could be that *grk-MS2* is not subject to endogenous control, and unlabelled *grk* particles do move with the same factors as the endogenous mRNA. However, given that on the DeltaVision very small motile particles of Me31B (of comparable size to *grk* particles) are visible, it is unlikely that I am failing to detect a subset of P bodies or Vasa protein particles. Furthermore, endogenous *grk* particles labelled with FISH do not colocalise with P bodies, and *grk*-MS2 is not translated in nurse cells, which suggests it is silenced during transport.

More interesting is the observation that *grk-MS2* particles do not move with any proteins in the nurse cells. In the oocyte, *grk* is transported with Sqd protein (Delanoue et al. 2007). However, my data suggest that there are no motile particles of Sqd, Heph UAP56 and BicD in nurse cells (Chapter 5), and *grk* does not move with P body proteins or Vasa. It is difficult to reconcile these data with the model that *grk* moves with its key trans-acting factors in the nurse cells. The accepted model is that mRNAs do not travel alone (Kato & Nakamura 2011), and it seems unlikely that *grk* is an exception. Improving the sensitivity of the MS2 system should be explored, along with more protein traps for putative regulators of *grk*, to test this further.

Final conclusions

In this chapter I have shown that *grk* is not translationally silenced in nurse cells by the same mechanisms as *osk*. In chapters 3, 4 and 5, I examined mRNA transport, P body composition and dynamics in nurse cells, and again the data indicate that both proteins and mRNA behave differently in the nurse cells compared to the oocyte. In Chapter 7, I will explore a novel mechanism for translational silencing of *grk* in the nurse cells which is distinct from the mechanisms for translational silencing proposed for the oocyte thus far.

Tables and statistics

Genotype (n of particles)	*% grk* particles moving with P bodies	% *grk* particles moving independently of P bodies
Me31B::GFP (89)	5	95
Tral::YFP (90)	2	98
Growl::GFP (68)	7	93
eIF4E::GFP (70)	3	97
Cup::YFP (84)	7	93
YPS::GFP (67)	3	97

Table 6-1: *grk* mRNA does not move with P bodies in the nurse cells.

Analysis of tracking data from live imaging of *grk*mCherry* and P body components, as detailed in Appendix F. With all P body markers, the majority of *grk* particles which were classed as actively transported move independently of P bodies.

Genotype	% *grk* particles moving from P bodies	% *grk* particles docking at P bodies	% *grk* particles moving through P bodies	% *grk* particles moving with P bodies	Total % *grk* particles interacting with P bodies	% *grk* particles not interacting with P bodies
Me31B:: GFP	7	8	0	5	20	80
Tral:: YFP	8	13	4	2	27	73
Growl:: GFP	9	9	6	7	31	69
eIF4E:: GFP	3	0	13	3	19	81
Cup:: YFP	2	5	4	7	18	82
YPS:: GFP	7	9	4	3	23	77

Table 6-2: *grk* mRNA interacts with P bodies in the nurse cells less frequently than at the oocyte DA corner.

Analysis of tracking data from live imaging of *grk*mCherry* and P body components (the same data as in table 6-1). In the oocyte, 41% (n=50) of *grk* particles dock at the edge of P bodies (Weil et al. 2012b). With all P body markers, the majority of *grk* particles which were classed as actively transported and do not move with P bodies (four left-most columns), also do not move from, dock at, or move through P bodies. An absolute majority of particles (right-most column) do not interact with P bodies in any way in the nurse cells.

Chapter 7: Translational control of *grk* in nurse cells by restricted spatial access to Orb

Introduction

The data presented in Chapter 6 suggest that *grk* is not translationally repressed in the nurse cells by single translational repressor proteins. In chapter 5 I showed that expression of the *Drosophila* CPEB homolog Orb is lower in nurse cell P bodies than those in the oocyte. CPEB proteins are key translational regulators in many organisms (Ivshina et al. 2014, Richter & Lasko 2011). In this chapter I will test whether lower levels of Orb in the nurse cells prevent *grk* translation in this tissue.

The CPEB proteins

Two subgroups of CPEB proteins exist; *Xenopus* CPEB1 is closely related to Human and mouse CPEB1, *Drosophila* Orb, and zebrafish Zorba. Conversely, mouse CPEB2-4, *C.elegans* CPB-1-3 and FOG-1, *Drosophila* Orb2 and *Aplysia* CPEB are more closely related to each other (Bally-Cuif et al. 1998, Huang et al. 2006, Luitjens et al. 2000, Méndez & Richter 2001). All CPEB proteins contain two RNA recognition motifs (RRMs) and two zinc finger domains in their C terminal domains (Figure 7-1, Hake & Richter 1994, Lantz et al. 1994). However, systematic evolution of ligands by exponential enrichment (SELEX) data suggest that the CPEB1-like RRMs have a high affinity for CPE sequences, but CPEB2-like RRMs do not (Huang et al. 2006, Krüttner et al. 2012). Some CPEB proteins also contain polyglutamine (polyQ) regions in their N terminal domain which are important for prion-like activity and formation of plaques, and are required for their function (Heinrich & Lindquist 2011, Keleman et al. 2007, Majumdar et al. 2012, Raveendra et al. 2013, Si et al. 2003, Si et al. 2010).

Figure 7-1: CPEB homology between species

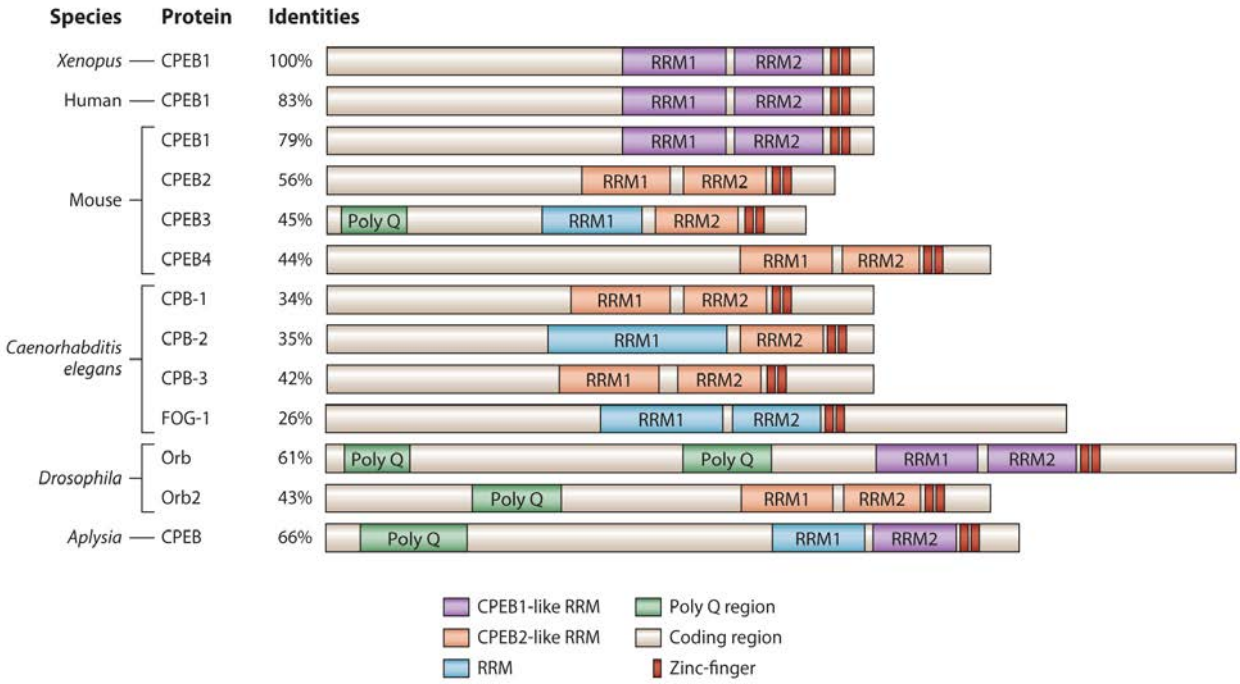

Figure 7-1: (Adapted from Ivshina et al 2014).

Alignment of CPEB proteins from *Xenopus*, Human, Mouse, *C.elegans*, *Drosophila* and *Aplysia* by BLAST and Cobalt programs. Proteins with the same colour (purple or orange) RRMs denote those with a strong similarity, RRMs in blue are not more closely related to either CPEB1-like or CPEB2-like RRMs. Poly Q refers to polyglutamine regions of normally greater than 25 residues, however the region in CPEB3 is smaller. Percentage idenities are relative to *Xenopus* CPEB. *Drosophila* Orb contains two poly Q regions, two CPEB1-like RRM domains, and two zinc finger domains.

orb encodes the *Drosophila* CPEB homolog in ovaries (Lantz et al. 1992, Lantz et al. 1994), and *orb* mRNA is alternatively spliced to generate 7 transcripts and 4 unique polypeptides. The predominant isoforms in the oocyte are the 915 and 913 amino acid (AA) proteins, OrbA/G and OrbB/D (Lantz et al. 1992). Orb protein contains two CPEB1-like RRM domains surrounded by conserved residues which are important for RNA binding (Bandziulis et al. 1989, Hoffman et al. 1990, Lantz et al. 1992, Nagai et al. 1990) and zinc finger domains (Figure 7-1). Both Orb and Orb2 contain polyQ stretches in their N terminal domains.

***orb* function and regulation during oogenesis**

In early oogenesis, *orb* mRNA and protein are required for the formation of the cyst, specification of the oocyte, and correct positioning of the presumptive oocyte (Huynh & St Johnston 2000, Lantz et al. 1994). Both accumulate transiently in the pro-oocytes, and are then restricted to the oocyte in the germarium (Lantz et al. 1994).

Throughout oogenesis *orb* mRNA and Orb protein are expressed in the nurse cells, but not in follicle cells, and Orb protein is not localised in the nurse cell nuclei. From stage 1-6 both *orb* and Orb accumulate at higher levels in the oocyte and are enriched at the posterior at stage 7. From stage 8-10 *orb* relocates to the anterior margin of the oocyte, with enrichment at the dorsal and ventral corners, mediated by regions within the *orb* 3' UTR. *orb* expression is reduced from stage 11 onwards (Lantz et al. 1992) (Lantz et al. 1994, Wong & Schedl 2011).

From stage 8-10 Orb protein is also enriched along the oocyte cortex, including the anterior and posterior poles (Lantz et al. 1994). IEM data also suggest that Orb protein is in P bodies throughout the oocyte (C. Rabouille, personal communication).

Orb protein expression in the nurse cells is markedly lower than in the oocyte throughout oogenesis, and is in a graded distribution, with the nurse cells nearest the oocyte containing more Orb than the anterior nurse cells (Lantz et al. 1994).

In severe *orb* mutants, oogenesis arrests early and the oocyte is not specified or is positioned inappropriately in the cyst (Christerson & McKearin 1994, Lantz et al. 1994). orb^{mel} is a recessive hypomorphic loss-of-function allele which expresses a truncated *orb* mRNA. Protein expression is normal in early oogenesis but is significantly reduced from stage 7 onwards. In orb^{mel} mutants, oogenesis is not arrested and homozygous females lay eggs (Christerson & McKearin 1994). Analysis of these mutants elucidated the role of *orb* in controlling the translation of localised mRNAs, in a similar manner to *Xenopus* CPEB.

Orb is required for the localisation and translation of *grk* mRNA (Chang et al. 2001, Lantz et al. 1994, Neuman-Silberberg & Schupbach 1996, Roth & Schupbach 1994), and is thought to activate *grk* translation when the mRNA anchors at the edge of P bodies in the DA corner, where Orb protein is enriched (Weil et al. 2012b). Both *grk* and Orb are present in heavier, translationally competent complexes, but only *grk* in translationally repressed RNPs, supporting this theory (Li et al. 2014). orb^{mel} females lay eggs with fused or missing dorsal appendages indicative of a lack of Grk signalling (Christerson & McKearin 1994). Orb also binds and translationally activates *osk* and *K10* mRNAs, and mediates their poly(A) tail length (Castagnetti & Ephrussi 2003, Chang et al. 1999, Chang et al. 2001, Christerson & McKearin 1994, Juge et al. 2002, Markussen et al. 1995). These data suggest Orb activates translation in a similar manner to CPEB. However, there is evidence that Orb does not bind directly

to *grk* mRNA, suggesting it may act through intermediate proteins (Chang et al. 2001), and whether Orb regulates *grk* poly(A) tail length is unknown.

orb mRNA is translationally activated by Orb protein, which binds to the 3' UTR of *orb* mRNA and elongates its poly(A) tail (Tan et al. 2001). High levels of Orb protein expression in the nurse cells is prevented by *Drosophila* Fragile X mental retardation protein (dFMR1, Costa et al. 2005), and Cup (Wong & Schedl 2011). In *cup* mutants, *orb* mRNA has longer poly(A) tails and its translation is increased in the nurse cells (Wong & Schedl 2011). How Cup represses *orb* translation is unclear, but the increase in poly(A) tail lengths in *cup* mutants suggests that Cup may deadenylate *orb* mRNA, similar to its action on *osk* or *nos* mRNA (Chicoine et al. 2007, Igreja & Izaurralde 2011, Jeske et al. 2011, Nelson et al. 2004, Saffman et al. 1998).

Although Cup is functionally homologous to *Xenopus* Maskin, the two do not share primary sequence homology outside of the eIF4E binding domain (Nelson et al. 2004, Nakamura et al. 2004). The *Drosophila* transforming acidic coiled-coil (D-TACC) protein C-terminus is 70% identical to Maskin, and both contain similar coiled-coil domains and are targeted to centrosomes by Aurora-A kinase mediated phosphorylation (Barros et al. 2005, Gergely et al. 2000, Groisman et al. 2000, Kinoshita et al. 2005, Lee et al. 2001, Stebbins-Boaz et al. 1999). Whether D-TACC regulates localised mRNAs is not known.

Orb, like CPEB, is regulated by phosphorylation. Orb phosphorylation by Casein Kinase 2 (CK2, Wong et al. 2011) is required for its function in dorsoventral patterning. Orb which is "hyperphosphorylated" associates with Wisp, the fly Gld2 poly(A) polymerase homolog (Benoit et al. 2008), and ribosomes, whereas the

"hypophosphorylated" form interacts with the translational repressors Bruno and Me31B (Wong et al. 2011). This suggests that, like CPEB, phosphorylation may switch Orb from a repressor to an activator of translation.

Differences between Orb and CPEB mechanisms of action

CPEB translationally represses mRNAs in immature oocytes, and activates translation at fertilisation (Ivshina et al. 2014). This involves CPEB binding to CPE sequences in the 3' UTR and recruiting Maskin, which binds eIF4E at the 5' Cap and prevents translation initiation (Cao & Richter 2002, Minshall et al. 2007, Piqué et al. 2008, Richter & Sonenberg 2005, Stebbins-Boaz et al. 1999).

Does Orb act in a similar mechanism to repress and activate translation in *Drosophila* oogenesis? Orb is required for the translation of *osk*, *grk*, *K10* and *orb* mRNA, suggesting it fulfils a similar role to CPEB in activating translation by extending the poly(A) tail (Chang et al. 1999, Chang et al. 2001, Tan et al. 2001). Both CPEB and Orb require phosphorylation to translationally activate localised mRNAs (Kim & Richter 2007, Mendez et al. 2000b, Wong et al. 2011). Orb is not only found in a complex with many localised mRNAs, but also interacts with Bic-C, Bruno and Me31B (Benoit et al. 2008, Castagnetti & Ephrussi 2003, Chicoine et al. 2007, Wong et al. 2011). Similarly, the *Xenopus* homolog of Me31B (p54/DDX6/RCK1) is associated with the CPEB complex (Minshall et al. 2001, Minshall et al. 2009), suggesting that, like CPEB, Orb is part of a complex with both translational repressors and activators. This is further supported by the fact that when phosphorylated, Orb associates with Wisp and polysomes, and when hypophosphorylated associates with Bruno (Wong et al. 2011). Finally Cup interacts with Orb, like Maskin and CPEB (Wong & Schedl 2011).

However, Orb does not function like CPEB in several respects. First, in *orb*^{mel} egg chambers where *grk*, *osk* and *K10* mRNAs are mislocalised, there is no ectopic Osk, Grk or K10 protein expression (Chang et al. 1999, Chang et al. 2001, Christerson & McKearin 1994, Roth & Schupbach 1994). Although there may be redundancy in the repression of unlocalised transcripts, this result suggests Orb does not translationally repress unlocalised mRNAs.

Second, CK2 may not directly phosphorylate Orb, or be the only kinase involved in its regulation (Wong et al. 2011). In *Xenopus*, CPEB phosphorylation is initiated by progesterone secretion at egg activation (Cao & Richter 2002, Mendez et al. 2000a) (Mendez et al. 2000b, Kim & Richter 2006, Sarkissian et al. 2004), but no cue for CK2 phosphorylation of Orb has been identified. Orb seems to exist in different phosphorylation states simultaneously during oogenesis (Wong et al. 2011), and it has been suggested that the phosphorylation state of Orb varies spatially rather than temporally; Orb at the DA corner or at the posterior may be hyperphosphorylated and active, whereas Orb elsewhere is hypophosphorylated and inactive.

Third, the regulation of *orb* by Cup seems distinct from the Maskin-CPEB interaction in *Xenopus*. Although Cup has a Maskin-like function in binding eIF4E to repress *osk* translation in the oocyte, (Chekulaeva et al. 2006, Nakamura et al. 2004, Wilhelm 2003), *orb* mRNA translational repression is independent of Cup's eIF4E binding activity (Wong & Schedl 2011). Although 4E-T is found in a complex with CPEB in *Xenopus* (Minshall et al. 2007) there is no evidence that Maskin or 4E-T represses the translation of *cpeb* mRNA. Finally, CPEB is a nucleocytoplasmic shuttling protein which binds transcripts initially in the nucleus (Fox et al. 1989, Lin et al. 2010). However, Orb protein is not expressed in nurse cell nuclei (Lantz et al. 1994).

One hypothesis is that Orb represses unlocalised mRNAs by binding them during their transport in the nurse cells. In this case, *grk* would be expected to colocalise with Orb, perhaps in nurse cell P bodies. However, my data show that Orb is expressed at markedly lower levels in the nurse cells than in the oocyte, and *grk* rarely colocalises with nurse cell P bodies. This raises the possibility that in *Drosophila* Orb is acting only as a translational activator, and its association with repressors like Bruno and Cup mediate Orb protein activity, rather than repressing the translation of its target mRNAs. In this case, lower levels of Orb protein in the nurse cells may be a key determinant which prevents *grk* translation in this tissue.

Aims of this chapter and experimental rationale

In this chapter I test whether *grk* translation in the nurse cells is prevented by lower levels of Orb in nurse cell P bodies. Specific questions include:

- **Is *grk* translated in the nurse cells of *cup* mutant egg chambers where Orb is overexpressed?**
- **Does overexpression of orb cause *grk* translation in the nurse cells?**
- **Does the Cup-eIF4E interaction have a role in *grk* transational repression?**
- **Does Orb modulate *grk* poly(A) tail length?**
- **Is Orb present in P bodies when it is overexpressed in the nurse cells?**
- **Does Orb control the interaction of *grk* mRNA with P bodies?**

To determine whether Orb regulates *grk* translation in the nurse cells, I examined fixed *cup* mutant and *orb* overexpression egg chambers with immunofluorescence using Grk and Orb protein antibodies. To test whether Orb is expressed in P bodies when it is overexpressed in nurse cells, I used 3D-SIM, which provides double the

resolution of conventional light microscopy in each dimension (Dobbie et al. 2011). To examine the association of *grk* with P bodies in these egg chambers, I covisualised *grk* with sm-FISH and *Me31B::GFP* or *Tral::YFP* as P body markers. These methods allow specific examination of the nurse cells, which cannot be isolated by biochemical means. To test the role of Orb in modulating *grk* mRNA poly(A) tail length, I used the sPAT assay (Minasaki et al. 2014), which enables highly sensitive analysis of poly(A) tail length for specific mRNAs.

Results

In *cup* mutant egg chambers Orb and Grk are expressed in the nurse cells

orb mRNA is present in the nurse cells as well as the oocyte (Lantz et al. 1992) (Wong & Schedl 2011) and *orb* translation in nurse cells is repressed by Cup (Wong & Schedl 2011). To confirm these data, I visualised Orb protein in *cup*^{1355} mutant egg chambers, where a P element insertion into *cup* untranslated exon 1 reduces Cup protein expression (Karpen & Spradling 1992). This is a weak allele where ovarian development does not arrest until late oogenesis (Wong & Schedl 2011).

In wild-type egg chambers, Orb protein is higher in the oocyte and at the oocyte cortex compared to the nurse cells (Figure 7-2 (A), Table 7-1). In *cup*^{1355} egg chambers Orb protein levels in the nurse cells are comparable to the oocyte (Figure 7-2 (A'), Table 7-1). To quantify this, I measured fluorescence intensity along an anteroposterior transect in projected Z stacks of individual egg chambers (Appendix F). In wild-type egg chambers, fluorescence intensity at the oocyte cortex is 2-3 fold higher than in the two nurse cells nearest to the oocyte, and 5 fold higher than in the anterior nurse cells (Figure 7-2 (B)). In *cup*^{1355} egg chambers, fluorescence intensity in the nurse cells is similar to or higher than at the oocyte cortex (Figure 7-2 (B')). I then measured the mean fluorescence intensity in different regions of 10 egg chambers from each genotype, (Appendix F). In wild-type egg chambers, the fluorescence in the nurse cells nearest to the oocyte is 63% of the intensity at the oocyte cortex, decreasing to 40% and 28% for the second row and anterior nurse cells respectively. In *cup*^{1355} egg chambers, the fluorescence intensity is significantly higher in all nurse cells compared to the oocyte cortex (Figure 7-2 (C)).

Figure 7-2: Orb protein expression is upregulated in the nurse cells of *cup*^{1355} egg chambers

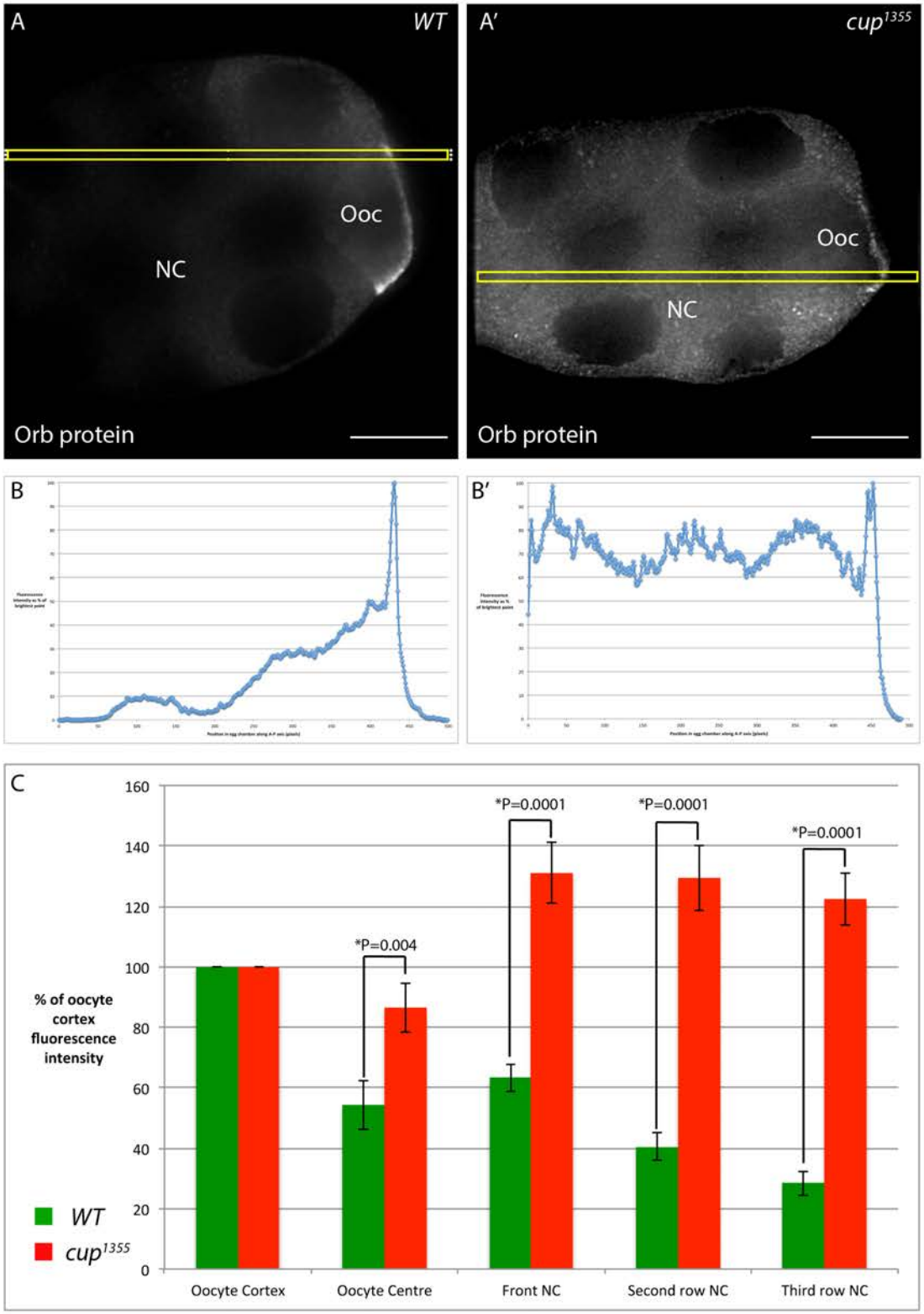

Figure 7-2:

(A-A'): Egg chambers stained for with anti-Orb. (A): In *WT* egg chambers Orb protein expression at the oocyte cortex is significantly higher than it is in the nurse cells. (A'): In cup^{1355} egg chambers, Orb expression is higher in all nurse cells than at the oocyte cortex. (B-B'): Fluorescence intensity readings along anteroposterior transects from yellow boxed regions in images in (A) and (A'). (B): In *WT* egg chambers there is a significant decrease in fluorescence intensity away from the oocyte cortex. (B'): In cup^{1355} egg chambers, the fluorescence intensity in the nurse cells is closer to, or greater than, that at the oocyte cortex. (C). Analysis of mean fluorescence intensity in different regions of the egg chamber (n=10 egg chambers for each condition). Error bars represent standard error of the mean. There is a statistically significant difference between the fluorescence intensity in the oocyte centre and all nurse cells when compared to the oocyte cortex between *WT* and cup^{1355} egg chambers. P values of significance were generated by a two tailed t-test, * indicates a statistically significant difference ($P<0.05$). Images in (A-A') were collected at 100x magnification, and deconvolved. NC, nurse cells; Ooc, oocyte. Scale bars 15 μm.

Figure 7-3: Grk protein is ectopically expressed in the nurse cells of *cup*^{1355} egg chambers

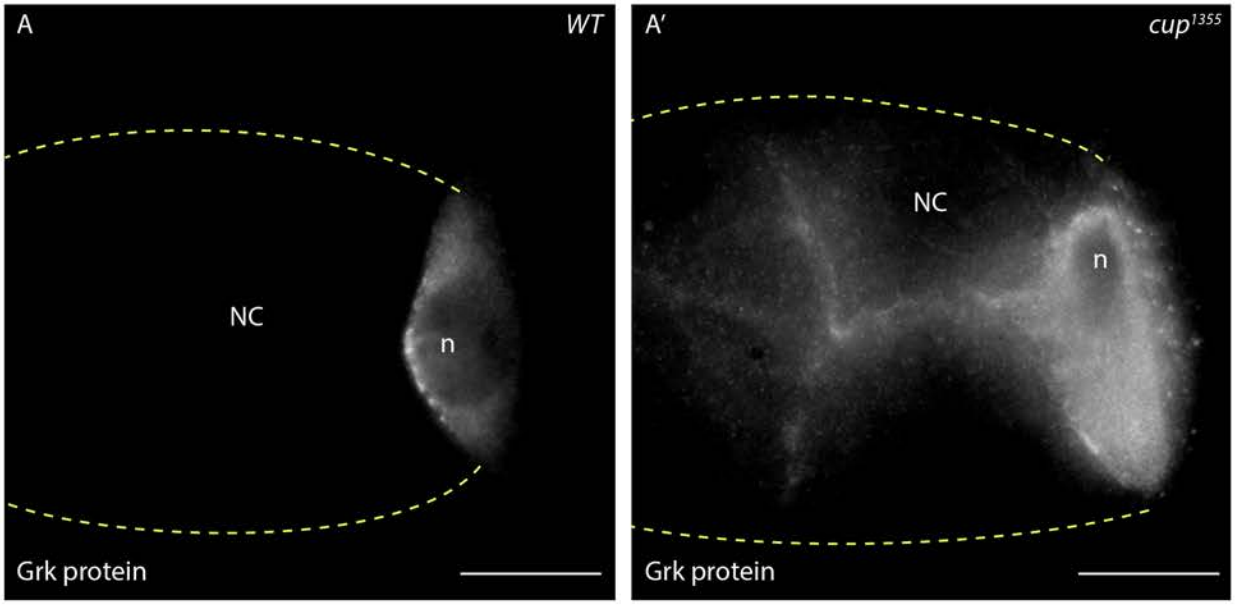

Figure 7-3:

(A-A'): Egg chambers stained for with anti-Grk. (A): In *WT* egg chambers Grk expressed is restricted to the oocyte. (A'): In *cup*^{1355} egg chambers Grk is expressed in the nurse cells along cell-cell boundaries. Dotted yellow lines indicate the edge of the egg chamber. Images collected at 100x magnification. NC, nurse cells; n, oocyte nucleus. Scale bars 15μm.

To test whether increased Orb expression alters *grk* mRNA translation, I visualised Grk protein in *cup*^{1355} egg chambers. Grk protein is expressed in a highly reproducible pattern along nurse cell boundaries that is not seen in wild-type egg chambers (Figure 7-3, Table 7-2). This distribution is expected for Grk, a secreted protein that is normally trafficked to the overlying follicle cells at the DA corner (Queenan et al. 1999), and was previously seen when *grk* was translated in the nurse cells of *aret* and *S*^{1} double mutants (Yan & Macdonald 2004). Grk protein is also expressed throughout the oocyte in these egg chambers (Figure 7-3).

Conclusion: In *cup*^{1355} egg chambers, Orb protein expression is significantly increased and *grk* mRNA is ectopically translated in the nurse cells.

Cup does not repress *grk* in the nurse cells by binding eIF4E

Cup has multiple functions during oogenesis (Piccioni et al. 2005), and translationally represses *osk* mRNA by binding eIF4E (Chekulaeva et al. 2006, Nakamura et al. 2004, Wilhelm 2003). To test whether ectopic Grk expression in *cup*^{1355} mutants is due to reduced Cup-mediated *grk* translation, I examined Grk protein distribution in *cup*$^{\Delta 212}$ mutant egg chambers. Imprecise excision of a P element insertion in these mutants produces a truncated protein which lacks the amino-terminal third of the peptide, disrupting the eIF4E binding domain and preventing Cup from binding eIF4E (Nakamura et al. 2004). Grk protein is absent from the nurse cells in *cup*$^{\Delta 212}$ mutants, and Orb protein expression was also normal in these egg chambers (Figure 7-4 (A-A', B-B'), Tables 7-1 and 7-2) as previously shown (Wong & Schedl 2011). Given the absence of an obvious phenotype, I verified that these flies were *cup*$^{\Delta 212}$ mutants by examining Osk protein distribution. As previously reported (Nakamura et al. 2004),

Figure 7-4: Grk and Orb protein distribution is unaffected in *cup*$^{\Delta 212}$ egg chambers

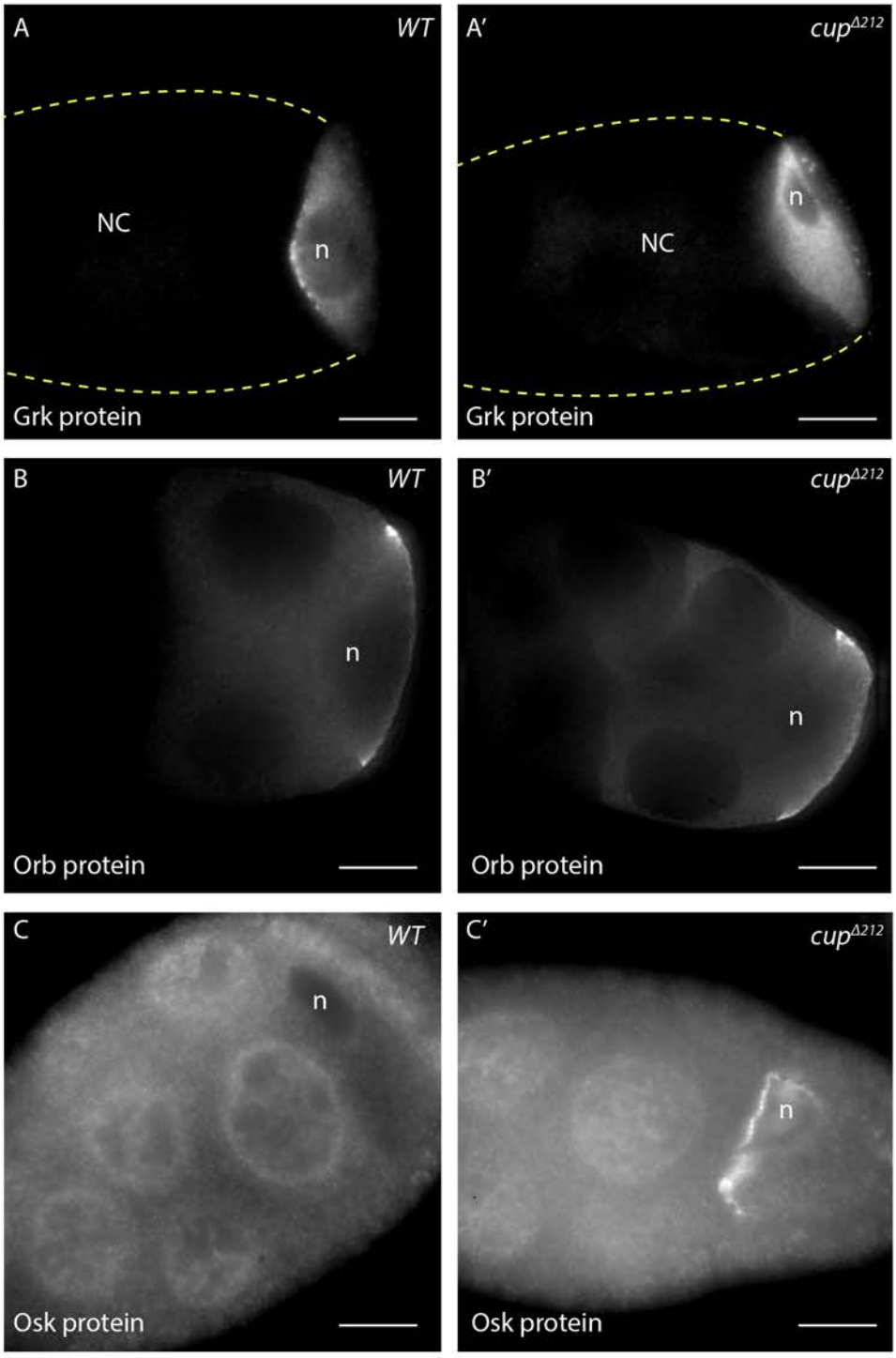

Figure 7-4:

(A-A') Egg chambers stained for with anti-Grk. In both *WT* (A) and *cup*$^{\Delta 212}$ (A') egg chambers Grk expression is restricted to the oocyte. (B-B'): Egg chambers stained for with anti-Orb. Orb expression is significantly higher at the oocyte cortex than in the nurse cells in both *WT* (B) and *cup*$^{\Delta 212}$ (B') egg chambers. (C-C'): Egg chambers stained for with anti-Osk. (C): In WT stage 6 egg chambers, no Osk is expressed in the oocyte. (C'): In stage 6 *cup*$^{\Delta 212}$ egg chambers Osk is expressed at the DA corner and anterior margin of the oocyte. In both cases, there is a high level of staining in the nurse cells and nurse cell nuclei with this antibody. Dotted yellow lines indicate the edge of the egg chamber. All images acquired at 100x magnification. NC, nurse cells; n, oocyte nucleus. Scale bars 15 μm.

Osk protein is expressed prematurely in the oocyte in stage 6 egg chambers (Figure 7-4 (C-C')). Recently, the validity of the *cup*$^{\Delta 212}$ mutants has recently been called into question, as it may not completely block Cup-eIF4E binding. However, my results indicate that there are differences in the extent to which Cup regulates *osk* and *grk* translation, as *osk* is ectopically translated in *cup*$^{\Delta 212}$ mutants and *grk* is not.

Conclusion: Ectopic translation of *grk* mRNA in *cup*^{1355} mutant egg chambers is mediated by an upregulation of Orb protein in the nurse cells of these mutants, rather than by disruption of the eIF4E binding activity of Cup.

Overexpressing *orb* causes ectopic Orb and Grk expression in nurse cells

To further test the role of Orb in *grk* translational control in the nurse cells, I overexpressed *orb* using a *UAS-orb* transgene (Li et al. 2012b) driven by *TubulinGal4VP16* (from now on referred to as *UAS-orb*). In these egg chambers, Orb protein expression in both the nurse cells and the oocyte is increased compared to wild-type egg chambers, with Orb expressed in puncta throughout the oocyte and nurse cell cytoplasm (Figure 7-5 (A'), Table 7-1). Analysis of fluorescence intensity along an anteroposterior transect of individual egg chambers reveals higher fluorescence in the nurse cells compared to the oocyte than in wild-type egg chambers (Figure 7-5 (B-B')). The mean fluorescence in all nurse cells compared to the oocyte is greater for all rows of nurse cells by roughly a third, but this is only statistically significant in the most anterior nurse cells (Figure 7-5 (C)).

To test whether upregulation of Orb protein in the nurse cells affects *grk* mRNA translation, I visualised Grk protein in *UAS-orb* egg chambers. Grk protein is expressed in the nurse cells along the cell-cell boundaries, as seen in *cup*^{1355} mutant

Figure 7-5: Orb protein expression is upregulated in the nurse cells of *UAS-orb* egg chambers

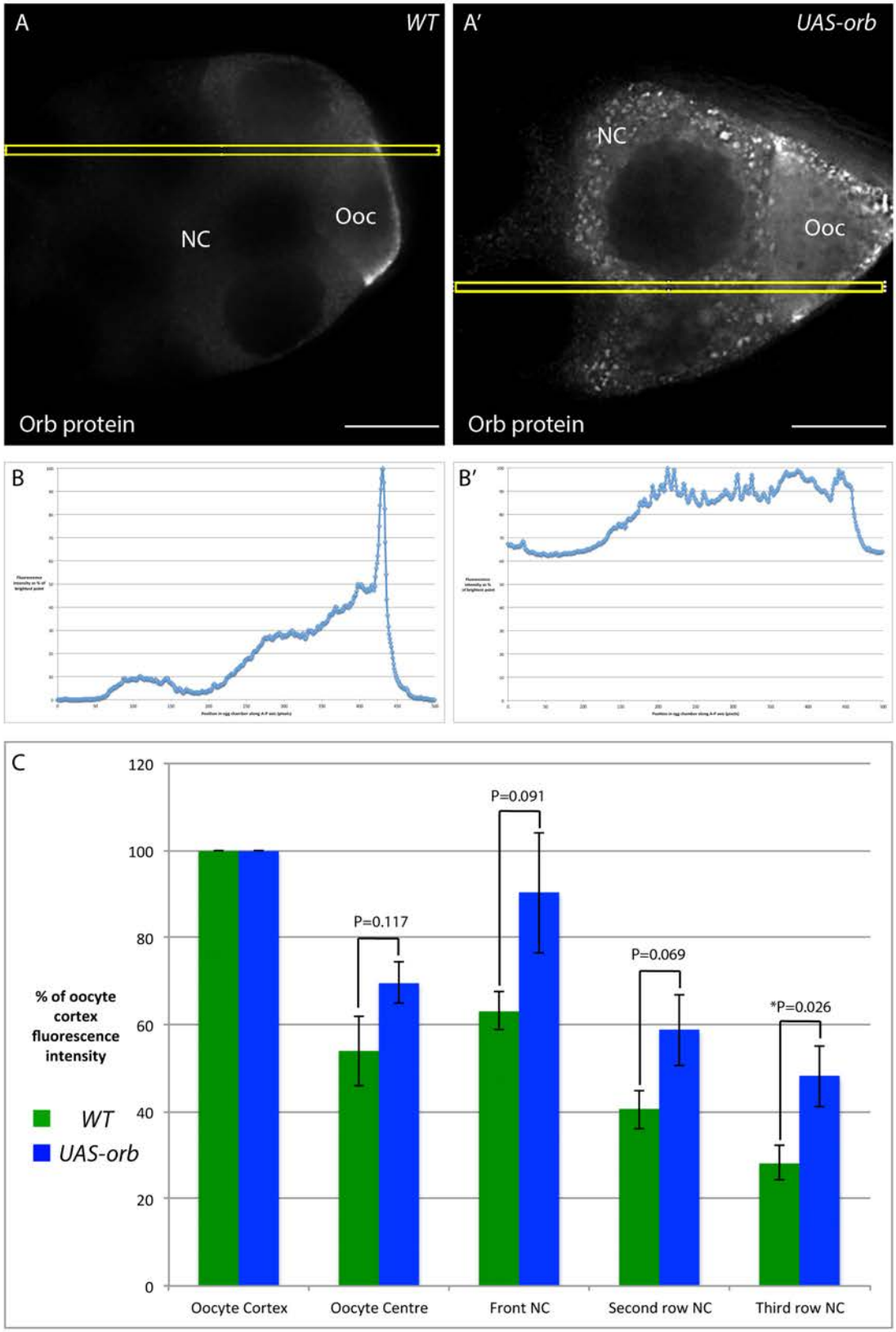

Figure 7-5:

(A-A'): Egg chambers stained for with anti-Orb. (A): In *WT* egg chambers Orb protein expression at the oocyte cortex is significantly higher than it is in the nurse cells. (A'): In *UAS-orb* egg chambers, Orb is highly expressed in puncta in the nurse cell cytoplasm. (B-B'): Fluorescence intensity readings along anteroposterior transects from yellow boxed regions in images in (A) and (A'). (B): In *WT* egg chambers there is a significant decrease in fluorescence intensity away from the oocyte cortex. (B'): In *UAS-orb* egg chambers, the fluorescence intensity in the nurse cells is closer to, or greater than, that at the oocyte cortex in this example. (C). Analysis of mean fluorescence intensity in different regions of the egg chamber (n=10 egg chambers for each condition). Error bars represent standard error of the mean. There is not a statistically significant difference between the fluorescence intensity in the oocyte centre and the first two rows of nurse cells when compared to the oocyte cortex between *WT* and *UAS-orb* egg chambers. P values of significance were generated by a two tailed t-test, * indicates a statistically significant difference ($P<0.05$). Only in the third row of nurse cells is *UAS-orb* significantly different to wild-type. Images in (A-A') were acquired at 100x magnification and are deconvolved. NC, nurse cells; Ooc, oocyte. Scale bars 15μm.

Figure 7-6: Grk protein is ectopically expressed in the nurse cells of *UAS-orb* egg chambers

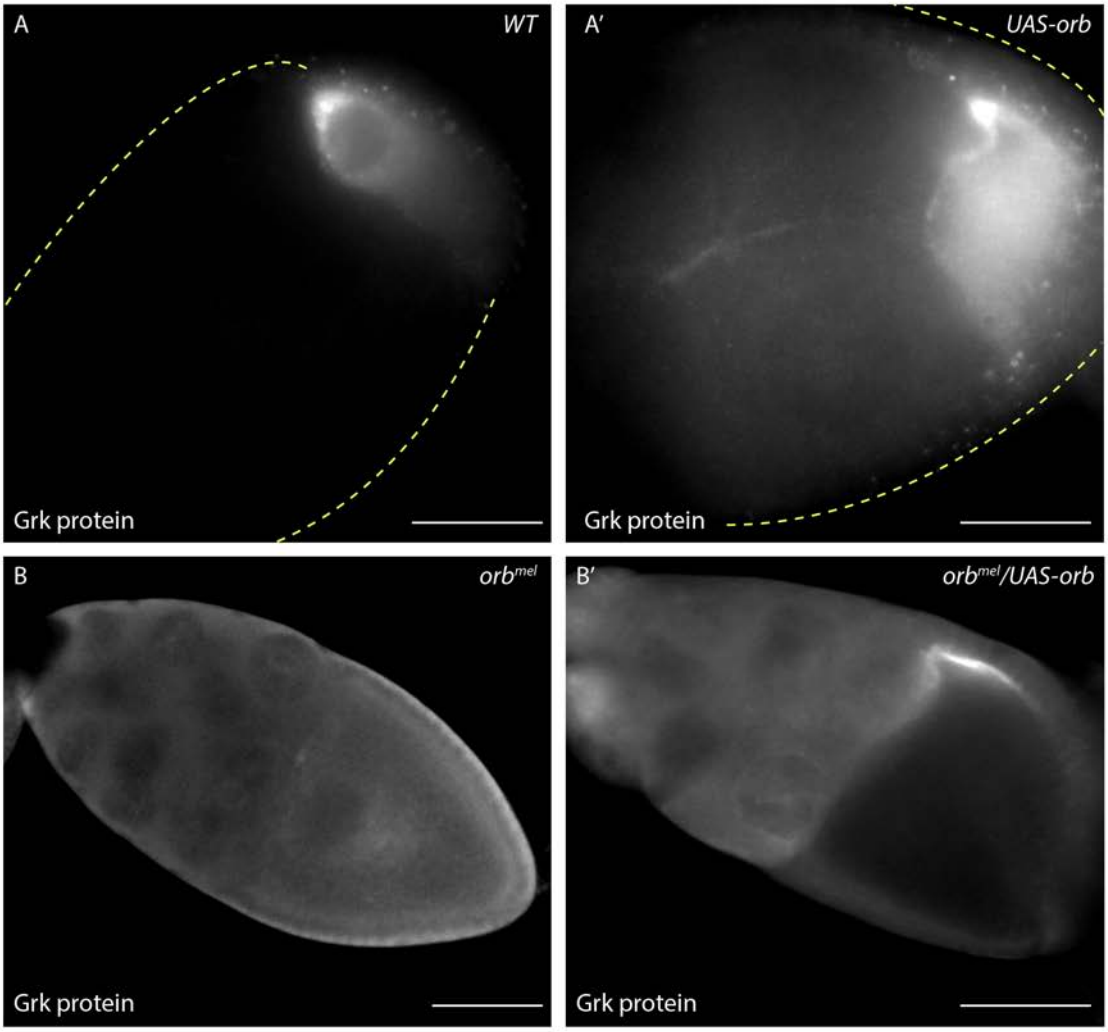

Figure 7-6:

(A-B'): Egg chambers stained for with anti-Grk. (A): In *WT* egg chambers Grk expression is restricted to the oocyte. (A'): In *UAS-orb* egg chambers Grk is expressed in the nurse cells along cell-cell boundaries. (B): In orb^{mel} egg chambers, Grk protein is not expressed. (B'): This expression is rescued in orb^{mel} egg chambers which also express *UAS-orb* driven by *TubulinGal4VP16*. Dotted yellow lines indicate the edge of the egg chamber. Images in (B) and (B') have been contrasted to show the egg chamber, nurse cell fluorescence in (B) and (B') is background. Images in (A-A') acquired at 100x magnification, images in (B-B') acquired at 20x magnification. NC, nurse cells; n, oocyte nucleus. Scale bars 15 μm (A-A'), 50 μm (B-B').

egg chambers, although Grk expression in the nurse cells is weaker than in *cup*^{1355} mutant egg chambers (Figure 7-6 (A-A'), Table 7-2). Grk is still enriched at the oocyte DA corner, but is also expressed more throughout the oocyte compared to wild-type (Figure 7-6 (A')). However, this pattern is not reproducibly seen.

To verify that this transgene expresses functional Orb protein, I generated flies expressing driven *UAS-orb* in an *orb*^{mel} mutant background. In *orb*^{mel} egg chambers Grk protein is not expressed (Figure 7-6 (B), Chang et al. 2001), but when coexpressed with driven *UAS-orb*, Grk expression is restored (Figure 7-6 (B')). In the nurse cells of these flies, Grk protein is not expressed, presumably because Cup still limits Orb expression to the low levels seen in wild-type nurse cells.

Conclusion: *orb* overexpression overwhelms its translational repression by Cup, and causes ectopic Orb protein expression throughout the egg chamber. Grk protein is expressed in the nurse cells when *orb* is overexpressed, suggesting that Orb is sufficient to activate *grk* mRNA translation in the nurse cells. These data argue that *grk* is translationally silenced in the nurse cells by low Orb expression in this tissue.

***UAS-orb* females lay eggs with dorsal appendage morphology defects**

To test whether overexpression of Orb causes ectopic dorsoventral patterning defects indicative of changes in Grk signalling (Neuman-Silberberg & Schupbach 1994), I examined eggs laid by *UAS-orb* females. 5% of eggs have fused dorsal appendages with extra dorsal cuticle material between them, and 32% of eggs have a "moose antler" dorsal appendage phenotype (Figure 7-7 (E, E'), Table 7-3). These appendages are shorter and have a more elaborate distal morphology, similar to the *bullwinkle* (*bwk,* (Dorman et al. 2004, Rittenhouse & Berg 1995, Tran & Berg 2003)

Figure 7-7: *UAS-orb* females lay eggs with dorsal appendage morphology defects

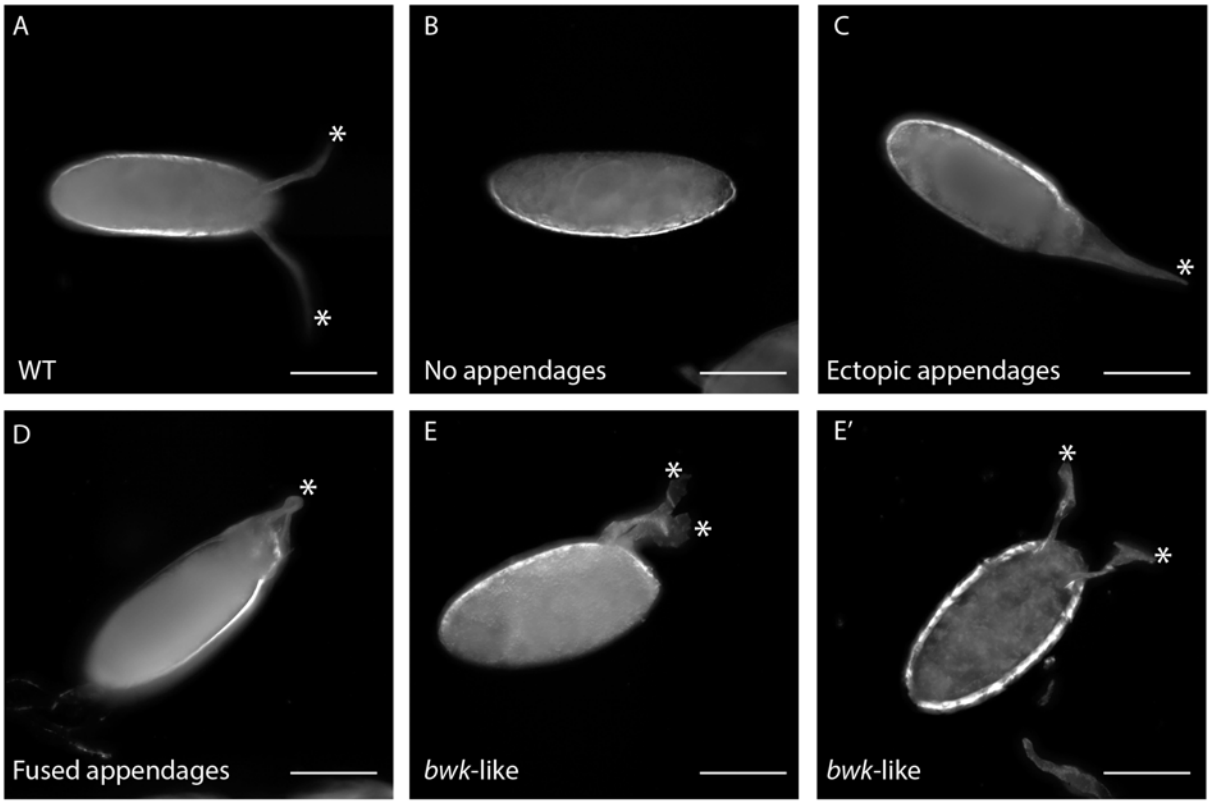

Figure 7-7:

(A-E'): Darkfield images of egg chambers laid by *WT*, *UAS-orb*, and *UAS-grk* females. Eggs were scored as belonging to one of 5 classes. (A) wild-type dorsal appendage morphology. (B) No appendages. (C) Ectopic appendages. (D) Fused appendage with extra dorsal material. (E, E') Two examples of "bwk-like" appendages. The morphology of the end of the appendage is elaborate and not like the "flattened paddle" seen in normal dorsal appendages. Images are contrasted for best display and oriented with posterior to the right. In all images the left of the egg chambers faces the top of the page, except E where the dorsal side faces the top of the page. White asterisks mark the end of the dorsal appendages. Images acquired at 10x magnification. Scale bars 150μm.

and *syncrip* mutants (McDermott et al. 2012). No eggs have ectopic dorsal appendages, a phenotype caused *grk* overexpression or mislocalisation (Bökel et al. 2006) (Kelley 1993). *cup*^{1355} females do not lay eggs, and were not assessed.

Conclusion: *orb* overexpression causes dorsal appendage morphology defects, suggesting Orb may regulate mRNAs with roles in follicle cell morphogenesis.

grk mRNA is localised in the oocyte in _cup_^{1355} and _orb_ overexpression mutants

Many proteins affect both *grk* localisation and translational control, including Sqd, K10, Syncrip and Cup (Clouse et al. 2008, McDermott et al. 2012, Norvell et al. 1999, Roth & Schupbach 1994). In *spoon* mutants, both *grk* mRNA and Grk protein are present at reduced levels in the oocyte, suggesting the mRNA is trapped and translated in the nurse cells (Motola & Neuman-Silberberg 2004). To test whether the expression of Grk protein in the nurse cells in *cup*^{1355} and *UAS-orb* egg chambers is a side effect of *grk* mRNA not being trafficked into the oocyte, I performed sm-FISH. In both genotypes, *grk* is still present in the oocyte. In *cup*^{1355} egg chambers the mRNA is mislocalised along the entire oocyte cortex (Figure 7-8 (A')). However, the misshapen oocyte in these egg chambers makes assessing mRNA localisation difficult, and egg chambers do not develop to mid-oogenesis when *grk* mRNA localises to the DA corner. In UAS-*orb* egg chambers, *grk* is localised correctly to the DA corner of the oocyte (Figure 7-8 (B')). In both instances, levels of *grk* mRNA in the nurse cells appear comparable to wild-type.

Conclusion: *grk* mRNA is correctly trafficked into the oocyte in *cup*^{1355} and *UAS-orb* egg chambers. These data argue that Grk expression in the nurse cells of these

Figure 7-8: *grk* mRNA localises to the oocyte in *UAS-orb* and *cup*^{1355} egg chambers

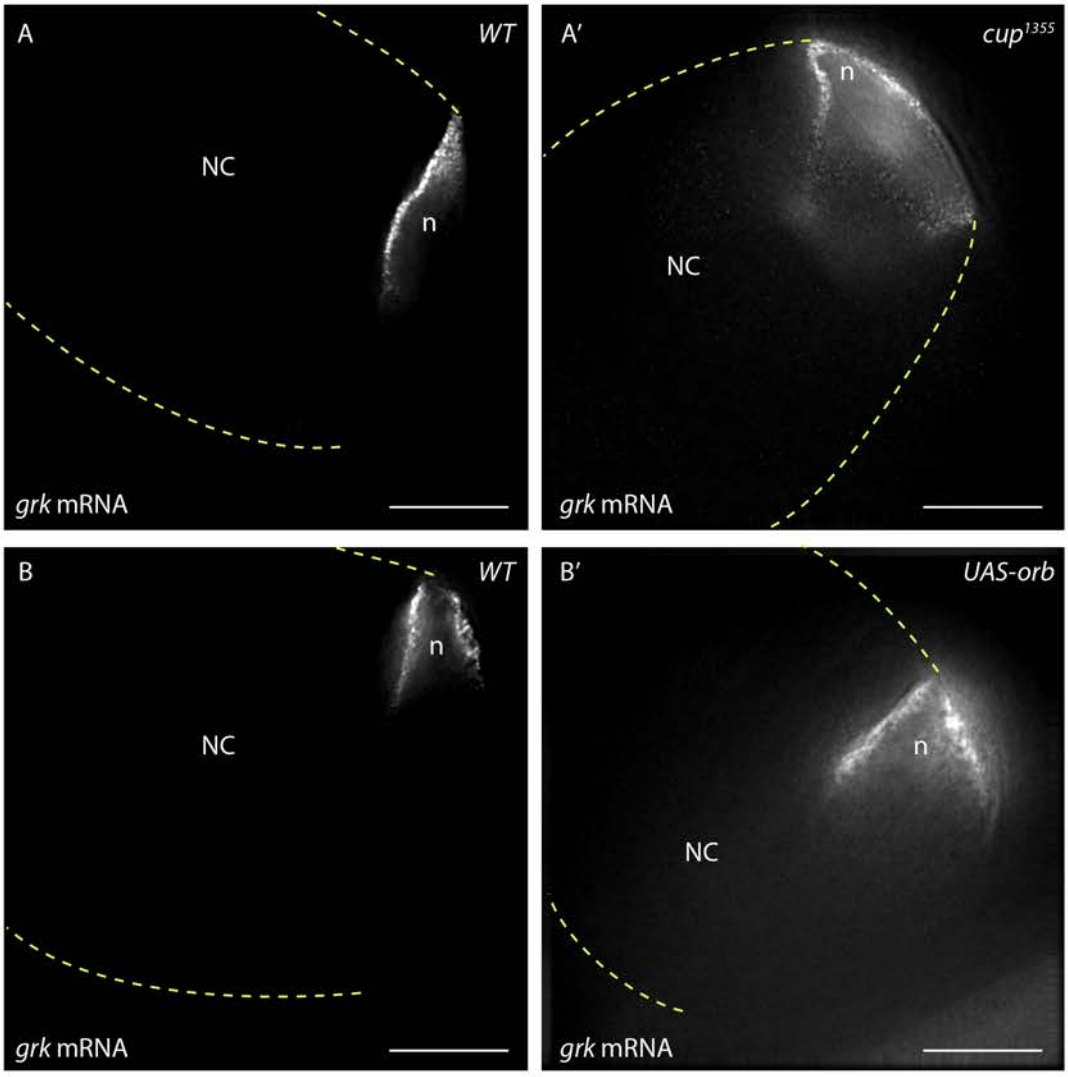

Figure 7-8:

(A-B'): Egg chambers labelled with *grk* sm-FISH probes. (A'): In *cup*^{1355} egg chambers, *grk* mRNA is deposited in the oocyte. However it is hard to assess whether it is correctly localised because the oocytes are abnormally shaped and die during mid-oogenesis. In both *WT* (B) and *UAS-orb* egg chambers (B'), *grk* mRNA localises to the DA corner of the oocyte. Dotted yellow lines indicate the edge of the egg chamber. Images acquired at 100x magnification and deconvolved. NC, nurse cells; n, oocyte nucleus. Scale bars 15μm.

mutants is a result of ectopic translation of *grk* mRNA in the nurse cells, not an increase in *grk* mRNA in nurse cells because of *grk* trafficking defects.

Assays to measure changes in *grk* the poly(A) tail length were inconclusive

Xenopus CPEB controls translation by modulating poly(A) tail length (Cao & Richter 2002), and Orb activity affects the poly(A) tail length of *osk*, *K10* and *orb* mRNAs (Chang et al. 1999, Chang et al. 2001, Wong & Schedl 2011). I verified the site of polyadenylation in the *grk* 3' UTR, which contains two conserved hexanucleotide sequences (AUUAAA, Retelska et al. 2006). From PCR of whole ovary RNA extracts, I sequenced the 3' end of the *grk* 3'UTR. Sequencing confirms that the poly(A) tail starts between 29 and 33 nucleotides downstream of the first hexanucleotide sequence at position 408 in the *grk* 3' UTR (Neuman-Silberberg & Schupbach 1993), suggesting that *grk* only uses this poly(A) site, and is not alternatively polyadenylated from its second, downstream hexanucleotide (Figure 7-9, (A)).

To test whether Orb controls *grk* translation by modulating its poly(A) tail length, I attempted to measure *grk* poly(A) tail length using the sPAT assay (Minasaki et al. 2014, in collaboration with L. Yang) when Orb activity is altered in orb^{mel}, cup^{1355} and *UAS-orb* egg chambers, compared to wild-type. Published results of this assay, and data obtained from L.Yang, identified heterogenous populations of poly(A) tail lengths for a single mRNA species, visualised as smears on agarose gels, which shift when the poly(A) tail is shortened or lengthened (Minasaki et al. 2014), L.Yang personal communication). The negative control for this experiment is treating samples with RNase-H, which specifically degrades the poly(A) tail. In these controls, only one discrete band should be observed on the gel instead of a smear. When I analysed sPAT products using primers designed for mapping the *grk* 3' UTR, one discrete band

is detected with faint smears in all samples (Figure 7-9 (B, C)). However, these smears are also present in RNase treated controls (Figure 7-9 (B, C)). Moreover, when this assay was repeated multiple times, no bands were detected. Due to the lack of observable difference between the samples and the controls, and the lack of reproducibility, this assay was not pursued further.

Conclusion: For measuring *grk* mRNA poly(A) tail length in whole ovary extracts, the sPAT assay does not yield reproducible results.

Orb protein is expressed at the P body edge when overexpressed in the nurse cells

Orb is enriched at the edge of P bodies at the DA corner of the oocyte where *grk* mRNA is translated, (Weil et al. 2012b), but is expressed at low levels in P bodies in wild-type nurse cells (Chapter 5). To test whether overexpressed Orb in the nurse cells is present in P bodies, I examined Orb protein distribution in either egg *cup*^{1355} chambers coexpressing *Tral::YFP*, or *UAS-orb* egg chambers coexpressing *Me31B::GFP*. Orb protein colocalises with Tral and Me31B respectively in the nurse cell cytoplasm of these egg chambers (Figure 7-10 (A-A", B-B")). To test whether Orb is enriched at the edge of these P bodies, I performed 3D-SIM microscopy on these egg chambers (collaboration with R. Parton). Although widefield images cannot resolve the precise distribution of Orb, 3D-SIM reveals that Orb protein is not extensively colocalised with Me31B, and appears to be in puncta at the edge of Me31B labelled P bodies (Figure 7-10 (C-C")).

Conclusion: Ectopic Orb protein in the nurse cells is enriched at the P body edge.

Figure 7-9: Changes in *grk* poly(A) tail length were not detected by the sPAT assay

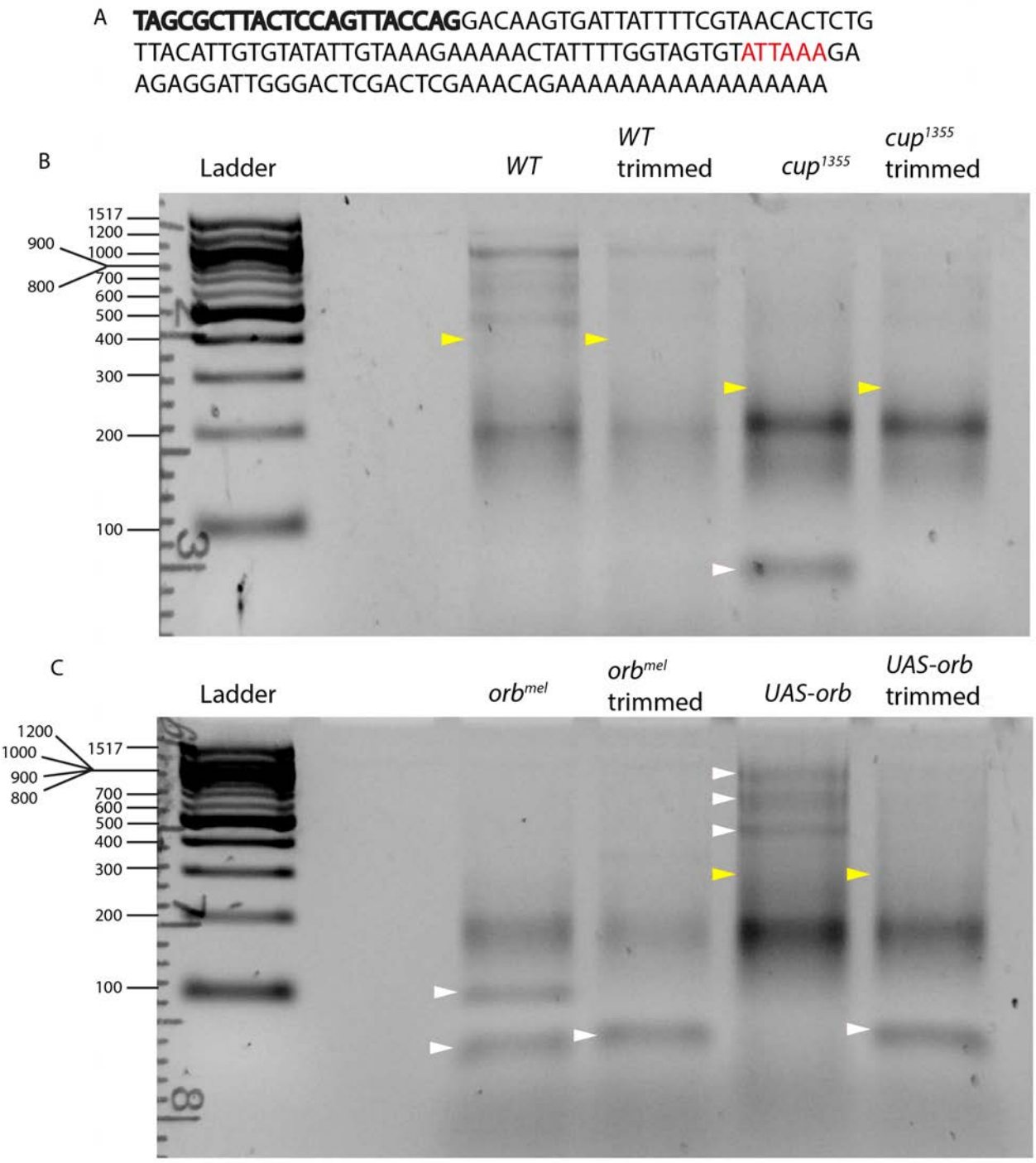

Figure 7-9:

(A): Position of the *grk* poly(A) site, with the poly(A) tail beginning 29 nucleotides downstream of the first hexanucleotide seuquence (red, ATTAAA). (B, C). sPAT analysis (in collaboration with L. Yang) detects one band at the expected size of the 3' end of the *grk* 3' UTR with a minimal poly(A) tail (~200 bp) in all genotypes (WT, cup^{1355}, orb^{mel} and *UAS-orb*). Some unidentified bands are detectable in certain genotypes (white arrowheads) but are not reproducibly seen and are most likely rRNAs. Smears (yellow arrowheads) are also seen in trimmed controls. There is sometimes a difference in the intensity of bands or smears, but there is no significant shift in the position of bands or smears in different genotypes.

Figure 7-10: Orb protein is expressed at the edge of P bodies when overexpressed in the nurse cells

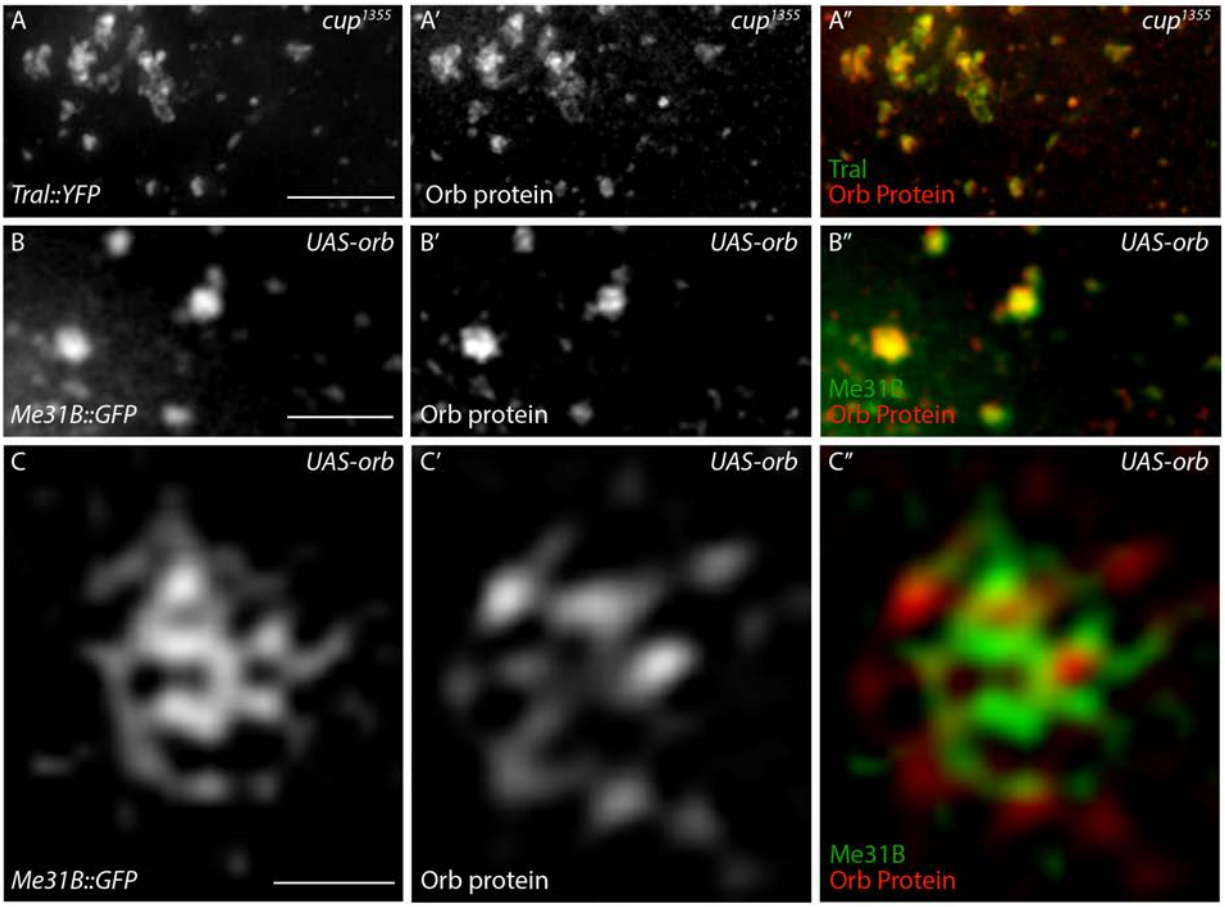

Figure 7-10:

(A-A") *cup*^{1355} egg chambers expressing *Tral::YFP* stained with anti-Orb. Orb (red) colocalises extensively with P bodies (green). (B-B") *UAS-orb* egg chambers expressing *Me31B::GFP* stained with anti-Orb. Orb (red) colocalises extensively with P bodies (green). (C-C") *UAS-orb* egg chambers expressing *Me31B::GFP* stained with anti-Orb, imaged using 3D-SIM. Puncta of Orb (red) are at the edge of continuous, reticulate P bodies (green). Images in (A-A") are 4 μm maximum intensity projections, images in (A-A") and (B-B") were acquired at 100x magnification and are deconvolved, images in (C-C") are 3D-SIM reconstructions of 1 μm maximum intensity projections collected at 60x magnification on the OMX V3. Scale bars 2μm (A,B), 1μm (C).

grk mRNA associates with P bodies when Orb is overexpressed in nurse cells

At the oocyte DA corner, *grk* mRNA docks at the edge of P bodies where Orb protein is enriched, and is thought to be translated here (Weil et al. 2012b). In the nurse cells of wild-type egg chambers, *grk* rarely colocalises with P bodies (Figure 6-9). To test whether increased Orb protein expression at the edge of nurse cell P bodies causes *grk* to associate with P bodies and become translated, I performed sm-FISH in either *cup*^{1355} egg chambers coexpressing *Tral::YFP* or driven *UAS-orb* egg chambers coexpressing *Me31B::GFP*. In both genotypes, there is a significant increase in the proportion of *grk* mRNA which colocalises with nurse cell P bodies (53% and 52% of particles are at the P body edge, n=395 and 429 particles respectively, Figure 7-11, Table 7-4). Although widefield imaging cannot resolve the exact position of *grk* particles relative to P bodies, it is clear that in wild-type egg chambers they are separate from P bodies, and in *cup*^{1355} or *UAS-orb* egg chambers they are closely associated with P bodies. *grk* particles were rarely in the core of large P bodies

(Table 7-4). Interestingly, there is also a significant increase in the number of *grk* particles in the P body core in both genotypes compared to wild-type (12% in *cup*^{1355} compared to 3% in *Tral::YFP* and 6% in *UAS-orb* compared to 1% in *Me31B::GFP*, Table 7-4), however this is still a small proportion of particles, and there are more particles not associated with P bodies than in the P body core.

Conclusion: Significantly more *grk* mRNA particles dock at the edge and are targeted to the core of nurse cell P bodies when Orb is overexpressed, suggesting that Orb expression at the P body edge is sufficient to target *grk* mRNA to P bodies.

Figure 7-11: *grk* mRNA associates with P bodies when Orb is overexpressed in nurse cells

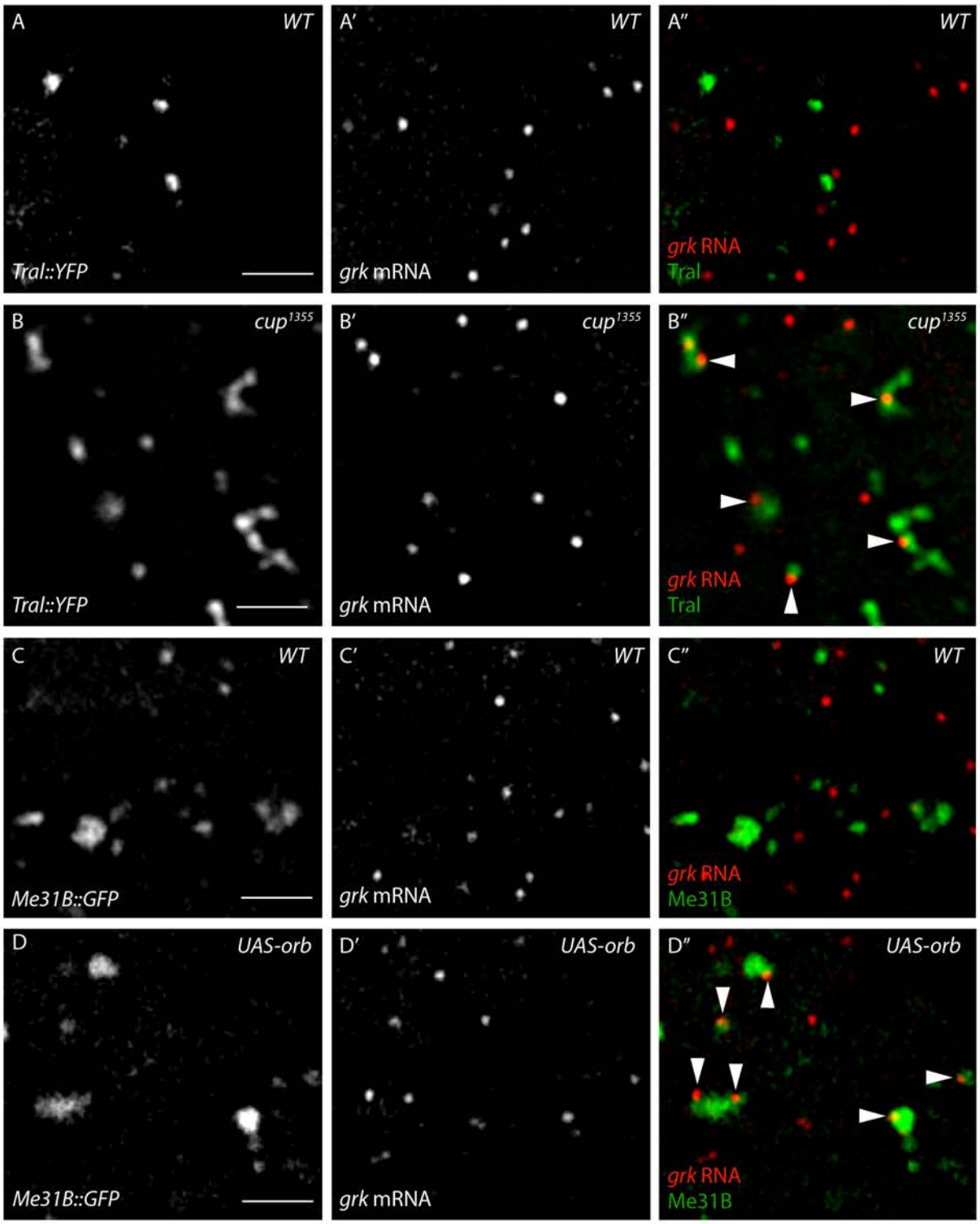

Figure 7-11:

(A-A") *WT* egg chambers expressing *Tral::YFP* with *grk* sm-FISH. *grk* mRNA (red) rarely colocalises with P bodies (green, 14% of particles colocalise, n=322). (B-B") *cup*^{1355} egg chambers expressing *Tral::YFP* with *grk* sm-FISH. *grk* mRNA (red) colocalises extensively with the edge of P bodies (green, white arrowheads mark particles at the P body edge, 52% of particles are at the edge, n=429). (C-C") *WT* egg chambers expressing *Me31B::GFP* with *grk* FISH. *grk* mRNA (red) rarely colocalises P bodies (green, 16% of particles colocalise, n=297). (D-D") *UAS-orb* egg chambers expressing *Me31B::GFP* with *grk* FISH. *grk* mRNA (red) colocalises extensively with the edge of P bodies (green, white arrowheads mark particles at the P body edge, 53% of particles are at the edge, n=395). There is a statistically significant difference in the proportion of grk particles which associated with the P body edge between *WT* and *cup*^{1355} and *WT* and *UAS-orb* egg chambers (Table 7-4). All images acquired at 100x magnification and deconvolved. Scale bars 2 μm

Discussion

Translation of *grk* mRNA in the nurse cells is prevented by spatially restricted access to Orb

My data highlight a new mechanism of translational control by restricted spatial access to translational activators. I propose a model whereby *grk* translation is prevented in the nurse cells by restricting high levels of Orb protein expression to the oocyte (Figure 7-12). In wild-type egg chambers, where Cup represses *orb* mRNA translation in the nurse cells (Wong & Schedl 2011), low levels of Orb protein expression in the nurse cells are not sufficient to target *grk* mRNA to nurse cell P bodies for translation (Figures 6-9, 7-11). In the oocyte, localised *grk* at the DA corner docks at the edge of P bodies, where high levels of Orb protein activate its translation (Weil et al. 2012b). In *cup* mutant or *UAS-orb* egg chambers, Orb protein is upregulated at the edge of nurse cell P bodies (Figures 7-2, 7-5, 7-10). *grk* mRNA now docks at the edge of these P bodies (Figure 7-11), is translated, and this Grk protein is trafficked to the nearest nurse cell-nurse cell boundary (Figures 7-3, 7-6). Significantly, my data also suggest that Orb is a key determinant of *grk* mRNA interaction with P bodies, as it is sufficient to target *grk* mRNA to nurse cell P bodies.

Orb and Grk are expressed in the nurse cells of *cup^{1355}* and *UAS-orb* egg chambers

In *cup^{1355}* egg chambers, Orb protein is upregulated in the nurse cells, is enriched in P bodies, but is also found in a diffuse cytoplasmic background in all of the nurse cells at a higher level than in the oocyte cortex (Figure 7-2). In contrast, in *UAS-orb* egg chambers, Orb protein is enriched almost exclusively P bodies, and there is still a gradient with the highest Orb expression in the posterior nurse cells (Figure 7-5).

Figure 7-12: Translation of *grk* mRNA in the nurse cells is prevented by restricted spatial access to Orb

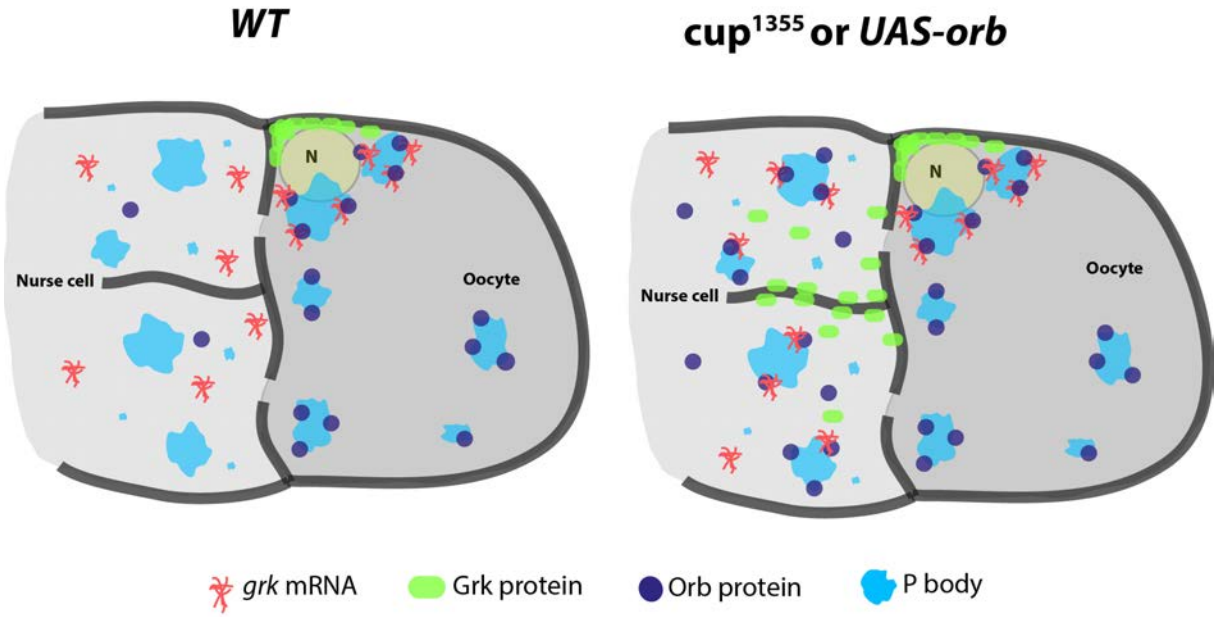

Figure 7-12:

In *WT* egg chambers, Orb (purple) is expressed at low levels in the nurse cells, and *grk* mRNA (red) does not dock at the edge of nurse cell P bodies (blue). At the DA corner of the oocyte, *grk* anchors at the P body edge where Orb is enriched, and is translated into Grk protein (green), which is secreted to the overlying follicle cells. In *cup*^{1355} or *UAS-orb* egg chambers, Orb is highly expressed at the edge of nurse cell P bodies. *grk* interacts with these P bodies and is translated. The Grk protein is trafficked to the boundaries between nurse cells. N, oocyte nucleus.

This difference in Orb distribution could be accounted for by the fact that in *cup*^{1355} egg chambers, Orb is presumably translated in the oocyte at normal levels, as Cup is not thought to repress *orb* mRNA translation in wild-type oocytes. Therefore, there is a significant increase in Orb protein expression in the nurse cells compared to the oocyte. However, in *UAS-orb* egg chambers, Cup still represses *orb* mRNA translation in the nurse cells. This repression machinery appears to be saturated, causing increased Orb protein expression, but this is accompanied by an increase in Orb protein expression in the oocyte. Hence, there is not as great a difference in the expression of the protein between the two tissues (Figures 7-2, 7-5). The expression of Orb protein largely in P bodies in *UAS-orb,* but not *cup*^{1355} mutant egg chambers, may reveal a role for Cup in restricting Orb expression to P bodies. How Orb is enriched in P bodies when overexpressed, and expressed only at the edge of oocyte P bodies, should be investigated further using ultra-structural analysis with IEM or 3D-SIM of Orb distribution in *cup* mutant egg chambers.

In both *cup*^{1355} and *UAS-orb* egg chambers, Grk protein is expressed along cell-cell boundaries in the nurse cells (Figures 7-3, 7-6). Grk protein at the oocyte DA corner is secreted into the follicle cells (Queenan et al. 1999). This pattern of nurse cell expression was also seen when Grk was translated in the nurse cells of *aret* and *S*^{1} mutants (Yan & Macdonald 2004), and when Osk protein was ectopically expressed using a *UAS-osk::GFP* construct lacking the *osk* 3' UTR (Kim et al. 2015). Although the expression of Osk protein in a similar pattern raises the possibility that all proteins expressed in nurse cells are trafficked to cell-cell boundaries by default, this seems unlikely, as numerous trans-acting proteins in the nurse cell cytoplasm are not expressed in this pattern (Chapter 5). Moreover, the Osk protein seen in this pattern is driven by a *UAS* construct, lacks the *osk* 3' UTR, and is not under the correct

endogenous control (Snee & Macdonald 2004). Finally, ectopic Grk protein present in the nurse cells of *spoon* mutants is not expressed in this pattern, but is expressed around the nurse cell nuclei (Motola & Neuman-Silberberg 2004). Why Grk expression is to be restricted to boundaries between nurse cells, and not at follicle cell boundaries, is unclear. This could be further examined by covisualising Grk with fluorescently labelled cell boundaries, like Phalloidin to label cortical actin (Spracklen et al. 2014), and investigating the differences of the cell boundaries between neighbouring nurse cells, and those between nurse cells and the follicle cells.

Grk expression in the nurse cells is stronger in cup^{1355} than *UAS-orb* egg chambers. This could be explained by the fact that in *UAS-orb* egg chambers, Cup protein presumably still represses some *orb* mRNA translation. This would cause lower levels of Orb protein expression in these nurse cells, and less *grk* mRNA translation. However, this interpretation is not supported by FISH data suggesting that a similar percentage of *grk* mRNA particles dock at the edge of P bodies in the nurse cells of cup^{1355} and *UAS-orb* egg chambers (Figure 7-11 and Table 7-4), and should be further investigated with different strengths of Gal4 driver for the *UAS-orb* construct.

The most likely explanation for Grk expression in the nurse cells of these egg chambers is that *grk* mRNA docks at the edge of P bodies and is ectopically translated, as increased levels of Orb protein transform the nurse cells into an environment conducive to translation, like the oocyte of wild-type egg chambers. However, there remains the unlikely possibility that this Grk protein is expressed in the oocyte and is somehow trafficked back into the nurse cells, and that *cup* mutations or *orb* overexpression causes Grk secretion defects. Although there is no evidence for this mechanism, it could be tested by disrupting the secretory pathway

of wild-type egg chambers and examining whether Grk protein accumulates in nurse cells, for example using S^{1} mutants (Yan & Macdonald 2004). The pioneer round of *grk* translation could be visualised in nurse cells of wild-type, cup^{1355} and *UAS-orb* egg chambers using using MS2 and PP7 loops in "translating RNA imaging by coat protein knock-off" (TRICK Halstead et al. 2015), or using photoconvertible injected proteins such as Kaede to visualise newly synthesised proteins (Leung & Holt 2008).

It is also possible that although overexpressing Orb in the nurse cells is sufficient to activate *grk* translation, low levels of Orb may not be the only mechanism which maintains translational silencing of *grk* in the nurse cells. Given that many proteins, including trans-acting factors of *grk*, *osk* and *bcd*, are expressed in the nurse cells, does another mechanism exist to repress *grk* and prevent it from interacting with this active translational machinery? I tested the main candidate proteins for translational repressors of *grk* (Chapter 6), but Orb could activate *grk* translation by removing multiple repressor proteins, or a (currently unknown) repressor protein. Low Orb expression may be just one layer of *grk* translation regulation in the nurse cells; perhaps removal of repressors from *grk* is not sufficient to cause Grk expression, because Orb levels in the nurse cells are still to low to activate *grk* translation. These hypotheses could be tested by visualising Grk protein in double mutants for repressor proteins, and biochemical analysis of the interactions between Orb and these repressor proteins in orb^{mel} and *UAS-orb* egg chambers.

Another interpretation of these data is that low levels of Orb expression in the nurse cells represses translation, whereas high levels in the oocyte activate translation. However, when *orb* is mutated, Grk and Osk proteins are not ectopically expressed, suggesting that Orb is not a key translational repressor of these mRNAs. Whether

Orb can repress translation, perhaps in conjuction with other proteins, requires further biochemical analysis of the translation initiation machinery and Orb interacting proteins in *Drosophila*. Whether Orb performs two distinct roles at different dosages could be address by *in-vitro* analysis of Orb activity at different expression levels.

It would also be interesting to test whether Osk, Bcd and Nos protein expression are altered in *cup* mutant or *UAS-orb* egg chambers. Orb is required for *osk* translation (Chang et al. 1999), and one hypothesis is that upregulation of Orb in nurse cells would cause ectopic Osk expression in this tissue. This was not tested because the Osk antibody causes high levels of nurse cell fluorescence (Figure 7-4), but should be investigated. How *nos* is translated in the nurse cells (Forrest et al. 2004) when Orb is expressed at low levels in this tissue, should also be investigated.

***orb* overexpression affects dorsal appendage morphology**

Eggs laid by *UAS-orb* females display dorsoventral patterning defects (Figure 7-7 table 7-3). I expected these egg chambers to show dorsal appendage defects indicative of incorrect Grk signalling. I hypothesised that either 1.) *grk* translation in the nurse cells would trap this mRNA in the nurse cells and prevent it's transport into the oocyte, leading to a lower concentration of *grk* at the DA corner and cause poorly formed appendages, or 2.) Grk protein expressed in the nurse cells would enter the oocyte at nurse cell dumping and diffuse throughout the ooplasm, causing ectopic dorsal appendage formation. However neither phenotypes was observed. 32% of eggs were laid with short, "bwk-like" appendages (McDermott et al. 2012, Rittenhouse & Berg 1995, Tran & Berg 2003). The *bwk* gene is required for dorsal appendage morphogenesis (Dorman et al. 2004), and my data indicate that when *orb* is overexpressed, the migration of follicle cells during dorsal appendage

morphogenesis is affected. This suggests that *orb* operates upstream of genes like *bwk* or *shark*, involved in dorsal appendage morphogenesis (Tran & Berg 2003). This could be further investigated by examining dorsal appendage morphogenesis and follicle cell gene expression in *UAS-orb* egg chambers (Dorman et al. 2004).

To understand the *UAS-orb* phenotype it is also important to examine the fate of Grk protein expressed in the nurse cells; is it able to activate EGFR signalling as it does in the oocyte? In *spoon* mutants, Grk protein in the nurse cells does not increase expression of *kekkon*, a downstream target of the *grk*/EGFR signalling pathway (Ghiglione et al. 1999, Motola & Neuman-Silberberg 2004). Whether Grk in the nurse cells of cup^{1355} and *UAS-orb* egg chambers activates the EGFR pathway could help assess the eggshell phenotype of these mutants. If this Grk is not signalling, is it an inactive protein, or are the nurse cells not competent to respond to Grk signalling?

sPAT analysis could not be used to determine the poly(A) tail length of *grk*

My results raise questions about the poly(A) state of *grk*; if Orb is required to translationally activate *grk*, is *grk* deadenylated in the nurse cells? If so, is this achieved by deadenylases like CCR4 (Igreja & Izaurralde 2011), or shortening of the poly(A) tail in the nucleus after transcription?

sPAT analysis has been used in other systems, including *Xenopus* oocytes and the *Drosophila* larval brain, to measure changes in poly(A) tail length (Minasaki et al. 2014, L. Yang personal communication). However, in my analysis, only one band is detected, rather than a smear of mRNAs with different poly(A) tail lengths (Figure 7-9). Any smears that are present in the samples are also seen in RNase treated controls, meaning the different genotypes cannot be compared based on the smear

position. The detected band is the approximate length of the *grk* 3' UTR region covered by the primer with a minimal poly(A) tail (~200bp). In other repeats of this experiment, no bands were detected, suggesting that the mRNA was degraded. This assay was attempted with fresh kits but no bands were detected.

The most likely explanation is that the RNase-H was not functioning, and so the samples appeared the same as the controls. However, the same reagents, including RNase-H, were used successfully in parallel sPAT assays by L. Yang. This suggests that the RNase-H was functional, and the smears detected in both the samples and the control are not different species of *grk* with different poly(A) tail lengths, but are more likely to be contaminants.

When I mapped the *grk* polyadenylation site with magnesium titration PCR of whole ovary RNA extracts (with *grk* and oligodT primers), smears are detected on the gel, and sequencing verified the smears as polyadenylated *grk* mRNA. This protocol is identical to sPAT, except sPAT requires the ligation of a DNA splint to the poly(A) tail. This allows addition of the RNA anchor, against which the reverse primer is designed (Minasaki et al. 2014). Logically, it seems that errors in the ligation of the DNA splint may be behind the differences in output between the two techniques.

Closer inspection of the genomic region of chromosome 2L, where *grk* is located, reveals that the genome is transcribed in both directions in this region, and just after the *grk* 3'UTR is an A rich region of the *Akap200* gene, encoding an A-kinase anchoring protein which is highly expressed during oogenesis (Figure 7-13, Jackson & Berg 2002, Li et al. 1999). One explanation for the issues with the sPAT assay could be that during *grk* is transcription, RNA polymerase transcribes through the

Figure 7-13: Potential problems with sPAT analysis of *grk* mRNA

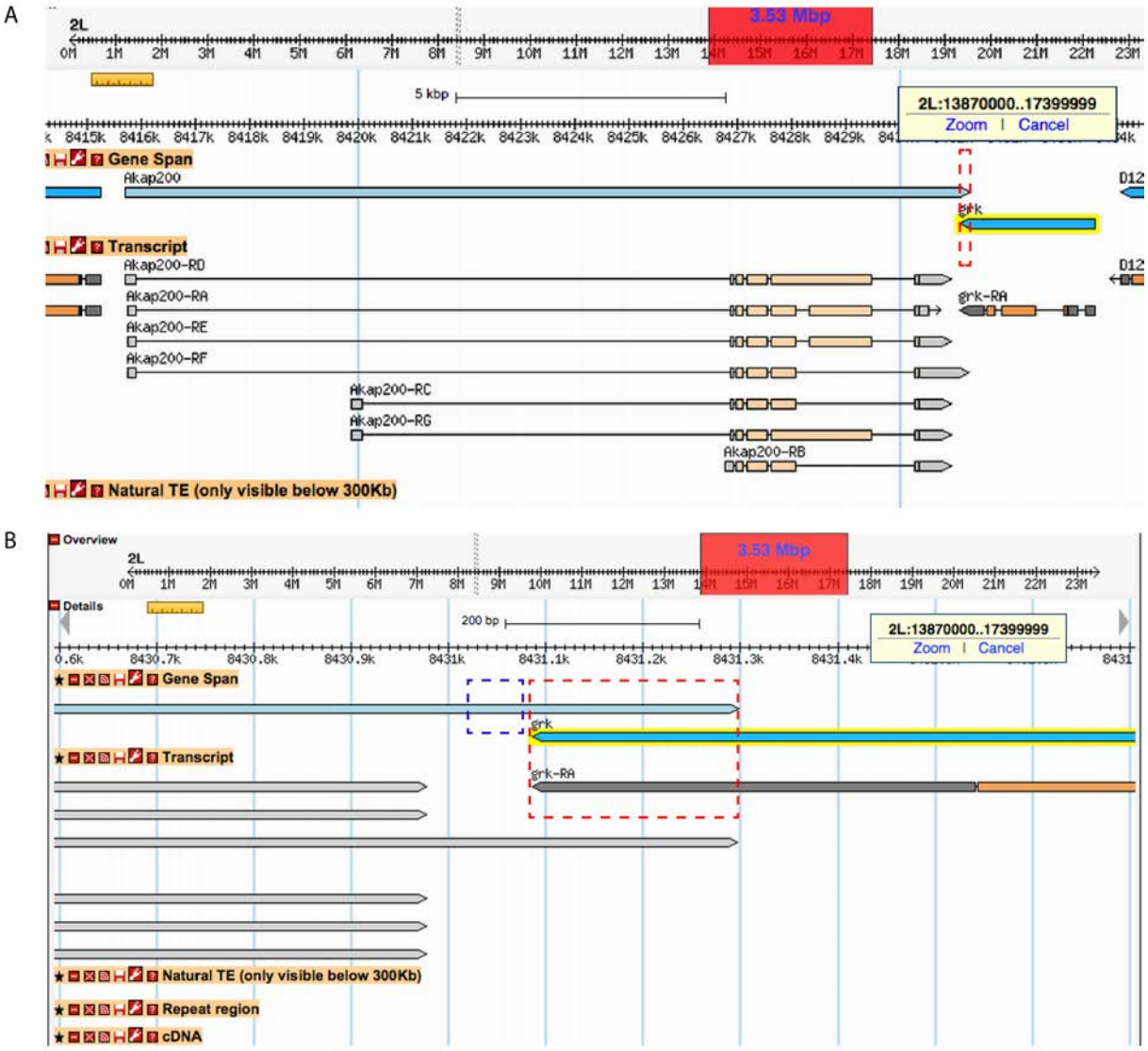

Figure 7-13:

(A): GBrowse view of *grk* and it's surrounding genes. The 3' UTR of *grk* overlaps with the 3' UTR of *Akap200*. (B) Close up of red boxed region in (A), red box highlights region of overlap, blue box highlights region just downstream of *grk*, sequence shown in (C) which is very A rich.

A-rich region of *Akap200*, and the *grk* nascent transcript is cleaved at the first polyadenylation site, followed by addition of the poly(A) tail. When mapping the polyadenylation site, it is theoretically possible that the oligodT primer, which contains 12-18 Ts, preferentially binds to the *grk* poly(A) tail rather than the A rich region of *Akap200* before it is cleaved. The DNA splint, however, contains only 9 Ts, and could discriminate less between the A-rich region in *Akap200* and the *grk* poly(A) tail. This, combined with the tendency of PCR to favour shorter products, could generate a band the size of the mapped *grk* 3'UTR region, plus a short region of *Akap200*, which would be a similar size to the mapped *grk* 3'UTR region with a minimal poly(A) tail.

This hypothesis could be tested by performing the sPAT assay with the DNA splint and the mapping with the oligodT primer alongside one another, and use the same RNase-H treatment on both to determine the identity of the bands in the mapping gels. Moreover, the bands and smears from the sPAT could be sequenced to identify whether they contain a poly(A) tail or part of the *Akap200* gene.

It is possible that *grk* poly(A) tail length is unaltered in *WT*, orb^{mel}, cup^{1355}, and *UAS-orb* egg chambers. However, due to the similarity between negative controls and all samples, conclusions cannot be drawn from this assay. Analysis of transcripts which are known to have altered poly(A) tail lengths in *orb* or *cup* mutants, for example *osk* and *orb* mRNAs (Chang et al. 1999, Tan et al. 2001, Wong & Schedl 2011) and alterations to the protocol including a modified DNA splint, could determine whether this assay can be used to study *grk* during oogenesis. If this or a similar assay can be used to monitor *grk* poly(A) state, it could be used to test whether deadenylases like CCR4 or Pum are required for the translational silencing of *grk* in the nurse cells by maintaining a short poly(A) tail. Indeed, at the time of writing (after these

experiments were completed) similar assays in aged ovaries confirm that *grk* translation at the DA corner requires Orb and Wispy dependent poly(A) tail elongation, and unlocalised *grk* is not polyadenylated (Norvell et al. 2015).

The molecular mechanism of the interaction between Orb and *grk* mRNA

Orb is required for the translation of *grk* mRNA (Chang et al. 2001), and my data suggest that Orb expression in the nurse cells is sufficient to activate *grk* translation. A simple model would be that at the P body edge, Orb binds to a CPE sequence in the *grk* 3' UTR and activates its translation by elongating its poly(A) tail. However, although Orb binds *osk*, *orb* and *K10* mRNAs and modulates their poly(A) tail length (Castagnetti & Ephrussi 2003, Chang et al. 1999, Chang et al. 2001, Juge et al. 2002, Tan et al. 2001), there is evidence that Orb does not bind to *grk* (Chang et al. 2001), although it does modulate *grk* poly(A) tail length (Norvell et al. 2015). Searches for a CPE sequence (consensus UUUUUAU Hake & Richter 1994, Fox et al. 1989) in the *grk* 3' UTR revealed one similar sequence, UUUAAUUU, 275 nucleotides upstream of the hexanucleotide. CPE sequence and position is variable, but is normally within 20-30, at most 100, nucleotides of the hexanucleotide (Méndez & Richter 2001). Although Orb may bind only weakly to *grk*, the fact that *K10* mRNA interacted with Orb in the same assay (Chang et al. 2001) forces us to consider that Orb and *grk* do not interact directly.

Mass spectrometry work revealed that Orb interacts with 170 proteins (Wong et al. 2011), including ribosomal proteins, translation initation factors, RNA helicases, RBPs, and P body proteins. This raises the possibility that Orb interacts with *grk* through one or more intermediate proteins. It is also possible that Orb polyadenylates and translationally activates an mRNA which encodes a translational activator of *grk*.

Further biochemical analysis of the Orb and *grk* mRNA interaction was planned for this Thesis, however: 1.) the Orb antibody failed to reproducibly label all Orb isoforms by Western blot, 2.) flies expressing *UAS-orb::HA* did not express this transgene correctly when driven by *TubulinGal4VP16* and examined using anti-HA antibodies by immunofluorescence, 3.) An *orb-eGFP* MiMIC line (Venken et al. 2011) is homozygous lethal, and Orb-eGFP expression did not correlate with antibody-labelled Orb protein in the same egg chamber.

Generation of an Orb::GFP protein trap line, a functional HA tagged Orb, or a new Orb antibody would allow biochemical analysis of *grk* and Orb interaction, the regions of *grk* required for interactions with Orb, or the necessary intermediate proteins. Mutational analysis of *grk* mRNA lacking candidate Orb interacting sequences, and the effect of *orb* mutation or overexpression on this mutant RNA, would help to elucidate the molecular mechanism of *grk* translational control by Orb. Individual-nucleotide resolution Cross-linking and ImmunoPrecipitation (iCLIP, (Darnell 2012, Huppertz et al. 2014) could also reveal other target mRNAs of Orb and the binding domains necessary for these interactions, improving our understanding of the role of Orb during oogenesis.

The mechanism of Cup mediated *orb* translational repression

My model of *grk* translational silencing by restricted access to Orb suggests that Cup repression of *orb* translation is central to *grk* translational regulation. However, the mechanism of Cup-mediated *orb* repression is unknown. Cup is the functional homolog of *Xenopus* Maskin. However, $cup^{\Delta 212}$ mutants do not show increased Orb protein expression in the nurse cells (Figure 7-4, (Wong & Schedl 2011), suggesting Cup and Orb do not interact in a similar way to CPEB and Maskin.

How *orb* mRNA translational repression by Cup is lifted in the oocyte is also unclear. Cup is present in P bodies in the nurse cells and in the oocyte (Figure 5-2, (Weil et al. 2012b), so it seems unlikely that spatial distribution of Cup controls *orb* mRNA translation. Biochemical analysis could elucidate the interactions between Cup, *orb*, and other proteins in this complex, as well as how these change throughout development and between the nurse cells and the oocyte. Moreover, *UAS-cup* constructs could be used to overexpress Cup protein, and test how this affects *orb* and *grk* translation in the oocyte and the nurse cells.

Orb targets *grk* to P bodies

Here I have shown that *grk* mRNA rarely interacts with nurse cell P bodies in wild-type egg chambers, but when Orb protein is upregulated in the nurse cells, *grk* docks at the edge of P bodies (Figure 7-11), as seen at the oocyte DA corner (Weil et al. 2012b). In Chapter 6 I hypothesised that *grk* could be targeted to P bodies by cis-acting regions with the mRNA, or by expression of different P body components in different regions of the egg chamber. My data suggest that the presence or absence of Orb in P bodies, determines association of *grk* with these bodies.

Interestingly, some *grk* mRNA (16% of particles) is associated with P bodies in wild-type nurse cells (Figures 6-9, 7-11). As Orb is expressed at low levels in the nurse cells, if a proportion of *grk* docked at the edge of P bodies, one would expect some *grk* to be translated in the nurse cells. However, this does not seem to be the case. I would hypothesise that *grk* mRNA associates with P bodies in wild-type nurse cells only transiently, and is not “docked” at the P body edge as seen in the oocyte (Weil et al. 2012b). The sm-FISH data provide only a snapshot of the interaction between *grk*

and P bodies, and my live imaging data (Chapter 6) does not suggest any stable interactions between the two.

My data also indicate that when Orb is upregulated there is a significant increase in the number of *grk* particles which associate with both the P body edge and the P body core, but the proportion of particles associated with the edge is much higher. I hypothesise that these particles are translated at the edge of P bodies, similar to those at the oocyte DA corner (Weil et al. 2012b). Whether the particles seen in the P body core are translationally repressed, and this represents some mechanism of controlling dosage as seen when *grk* mRNA is upregulated in the oocyte (Weil et al. 2012b), could be tested by imaging the interactions between injected and overexpressed *grk* with P bodies. It is also possible that widefield imaging is unable to accurately resolve the position of *grk* particles in relation to the core or the edge, which may be producing misleading results. 3D-SIM experiments could more accurately test these interactions, as they have in the oocyte (Weil et al. 2012b).

How Orb causes *grk* targeting to P bodies is unclear, and could be further tested by examining the interaction between *grk* and Orb using biochemical methods. Whether particular regions of *grk* are required for the association with P bodies could be tested by examining *grk* regions with NMR. This could inform generation of either mutant *in-vitro* synthesised *grk* for injection, or flies which express *grk* which lacks specific sequences (Van De Bor et al. 2005), and examining which sequences, if any, are required for *grk* association with P bodies.

The role of Orb in targeting *grk* to P bodies could also be assessed by examining *orb* mutant egg chambers. When *orb* is mutated, *grk* mRNA is mislocalised in the oocyte

(Christerson & McKearin 1994, Roth & Schupbach 1994). Similarly, in *sqd*^{1} mutant egg chambers, P bodies disassemble at the DA corner of the oocyte and *grk* is found in transport particles along the anterior margin (Delanoue et al. 2007). ISH combined with IEM (Weil et al. 2012b) could determine whether *grk* is still associated with P bodies at the DA corner of the oocyte in *orb*^{mel} egg chambers. Other P body proteins may also be necessary, but not sufficient, for *grk* association with P bodies. Analysis of P body structure and the association between *grk* and P bodies in mutant egg chambers for other P body proteins could answer these questions.

Whether Orb alters the structure of P bodies so they are able to associate with *grk* could be examined by ultrastructural analysis of P bodies when Orb expression is altered. In yeast, stress granules are assembled by self-aggregation of proteins with QN-rich domains (DePace et al. 1998, Gilks et al. 2004, Kedersha et al. 1999). Some CPEB proteins contain similar prion-like polyQ domains in their N terminal regions. In the *Aplysia* neuronal isoform of CPEB, this region is required for prion-like properties of the protein, and is essential for its function (Fiumara et al. 2010, Raveendra et al. 2013, Si et al. 2003, Si et al. 2010). The *Drosophila* Orb2 protein resembles *Aplysia* neuronal CPEB and contains a similar polyQ domain which is required for the formation of amyloid-like fibres, and are essential for its function in memory formation and courtship behaviour in adults (Keleman et al. 2007, Majumdar et al. 2012, Pai et al. 2013). Orb protein also contains two polyQ stretches (13 and 29 residues long). However, their tertiary structure has not been established, and whether Orb forms functional plaques, exhibits monomeric and multimeric states, or displays prion-like inheritance, is unknown.

Similarly, analysis of the frequency of *grk* mRNA docking at the edge of P bodies in the nurse cells of *UAS-orb* egg chambers could help to further characterise the interactions of *grk* and P bodies when Orb expression is altered. Is there a higher proportion of static *grk* particles, which are anchored at the P body edge, observed when Orb is upregulated in nurse cells? Do P bodies display different dynamics in these egg chambers? Do *grk* mRNA particles move with P bodies when Orb is overexpressed? Is mislocalised *grk* in the oocyte dynamic in *orb* mutants? Does altering the level of Orb protein expression affect the interactions between *bcd*, *osk* and *nos* with P bodies in the nurse cells and the oocyte?

However, the model that *grk* associates only with P bodies containing Orb is complicated by the fact that data from T. Weil, B. Herpers and C. Rabouille indicates that Orb, and Sqd, are expressed in P bodies throughout the oocyte, not just at the DA corner (Figure 7-14). Similarly, when Orb is overexpressed, *grk* is correctly localised at the DA corner, suggesting that Orb alone does not control the *grk*-P body interaction (see Chapter 8). These data also raise the question of why *grk* in the nurse cells is not translated by association with cytoplasmic ribosomes. *grk* RNP composition in nurse cells should be analysed to determine which proteins prevent *grk* interacting with ribosomes, and EM analysis of transport particles containing *grk* could test whether these particles contain ribosomes.

Differences between Orb and other CPEB proteins

Orb activates translation of *osk*, *K10* and *orb* mRNAs through a similar mechanism to CPEB. However; 1.) there is no evidence that Orb translationally represses unlocalised mRNAs, 2.) the role of Orb phosphorylation in its regulation, and the trigger for this phosphorylation are unknown, 3.) Orb affects mRNA interactions with

Figure 7-14: P bodies throughout the oocyte contain Sqd and Orb

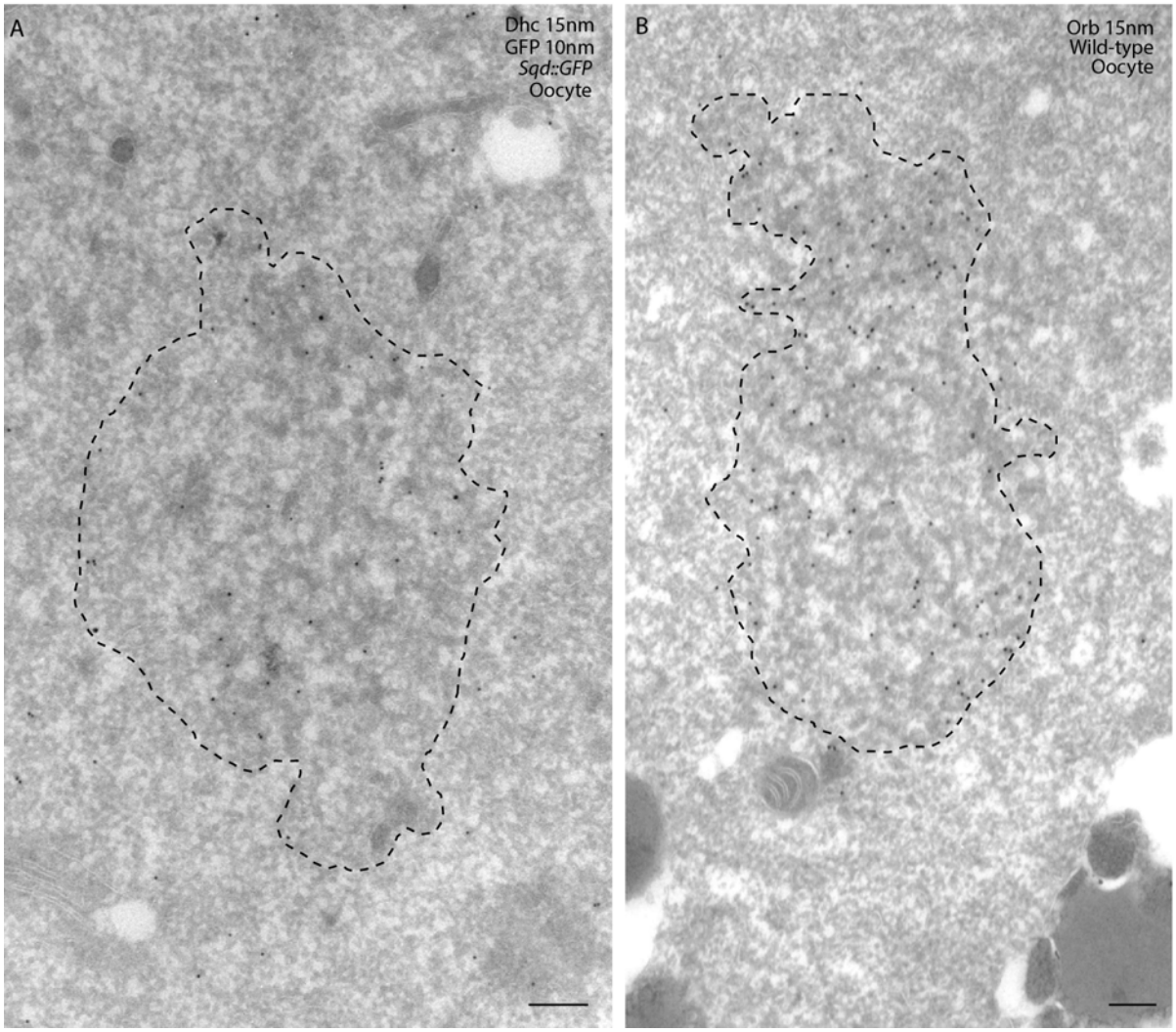

Figure 7-14:

(A): Protein detection by IEM on ultra-thin sections of the oocyte, carried out by T. Weil, B. Herpers and C. Rabouille. Both Sqd (A) and Orb (B) are present in P bodies in the centre of the oocyte, away from the DA corner. Dashed black lines mark the edge of P bodies as determined by C. Rabouille based on electron density. Scale bars 200nm.

P bodies, which is not a known a role of CPEB, 4.) Orb modulates *grk* by differential spatial, not temporal, expression like CPEB, and 5.) although Cup is functionally similar to Maskin it does not have sequence homology, and they may not fulfil the same role of translational repression via CPEB and eIF4E binding. The fact that *cup*$^{\Delta 212}$ mutants do not affect Orb or Grk expression (Figure 7-4) suggests Cup translational regulation by sequestering eIF4E is not a general mechanism for control of unlocalised mRNAs by cooperation of Orb and Cup. Moreover, my data indicating that *grk* does not move with Orb, Vasa, or translational repressor proteins in the nurse cells suggest that *grk*, at least, is not packaged with its translational repressors and activators during its transport.

Biochemical analysis could elucidate the protein complement of the translational repression and activation machinery for localised mRNAs during oogenesis. In particular, the role and interactions of the *Drosophila* CPSF homolog, the Gld2 homolog Wisp, PABP, Orb, and Cup/D-TACC is not clear. Understanding how these proteins interact with each other, and with mRNA, is key to establishing a model for mRNA translational repression and activation in *Drosophila* oogenesis comparable to the one we have for *Xenopus* oocytes.

Final conclusions

In this chapter I have shown that *grk* translational silencing in the nurse cells is controlled, at least in part, by restricted access to its translational activator, Orb. I have also revealed a role in Orb for targeting *grk* to P bodies. In Chapter 8, I will explore the implications of my findings for our understanding of the translational regulation of localised mRNAs during *Drosophila* oogenesis, and in other organisms.

Tables and statistics

Maternal Genotype (n)	% normal Orb expression	% Orb upregulated in nurse cells
WT (258)	94	6
cup^{1355} (238)	20	80
cup$^{\Delta 212}$ (50)	86	14
UAS-orb (60)	17	83

Table 7-1: Quantitation of Orb expression in the nurse cells from *OrR*, *cup^{1355}*, *cup$^{\Delta 212}$*, and *UAS-orb* egg chambers

In the majority of *WT* and *cup$^{\Delta 212}$* egg chambers, Orb expression is normal in the nurse cells, whereas in the majority of *cup^{1355}* and *UAS-orb* egg chambers, Orb expression is upregulated in the nurse cells.

Maternal Genotype (n)	% Normal Grk expression	% Grk expressed in nurse cells
WT (300)	97	3
cup^{1355} (274)	2	98
***cup$^{\Delta 212}$* (79)**	96	4
UAS-orb (60)	10	90

Table 7-2: Quantitation of Grk expression in the nurse cells from *OrR*, *cup^{1355}*, *cup$^{\Delta 212}$*, and *UAS-orb* egg chambers

In the majority of *WT* and *cup$^{\Delta 212}$* egg chambers, Grk expression is normal in the nurse cells, whereas in the majority of *cup^{1355}* and *UAS-orb* egg chambers, Grk is expressed in the nurse cells.

Maternal Genotype (n)	% WT	% No appendages	% Ectopic appendages	% Fused appendages	% *bwk*-like appendages
WT (120)	93	6	0	0	0
UAS-orb (90)	62	1	0	5	32
UAS-grk (90)	36	2	62	0	0

Table 7-3: Quantitation of eggshell phenotypes from *OrR*, *UAS-orb* and *UAS-grk* egg chambers

Although the majority of *UAS-orb* eggs laid have normal dorsal appendage morphology, some have fused appendages with extra dorsal material, and about a third have "*bwk*-like" appendages. These are shorted and have more elaborate distal ends rather than the "flattened paddle" morphology of wild-type egg chambers. Eggs laid by *UAS-grk* were scored for reference. Eggs with ectopic appendages indicative of upregulation of Grk signalling were not seen in *UAS-orb* egg chambers. The high percentage of eggs laid with no appendages from all genotypes is most likely due to damage during the preparation of the egg chambers.

Maternal Genotype (n of particles)	% *grk* particles not associated with P bodies	% *grk* particles at the P body edge	% *grk* particles in the P body core
Tral::YFP (322)	83	14	3
Me31B::GFP (297)	83	16	1
cup^{1355}/Tral::YFP (429)	36	52	12
UAS-orb/ Me31B::GFP (395)	41	53	6

Table 7-4: Quantitation of *grk* mRNA association with P bodies in *UAS-orb* and *cup^{1355}* egg chambers

For all conditions 30 egg chambers were scored as described in Appendix F. Results were compared by a Chi-square test. Comparing particles at the edge and all other particles between *Tral::YFP* and *cup^{1355}/Tral::YFP* egg chambers, there is a significant difference ($p < 0.001$). Comparing particles at the core and all other particles between *Tral::YFP* and *cup^{1355}/Tral::YFP* egg chambers, there is a significant difference ($p < 0.001$). Comparing particles at the edge and all other particles between *Me31B::GFP* and *UAS-orb/Me31B::GFP* egg chambers, there is a significant difference ($p < 0.001$). Comparing particles at the core and all other particles between *Me31B::GFP* and *UAS-orb/Me31B::GFP* egg chambers, there is a significant difference ($p = 0.002$).

Chapter 8: Discussion and Future Perspectives

Visualising mRNA throughout it's life cycle

The processing of mRNA from transcription to degradation influences where it is localised and translated. Imaging mRNA at different stages of its journey is key to understanding how and where RNPs are remodelled, and how transcripts with a common origin are sorted to distinct subcellular locations.

In *Drosophila* oogenesis, localised mRNAs require exposure to the nurse cell nuclei and cytoplasm for their correct regulation (Cáceres & Nilson 2009, Cha et al. 2001, Glotzer et al. 1997, Weil et al. 2012b). Here, I have imaged endogenous *grk* transcripts in live and fixed nurse cells for the first time, and have investigated the mechanism of *grk* translational regulation. I have found that *grk* and *osk* mRNAs move significantly faster in the nurse cells than in the oocyte, and my data suggest a difference in the multimerisation state of *grk* throughout its life cycle. *In-vitro* data indicate that the packaging of an mRNA can alter how it is transported, and that the number and activity of motors recruited to mRNAs is controlled by cis-acting regions within the transcript (Amrute-Nayak & Bullock 2012, Soundararajan & Bullock 2014). Indeed, *osk* and *nos* are packaged into higher order complexes as they are transported into the oocyte, and multimerisation also has a role in *osk* translational regulation (Chekulaeva et al. 2006, Little et al. 2015).

My data suggest that *grk* RNPs in the oocyte contain more transcripts than those in the nurse cells. This could be necessary for it's association with different numbers of motors, or a distinct set of microtubules on which the mRNA localises to the DA corner (MacDougall et al. 2003). *grk* RNPs in the oocyte could contain different trans-

acting factors, which repress translation of the mRNA specifically in the oocyte (Clouse et al. 2008), or could control the association of *grk* with the edge of P bodies (Weil et al. 2012b). Further sm-FISH, RT-qPCR, and mutational analysis could test the significance of this change in particle composition between the two tissues.

Visualisation of these particles required extensive optimisation of the imaging parameters, and I have used the state-of-the-art OMX system with a Z sweep function to image mRNA and protein particles moving in 3D with high temporal resolution. Developing imaging approaches is key to moving the field forward, including; using two-photon systems to image particle dynamics in the *Drosophila* oocyte (Sinsimer et al. 2013), characterising nuclear export dynamics using super-registration imaging in mammalian cells (Grünwald & Singer 2010), investigating mRNA-motor complex behaviour using total internal reflection microscopy (TIRF) *in vitro* (Amrute-Nayak & Bullock 2012) and examining mRNA multimerisation and transcription rates in mammalian tissues using fluorescence fluctuation microscopy (FFS, Wu et al. 2012). Although RNP formation and remodelling is well studied in yeast and mammalian cell lines (Buxbaum et al. 2015), it is poorly understood in *Xenopus* oocytes, the developing nervous system, and the *Drosophila* oocyte and embryo. Application of the imaging protocol I have optimised, combined with new MS2/PP7 tagging techniques to improve visualisation of these mRNAs, could help to investigate these processes in other systems.

Translational regulation of *grk* mRNA by restricted spatial access to translational activators

How mRNAs are translationally repressed during their transport, but translationally activated once localised, is a key question in biology. Here, I have determined that

grk is not translationally repressed by a number of individual candidate repressor proteins, or by targeting to the translationally silent core of nurse cell P bodies. I have shown that increasing Orb protein expression in the nurse cells causes Orb enrichment at the edge of nurse cell P bodies, *grk* targeting to these P bodies, and ectopic *grk* translation in the nurse cells. I present a model for translational control through restricted spatial access to translational activators.

My data highlight several unresolved questions regarding *grk* localisation and translational control. Although *grk* is thought to be translationally repressed in the oocyte by translational repressor proteins including Bruno, Sqd and Cup (Clouse et al. 2008, Li et al. 2014, Norvell et al. 1999), I did not detect increased Grk protein levels in the oocyte of *aret* or *me31B* mutants. In *sqd*^{1}, *K10,* and *cup* mutants, *grk* mRNA is mislocalised and the protein is ectopically translated along the anterior of the oocyte (Clouse et al. 2008, Jaramillo et al. 2008, Neuman-Silberberg & Schupbach 1993, Norvell et al. 1999, Roth & Schupbach 1994). The inability to dissect *grk* localisation and translational control in the oocyte makes identifying proteins with roles in *grk* translational control independent of its localisation difficult. However, overexpression or injection of *grk* does cause ectopic translation of the mRNA (Weil et al. 2012b), suggesting that there is saturable *grk* repression machinery in the oocyte.

Sqd is thought to repress *grk* translation (Clouse et al. 2008, Li et al. 2014, Norvell et al. 1999), but where and how Sqd acts on *grk* is unclear. *grk* must be exposed to Sqd in the nurse cell nuclei (Cáceres & Nilson 2009), and injected *grk* is translated ectopically along the anterior (Weil et al. 2012b), suggesting that *grk* translational control requires Sqd in the nurse cells. However, in *sqd*^{1} mutants *grk* is not translated

in the nurse cells. Sqd binds *grk* (Norvell et al. 1999), but these data from whole ovary extracts do not demonstrate that Sqd and *grk* interact in the nurse cells. Further biochemical and imaging analysis could clarify where and how Sqd interacts with *grk*, as it seems likely the two do interact in the nurse cell nuclei and the oocyte.

Although levels of Orb expression seem to be the key factor in preventing *grk* translation in the nurse cells, Orb is present throughout the oocyte, not exclusively at the DA corner. Moreover, when Orb expression is upregulated in both the nurse cells and the oocyte, eggs do not display dorsal appendage defects indicative of upregulated Grk signalling. This suggests that *grk* translation is not restricted to the DA corner by the distribution of Orb, and may be regulated by two distinct mechanisms in the nurse cells and the oocyte. This could be investigated with biochemical analysis of the two tissues separately, and live cell imaging of *grk* with its trans-acting factors to determine how and where the *grk* RNP is remodelled.

My data also highlight unclear aspects of *grk* translation and interaction with P bodies in the oocyte. *grk* does not interact with nurse cell P bodies, but at the oocyte DA corner of the oocyte docks at the edge of P bodies and is translated (Weil et al. 2012b). However, P bodies exist throughout the oocyte (C.Rabouille personal communication), which *grk* travels past on its way to the DA corner. Data suggests that *grk* does not anchor and become translated at the P body edge until Dynein is converted into an anchor at the DA corner by Sqd (Delanoue et al. 2007) (Weil et al. 2012b). However, several lines of evidence do not support this hypothesis.

First, Sqd is enriched in P bodies throughout the oocyte, and in the nurse cells where *grk* does not dock at the P body edge. Similarly, Orb, which I have shown here is

involved in targeting *grk* to P bodies and is required for *grk* translation (Chang et al. 2001), is expressed in P bodies throughout the oocyte, not exclusively at the DA corner. Ultrastructural analysis of P bodies along the anterior margin could establish whether unlocalised *grk* associates with these P bodies when various P body components or sequences in *grk* are mutated, and elucidate which factors prevent *grk* from docking to the edge of these P bodies, or which sequences within *grk* control this interaction. Other factors involved in *grk* translation, such as Vasa or Encore, which is enriched at the DA corner (Van Buskirk et al. 2000), could be required for P body targeting. This could be investigated with ultrastructural and analysis of *grk* and P bodies in mutants for these proteins.

Second, in *sqd*^{1} mutants, *grk* both fails to anchor at the DA corner (Delanoue et al. 2007, Jaramillo et al. 2008), and is ectopically translated along the anterior margin (Norvell et al. 1999). Therefore, Sqd is not required for *grk* mRNA translation by anchoring at the edge of P bodies, as *grk* is translated in *sqd*^{1} mutants. Third, in *UAS-grk* egg chambers, ectopic *grk* is translated along the anterior margin, even though Sqd is functional. Whether this *grk* is anchored at the edge of P bodies, and whether Sqd is still restricted to the DA corner in these egg chambers, could help identify whether these *grk* transcripts are translated independently of P bodies.

Finally, when excess *grk* is produced, more *grk* is targeted to the core of P bodies, where it is presumably translationally repressed (Weil et al. 2012b). However, ectopic *grk* is translated along the anterior (Weil et al. 2012b). Is the internalisation of transcripts in P bodies a mechanism for repressing excess *grk* translation, which is saturated in these egg chambers? *grk* may contain an IRES, and can be translated independently of the canonical cap-dependent mechanism under nutrient stress

conditions (Ferguson et al. 2012). Perhaps *grk* translation under normal conditions is restricted to the edge of P bodies at the DA corner and requires Orb, but there is another mechanism of *grk* translation independent of P bodies, Orb, and Sqd, ensuring oocyte patterning is not compromised under stress conditions. Whether *grk* can be translated in *orb* mutants when it is injected or overexpressed, and biochemical analysis of the interactions between *grk* and the translation machinery in *sqd*^{1} mutants or starved egg chambers, could test this model.

Translational control of localised mRNAs

My data suggest that levels of Orb protein regulate *grk* translation in the nurse cells. Are other localised mRNAs controlled by a similar mechanism? Can the restriction of high levels of translational activator expression to one tissue generate a region in which localised mRNAs cannot be translated, and hence inhibit the translation of multiple mRNAs through a single mechanism?

osk translation requires Orb and a long poly(A) tail (Castagnetti & Ephrussi 2003, Chang et al. 1999), but *osk* translation seems to be predominantly repressed by the action of repressor proteins, rather than control of poly(A) tail length (Chekulaeva et al. 2006, Kim-Ha et al. 1995, Nakamura et al. 2001, Nakamura et al. 2004, Wilhelm 2003). Low Orb levels in the nurse cells may add another layer of *osk* translational control, or may be inconsequential. RT-qPCR and Western blot analysis of *cup*^{1355} mutant egg chambers indicates that levels of *osk* mRNA are decreased, but levels of Osk protein are increased, when *cup* is mutated, suggesting that *osk* translation is upregulated in these mutants (Wong & Schedl 2011).

However, this increase in Osk protein could be due to either increased Orb expression, or loss of Cup-mediated *osk* translational repression in these mutants. Moreover, as this analysis was performed on whole ovary extracts, it is not clear that *osk* mRNA is prematurely translated in the nurse cells. Whether increasing levels of Orb in the nurse cells is sufficient to overcome *osk* translational repression could be investigated with Osk antibody staining in *UAS-orb* or *cup*^{1355} egg chambers. However, this antibody caused high levels of fluorescence in the nurse cells of wild-type egg chambers. This staining was not lessened with lower antibody concentrations, additional washing steps, or pre-absorption on wild-type embryos. Western blot analysis of the nurse cells of these mutants, or methods of visualising translation, including TRICK (Halstead et al. 2015), could answer this question.

osk mRNA also colocalises with Me31B granules in the nurse cells (Nakamura et al. 2001), and biochemical analysis reveals that *osk* silencing particles induced by Bruno also contain Me31B and Cup (Besse et al. 2009, Chekulaeva et al. 2006). These are P body markers, and suggest that *osk* may be translationally repressed by being transported within nurse cell P bodies. This could be assessed with imaging of MS2-tagged or sm-FISH labelled *osk* and fluorescently labelled P body proteins, and ultrastructural analysis of *osk* mRNA and P bodies with ISH-IEM.

bcd translation is controlled by PAP-mediated poly(A) tail extension (Juge et al. 2002, Lieberfarb et al. 1996, Sallés et al. 1994), but elongating the poly(A) tail by overexpressing PAP cannot induce *bcd* translation in the oocyte (Juge et al. 2002). Moreover, Orb does not have a known role in controlling *bcd* translation, and there is no canonical CPE in the *bcd* 3' UTR. *bcd* is translationally repressed in the oocyte by targeting to the core of P bodies until egg activation (Weil et al. 2012b), but whether

bcd is associated with P bodies in the nurse cells is unclear. Covisualisation of MS2 or sm-FISH labelled *bcd* with fluorescently labelled proteins could test whether *bcd* is repressed by being transported within the translationally silent core of P bodies in the nurse cells. If *bcd* is not transported within P bodies in the nurse cells, this begs the question of how it is repressed. Biochemical analysis of the proteins which bind *bcd* during oogenesis, followed by mutational analysis, could identify key proteins required for *bcd* translational control.

The diversity of translational regulation mechanisms also begs the question; why are *grk*, *osk* and *bcd* translationally regulated by different mechanisms during oogenesis? Do these mechanisms exist to ensure that protein expression is not only spatially restricted by differential localisation of the mRNA, but also by distinct modes of translational repression? It may be that because the axis determining transcripts must be translated in such precise, yet distinct, temporal and spatial profiles, discrete translation of these transcripts may only be achievable with multiple mechanisms. Why and how organisms have evolved so many different ways of regulating translation is a key question in the field, and should be examined with a thorough molecular analysis of numerous model organisms.

Unlike *grk*, *osk* and *bcd*, *nos* is translated in the nurse cells (Forrest et al. 2004). The role of the poly(A) tail in *nos* translation is unclear (Jeske et al. 2011, Rangan et al. 2009, Rouget et al. 2010, Semotok et al. 2005, Zaessinger et al. 2006), there is no known role for Orb in *nos* translation, and there are no canonical CPEs in the *nos* 3' UTR. Together, these data suggest that *nos* translation is not regulated by Orb. Moreover, the transition which must occur from the translation of *nos* in the nurse cells, to the translational repression of the unlocalised mRNA once it enters the

oocyte, suggests a fundamentally different mechanism of translational regulation to that of *grk*, *osk* and *bcd*. Although Glo has been identified as a repressor of *nos* translation during oogenesis (Kalifa et al. 2006), mutant phenotypes suggest there is another level of translational regulation which has yet to be identified, and how translation is regulated differentially in the two tissues is unclear.

Numerous trans-acting proteins are present in the nurse cell cytoplasm, suggesting that there is active translation machinery in this tissue throughout oogenesis. *nos* mRNA could be translated through this pathway independently of Orb. Biochemical analysis of proteins which interact with *nos* specifically in the nurse cells and the oocyte could identify key regulators of *nos* translation, and elucidate how *nos* is translated in the nurse cells when other localised mRNAs are translationally silent.

These data seem to argue against a model where translation of all localised mRNAs is prevented in the nurse cells by restricting high levels of Orb protein expression to the oocyte. Indeed, only *osk* and *grk* seem to be modulated by Orb, and only *osk* contains canonical CPE sequences in its 3' UTR. Whether inhibiting *orb* translation in the nurse cells only controls the translation of *grk*, or whether other mRNAs like *K10* are also translationally repressed in the nurse cells by this mechanism, could be further explored using quantitative mass spectrometry to examine changes in protein levels when *orb* is mutated or over-expressed (Kronja et al. 2014).

It is unclear what role, if any, Orb plays later in *Drosophila* development. As Orb regulates of translation during oogenesis, if it does not play a role in the embryo, how is it cleared or suppressed at egg activation? Many developmental transitions occur at the onset of egg activation or fertilisation, including the MZT (Tadros & Lipshitz

2009), changes in mRNA localisation and P body disassembly in *Drosophila* (Weil et al. 2008) (Weil et al. 2012b), and hormone-regulated cytoplasmic polyadenylation and translation in *Xenopus* (Cao & Richter 2002, Kim & Richter 2007). If the proteins involved in translational control are reorganised at fertilisation, this could provide important insights into how key processes during early embryogenesis are regulated, and could shed light on the underlying principles involved in the MZT.

CPEB proteins regulate translation in many organisms (Ivshina et al. 2014). However, the mechanism I propose here highlights differences between Orb and the canonical *Xenopus* CPEB. First, Orb modulates *grk* translation by differential spatial, rather than temporal expression as in *Xenopus* (Cao & Richter 2002, Kim & Richter 2006, Mendez, Hake, et al. 2000a, Sarkissian et al. 2004). Second, my data agrees with previous work which finds no evidence for Orb as a translational repressor, unlike CPEB and Maskin (Chang et al. 1999, Chang et al. 2001). Third, although Cup has a Maskin-like role in binding eIF4E to regulate *osk* translation (Nakamura et al. 2004, Wilhelm 2003) it does not seem to regulate *grk* in the nurse cells in this manner. Instead, it represses *orb* translation (Wong & Schedl 2011), a function which has not been shown for Maskin. Finally, I have shown that Orb is a key regulator of the interaction between *grk* and P bodies, which is not a canonical function of CPEB-1 superfamily members (Ivshina et al. 2014).

Spatial restriction of translational activators could be employed in other organisms to generate translationally silent tissues. Which proteins Orb interacts with, and how it interacts with localised mRNAs is poorly understood, and must be elucidated to gain a full understanding of its mechanisms of action during oogenesis. This, coupled with studies of CPEB proteins in other organisms to test whether they perform similar

functions, and which domains of the protein are required for these functions, could elucidate whether the the mechanism of I have uncovered is conserved.

P body function and regulation

Electron dense cellular structures process mRNA in a number of organisms. These include the mitochondrial cloud in *Xenopus* (King et al. 2005), Balbiani bodies in Zebrafish (Gupta et al. 2010), nematode P granules (Updike & Strome 2010), and P bodies in mammalian cells (Buchan et al. 2013). At the oocyte DA corner, *grk* mRNA docks at the edge of P bodies and is translated, yet *bcd* is internalised within these bodies and is translationally repressed (Weil et al. 2012b). However, I have shown that *grk* does not associate with nurse cell P bodies, but that upregulating Orb expression causes *grk* to be targeted to nurse cell P bodies and translated. My data continues to build the case that P bodies are key sites of translational regulation.

How mRNAs interact with P bodies is poorly understood. Although Orb can target *grk* to the edge of P bodies, many lines of evidence indicate that the protein complement of P bodies is not the sole factor determining mRNA - P body interactions. First, *bcd* mRNA is targeted to the core of P bodies at the DA corner where it is translationally repressed, whereas *grk* is targeted to the edge of these bodies (Weil et al. 2012b). There is no evidence that *bcd* and *grk* associate with distinct sub-classes of P bodies, or that different spatial distributions of proteins within P bodies control these interactions. These data raise the possibility that mRNAs may contain cis-acting regions which mediate their interaction with different parts of the P body. This could be regulated by altering the conformation of IDPs in P body protein components to mediate docking at the edge or trafficking to the core. Such motifs have not been

identified, and would require NMR and mutational analysis to elucidate whether these regions exist and how they control mRNA targeting to P bodies.

Second, when levels of *grk* mRNA are increased by injection or overexpression, *grk* is targeted to the core of P bodies, not the edge (Weil et al. 2012b). Moreover, there is evidence that nutrient stress alters the association of localised mRNAs with P bodies (Burn et al. 2015), and in other systems specific mRNAs are translated under physiological stress conditions (Halstead et al. 2015). This differential association of mRNAs with P bodies under different conditions raises two possibilities. The first, that trans-acting factors moving with the mRNA are the key regulators of P body interactions, and the protein complement of these RNPs is remodelled under stress. The second, that cis-acting regions in the mRNA which mediate interactions with different regions of the P body can be masked or revealed in different cellular circumstances, by changes in the conformation of the mRNA or RBP binding. These hypotheses could be tested with molecular analysis of which trans-acting factors and regions of mRNA, if any, are required for targeting *grk* and *bcd* to P bodies. Changes under stress could then be investigated with imaging and biochemical analysis.

P body assembly has been explored in yeast (Decker & Parker 2012), but not in *Drosophila*. In *sqd*^{1} mutants, P bodies disassemble completely, and *grk* is found in transport particles (Delanoue et al. 2007). This suggests that Sqd may have a role in P body assembly. Overexpression of Sqd by Gal4 driven *UAS-sqd*, or injection of *sqd* mRNA, could test whether Sqd is necessary and/or sufficient for Orb-mediated *grk* targeting to nurse cell P bodies. Further elucidation of how *grk* interacts with P bodies, and whether this is controlled completely by Orb, by Orb and Sqd, or in

conjunction with specific sequences in *grk*, could shed light on whether homologs of these proteins are involved in P body assembly in other systems.

Similarly, the key regulators of the mRNA cycle between P bodies, stress granules and polysomes have not been clearly identified in flies. The *Drosophila* egg chamber could provide an ideal system to understand changes in mRNA regulation under stress, and to investigate oocyte maintenance and regulation of fertility.

Final conclusions

Translational regulation of localised mRNAs is key for their function in a multitude of cellular processes. It is becoming clear that numerous mechanisms act to control translation between and within organisms and tissues. Here, I have identified a novel mechanism of translational control through restricted spatial access to a translational activator. Whether a similar mechanism acts to regulate translation in other organisms, perhaps in concert with translational repressor proteins or temporal control of translational activators, should be explored. Such studies could elucidate how cells coordinate simultaneous translational repression and activation of different transcripts, and help to understand the role of translational regulation in development, key cellular processes, and disease.

Chapter 9: References

Abdu, U., Brodsky, M. & Schüpbach, T., 2002. Activation of a meiotic checkpoint during *Drosophila* oogenesis regulates the translation of *gurken* through Chk2/Mnk. *Current biology : CB*, 12(19), pp.1645–1651.

Ainger, K. et al., 1993. Transport and localization of exogenous myelin basic protein mRNA microinjected into oligodendrocytes. *The Journal of Cell Biology*, 123(2), pp.431–441.

Aizer, A., Brody Y., Wee Ler L., Sonenberg N., Singer R., Shav-Tal Y., 2008. The dynamics of mammalian P body transport, assembly, and disassembly in vivo. *Molecular biology of the cell*, 19(10), pp.4154–4166.

Akam, M.E., 1983. The location of Ultrabithorax transcripts in *Drosophila* tissue sections. *The EMBO journal*, 2(11), pp.2075–2084.

Alami, N.H., Smith, R.B., Carrasco, M.A., Williams, L.A., Winborn, C.S., Han, S.S.W., Kiskinis, E., Winborn, B., Freibaum, B.D., Kanagarj, A., Clare, A.J, Badders, N.M, Biliban, B., Chaum, E., Chandran, S., Shaw, C.E., Eggan, K.C, Maniatis, T., Taylor, J.P., 2014. Axonal transport of TDP-43 mRNA granules is impaired by ALS-causing mutations. *Neuron*, 81(3), pp.536–543.

Amrute-Nayak, M. & Bullock, S.L., 2012. Single-molecule assays reveal that RNA localization signals regulate Dynein-dynactin copy number on individual transcript cargoes. *Nature cell biology*, 14(4), pp.416–423.

Anderson, J.S. & Parker, R.P., 1998. The 3' to 5' degradation of yeast mRNAs is a general mechanism for mRNA turnover that requires the SKI2 DEVH box

protein and 3“ to 5” exonucleases of the exosome complex. *The EMBO journal*, 17(5), pp.1497–1506.

Bally-Cuif, L., Schatz, W.J. & Ho, R.K., 1998. Characterization of the zebrafish Orb/CPEB-related RNA-binding protein and localization of maternal components in the zebrafish oocyte. *Mechanisms of development*, 77(1), pp.31–47.

Bandziulis, R.J., Swanson, M.S. & Dreyfuss, G., 1989. RNA-binding proteins as developmental regulators. *Genes & Development*, 3(4), pp.431–437.

Barbee, S.A. et al., 2006. Staufen- and FMRP-containing neuronal RNPs are structurally and functionally related to somatic P bodies. *Neuron*, 52(6), pp. 997–1009.

Barkoff, A.F. et al., 2000. Translational control of *cyclin B1* mRNA during meiotic maturation: coordinated repression and cytoplasmic polyadenylation. *Developmental Biology*. 220(1), pp. 97-109

Barnard, D.C. et al., 2004. Symplekin and xGLD-2 are required for CPEB-mediated cytoplasmic polyadenylation. *Cell*, 119(5), pp.641–651.

Barnard, D.C., Cao, Q. & Richter, J.D., 2005. Differential phosphorylation controls Maskin association with eukaryotic translation initiation factor 4E and localization on the mitotic apparatus. *Molecular and cellular biology*, 25(17), pp.7605–7615.

Barros, C.S., Phelps, C.B. & Brand, A.H., 2003. *Drosophila* nonmuscle myosin II promotes the asymmetric segregation of cell fate determinants by cortical exclusion rather than active transport. *Developmental Cell*, 5(6), pp.829–840.

Barros, T.P. et al., 2005. Aurora A activates D-TACC-Msps complexes exclusively at centrosomes to stabilize centrosomal microtubules. *The Journal of Cell Biology*, 170(7), pp.1039–1046.

Bartel, D.P., 2004. MicroRNAs: genomics, biogenesis, mechanism, and function. *Cell*, 116(2), pp.281–297.

Bashirullah, A. et al., 1999. Joint action of two RNA degradation pathways controls the timing of maternal transcript elimination at the midblastula transition in Drosophila melanogaster. *The EMBO journal*, 18(9), pp.2610–2620.

Bassell, G.J. & Warren, S.T., 2008. Fragile X syndrome: loss of local mRNA regulation alters synaptic development and function. *Neuron*, 60(2), pp.201–214.

Battich, N., Stoeger, T. & Pelkmans, L., 2013. Image-based transcriptomics in thousands of single human cells at single-molecule resolution. *Nature Methods*, 10(11), pp.1127–1133.

Baugh, L.R. et al., 2003. Composition and dynamics of the *Caenorhabditis elegans* early embryonic transcriptome. *Development*, 130(5), pp.889–900.

Baurén, G. & Wieslander, L., 1994. Splicing of Balbiani ring 1 gene pre-mRNA occurs simultaneously with transcription. *Cell*, 76(1), pp.183–192.

Beckham, C.J. & Parker, R., 2008. P bodies, stress granules, and viral life cycles. *Cell host & microbe*, 3(4), pp.206–212.

Bellen, H.J., Levis, R.W., He, Y., Carlson, J.W., Tsang, G., Evans-Holm, M., Hiesinger, P.R., Schulze, K.L., Rubin, G.M., Hoskins, R.A., Spradling, A.C.,

2004. The BDGP gene disruption projection: single transposon insertions associated with 40% of all *Drosophila* genes. *Genetics*, 176(2), pp.761-781

Benoit, B. et al., 2005. An essential cytoplasmic function for the nuclear poly(A) binding protein, PABP2, in poly(A) tail length control and early development in *Drosophila*. *Developmental Cell*, 9(4), pp.511–522.

Benoit, P. et al., 2008. PAP- and GLD-2-type poly(A) polymerases are required sequentially in cytoplasmic polyadenylation and oogenesis in *Drosophila*. *Development*, 135(11), pp.1969–1979.

Bergsten, S.E. & Gavis, E.R., 1999. Role for mRNA localization in translational activation but not spatial restriction of *nanos* RNA. *Development*, 126(4), pp. 659–669.

Berleth, T. et al., 1988. The role of localization of *bicoid* RNA in organizing the anterior pattern of the Drosophila embryo. *The EMBO journal*, 7(6), pp.1749–1756.

Bertrand, E. et al., 1998. Localization of *ASH1* mRNA particles in living yeast. *Molecular cell*, 2(4), pp.437–445.

Besse, F. & Ephrussi, A., 2008. Translational control of localized mRNAs: restricting protein synThesis in space and time. *Nature Reviews Molecular Cell Biology*, 9(12), pp.971–980.

Besse, F. et al., 2009. *Drosophila* PTB promotes formation of high-order RNP particles and represses *oskar* translation. *Genes & Development*, 23(2), pp. 195–207.

Bhattacharyya, S.N. et al., 2006. Relief of microRNA-mediated translational repression in human cells subjected to stress. *Cell*, 125(6), pp.1111–1124.

Bicker, S. et al., 2013. The DEAH-box helicase DHX36 mediates dendritic localization of the neuronal precursor-microRNA-134. *Genes & Development*, 27(9), pp.991–996.

Bilger, A. et al., 1994. Nuclear polyadenylation factors recognize cytoplasmic polyadenylation elements. *Genes & Development*, 8(9), pp.1106–1116.

Blichenberg, A. et al., 1999. Identification of a cis-acting dendritic targeting element in MAP2 mRNAs. *Journal of Neuroscience*, 19(20), pp.8818–8829.

Blichenberg, A., Rehbein, M. & Müller, R., 2001. Identification of a cis-acting dendritic targeting element in the mRNA encoding the alpha subunit of Ca2+/ calmodulin-dependent protein kinase II. *European Journal of neuroscience*. 13, pp.1881-1888

Bolívar, J. et al., 2001. Centrosome migration into the *Drosophila* oocyte is independent of BicD and Egl, and of the organisation of the microtubule cytoskeleton. *Development*, 128(10), pp.1889–1897.

Botchan, M. & Levine, M., 2004. A genome analysis of endoreplication in the *Drosophila* ovary. *Developmental Cell*, 6(1), pp.4–5.

Bouveret, E. et al., 2000. A Sm-like protein complex that participates in mRNA degradation. *The EMBO journal*, 19(7), pp.1661–1671.

Bökel, C. et al., 2006. *Drosophila* Cornichon acts as cargo receptor for ER export of the TGFalpha-like growth factor Gurken. *Development*, 133(3), pp.459–470.

Brangwynne, C.P., 2013. Phase transitions and size scaling of membrane-less organelles. *The Journal of Cell Biology*, 203(6), pp.875–881.

Brangwynne, C.P. et al., 2009. Germline P granules are liquid droplets that localize by controlled dissolution/condensation. *Science*, 324(5935), pp.1729–1732.

Bratu, D.P., 2006. Molecular Beacons. Fluorescent probes for detection of endogenous mRNAs in living cells. *Methods in molecular biology*. 319, pp. 1-14

Braunschweig, U. et al., 2014. Widespread intron retention in mammals functionally tunes transcriptomes. *Genome research*. 24(11), 1744-1786

Brechbiel, J.L. & Gavis, E.R., 2008. Spatial regulation of *nanos* is required for its function in dendrite morphogenesis. *Current biology : CB*, 18(10), pp.745–750.

Brengues, M., 2005. Movement of Eukaryotic mRNAs Between Polysomes and Cytoplasmic Processing Bodies. *Science*, 310(5747), pp.486–489.

Broadus, J., Fuerstenberg, S. & Doe, C.Q., 1998. Staufen-dependent localization of *prospero* mRNA contributes to neuroblast daughter-cell fate. *Nature*, 391(6669), pp.792–795.

Buchan, J.R. & Parker, R., 2009. Eukaryotic Stress Granules: The Ins and Outs of Translation. *Molecular cell*, 36(6), pp.932–941.

Buchan, J.R. et al., 2013. Eukaryotic Stress Granules Are Cleared by Autophagy and Cdc48/VCP Function. *Trends in Cell Biology*, 153(7), pp.1461–1474.

Buchan, J.R., Muhlrad, D. & Parker, R., 2008. P bodies promote stress granule assembly in *Saccharomyces cerevisiae*. *The Journal of Cell Biology*, 183(3), pp.441–455.

Buchan, J.R., Yoon, J.-H. & Parker, R., 2011. Stress-specific composition, assembly and kinetics of stress granules in Saccharomyces cerevisiae. *Journal of Cell Science*, 124(Pt 2), pp.228–239.

Bullock, S.L. & Ish-Horowicz, D., 2001. Conserved signals and machinery for RNA transport in *Drosophila* oogenesis and embryogenesis. *Nature*, 414(6864), pp. 611–616.

Bullock, S.L., Zicha, D. & Ish-Horowicz, D., 2003. The *Drosophila hairy* RNA localization signal modulates the kinetics of cytoplasmic mRNA transport. *The EMBO journal*, 22(10), pp.2484–2494.

Burgess, S.A. & Knight, P.J., 2004. Is the Dynein motor a winch? *Current opinion in structural biology*, 14(2), pp.138–146.

Burn, K.M. et al., 2015. Somatic insulin signaling regulates a germline starvation response in *Drosophila* egg chambers. *Developmental Biology*, 398(2), pp. 206–217.

Bushati, N. & Cohen, S.M., 2008. microRNAs in neurodegeneration. *Current Opinion in Neurobiology*, 18(3), pp.292–296.

Buxbaum, A.R., Haimovich, G. & Singer, R.H., 2015. In the right place at the right time visualizing and understanding mRNA localization. *Nature Reviews Molecular Cell Biology*, 16(2), pp.95–109.

Buxbaum, A.R., Wu, B. & Singer, R.H., 2014. Single b-Actin mRNA Detection in Neurons Reveals a Mechanism for Regulating Its Translatability. *Science* 343 pp.419-422

Caceres, L., 2005. Production of *gurken* in the nurse cells is sufficient for axis determination in the *Drosophila* oocyte. *Development*, 132(10), pp.2345–2353.

Calvi, B.R. & Spradling, A.C., 1999. Chorion gene amplification in *Drosophila*: A model for metazoan origins of DNA replication and S-phase control. *Methods (San Diego, Calif.)*. 99, pp.407-417.

Cao, Q. & Richter, J.D., 2002. Dissolution of the Maskin–eIF4E complex by cytoplasmic polyadenylation and poly (A)-binding protein controls *cyclin B1* mRNA translation and oocyte maturation. *The EMBO journal*. 21(14), pp. 3852-3862

Cao, Q., Kim, J.H. & Richter, J.D., 2006. CDK1 and calcineurin regulate Maskin association with eIF4E and translational control of cell cycle progression. *Nature Structural & Molecular Biology*, 13(12), pp.1128–1134.

Cao, Q., Padmanabhan, K. & Richter, J.D., 2010. Pumilio 2 controls translation by competing with eIF4E for 7-methyl guanosine cap recognition. *RNA*, 16(1), pp. 221–227.

Carlton, P.M. et al., 2010. Fast live simultaneous multiwavelength four-dimensional optical microscopy. *Proceedings of the National Academy of Sciences*, 107(37), pp.16016–16022.

Carrocci, T.J. & Hoskins, A.A., 2014. Imaging of RNAs in live cells with spectrally diverse small molecule fluorophores. *The Analyst*, 139(1), pp.44–47.

Carson, J.H. et al., 1997. Translocation of myelin basic protein mRNA in oligodendrocytes requires microtubules and kinesin. *Cell Motility and the Cytoskeleton*, 38(4), pp.318–328.

Castagnetti S., Ephrussi, A. 2003. Orb and a long poly(A) tail are required for efficient *oskar* translation at the posterior pole of the *Drosophila* oocyte. *Development*, 130(5), pp.835–843.

Castello, A. et al., 2012. Insights into RNA Biology from an Atlas of Mammalian mRNA-Binding Proteins. *Trends in Cell Biology*, 149(6), pp.1393–1406.

Castello, A. et al., 2013. RNA-binding proteins in Mendelian disease. *Trends in Genetics*, 29(5), pp.318–327.

Caviston, J.P. & Holzbaur, E.L.F., 2006. Microtubule motors at the intersection of trafficking and transport. *Trends in Cell Biology*, 16(10), pp.530–537.

Cáceres, L. & Nilson, L.A., 2009. Translational repression of *gurken* mRNA in the *Drosophila* oocyte requires the hnRNP Squid in the nurse cells. *Developmental Biology*, 326(2), pp.327–334.

Cha, B.-J. et al., 2002. Kinesin I-dependent cortical exclusion restricts pole plasm to the oocyte posterior. *Nature cell biology*, 4(8), pp.592–598.

Cha, B.J., Koppetsch, B.S. & Theurkauf, W.E., 2001. In vivo analysis of *Drosophila bicoid* mRNA localization reveals a novel microtubule-dependent axis specification pathway. *Cell*, 106(1), pp.35–46.

Chang, J.S. et al., 2001. Functioning of the *Drosophila orb* gene in *gurken* mRNA localization and translation. *Development*, 128(16), pp.3169–3177.

Chang, J.S., Tan, L. & Schedl, P., 1999. The *Drosophila* CPEB Homolog, Orb, Is Required for Oskar Protein Expression in Oocytes. *Developmental Biology*, 215(1), pp.91–106.

Chang, P. et al., 2004. Localization of RNAs to the mitochondrial cloud in *Xenopus* oocytes through entrapment and association with endoplasmic reticulum. *Molecular biology of the cell*, 15(10), pp.4669–4681.

Chao, J.A. et al., 2008. Structural basis for the coevolution of a viral RNA–protein complex. *Nature Structural & Molecular Biology*, 15(1), pp.103–105.

Chekulaeva, M., Hentze, M.W. & Ephrussi, A., 2006. Bruno Acts as a Dual Repressor of *oskar* Translation, Promoting mRNA Oligomerization and Formation of Silencing Particles. *Cell*, 124(3), pp.521–533.

Chen, Y., Pane, A. & Schüpbach, T., 2007. Cutoff and aubergine mutations result in retrotransposon upregulation and checkpoint activation in *Drosophila*. *Current biology : CB*, 17(7), pp.637–642.

Cherny, D. et al., 2010. Stoichiometry of a regulatory splicing complex revealed by single-molecule analyses. *The EMBO journal*, 29(13), pp.2161–2172.

Chicoine, J. et al., 2007. Bicaudal-C recruits CCR4-NOT deadenylase to target mRNAs and regulates oogenesis, cytoskeletal organization, and its own expression. *Developmental Cell*. 13(5), pp. 691-704

Chlebowski, A. et al., 2013. RNA decay machines: the exosome. *Biochimica et biophysica acta*, 1829(6-7), pp.552–560.

Cho, P.F. et al., 2005. A new paradigm for translational control: inhibition via 5“-3” mRNA tethering by Bicoid and the eIF4E cognate 4EHP. *Cell*, 121(3), pp.411–423.

Chowdhury, S. et al., 2015. Structural organization of the Dynein-dynactin complex bound to microtubules. *Nature Structural & Molecular Biology*, 22(4), pp.345–347.

Christerson, L.B. & McKearin, D.M., 1994. *orb* is required for anteroposterior and dorsoventral patterning during Drosophila oogenesis. *Genes & Development*, 8(5), pp.614–628.

Chu, C.-Y. & Rana, T.M., 2006. Translation repression in human cells by microRNA-induced gene silencing requires RCK/p54. *PLoS Biology*, 4(7), p.e210.

Clark, A., Meignin, C. & Davis, I., 2007. A Dynein-dependent shortcut rapidly delivers axis determination transcripts into the *Drosophila* oocyte. *Development*, 134(10), pp.1955–1965.

Clark, I. et al., 1994. Transient posterior localization of a kinesin fusion protein reflects anteroposterior polarity of the *Drosophila* oocyte. *Current biology : CB*, 4(4), pp.289–300.

Clark, I.E., Jan, L.Y. & Jan, Y.N., 1997. Reciprocal localization of Nod and kinesin fusion proteins indicates microtubule polarity in the *Drosophila* oocyte, epithelium, neuron and muscle. *Development*, 124(2), pp.461–470.

Clark, I.E., Wyckoff, D. & Gavis, E.R., 2000. SynThesis of the posterior determinant Nanos is spatially restricted by a novel cotranslational regulatory mechanism. *Current biology : CB*, 10(20), pp.1311–1314.

Clouse, K.N., Ferguson, S.B. & Schüpbach, T., 2008. Squid, Cup, and PABP55B function together to regulate *gurken* translation in *Drosophila*. *Developmental Biology*, 313(2), pp.713–724.

Cody, N.A.L., Iampietro, C. & Lécuyer, E., 2013. The many functions of mRNA localization during normal development and disease: from pillar to post. *Wiley Interdisciplinary Reviews: Developmental Biology*, 2, pp.781-796

Cook, H.A. et al., 2004. The *Drosophila* SDE3 homolog armitage is required for *oskar* mRNA silencing and embryonic axis specification. *Cell*, 116(6), pp.817–829.

Costa, A. et al., 2005. The *Drosophila* fragile X protein functions as a negative regulator in the *orb* autoregulatory pathway. *Developmental Cell*, 8(3), pp.331–342.

Cougot, N., Babajko, S. & Séraphin, B., 2004. Cytoplasmic foci are sites of mRNA decay in human cells. *The Journal of Cell Biology*, 165(1), pp.31–40.

Cox, D.N. et al., 2001. *Drosophila* par-1 is required for oocyte differentiation and microtubule organization. *Current biology : CB*, 11(2), pp.75–87.

Cox, R.T. & Spradling, A.C., 2003. A Balbiani body and the fusome mediate mitochondrial inheritance during *Drosophila* oogenesis. *Development*, 130(8), pp.1579–1590.

Craig, A. et al., 1998. Interaction of polyadenylate-binding protein with the eIF4G homologue PAIP enhances translation. *Nature*. 392(6675), pp. 520-523

Crucs, S., Chatterjee, S. & Gavis, E.R., 2000. Overlapping but distinct RNA elements control repression and activation of *nanos* translation. *Molecular cell*, 5(3), pp. 457–467.

Cui, J. et al., 2013. Cytoplasmic polyadenylation is a major mRNA regulator during oogenesis and egg activation in *Drosophila*. *Developmental Biology*, 383(1), pp.121–131.

Dahlgaard, K. et al., 2007. Capu and Spire assemble a cytoplasmic actin mesh that maintains microtubule organization in the *Drosophila* oocyte. *Developmental Cell*, 13(4), pp.539–553.

Darnell, R., 2012. CLIP (Cross-Linking and Immunoprecipitation) Identification of RNAs Bound by a Specific Protein. *Cold Spring Harbor Protocols*, 2012(11).

Daugeron, M.C., Mauxion, F. & Séraphin, B., 2001. The yeast POP2 gene encodes a nuclease involved in mRNA deadenylation. *Nucleic Acids Research*, 29(12), pp.2448–2455.

Davis, I., Ish-Horowicz, D., 1991. Apical localisation of pair-rule transcripts requires 3' sequences and limits protein diffusion in the *Drosophila* blastoderm embryo. *Cell*, 67, pp.927-940

de Cuevas, M. & Spradling, A.C., 1998. Morphogenesis of the *Drosophila* fusome and its implications for oocyte specification. *Development*, 125(15), pp.2781–2789.

de Cuevas, M., Lee, J.K. & Spradling, A.C., 1996. alpha-spectrin is required for germline cell division and differentiation in the *Drosophila* ovary. *Development*, 122(12), pp.3959–3968.

de Moor, C.H. & Richter, J.D., 1997. The Mos pathway regulates cytoplasmic polyadenylation in *Xenopus* oocytes. *Molecular and cellular biology*, 17(11), pp.6419–6426.

De Renzis, S. et al., 2007. Unmasking activation of the zygotic genome using chromosomal deletions in the *Drosophila* embryo. *PLoS Biology*. 5(5), e117

de Valoir, T. et al., 1991. A second maternally expressed *Drosophila* gene encodes a putative RNA helicase of the“ DEAD box” family. *Proceedings of the National Academy of Sciences of the United States of America*, 88(6), pp.2113–2117.

Decker, C.J. & Parker, R., 1993. A turnover pathway for both stable and unstable mRNAs in yeast: evidence for a requirement for deadenylation. *Genes & Development*, 7(8), pp.1632–1643.

Decker, C.J. & Parker, R., 2012. P-bodies and stress granules: possible roles in the control of translation and mRNA degradation. *Cold Spring Harbor perspectives in biology*, 4(9), p.a012286.

Decker, C.J., Teixeira, D. & Parker, R., 2007. Edc3p and a glutamine/asparagine-rich domain of Lsm4p function in processing body assembly in Saccharomyces cerevisiae. *The Journal of Cell Biology*, 179(3), pp.437–449.

Delanoue, R. & Davis, I., 2005. Dynein Anchors Its mRNA Cargo after Apical Transport in the *Drosophila* Blastoderm Embryo. *Cell*, 122(1), pp.97–106.

Delanoue, R. et al., 2007. *Drosophila* Squid/hnRNP Helps Dynein Switch from a gurken mRNA Transport Motor to an Ultrastructural Static Anchor in Sponge Bodies. *Developmental Cell*, 13(4), pp.523–538.

Deng, W.M. & Bownes, M., 1997. Two signalling pathways specify localised expression of the Broad-Complex in *Drosophila* eggshell patterning and morphogenesis. *Development*, 124(22), pp.4639–4647.

Deng, W.M. & Ruohola-Baker, H., 2000. Laminin A is required for follicle cell-oocyte signaling that leads to establishment of the anterior-posterior axis in *Drosophila*. *Current biology : CB*, 10(11), pp.683–686.

DePace, A.H. et al., 1998. A critical role for amino-terminal glutamine/asparagine repeats in the formation and propagation of a yeast prion. *Cell*, 93(7), pp. 1241–1252.

Di Giammartino, D.C., Nishida, K. & Manley, J.L., 2011. Mechanisms and Consequences of Alternative Polyadenylation. *Molecular cell*, 43(6), pp.853–866.

Dickson, K.S. et al., 1999. The Cleavage and Polyadenylation Specificity Factor in *Xenopus laevis* Oocytes Is a Cytoplasmic Factor Involved in Regulated Polyadenylation. *Molecular and cellular biology* pp.5707-5717

Dienstbier, M. et al., 2009. Egalitarian is a selective RNA-binding protein linking mRNA localization signals to the Dynein motor. *Genes & Development*, 23(13), pp.1546–1558.

Dimitrova, N. et al., 2014. LincRNA-p21 activates p21 in cis to promote Polycomb target gene expression and to enforce the G1/S checkpoint. *Molecular cell*, 54(5), pp.777–790.

Dobbie, I.M. et al., 2011. OMX: A New Platform for Multimodal, Multichannel Wide-Field Imaging. *Cold Spring Harbor Protocols*, 2011(8), pp.pdb.top121–pdb.top121.

Doe, C.Q. et al., 1991. The *prospero* gene specifies cell fates in the *Drosophila* central nervous system. *Cell*, 65(3), pp.451–464.

Dolgosheina, E.V. et al., 2014. RNA mango aptamer-fluorophore: a bright, high-affinity complex for RNA labeling and tracking. *ACS chemical biology*, 9(10), pp.2412–2420.

Doma, M.K. & Parker, R., 2006. Endonucleolytic cleavage of eukaryotic mRNAs with stalls in translation elongation. *Nature*, 440(7083), pp.561–564.

Dorman, J.B. et al., 2004. *bullwinkle* is required for epithelial morphogenesis during *Drosophila* oogenesis. *Developmental Biology*, 267(2), pp.320–341.

Dunckley, T. & Parker, R., 1999. The DCP2 protein is required for mRNA decapping in *Saccharomyces cerevisiae* and contains a functional MutT motif. *The EMBO journal*, 18(19), pp.5411–5422.

Dyson, H.J. & Wright, P.E., 2005. Elucidation of the protein folding landscape by NMR. *Methods in enzymology*, 394, pp.299–321.

Eckley, D.M. et al., 1999. Analysis of dynactin subcomplexes reveals a novel actin-related protein associated with the arp1 minifilament pointed end. *The Journal of Cell Biology*, 147(2), pp.307–320.

Edgar, B.A., Odell, G.M. & Schubiger, G., 1987. Cytoarchitecture and the patterning of *fushi tarazu* expression in the *Drosophila* blastoderm. *Genes & Development*, 1(10), pp.1226–1237.

Ephrussi, A., Dickinson, L.K. & Lehmann, R., 1991. *oskar* organizes the germ plasm and directs localization of the posterior determinant *nanos*. *Cell*, 66(1), pp.37–50.

Fallini, C., Bassell, G.J. & Rossoll, W., 2012. Spinal muscular atrophy: the role of SMN in axonal mRNA regulation. *Brain research*, 1462, pp.81–92.

Farina, K.L. et al., 2003. Two ZBP1 KH domains facilitate beta-actin mRNA localization, granule formation, and cytoskeletal attachment. *The Journal of Cell Biology*, 160(1), pp.77–87.

Femino, A.M. et al., 1998. Visualization of single RNA transcripts in situ. *Science*, 280(5363), pp.585–590.

Fenger-Grøn, M. et al., 2005. Multiple processing body factors and the ARE binding protein TTP activate mRNA decapping. *Molecular cell*, 20(6), pp.905–915.

Ferguson, S.B. et al., 2012. Modulation of *gurken* translation by insulin and TOR signaling in *Drosophila*. *Journal of Cell Science*, 125(Pt 6), pp.1407–1419.

Ferrandon, D., 1997. RNA-RNA interaction is required for the formation of specific *bicoid* mRNA 3' UTR-STAUFEN ribonucleoprotein particles. *The EMBO journal*, 16(7), pp.1751–1758.

Filardo, P. & Ephrussi, A., 2003a. Bruno regulates *gurken* during *Drosophila* oogenesis. *Mechanisms of development*, 120(3), pp.289–297.

Findley, S.D. et al., 2003. Maelstrom, a *Drosophila* spindle-class gene, encodes a protein that colocalizes with Vasa and RDE1/AGO1 homolog, Aubergine, in nuage. *Development*, 130(5), pp.859–871.

Firestone, A.J. et al., 2013. Small-molecule inhibitors of the AAA+ ATPase motor cytoplasmic Dynein. *Nature*, 484(7392), pp.125–129.

Fiumara, F. et al., 2010. Essential role of coiled coils for aggregation and activity of Q/N-rich prions and PolyQ proteins. *Cell*, 143(7), pp.1121–1135.

Forrest, K.M. & Gavis, E.R., 2003. Live Imaging of Endogenous RNA Reveals a Diffusion and Entrapment Mechanism for *nanos* mRNA Localization in Drosophila. *Current Biology*, 13(14), pp.1159–1168.

Forrest, K.M. et al., 2004. Temporal complexity within a translational control element in the *nanos* mRNA. *Development*, 131(23), pp.5849–5857.

Fox, C.A., Sheets, M.D. & Wickens, M.P., 1989. Poly(A) addition during maturation of frog oocytes: distinct nuclear and cytoplasmic activities and regulation by the sequence UUUUUAU. *Genes & Development*, 3(12B), pp.2151–2162.

Frank-Vaillant, M. et al. 1999, Two Distinct Mechanisms Control the Accumulation of Cyclin B1 and Mos in *Xenopus* Oocytes in Response to Progesterone. 10(10), pp. 3279-3288

Frischmeyer, P.A. et al., 2002. An mRNA surveillance mechanism that eliminates transcripts lacking termination codons. *Science*, 295(5563), pp.2258–2261.

Frohnhöfer, H.G., Lehmann, R. & Nüsslein-Volhard, C., 1986. Manipulating the anteroposterior pattern of the *Drosophila* embryo. *Journal of embryology and experimental morphology*, 97 Suppl, pp.169–179.

Frydman, H.M. & Spradling, A.C., 2001. The receptor-like tyrosine phosphatase lar is required for epithelial planar polarity and for axis determination within *Drosophila* ovarian follicles. *Development*, 128(16), pp.3209–3220.

Gagnon, J.A. et al., 2013. Directional Transport Is Mediated by a Dynein-Dependent Step in an RNA Localization Pathway. *PLoS Biology*, 11(4), p.e1001551.

Gamberi, C. et al., 2002. An anterior function for the *Drosophila* posterior determinant Pumilio. *Development*, 129(11), pp.2699–2710.

Garcia, J.F. & Parker, R., 2015. MS2 coat protein bound to yeast mRNAs block 5“ to 3” degradation and trap mRNA decay products: implications for the localization of mRNAs by MS2-MCP system. *RNA*. 21(8), pp. 1393-1395

Garcia, S.M.D.A. et al., 2014. Identification of genes in toxicity pathways of trinucleotide-repeat RNA in *C. elegans*. *Nature Structural & Molecular Biology*, 21(8), pp.712–720.

Garneau, N.L., Wilusz, J. & Wilusz, C.J., 2007. The highways and byways of mRNA decay. *Nature Reviews Molecular Cell Biology*, 8(2), pp.113–126.

Gaspar, I. et al., 2014. Klar ensures thermal robustness of *oskar* localization by restraining RNP motility. *The Journal of Cell Biology*, 206(2), pp.199–215.

Gavin, A.-C. et al., 2006. Proteome survey reveals modularity of the yeast cell machinery. *Nature*, 440(7084), pp.631–636.

Gavis, E.R. & Lehmann, R., 1992. Localization of *nanos* RNA controls embryonic polarity. *Cell*, 71(2), pp.301–313.

Gavis, E.R., Curtis, D. & Lehmann, R., 1996a. Identification of cis-acting sequences that control *nanos* RNA localization. *Developmental Biology*, 176(1), pp.36–50.

Gavis, E.R., Lunsford, L., et al., 1996b. A conserved 90 nucleotide element mediates translational repression of *nanos* RNA. *Development*, 122(9), pp.2791–2800.

Geng, C. & Macdonald, P.M., 2006. Imp associates with squid and Hrp48 and contributes to localized expression of *gurken* in the oocyte. *Molecular and cellular biology*, 26(24), pp.9508–9516.

Gennerich, A. & Vale, R.D., 2009. Walking the walk: how kinesin and Dynein coordinate their steps. *Current Opinion in Cell Biology*, 21(1), pp.59–67.

Gergely, F. et al., 2000. D-TACC: a novel centrosomal protein required for normal spindle function in the early *Drosophila* embryo. *The EMBO journal*, 19(2), pp. 241–252.

Ghabrial, A. & Schupbach, T., 1999. Activation of a meiotic checkpoint regulates translation of Gurken during *Drosophila* oogenesis. *Nature cell biology*, 1(6), pp.354–357.

Ghiglione, C. et al., 2002. Mechanism of activation of the *Drosophila* EGF Receptor by the TGFalpha ligand Gurken during oogenesis. *Development*, 129(1), pp. 175–186.

Ghiglione, C. et al., 1999. The transmembrane molecule kekkon 1 acts in a feedback loop to negatively regulate the activity of the *Drosophila* EGF receptor during oogenesis. *Cell*, 96(6), pp.847–856.

Ghosh, S. et al., 2012. Control of RNP motility and localization by a splicing-dependent structure in *oskar* mRNA. *Nature Publishing Group*, 19(4), pp.441–449.

Gilks, N. et al., 2004. Stress granule assembly is mediated by prion-like aggregation of TIA-1. *Molecular biology of the cell*, 15(12), pp.5383–5398.

Giraldez, A.J. et al., 2006. Zebrafish MiR-430 promotes deadenylation and clearance of maternal mRNAs. *Science*, 312(5770), pp.75–79.

Glotzer, J.B. et al., 1997. Cytoplasmic flows localize injected *oskar* RNA in *Drosophila* oocytes. *Current biology : CB*, 7(5), pp.326–337.

Godt, D. & Tepass, U., 1998. *Drosophila* oocyte localization is mediated by differential cadherin-based adhesion. *Nature*, 395(6700), pp.387–391.

Goldstein, L.S., 2001. Kinesin molecular motors: transport pathways, receptors, and human disease. *Proceedings of the National Academy of Sciences of the United States of America*, 98(13), pp.6999–7003.

Gonzalez-Reyes, A., Elliot, H. & St Johnston, D., 1995. Polarisation of both major body axes in *Drosophila* by *gurken-torpedo* signalling. 375(6533), pp. 654-658

González-Reyes, A. & St Johnston, D., 1998. Patterning of the follicle cell epithelium along the anterior-posterior axis during *Drosophila* oogenesis. *Development*, 125(15), pp.2837–2846.

Goodrich, J.S., Clouse, K.N. & Schüpbach, T., 2004. Hrb27C, Sqd and Otu cooperatively regulate *gurken* RNA localization and mediate nurse cell chromosome dispersion in *Drosophila* oogenesis. *Development*, 131(9), pp. 1949–1958.

Grammont, M. & Irvine, K.D., 2001. fringe and Notch specify polar cell fate during *Drosophila* oogenesis. *Development*, 128(12), pp.2243–2253.

Grieder, N.C., de Cuevas, M. & Spradling, A.C., 2000. The fusome organizes the microtubule network during oocyte differentiation in *Drosophila*. *Development*, 127(19), pp.4253–4264.

Groisman, I. et al., 2000. CPEB, maskin, and cyclin B1 mRNA at the mitotic apparatus: implications for local translational control of cell division. *Cell*, 103(3), pp.435–447.

Gross, S.P., 2004. Hither and yon: a review of bi-directional microtubule-based transport. *Physical Biology*, 1(1-2), pp.R1–11.

Groušl, T. et al., 2009. Robust heat shock induces eIF2α-phosphorylation-independent assembly of stress granules containing eIF3 and 40S ribosomal subunits in budding yeast, *Saccharomyces cerevisiae*. 122(Pt 12), pp. 2078-2088

Grünwald, D. & Singer, R.H., 2010. In vivo imaging of labelled endogenous *β-actin* mRNA during nucleocytoplasmic transport. *Nature*, 467(7315), pp.604–607.

Gu, W. et al., 2004. A new yeast PUF family protein, Puf6p, represses *ASH1* mRNA translation and is required for its localization. *Genes & Development*, 18(12), pp.1452–1465.

Gu, W. et al., 2012. Regulation of local expression of cell adhesion and motility-related mRNAs in breast cancer cells by IMP1/ZBP1. *The Journal of cell science*. 125(Pt 1), pp. 81-91

Gupta, I. et al., 2014. Alternative polyadenylation diversifies post-transcriptional regulation by selective RNA-protein interactions. *Molecular Systems Biology*, 10(2), pp.719–719.

Gupta, T. et al., 2010. Microtubule actin crosslinking factor 1 regulates the Balbiani body and animal-vegetal polarity of the zebrafish oocyte. *PLoS genetics*, 6(8), p.e1001073.

Gutzeit, H.O., 1986. The role of microfilaments in cytoplasmic streaming in *Drosophila* follicles. *Journal of Cell Science*, 80, pp.159–169.

Hachet, O. & Ephrussi, A., 2001. *Drosophila* Y14 shuttles to the posterior of the oocyte and is required for *oskar* mRNA transport. *Current biology : CB*, 11(21), pp.1666–1674.

Hachet, O. & Ephrussi, A., 2004. Splicing of *oskar* RNA in the nucleus is coupled to its cytoplasmic localization. *Nature*, 428(6986), pp.959–963.

Hake, L.E. & Richter, J.D., 1994. CPEB is a specificity factor that mediates cytoplasmic polyadenylation during *Xenopus* oocyte maturation. *Cell*, 79(4), pp.617–627.

Halstead, J.M. et al., 2014. Syncrip/hnRNP Q influences synaptic transmission and regulates BMP signaling at the Drosophila neuromuscular synapse. *Biology Open*, 3(9), pp.839–849.

Halstead, J.M. et al., 2015. Translation. An RNA biosensor for imaging the first round of translation from single cells to living animals. *Science*, 347(6228), pp.1367–1671.

Hamada, S. et al., 2003. The Transport of Prolamine RNAs to Prolamine Protein Bodies in Living Rice Endosperm Cells. *Plant cell*. 15(10), pp. 2253-2264

Hamatani, T., Daikoku, T. & Wang, H., 2004. Global gene expression analysis identifies molecular pathways distinguishing blastocyst dormancy and activation. *Proceedings of the National Academy of Sciences*. 101(28), pp. 10326-10331

Hamilton, R.S. & Davis, I., 2007. RNA localization signals: Deciphering the message with bioinformatics. *Seminars in Cell and Developmental Biology*, 18(2), pp. 178–185.

Han, T.W. et al., 2012. Cell-free formation of RNA granules: bound RNAs identify features and components of cellular assemblies. *Cell*, 149(4), pp.768–779.

Harigaya, Y. & Parker, R., 2010. No-go decay: a quality control mechanism for RNA in translation. *Wiley Interdisciplinary Reviews: RNA*, 1(1), pp.132–141.

Harris, A.N. & Macdonald, P.M., 2001. Aubergine encodes a *Drosophila* polar granule component required for pole cell formation and related to eIF2C. *Development*, 128(14), pp.2823–2832.

Hawkins, N.C. et al., 1997. Post-transcriptional regulation of *gurken* by Encore is required for axis determination in *Drosophila*. *Development*, 124(23), pp. 4801–4810.

Hawkins, N.C., Thorpe, J. & Schupbach, T., 1996. Encore, a gene required for the regulation of germ line mitosis and oocyte differentiation during *Drosophila* oogenesis. *Development*, 122(1), pp.281–290.

Hayashi, R. et al., 2014. A Genetic Screen Based on in Vivo RNA Imaging Reveals Centrosome-Independent Mechanisms for Localizing *gurken* Transcripts in *Drosophila*. *G3*. 4(4), pp. 749-760

Heinrich, S.U. & Lindquist, S., 2011. Protein-only mechanism induces self-perpetuating changes in the activity of neuronal Aplysia cytoplasmic polyadenylation element binding protein (CPEB). *Proceedings of the National Academy of Sciences of the United States of America*, 108(7), pp.2999–3004.

Herpers, B. & Rabouille, C., 2004. mRNA localization and ER-based protein sorting mechanisms dictate the use of transitional endoplasmic reticulum-golgi units

involved in *gurken* transport in *Drosophila* oocytes. *Molecular biology of the cell*, 15(12), pp.5306–5317.

Herpers, B., Xanthakis, D. & Rabouille, C., 2010. ISH–IEM: a sensitive method to detect endogenous mRNAs at the ultrastructural level. *Nature Protocols*, 5(4), pp.678–687.

Hilleren, P. & Parker, R., 1999. Mechanisms of mRNA surveillance in eukaryotes. *Annual review of genetics*, 33, pp.229–260.

Hocine, S. et al., 2013. Single-molecule analysis of gene expression using two-color RNA labeling in live yeast. *Nature Methods*, 10(2), pp.119–121.

Hoffman, A. et al., 1990. Highly conserved core domain and unique N terminus with presumptive regulatory motifs in a human TATA factor (TFIID). *Nature*, 346(6282), pp.387–390.

Holt, C.E. & Bullock, S.L., 2009. Subcellular mRNA localization in animal cells and why it matters. *Science*, 326(5957), pp.1212–1216.

Horne-Badovinac, S. & Bilder, D., 2008. Dynein regulates epithelial polarity and the apical localization of stardust A mRNA. *PLoS genetics*, 4(1), p.e8.

Horne-Badovinac, S. & Bilder, D., 2005. Mass transit: epithelial morphogenesis in the *Drosophila* egg chamber. *Developmental Dynamics*, 232(3), pp.559–574.

Hsu, C.L. & Stevens, A., 1993. Yeast cells lacking 5'--> 3‘exoribonuclease 1 contain mRNA species that are poly (A) deficient and partially lack the 5’cap structure. *Molecular and cellular biology*. 13(8), pp. 4826-4835

Hsu, H.-J., LaFever, L. & Drummond-Barbosa, D., 2008. Diet controls normal and tumorous germline stem cells via insulin-dependent and -independent mechanisms in Drosophila. *Developmental Biology*, 313(2), pp.700–712.

Hu, W. et al., 2009. Co-translational mRNA decay in *Saccharomyces cerevisiae*. *Nature*, 461(7261), pp.225–229.

Huang, Y.-S. et al., 2006. CPEB3 and CPEB4 in neurons: analysis of RNA-binding specificity and translational control of AMPA receptor GluR2 mRNA. *The EMBO journal*, 25(20), pp.4865–4876.

Huarte, J. et al., 1992. Transient translational silencing by reversible mRNA deadenylation. *Cell*, 69(6), pp.1021–1030.

Huppertz, I. et al., 2014. iCLIP: protein-RNA interactions at nucleotide resolution. *Methods (San Diego, Calif.)*, 65(3), pp.274–287.

Huynh, J.-R. & St Johnston, D., 2004. The origin of asymmetry: early polarisation of the *Drosophila* germline cyst and oocyte. *Current biology : CB*, 14(11), pp.R438–R449.

Huynh, J.-R. et al., 2004. The *Drosophila* hnRNPA/B Homolog, Hrp48, Is Specifically Required for a Distinct Step in *osk* mRNA Localization. *Developmental Cell*, 6(5), pp.625–635.

Huynh, J.R. & St Johnston, D., 2000. The role of BicD, Egl, Orb and the microtubules in the restriction of meiosis to the *Drosophila* oocyte. *Development*, 127(13), pp.2785–2794.

Huynh, J.R. et al., 2001. PAR-1 is required for the maintenance of oocyte fate in *Drosophila*. *Development*, 128(7), pp.1201–1209.

Hyman, A.A., Weber, C.A. & Jülicher, F., 2014. Liquid-liquid phase separation in biology. *Annual Review of Cell and Developmental Biology*, 30, pp.39–58.

Igreja, C. & Izaurralde, E., 2011. CUP promotes deadenylation and inhibits decapping of mRNA targets. *Genes & Development*, 25(18), pp.1955–1967.

Irie, K. et al., 2002. The Khd1 protein, which has three KH RNA-binding motifs, is required for proper localization of ASH1 mRNA in yeast. *The EMBO journal*, 21(5), pp.1158–1167.

Isken, O. & Maquat, L.E., 2007. Quality control of eukaryotic mRNA: safeguarding cells from abnormal mRNA function. *Genes & Development*, 21(15), pp.1833–1856.

Ivshina, M., Lasko, P. & Richter, J.D., 2014. Cytoplasmic polyadenylation element binding proteins in development, health, and disease. *Annual Review of Cell and Developmental Biology*, 30, pp.393–415.

Jackson, R.J., Hellen, C.U.T. & Pestova, T.V., 2010. The mechanism of eukaryotic translation initiation and principles of its regulation. *Nature Reviews Molecular Cell Biology*, 11(2), pp.113–127.

Jackson, S.M. & Berg, C.A., 2002. An A-kinase anchoring protein is required for protein kinase A regulatory subunit localization and morphology of actin structures during oogenesis in *Drosophila*. *Development*, 129(19), pp.4423–4433.

Jaeger, J., 2011. The gap gene network. *Cellular and molecular life sciences : CMLS*, 68(2), pp.243–274.

Jakt, L.M., Moriwaki, S. & Nishikawa, S., 2013. A continuum of transcriptional identities visualized by combinatorial fluorescent in situ hybridization. *Development*, 140(1), pp.216–225.

Jambor, H. et al., 2014. A stem–loop structure directs *oskar* mRNA to microtubule minus ends. *RNA*. 20(4), pp. 429-439

Jambor, H. et al., 2015. Systematic imaging reveals features and changing localization of mRNAs in *Drosophila* development. *eLife*, 4. doi 10.7554/eLife 05003

Jambor, H., Brunel, C. & Ephrussi, A., 2011. Dimerization of *oskar* 3' UTRs promotes hitchhiking for RNA localization in the *Drosophila* oocyte. *RNA*, 17(12), pp. 2049–2057.

Jankovics, F. et al., 2002. MOESIN crosslinks actin and cell membrane in *Drosophila* oocytes and is required for OSKAR anchoring. *Current biology : CB*, 12(23), pp.2060–2065.

Januschke, J. et al., 2002. Polar transport in the *Drosophila* oocyte requires Dynein and Kinesin I cooperation. *Current Biology*, 12(23), pp.1971–1981.

Jaqaman, K. et al., 2008. Robust single-particle tracking in live-cell time-lapse sequences. *Nature Methods*, 5(8), pp.695–702.

Jaramillo, A.M. et al., 2008. The dynamics of fluorescently labeled endogenous gurken mRNA in *Drosophila*. *Journal of Cell Science*, 121(6), pp.887–894.

Jeffery, W.R., Tomlinson, C.R. & Brodeur, R.D., 1983. Localization of actin messenger RNA during early ascidian development. *Developmental Biology*, 99(2), pp.408–417.

Jenny, A. et al., 2006. A translation-independent role of *oskar* RNA in early Drosophila oogenesis. *Development*. 133(15), pp. 2827-2833

Jeske, M. et al., 2011. Smaug assembles an ATP-dependent stable complex repressing *nanos* mRNA translation at multiple levels. *The EMBO journal*, 30(1), pp.90–103.

Ji, Z. et al., 2009. Progressive lengthening of 3' untranslated regions of mRNAs by alternative polyadenylation during mouse embryonic development. *Proceedings of the National Academy of Sciences*, 106(17), pp.7028–7033.

Johnstone, O. & Lasko, P., 2004. Interaction with eIF5B is essential for Vasa function during development. *Development*, 131(17), pp.4167–4178.

Jonas, S. & Izaurralde, E., 2013. The role of disordered protein regions in the assembly of decapping complexes and RNP granules. *Genes & Development*, 27(24), pp.2628–2641.

Juge, F. et al., 2002. Control of poly(A) polymerase level is essential to cytoplasmic polyadenylation and early development in *Drosophila*. *The EMBO journal*, 21(23), pp.6603–6613.

Jung, H., Yoon, B.C. & Holt, C.E., 2012. Axonal mRNA localization and local protein synThesis in nervous system assembly, maintenance and repair. *Nature reviews. Neuroscience*, 13(5), pp.308–324.

Kalifa, Y. et al., 2006. Glorund, a *Drosophila* hnRNP F/H homolog, is an ovarian repressor of *nanos* translation. *Developmental Cell*, 10(3), pp.291–301.

Kamenska, A. et al., 2014. Human 4E-T represses translation of bound mRNAs and enhances microRNA-mediated silencing. *Nucleic Acids Research*, 42(5), pp. 3298–3313.

Kanai, Y., Dohmae, N. & Hirokawa, N., 2004. Kinesin transports RNA: isolation and characterization of an RNA-transporting granule. *Neuron*, 43(4), pp.513–525.

Kanke, M. & Macdonald, P.M., 2015. Translational Activation of *oskar* mRNA: Reevaluation of the Role and Importance of a 5' Regulatory Element. *PLoS ONE*, 10(5), p.e0125849.

Kanke, M. et al., 2015. *oskar* RNA plays multiple noncoding roles to support oogenesis and maintain integrity of the germline/soma distinction. *RNA*. 21, pp.1096-1109

Karasawa, S. et al., 2004. Cyan-emitting and orange-emitting fluorescent proteins as a donor/acceptor pair for fluorescence resonance energy transfer. *The Biochemical journal*, 381(Pt 1), pp.307–312.

Karpen, G.H. & Spradling, A.C., 1992. Analysis of subtelomeric heterochromatin in the *Drosophila* minichromosome Dp1187 by single P element insertional mutagenesis. *Genetics*. 132)3), pp. 737-753

Kato, M. et al., 2012. Cell-free formation of RNA granules: low complexity sequence domains form dynamic fibers within hydrogels. *Cell*, 149(4), pp.753–767.

Kato, Y. & Nakamura, A., 2011. Roles of cytoplasmic RNP granules in intracellular RNA localization and translational control in the *Drosophila* oocyte. *Development, Growth & Differentiation*, 54(1), pp.19–31.

Katz, Z.B. et al., 2012. *β-Actin* mRNA compartmentalization enhances focal adhesion stability and directs cell migration. *Genes and development*. 26(17), pp 1885-1890

Kedersha, N. & Anderson, P., 2002. Stress granules: sites of mRNA triage that regulate mRNA stability and translatability. *Biochemical Society transactions*, 30(Pt 6), pp.963–969.

Kedersha, N. et al., 2005. Stress granules and processing bodies are dynamically linked sites of mRNP remodeling. *The Journal of Cell Biology*. 169(6), pp. 871-884

Kedersha, N.L. et al., 1999. RNA-binding proteins TIA-1 and TIAR link the phosphorylation of eIF-2 alpha to the assembly of mammalian stress granules. *The Journal of Cell Biology*, 147(7), pp.1431–1442.

Keleman, K. et al., 2007. Function of the *Drosophila* CPEB protein Orb2 in long-term courtship memory. *Nature Neuroscience*, 10(12), pp.1587–1593.

Kelley, R.L., 1993. Initial organization of the *Drosophila* dorsoventral axis depends on an RNA-binding protein encoded by the squid gene. *Genes & Development*, 7(6), pp.948–960.

Kiebler, M.A. & Bassell, G.J., 2006. Neuronal RNA Granules: Movers and Makers. *Neuron*, 51(6), pp.685–690.

Kim, G. et al., 2015. Region-Specific Activation of *oskar* mRNA Translation by Inhibition of Bruno-Mediated Repression. *PLoS genetics*, 11(2), p.e1004992.

Kim, J.H. & Richter, J.D., 2006. Opposing polymerase-deadenylase activities regulate cytoplasmic polyadenylation. *Molecular cell*, 24(2), pp.173–183.

Kim, J.H. & Richter, J.D., 2007. RINGO/cdk1 and CPEB mediate poly (A) tail stabilization and translational regulation by ePAB. *Genes & Development*. 21(20), pp. 2571-2579

Kim-Ha, J. et al., 1993. Multiple RNA regulatory elements mediate distinct steps in localization of *oskar* mRNA. *Development*, 119(1), pp.169–178.

Kim-Ha, J., Kerr, K. & Macdonald, P.M., 1995. Translational regulation of *oskar* mRNA by bruno, an ovarian RNA-binding protein, is essential. *Cell*, 81(3), pp. 403–412.

Kim-Ha, J., Smith, J.L. & Macdonald, P.M., 1991. *oskar* mRNA is localized to the posterior pole of the Drosophila oocyte. *Cell*, 66(1), pp.23–35.

Kimball, S.R. et al., 2003. Mammalian stress granules represent sites of accumulation of stalled translation initiation complexes. *American journal of physiology. Cell physiology*, 284(2), pp.C273–84.

King, R. C., 1970. Ovarian development in *Drosophila melanogaster*. Academic Press.

King, R. C. and Burnett R.G., 1959. An autoradiographic study of uptake of tritiated glycine, thymidine, and uridine by fruit fly ovaries. *Science*, 129(1), pp. 1674-1675

King, M.L., Messitt, T.J. & Mowry, K.L., 2005. Putting RNAs in the right place at the right time: RNA localization in the frog oocyte. *Biology of the Cell*, 97(1), pp. 19–33.

King, S.M., 2000. AAA domains and organization of the Dynein motor unit. *Journal of Cell Science*, 113 (Pt 14), pp.2521–2526.

Kinkelin, K. et al., 2012. Crystal structure of a minimal eIF4E-Cup complex reveals a general mechanism of eIF4E regulation in translational repression. *RNA*, 18(9), pp.1624–1634.

Kinoshita, K. et al., 2005. Aurora A phosphorylation of TACC3/maskin is required for centrosome-dependent microtubule assembly in mitosis. *The Journal of Cell Biology*, 170(7), pp.1047–1055.

Kislauskis, E.H., Zhu, X. & H, S.R., 1997. beta-Actin messenger RNA localization and protein synThesis augment cell motility. *The Journal of Cell Biology*, 136(6), pp.1263–1270.

Köhrmann, M. et al., 1999. Microtubule-dependent Recruitment of Staufen-Green Fluorescent Protein into Large RNA-containing Granules and Subsequent Dendritic Transport in Living Hippocampal Neurons. *Molecular cell biology*. 10(9), pp. 2945-2953

Kronja, I. et al., 2014. Quantitative proteomics reveals the dynamics of protein changes during *Drosophila* oocyte maturation and the oocyte-to-embryo transition. *Proceedings of the National Academy of Sciences*, 111(45), pp. 16023–16028.

Krüttner, S. et al., 2012. *Drosophila* CPEB Orb2A mediates memory independent of Its RNA-binding domain. *Neuron*, 76(2), pp.383–395.

Kwon, S., Zhang, Y. & Matthias, P., 2007. The deacetylase HDAC6 is a novel critical component of stress granules involved in the stress response. *Genes & Development*, 21(24), pp.3381–3394.

Lall, S. et al., 1999. Squid hnRNP protein promotes apical cytoplasmic transport and localization of *Drosophila* pair-rule transcripts. *Cell*, 98(2), pp.171–180.

Lan, L. et al., 2010. Evidence for a Transport-Trap Mode of *Drosophila* melanogaster gurken mRNA Localization B. D. McCabe, ed. *PLoS ONE*, 5(11), p.e15448.

Lantz, V. & Schedl, P., 1994. Multiple cis-acting targeting sequences are required for *orb* mRNA localization during *Drosophila* oogenesis. *Molecular and cellular biology*, 14(4), pp.2235–2242.

Lantz, V. et al., 1994. The *Drosophila orb* RNA-binding protein is required for the formation of the egg chamber and establishment of polarity. *Genes & Development*, 8(5), pp.598–613.

Lantz, V., Ambrosio, L. & Schedl, P., 1992. The *Drosophila orb* gene is predicted to encode sex-specific germline RNA-binding proteins and has localized transcripts in ovaries and early embryos. *Development*, 115(1), pp.75–88.

Lantz, V.A., Clemens, S.E. & Miller, K.G., 1999. The actin cytoskeleton is required for maintenance of posterior pole plasm components in the *Drosophila* embryo. *Mechanisms of development*, 85(1-2), pp.111–122.

Lasko, P., 1999. RNA sorting in *Drosophila* oocytes and embryos. *FASEB journal : official publication of the Federation of American Societies for Experimental Biology*, 13(3), pp.421–433.

Lasko, P.F. & Ashburner, M., 1988. The product of the *Drosophila* gene vasa is very similar to eukaryotic initiation factor-4A. *Nature Structural & Molecular Biology*, 335(6191), pp.611–617.

Lauriat, T.L. et al., 2008. Developmental expression profile of quaking, a candidate gene for schizophrenia, and its target genes in human prefrontal cortex and hippocampus shows regional specificity. *Journal of neuroscience research*, 86(4), pp.785–796.

Lawrence, J.B. & H, S.R., 1986. Intracellular localization of messenger RNAs for cytoskeletal proteins. *Cell*, 45(3), pp.407–415.

Le Hir, H., 2000. The spliceosome deposits multiple proteins 20-24 nucleotides upstream of mRNA exon-exon junctions. *The EMBO journal*, 19(24), pp.6860–6869.

LeCuyer, K.A., Behlen, L.S. & Uhlenbeck, O.C., 1996. Mutagenesis of a stacking contact in the MS2 coat protein-RNA complex. *The EMBO journal*, 15(24), p. 6847.

Lee, M.J. et al., 2001. Msps/XMAP215 interacts with the centrosomal protein D-TACC to regulate microtubule behaviour. *Nature cell biology*, 3(7), pp.643–649.

Lehmann, R. & Nüsslein-Volhard, C., 1986. Abdominal segmentation, pole cell formation, and embryonic polarity require the localized activity of *oskar*, a maternal gene in Drosophila. *Cell*, 47(1), pp.141–152.

Lehmann, R. & Nüsslein-Volhard, C., 1991. The maternal gene *nanos* has a central role in posterior pattern formation of the *Drosophila* embryo. *Development*, 112(3), pp.679–691.

Leung, K.-M. & Holt, C.E., 2008. Live visualization of protein synThesis in axonal growth cones by microinjection of photoconvertible Kaede into Xenopus embryos. *Nature Protocols*, 3(8), pp.1318–1327.

Leung, K.-M. et al., 2006. Asymmetrical beta-actin mRNA translation in growth cones mediates attractive turning to netrin-1. *Nature Neuroscience*, 9(10), pp.1247–1256.

Leung, L.C. et al., 2013. Coupling of NF-protocadherin signaling to axon guidance by cue-induced translation. *Nature Neuroscience*, 16(2), pp.166–173.

Levsky, J.M. et al., 2002. Single-cell gene expression profiling. *Science*. 297 pp. 836-840

Lécuyer, E. et al., 2007. Global analysis of mRNA localization reveals a prominent role in organizing cellular architecture and function. *Cell*, 131(1), pp.174–187.

Li, P. et al., 2012a. Phase transitions in the assembly of multivalent signalling proteins. *Nature*, 483(7389), pp.336–340.

Li, W., Klovstad, M. & Schüpbach, T., 2014. Repression of *gurken* translation by a meiotic checkpoint in *Drosophila* oogenesis is suppressed by a reduction in the dose of eIF1A. *Development*, 141(20), pp.3910–3921.

Li, Y. et al., 2012b. Mei-P26 regulates the maintenance of ovarian germline stem cells by promoting BMP signaling. *Development*, 139(9), pp.1547–1556.

Li, Z. et al., 1999. Generation of a Novel A Kinase Anchor Protein and a Myristoylated Alanine-rich C Kinase Substrate-like Analog from a Single Gene. *The Journal of Biological Chemistry* 274(38), pp.27191-27200

Liang, L., Diehl-Jones, W. & Lasko, P., 1994. Localization of Vasa protein to the *Drosophila* pole plasm is independent of its RNA-binding and helicase activities. *Development*, 120(5), pp.1201–1211.

Lianoglou, S. et al., 2013. Ubiquitously transcribed genes use alternative polyadenylation to achieve tissue-specific expression. *Genes & Development*, 27(21), pp.2380–2396.

Lie, Y.S. & Macdonald, P.M., 1999. Apontic binds the translational repressor Bruno and is implicated in regulation of *oskar* mRNA translation. *Development*, 126(6), pp.1129–1138.

Lieberfarb, M.E. et al., 1996. Mutations that perturb poly(A)-dependent maternal mRNA activation block the initiation of development. *Development*, 122(2), pp. 579–588.

Lim, A.K. & Kai, T., 2007. Unique germ-line organelle, nuage, functions to repress selfish genetic elements in *Drosophila melanogaster*. *Proceedings of the National Academy of Sciences*, 104(16), pp.6714–6719.

Lim, S. et al., 2012. Dorsal activity of maternal squint is mediated by a non-coding function of the RNA. *Development*, 139(16), pp.2903–2915.

Lin, C.-L. et al., 2010. The nuclear experience of CPEB: implications for RNA processing and translational control. *RNA*, 16(2), pp.338–348.

Lin, H., Yue, L. & Spradling, A.C., 1994. The *Drosophila* fusome, a germline-specific organelle, contains membrane skeletal proteins and functions in cyst formation. *Development*, 120(4), pp.947–956.

Lin, M.-D. et al., 2008. *Drosophila* processing bodies in oogenesis. *Developmental Biology*, 322(2), pp.276–288.

Lionnet, T. et al., 2011. A transgenic mouse for in vivo detection of endogenous labeled mRNA. *Nature Methods*, 8(2), pp.165–170.

Little, S.C. et al., 2015. Independent and coordinate trafficking of single Drosophila germ plasm mRNAs. *Nature cell biology*. 17(5), pp.558-568

Little, S.C. et al., 2011. PLOS Biology: The Formation of the Bicoid Morphogen Gradient Requires Protein Movement from Anteriorly Localized mRNA. *PLoS Biology*, 9(3), p.e1000596.

Liu, J. et al., 2005. A role for the P-body component GW182 in microRNA function. *Nature cell biology*, 7(12), pp.1261–1266.

Liu, Q., Greimann, J.C. & Lima, C.D., 2006. Reconstitution, activities, and structure of the eukaryotic RNA exosome. *Cell*, 127(6), pp.1223–1237.

Liu, Y. et al., 2013. Bicaudal-D uses a parallel, homodimeric coiled coil with heterotypic registry to coordinate recruitment of cargos to Dynein. *Genes and development*. 27(11), pp. 1233-1246

Loiseau, P. et al., 2010. *Drosophila* PAT1 is required for Kinesin-1 to transport cargo and to maximize its motility. *Development*, 137(16), pp.2763–2772.

Long, R.M. et al., 1997. Mating type switching in yeast controlled by asymmetric localization of ASH1 mRNA. *Science*, 277(5324), pp.383–387.

Low, W.-K. et al., 2005. Inhibition of eukaryotic translation initiation by the marine natural product pateamine A. *Molecular cell*, 20(5), pp.709–722.

Luitjens, C. et al., 2000. CPEB proteins control two key steps in spermatogenesis in C. elegans. *Genes & Development*, 14(20), pp.2596–2609.

Lyford, G.L. et al., 1995. Arc, a growth factor and activity-regulated gene, encodes a novel cytoskeleton-associated protein that is enriched in neuronal dendrites. *Neuron*. 14(2), 433-435

Macdonald, P.M. & Kerr, K., 1998. Mutational analysis of an RNA recognition element that mediates localization of *bicoid* mRNA. *Molecular and cellular biology*, 18(7), pp.3788–3795.

Macdonald, P.M. & Kerr, K., 1997. Redundant RNA recognition events in *bicoid* mRNA localization. *RNA*, 3(12), pp.1413–1420.

Macdonald, P.M. & Struhl, G., 1988. Cis-acting sequences responsible for anterior localisation of *bicoid* mRNA in *Drosophila* embryos. *Nature*. 336, pp.595-598

Macdonald, P.M., Leask, A. & Kerr, K., 1995. exl protein specifically binds BLE1, a *bicoid* mRNA localization element, and is required for one phase of its activity. *Proceedings of the National Academy of Sciences of the United States of America*, 92(23), pp.10787–10791.

MacDougall, N. et al., 2003. *Drosophila gurken* (TGF [alpha]) mRNA Localizes as Particles that Move within the Oocyte in Two Dynein-Dependent Steps. *Developmental Cell*, 4(3), pp.307–319.

MacDougall, N. et al., 2001. Merlin, the *Drosophila* homologue of neurofibromatosis-2, is specifically required in posterior follicle cells for axis formation in the oocyte. *Development*, 128(5), pp.665–673.

Mach, J.M. & Lehmann, R., 1997. An Egalitarian-BicaudalD complex is essential for oocyte specification and axis determination in *Drosophila*. *Genes & Development*, 11(4), pp.423–435.

Majumdar, A. et al., 2012. Critical role of amyloid-like oligomers of *Drosophila* Orb2 in the persistence of memory. *Cell*, 148(3), pp.515–529.

Mancebo, R. et al., 2001. BSF binds specifically to the *bicoid* mRNA 3' untranslated region and contributes to stabilization of *bicoid* mRNA. *Molecular and cellular biology*, 21(10), pp.3462–3471.

Mandel, C.R. et al., 2006. Polyadenylation factor CPSF-73 is the pre-mRNA 3'-end-processing endonuclease. *Nature*, 444(7121), pp.953–956.

Markussen, F.-H. et al., 1995. Translational control of *oskar* generates short OSK, the isoform that induces pole plasma assembly. *Development*, 121(11), pp.3723–3732.

Martin, S.G. & St Johnston, D., 2003. A role for *Drosophila* LKB1 in anterior–posterior axis formation and epithelial polarity. *Nature*, 421(6921), pp.379–384.

Mazzoni, C., D'Addario, I. & Falcone, C., 2007. The C-terminus of the yeast Lsm4p is required for the association to P-bodies. *FEBS letters*, 581(25), pp.4836–4840.

McDermott, S.M. & Davis, I., 2013. *Drosophila* Hephaestus/Polypyrimidine Tract Binding Protein Is Required for Dorso-Ventral Patterning and Regulation of Signalling between the Germline and Soma A. Singh, ed. *PLoS ONE*, 8(7), p.e69978.

McDermott, S.M. et al., 2012. *Drosophila* Syncrip binds the *gurken* mRNA localisation signal and regulates localised transcripts during axis specification. *Biology Open*, 1(5), pp.488–497.

McDermott, S.M. et al., 2014. *Drosophila* Syncrip modulates the expression of mRNAs encoding key synaptic proteins required for morphology at the neuromuscular junction. *RNA*, 20(10), pp.1593–1606.

McGrail, M. & Hays, T.S., 1997. The microtubule motor cytoplasmic Dynein is required for spindle orientation during germline cell divisions and oocyte differentiation in *Drosophila*. *Development*, 124(12), pp.2409–2419.

McGregor, J.R., Xi, R. & Harrison, D.A., 2002. JAK signaling is somatically required for follicle cell differentiation in *Drosophila*. *Development*, 129(3), pp.705–717.

McGrew, L.L. et al., Poly(A) elongation during *Xenopus* oocyte maturation is required for translational recruitment and is mediated by a short sequence element. *Genes and Development*. 3, pp.803-815

Medioni, C., Mowry, K. & Besse, F., 2012. Principles and roles of mRNA localization in animal development. *Development*, 139(18), pp.3263–3276.

Meignin, C. & Davis, I., 2008. UAP56 RNA helicase is required for axis specification and cytoplasmic mRNA localization in *Drosophila*. *Developmental Biology*, 315(1), pp.89–98.

Meignin, C. et al., 2007. The salvador-warts-hippo pathway is required for epithelial proliferation and axis specification in *Drosophila*. *Current biology : CB*, 17(21), pp.1871–1878.

Mendez, R., Barnard, D. & Richter, J.D., 2002. Differential mRNA translation and meiotic progression require Cdc2-mediated CPEB destruction. *The EMBO journal*. 21(7), pp.1833-1844

Mendez, R., Hake, L.E., et al., 2000a. Phosphorylation of CPE binding factor by Eg2 regulates translation of c-mos mRNA. *Nature*, 404(6775), pp.302–307.

Mendez, R., Murthy, K.G., et al., 2000b. Phosphorylation of CPEB by Eg2 mediates the recruitment of CPSF into an active cytoplasmic polyadenylation complex. *Molecular cell*, 6(5), pp.1253–1259.

Méndez, R. & Richter, J.D., 2001. Translational Control by CPEB: a means to the end. *Nature Molecular Cell Biology*. 2, pp.521-529

Mhlanga, M.M. et al., 2009. In vivo colocalisation of *oskar* mRNA and trans-acting proteins revealed by quantitative imaging of the *Drosophila* oocyte. *PLoS ONE*, 4(7), p.e6241.

Micklem, D.R., 2000. Distinct roles of two conserved Staufen domains in *oskar* mRNA localization and translation. *The EMBO journal*, 19(6), pp.1366–1377.

Micklem, D.R. et al., 1997. The *mago nashi* gene is required for the polarisation of the oocyte and the formation of perpendicular axes in *Drosophila*. *Current biology : CB*, 7(7), pp.468–478.

Minasaki, R., Rudel, D. & Eckmann, C.R., 2014. Increased sensitivity and accuracy of a single-stranded DNA splint-mediated ligation assay (sPAT) reveals poly (A) tail length dynamics of developmentally.*RNA biology*. 11(2), pp.111-123

Minshall, N. et al., 2007. CPEB Interacts with an Ovary-specific eIF4E and 4E-T in Early *Xenopus* Oocytes. *Journal of Biological Chemistry*, 282(52), pp.37389–37401.

Minshall, N. et al., 2009. Role of p54 RNA helicase activity and its C-terminal domain in translational repression, P-body localization and assembly. *Molecular biology of the cell*, 20(9), pp.2464–2472.

Minshall, N., Thom, G. & Standart, N., 2001. A conserved role of a DEAD box helicase in mRNA masking. *RNA*, 7(12), pp.1728–1742.

Mische, S. et al., 2007. Direct observation of regulated ribonucleoprotein transport across the nurse cell/oocyte boundary. *Molecular biology of the cell*, 18(6), pp. 2254–2263.

Mitchell, P. et al., 1997. The exosome: a conserved eukaryotic RNA processing complex containing multiple 3′→ 5′ exoribonucleases. *Cell*. 91, pp.457-466

Montell, D.J., 2003. Border-cell migration: the race is on. *Nature Reviews Molecular Cell Biology*, 4(1), pp.13–24.

Montpetit, B. et al., 2011. A conserved mechanism of DEAD-box ATPase activation by nucleoporins and InsP6 in mRNA export. *Nature*, 472(7342), pp.238–242.

Mor, A. et al., 2010. Dynamics of single mRNP nucleocytoplasmic transport and export through the nuclear pore in living cells. *Nature Publishing Group*, 12(6), pp.543–552.

Morais-de-Sá, E. et al., 2013. Oskar is targeted for degradation by the sequential action of Par-1, GSK-3, and the SCF-Slimb ubiquitin ligase. *Developmental Cell*, 26(3), pp.303–314.

Motola, S. & Neuman-Silberberg, F.S., 2004. *spoonbill*, a new *Drosophila* female-sterile mutation, interferes with chromosome organization and dorsal-ventral patterning of the egg. *Developmental Dynamics*, 230(3), pp.535–545.

Muddashetty, R.S. et al., 2011. Reversible Inhibition of PSD-95 mRNA Translation by miR-125a, FMRP Phosphorylation, and mGluR Signaling. *Molecular cell*, 42(5), pp.673–688.

Muhlrad, D. & Parker, R., 1994. Premature translational termination triggers mRNA decapping. *Nature*, 370(6490), pp.578–581.

Muhlrad, D., Decker, C.J. & Parker, R., 1994. Deadenylation of the unstable mRNA encoded by the yeast MFA2 gene leads to decapping followed by 5“--> 3”digestion of the transcript. *Genes & Development*. 8(7), pp. 855-866

Muhlrad, D., Decker, C.J. & Parker, R., 1995. Turnover mechanisms of the stable yeast PGK1 mRNA. *Molecular and cellular biology*, 15(4), pp.2145–2156.

Munro, T.P. et al., 2006. A repeated IMP-binding motif controls *oskar* mRNA translation and anchoring independently of *Drosophila* melanogaster IMP. *The Journal of Cell Biology*, 172(4), pp.577-588

Müller, C. et al., 2013. Making myelin basic protein -from mRNA transport to localized translation. *Frontiers in cellular neuroscience*, 7, p.169.

Nagai, K. et al., 1990. Crystal structure of the RNA-binding domain of the U1 small nuclear ribonucleoprotein A. *Nature*. 348, pp.515-520

Nakamura, A. et al., 2001. Me31B silences translation of oocyte-localizing RNAs through the formation of cytoplasmic RNP complex during *Drosophila* oogenesis. *Development*, 128(17), pp.3233–3242.

Nakamura, A., Sato, K. & Hanyu-Nakamura, K., 2004. *Drosophila* cup is an eIF4E binding protein that associates with Bruno and regulates *oskar* mRNA translation in oogenesis. *Developmental Cell*, 6(1), pp.69–78.

Natalizio, B.J. & Wente, S.R., 2013. Postage for the messenger: designating routes for nuclear mRNA export. *Trends in Cell Biology*. 23(28), pp.365-373

Navarro, C. et al., 2004. Egalitarian binds Dynein light chain to establish oocyte polarity and maintain oocyte fate. *Nature cell biology*, 6(5), pp.427–435.

Nelson, M.R., Leidal, A.M. & Smibert, C.A., 2004. *Drosophila* Cup is an eIF4E-binding protein that functions in Smaug-mediated translational repression. *The EMBO journal*, 23(1), pp.150–159.

Neuman-Silberberg, F.S. & Schupbach, T., 1994. Dorsoventral axis formation in *Drosophila* depends on the correct dosage of the gene *gurken*. *Development*, 120(9), pp.2457–2463.

Neuman-Silberberg, F.S. & Schupbach, T., 1993. The *Drosophila* dorsoventral patterning gene *gurken* produces a dorsally localized RNA and encodes a TGF alpha-like protein. *Cell*, 75(1), pp.165–174.

Neuman-Silberberg, F.S. & Schupbach, T., 1996. The *Drosophila* TGF-α-like protein Gurken: expression and cellular localization during *Drosophila* oogenesis. *Mechanisms of development*. 59(2), pp.105-113

Newmark, P.A. et al., 1997. mago nashi mediates the posterior follicle cell-to-oocyte signal to organize axis formation in *Drosophila*. *Development*, 124(16), pp. 3197–3207.

Nishida, H. & Sawada, K., 2001. macho-1 encodes a localized mRNA in ascidian eggs that specifies muscle fate during embryogenesis. *Nature*. 409(6281), pp. 724-729

Nishiura, M. et al., 2004. A single-headed recombinant fragment of *Dictyostelium* cytoplasmic Dynein can drive the robust sliding of microtubules. *The Journal of biological chemistry*, 279(22), pp.22799–22802.

Nissan, T. et al., 2010. Decapping activators in *Saccharomyces cerevisiae* act by multiple mechanisms. *Molecular cell*, 39(5), pp.773–783.

Norvell, A. et al., 1999. Specific isoforms of *squid*, a *Drosophila* hnRNP, perform distinct roles in Gurken localization during oogenesis. *Genes & Development*, 13(7), pp.864–876.

Norvell, A. et al., 2015. Wispy and Orb cooperate in the cytoplasmic polyadenylation of localized *gurken* mRNA. *Developmental Dynamics*. Epub ahead of print, doiL 10.10002/dvdy.24331

Nott, T.J. et al., 2015. Phase transition of a disordered nuage protein generates environmentally responsive membraneless organelles. *Molecular cell*, 57(5), pp.936–947.

Nüsslein-Volhard, C., Frohnhöfer, H.G. & Lehmann, R., 1987. Determination of anteroposterior polarity in *Drosophila*. *Science*, 238(4834), pp.1675–1681.

Olivier, C. et al., 2005. Identification of a conserved RNA motif essential for *She2p* recognition and mRNA localization to the yeast bud. *Molecular and cellular biology*, 25(11), pp.4752–4766.

Ostareck, D.H., Ostareck-Lederer, A. & Shatsky, I.N., 2001. Lipoxygenase mRNA silencing in erythroid differentiation: the 3′ UTR regulatory complex controls 60S ribosomal subunit joining. *Cell*. 104(2):281-290

Padmanabhan, K. & Richter, J.D., 2006. Regulated Pumilio-2 binding controls RINGO/Spy mRNA translation and CPEB activation. *Genes & Development*, 20(2), pp.199–209.

Pai, T.-P. et al., 2013. *Drosophila* ORB protein in two mushroom body output neurons is necessary for long-term memory formation. *Proceedings of the National Academy of Sciences*, 110(19), pp.7898–7903.

Paige, J.S., Wu, K.Y. & Jaffrey, S.R., 2011. RNA Mimics of Green Fluorescent Protein. *Science*, 333(6042), pp.642–646.

Palacios, I.M. et al., 2004. An eIF4AIII-containing complex required for mRNA localization and nonsense-mediated mRNA decay. *Nature Structural & Molecular Biology*, 427(6976), pp.753–757.

Pane, A., Wehr, K. & Schüpbach, T., 2007. zucchini and squash encode two putative nucleases required for rasiRNA production in the *Drosophila* germline. *Developmental Cell*, 12(6), pp.851–862.

Pare, C. & Suter, B., 2000. Subcellular localization of *Bic-D::GFP* is linked to an asymmetric oocyte nucleus. *Journal of Cell Science*, 113(12), pp.2119–2127.

Paris, J. & Richter, J.D., 1990. Maturation-specific polyadenylation and translational control: diversity of cytoplasmic polyadenylation elements, influence of poly(A) tail size, and formation of stable polyadenylation complexes. *Molecular and cellular biology*, 10(11), pp.5634–5645.

Park, H.Y. & Singer, R.H., 2014. Visualization of Dynamics of Single Endogenous mRNA Labeled in Live Mouse. *Science*. 343(6169), pp.422-424

Parker, R. & Sheth, U., 2007. P bodies and the control of mRNA translation and degradation. *Molecular cell*, 25(5), pp.635–646.

Parker, R. & Song, H., 2004. The enzymes and control of eukaryotic mRNA turnover. *Nature Structural & Molecular Biology*, 11(2), pp.121–127.

Parton, R. & Davis, I., 2006. Lifting the fog: Image restoration by deconvolution. *Cell biology (ed. JE Celis)*, pp.187–200.

Parton, R.M. et al., 2011. A PAR-1-dependent orientation gradient of dynamic microtubules directs posterior cargo transport in the *Drosophila* oocyte. *The Journal of Cell Biology*, 194(1), pp.121–135.

Parton, R.M. et al., 2010. Pushing the limits of live cell imaging in *Drosophila*. *Live cell imaging: a laboratory manual*, pp.387–418.

Parton, R.M. et al., 2014. Subcellular mRNA localisation at a glance. *Journal of Cell Science*, 127(Pt 10), pp.2127–2133.

Peng, Z. et al., 2014. A creature with a hundred waggly tails: intrinsically disordered proteins in the ribosome. *Cellular and molecular life sciences : CMLS*, 71(8), pp.1477–1504.

Peri, F. & Roth, S., 2000. Combined activities of Gurken and decapentaplegic specify dorsal chorion structures of the *Drosophila* egg. *Development*, 127(4), pp. 841–850.

Piccioni, F., Zappavigna, V. & Verrotti, A.C., 2005. A cup full of functions. *RNA biology*, 2(4), pp.125–128.

Pilkington, G.R. & Parker, R., 2008. Pat1 contains distinct functional domains that promote P-body assembly and activation of decapping. *Molecular and cellular biology*, 28(4), pp.1298–1312.

Pillai, R.S. et al., 2005. Inhibition of translational initiation by Let-7 MicroRNA in human cells. *Science*. 309(5740), 1573-1576

Pinder, B.D. & Smibert, C.A., 2013. microRNA-independent recruitment of Argonaute 1 to nanos mRNA through the Smaug RNA-binding protein. *Nature Publishing Group*, 14(1), pp.80–86.

Piqué, M. et al., 2008. A combinatorial code for CPE-mediated translational control. *Cell*, 132(3), pp.434–448.

Polesello, C. & Tapon, N., 2007. Salvador-warts-hippo signaling promotes *Drosophila* posterior follicle cell maturation downstream of notch. *Current Biology*. 17(21), pp.1864-1870

Powrie, E.A., Zenklusen, D. & H, S.R., 2011. A nucleoporin, Nup60p, affects the nuclear and cytoplasmic localization of *ASH1* mRNA in *S. cerevisiae*. *RNA*, 17(1), pp.134–144.

Prasad M., Jang A. C., Starz-Gaiano M., Melani M., Montell D. J., 2007. A protocol for culturing *Drosophila melanogaster* stage 9 egg chambers for live imaging. *Nature protocols*, 2(10), pp.2467-2473

Proudfoot, N.J., 2011. Ending the message: poly(A) signals then and now. *Genes & Development*, 25(17), pp.1770–1782.

Queenan, A.M. et al., 1999. The transmembrane region of Gurken is not required for biological activity, but is necessary for transport to the oocyte membrane in *Drosophila*. *Mechanisms of development*, 89(1-2), pp.35–42.

Raap, A.K. & Van de Corput, M., 1995. Ultra-sensitive FISH using peroxidase-mediated deposition of biotin-or fluorochrome tyramides. *Human Molecular Genetics*. 4(4), pp.529-534

Rabouille, C., 1999. Quantitative aspects of immunogold labeling in embedded and nonembedded sections. *Methods in molecular biology (Clifton, N.J.)*, 117, pp. 125–144.

Raj, A. et al., 2008. Imaging individual mRNA molecules using multiple singly labeled probes. *Nature Methods*, 5(10), pp.877–879.

Raj, A. et al., 2006. Stochastic mRNA synThesis in mammalian cells. *PLoS Biology*, 4(10), p.e309.

Rangan, P. et al., 2009. Temporal and Spatial Control of Germ-Plasm RNAs. *Current Biology*, 19(1), pp.72–77.

Raveendra, B.L. et al., 2013. Characterization of prion-like conformational changes of the neuronal isoform of *Aplysia* CPEB. *Nature Structural & Molecular Biology*, 20(4), pp.495–501.

Reck-Peterson, S.L. et al., 2006. Single-molecule analysis of Dynein processivity and stepping behavior. *Cell*, 126(2), pp.335–348.

Reijns, M.A.M. et al., 2008. A role for Q/N-rich aggregation-prone regions in P-body localization. *Journal of Cell Science*, 121(Pt 15), pp.2463–2472.

Retelska, D. et al., 2006. Similarities and differences of polyadenylation signals in human and fly. *BMC genomics*, 7, p.176.

Reveal, B. et al., 2010. BREs mediate both repression and activation of *oskar* mRNA translation and act in trans. *Developmental Cell*, 18(3), pp.496–502.

Reveal, B. et al., 2011. Multiple RNA binding domains of Bruno confer recognition of diverse binding sites for translational repression. *RNA biology*, 8(6), pp.1047–1060.

Reverte, C.G., Ahearn, M.D. & Hake, L.E., 2001. CPEB degradation during *Xenopus* oocyte maturation requires a PEST domain and the 26S proteasome. *Developmental Biology*. 231(2), 447-458

Richter, J.D. & Lasko, P., 2011. Translational control in oocyte development. *Cold Spring Harbor perspectives in biology*, 3(9), p.a002758.

Richter, J.D. & Sonenberg, N., 2005. Regulation of cap-dependent translation by eIF4E inhibitory proteins. *Nature*, 433(7025), pp.477–480.

Rittenhouse, K.R. & Berg, C.A., 1995. Mutations in the *Drosophila* gene *bullwinkle* cause the formation of abnormal eggshell structures and bicaudal embryos. *Development*, 121(9), pp.3023–3033.

Rodríguez-Navarro, S. & Hurt, E., 2011. Linking gene regulation to mRNA production and export. *Current Opinion in Cell Biology*, 23(3), pp.302–309.

Rongo, C., Gavis, E.R. & Lehmann, R., 1995. Localization of *oskar* RNA regulates *oskar* translation and requires Oskar protein. *Development*, 121(9), pp.2737–2746.

Ross, A.F. et al., 1997. Characterization of a beta-actin mRNA zipcode-binding protein. *Molecular and cellular biology*, 17(4), pp.2158–2165.

Rossoll, W. et al., 2003. Smn, the spinal muscular atrophy-determining gene product, modulates axon growth and localization of beta-actin mRNA in growth cones of motoneurons. *The Journal of Cell Biology*, 163(4), pp.801–812.

Roth, S., 2001. *Drosophila* oogenesis: coordinating germ line and soma. *Current Biology*. 11(19) pp.779-781

Roth, S. & Schupbach, T., 1994. The relationship between ovarian and embryonic dorsoventral patterning in *Drosophila*. *Development*, 120(8), pp.2245–2257.

Roth, S., Neuman-Silberberg, F.S. & Barcelo, G., 1995. cornichon and the EGF receptor signaling process are necessary for both anterior-posterior and dorsal-ventral pattern formation in *Drosophila*. *Cell*. 81(6), pp.967-978

Rouget, C. et al., 2010. Maternal mRNA deadenylation and decay by the piRNA pathway in the early *Drosophila* embryo. *Nature*, 467(7319), pp.1128–1132.

Röper, K. & Brown, N.H., 2004. A spectraplakin is enriched on the fusome and organizes microtubules during oocyte specification in *Drosophila*. *Current Biology*. 14(2), pp.99-110

Sachs, A. & Wahle, E., 1993. Poly(A) tail metabolism and function in eucaryotes. *The Journal of biological chemistry*, 268(31), pp.22955–22958.

Saffman, E.E. et al., 1998. Premature translation of *oskar* in oocytes lacking the RNA-binding protein bicaudal-C. *Molecular and cellular biology*, 18(8), pp. 4855–4862.

Sakato, M. & King, S.M., 2004. Design and regulation of the AAA+ microtubule motor Dynein. *Journal of structural biology*. 146(1-2), pp.58-71

Sakaue-Sawano, A. et al., 2008. Visualizing spatiotemporal dynamics of multicellular cell-cycle progression. *Cell*, 132(3), pp.487–498.

Sallés, F.J. et al., 1994. Coordinate initiation of *Drosophila* development by regulated polyadenylation of maternal messenger RNAs. *Science*. 266(5193), pp. 1966-1999

Sambrook, J., Russell, D. W., 1979. Molecular Cloning. A laboratory manual. Cold Spring Harbour Laboratory Press

Samsó, M. et al., 1998. Structural characterization of a Dynein motor domain. *Journal of molecular biology*, 276(5), pp.927–937.

Sapir, A., Schweitzer, R. & Shilo, B.Z., 1998. Sequential activation of the EGF receptor pathway during *Drosophila* oogenesis establishes the dorsoventral axis. *Development*, 125(2), pp.191–200.

Sarkissian, M., Méndez, R. & Richter, J.D., 2004. Progesterone and insulin stimulation of CPEB-dependent polyadenylation is regulated by Aurora A and glycogen synthase kinase-3. *Genes & Development*, 18(1), pp.48–61.

Saulière, J., Murigneux, V. & Wang, Z., 2012. CLIP-seq of eIF4AIII reveals transcriptome-wide mapping of the human exon junction complex. *Nature structural and molecular biology*. 19(11), pp.1124-1131

Saunders, C. & Cohen, R.S., 1999. The Role of Oocyte Transcription, the 5′UTR, and Translation Repression and Derepression in *Drosophila gurken* mRNA and Protein Localization. *Molecular cell*, 3(1), pp.43–54.

Schupbach, T., 1987. Germ Line and Soma Cooperate during Oogenesis to establish the Dorsoventral pattern of egg shell and embryo in Drosophila melanogaster. *Cell*. 49(5), pp.699-707

Schroer, T.A., 2004. Dynactin. *Annual Review of Cell and Developmental Biology*, 20, pp.759–779.

Schupbach, T. & Wieschaus, E., 1991. Female sterile mutations on the second chromosome of *Drosophila* melanogaster. II. Mutations blocking oogenesis or altering egg morphology. *Genetics*, 129(4), pp.1119–1136.

Schüpbach, T. & Wieschaus, E., 1986. Germline autonomy of maternal-effect mutations altering the embryonic body pattern of *Drosophila*. *Developmental Biology*, 113(2), pp.443–448.

Semotok, J.L. et al., 2005. Smaug recruits the CCR4/POP2/NOT deadenylase complex to trigger maternal transcript localization in the early *Drosophila* embryo. *Current biology : CB*, 15(4), pp.284–294.

Sen, G.L. & Blau, H.M., 2005. Argonaute 2/RISC resides in sites of mammalian mRNA decay known as cytoplasmic bodies. *Nature cell biology*. 7(6), pp. 633-636

Serbus, L.R. et al., 2005. Dynein and the actin cytoskeleton control kinesin-driven cytoplasmic streaming in *Drosophila* oocytes. *Development*, 132(16), pp. 3743–3752.

Setoyama, D., Yamashita, M. & Sagata, N., 2007. Mechanism of degradation of CPEB during *Xenopus* oocyte maturation. *Proceedings of the National Academy of Sciences*, 104(46), pp.18001–18006.

Shaffer, S.M. et al., 2013. Turbo FISH: a method for rapid single molecule RNA FISH. *PLoS ONE*, 8(9), p.e75120.

Shandilya, J. & Roberts, S.G.E., 2012. The transcription cycle in eukaryotes: from productive initiation to RNA polymerase II recycling. *Biochimica et biophysica acta*, 1819(5), pp.391–400.

Shaner, N.C. et al., 2004. Improved monomeric red, orange and yellow fluorescent proteins derived from Discosoma sp. red fluorescent protein. *Nature Biotechnology*, 22(12), pp.1567–1572.

Shatkin, A.J. & Manley, J.L., 2000. The ends of the affair: capping and polyadenylation. *Nature structural biology*, 7(10), pp.838–842.

Shcherbo, D. et al., 2007. Bright far-red fluorescent protein for whole-body imaging. *Nature Methods*, 4(9), pp.741–746.

Shcherbo, D. et al., 2009. Far-red fluorescent tags for protein imaging in living tissues. *The Biochemical journal*, 418(3), pp.567–574.

Sheth, U. & Parker, R., 2003. Decapping and decay of messenger RNA occur in cytoplasmic processing bodies. *Science*, 300(5620), pp.805–808.

Sheth, U. & Parker, R., 2006. Targeting of Aberrant mRNAs to Cytoplasmic Processing Bodies. *Cell*, 125(6), pp.1095–1109.

Shimada, Y. et al., 2011. Reversible response of protein localization and microtubule organization to nutrient stress during *Drosophila* early oogenesis. *Developmental Biology*, 355(2), pp.250–262.

Si, K. et al., 2010. Aplysia CPEB can form prion-like multimers in sensory neurons that contribute to long-term facilitation. *Cell*, 140(3), pp.421–435.

Si, K., Lindquist, S. & Kandel, E.R., 2003. A neuronal isoform of the aplysia CPEB has prion-like properties. *Cell*, 115(7), pp.879–891.

Simon, B. et al., 2015. The structure of the SOLE element of *oskar* mRNA. *RNA*, 21(8), pp.1444–1453.

Singh, G. et al., 2012. The Cellular EJC Interactome Reveals Higher-Order mRNP Structure and an EJC-SR Protein Nexus. *Trends in Cell Biology*, 151(4), pp. 750–764.

Sinsimer, K.S. et al., 2011. A late phase of germ plasm accumulation during *Drosophila* oogenesis requires lost and rumpelstiltskin. *Development*, 138(16), pp.3431–3440.

Sinsimer, K.S. et al., 2013. Germ Plasm Anchoring Is a Dynamic State that Requires Persistent Trafficking. *Cell Reports*, 5(5), pp.1169–1177.

Slaidina, M. & Lehmann, R., 2014. Translational control in germline stem cell development. *The Journal of Cell Biology*, 207(1), pp.13–21.

Slot, J.W. & Geuze, H.J., 2007. Cryosectioning and immunolabeling. *Nature Protocols*, 2(10), pp.2480–2491.

Smibert, C.A. et al., 1996. smaug protein represses translation of unlocalized *nanos* mRNA in the *Drosophila* embryo. *Genes & Development*, 10(20), pp.2600–2609.

Snee, M.J. & Macdonald, P.M., 2009. Dynamic organization and plasticity of sponge bodies. *Developmental Dynamics*, 238(4), pp.918–930.

Snee, M.J. & Macdonald, P.M., 2004. Live imaging of nuage and polar granules: evidence against a precursor-product relationship and a novel role for Oskar in stabilization of polar granule components. *Journal of Cell Science*, 117(Pt 10), pp.2109–2120.

Snee, M.J. et al., 2007. A late phase of Oskar accumulation is crucial for posterior patterning of the *Drosophila* embryo, and is blocked by ectopic expression of Bruno. *Differentiation; research in biological diversity*, 75(3), pp.246–255.

Snee, M.J. et al., 2005. Recognition of the *bcd* mRNA localization signal in *Drosophila* embryos and ovaries. *Molecular and cellular biology*, 25(4), pp. 1501–1510.

Soundararajan, H.C. & Bullock, S.L., 2014. The influence of Dynein processivity control, MAPs, and microtubule ends on directional movement of a localising mRNA. *eLife*, 3, p.e01596.

Spana, E.P. & Doe, C.Q., 1995. The prospero transcription factor is asymmetrically localized to the cell cortex during neuroblast mitosis in *Drosophila*. *Development*, 121(10), pp.3187–3195.

Speel, E.J., Ramaekers, F.C. & Hopman, A.H., 1997. Sensitive multicolor fluorescence in situ hybridization using catalyzed reporter deposition (CARD) amplification. *The journal of histochemistry and cytochemistry : official journal of the Histochemistry Society*, 45(10), pp.1439–1446.

Spies, N., Burge, C.B. & Bartel, D.P., 2013. 3′ UTR-isoform choice has limited influence on the stability and translational efficiency of most mRNAs in mouse fibroblasts. *Genome research*. 23(12), pp.2078-2090

Spradling, A.J., Stem, D.M., Kiss, I., Roote, J., Laverty, T., Rubin, G.M., 1995. Gene disruptions using P transposable elements: an integral component of the *Drosophila* genome project. *Proceedings of the National Academy of Sciences of the United States of America*, 92(24) pp.10824-10830

Spracklen, A.J. et al., 2014. The pros and cons of common actin labeling tools for visualizing actin dynamics during *Drosophila* oogenesis. *Developmental Biology*, 393(2), pp.209–226.

Spradling, A., 1993. Developmental genetics of oogenesis in the development of *Drosophila melanogaster*. *Cold Spring Harbour Press*, 1, pp 1-70

St Johnston, D., 2005. Developmental Cell Biology: Moving messages: the intracellular localization of mRNAs. *Nature Reviews Molecular Cell Biology*, 6(5), pp.363–375.

St Johnston, D. & Nüsslein-Volhard, C., 1992. The origin of pattern and polarity in the *Drosophila* embryo. *Cell*, 68(2), pp.201–219.

St Johnston, D. et al., 1989. Multiple steps in the localization of *bicoid* RNA to the anterior pole of the *Drosophila* oocyte. *Development*, 107 Suppl, pp.13–19.

St Johnston, D., Beuchle, D. & Nüsslein-Volhard, C., 1991. Staufen, a gene required to localize maternal RNAs in the *Drosophila* egg. *Cell*, 66(1), pp.51–63.

Stebbins-Boaz, B. et al., 1999. Maskin is a CPEB-associated factor that transiently interacts with eIF-4E. *Molecular cell*. 4(6), pp.1017-1027

Steiger, M. et al., 2003. Analysis of recombinant yeast decapping enzyme. *RNA*, 9(2), pp.231–238.

Steward, O. & Schuman, E.M., 2001. Protein synThesis at synaptic sites on dendrites. *Annual review of neuroscience*, 24, pp.299–325.

Styhler, S. et al., 1998. *vasa* is required for Gurken accumulation in the oocyte, and is involved in oocyte differentiation and germline cyst development. *Development*, 125(9), pp.1569–1578.

Subtelny, A.O. et al., 2014. Poly(A)-tail profiling reveals an embryonic switch in translational control. *Nature*, 508(7494), pp.66–71.

Sundell, C.L. & H, S.R., 1991. Requirement of microfilaments in sorting of actin messenger RNA. *Science*. 253(5025), pp.1275-1277

Sung, H.-H. et al., 2008. *Drosophila* ensconsin promotes productive recruitment of Kinesin-1 to microtubules. *Developmental Cell*, 15(6), pp.866–876.

Surdej, P. & Jacobs-Lorena, M., 1998. Developmental regulation of *bicoid* mRNA stability is mediated by the first 43 nucleotides of the 3' untranslated region. *Molecular and cellular biology*, 18(5), pp.2892–2900.

Suter, B. & Steward, R., 1991. Requirement for phosphorylation and localization of the Bicaudal-D protein in *Drosophila* oocyte differentiation. *Trends in Cell Biology*, 67(5), pp.917–926.

Suter, B., Romberg, L.M. & Steward, R., 1989. Bicaudal-D, a *Drosophila* gene involved in developmental asymmetry: localized transcript accumulation in ovaries and sequence similarity to myosin heavy chain tail domains. *Genes & Development*, 3(12A), pp.1957–1968.

Sutton, M.A. & schuman, E.M., 2006. Dendritic protein synThesis, synaptic plasticity, and memory. *Cell*, 127(1), pp.49–58.

Swan, A., Nguyen, T. & Suter, B., 1999. *Drosophila* Lissencephaly-1 functions with Bic-D and Dynein in oocyte determination and nuclear positioning. *Nature cell biology*, 1(7), pp.444–449.

Tadros, W. & Lipshitz, H.D., 2009. The maternal-to-zygotic transition: a play in two acts. *Development*, 136(18), pp.3033–3042.

Takatori, N. et al., 2010. Segregation of Germ Layer Fates by Nuclear Migration-Dependent Localization of Not mRNA. *Developmental Cell*, 19(4), pp.589–598.

Takizawa, P.A. & Vale, R.D., 2000. The myosin motor, Myo4p, binds Ash1 mRNA via the adapter protein, She3p. *Proceedings of the National Academy of Sciences of the United States of America*, 97(10), pp.5273–5278.

Takizawa, P.A. et al., 1997. Actin-dependent localization of an RNA encoding a cell-fate determinant in yeast. *Nature*. 389(6646), pp 90-93

Tan, L. et al., 2001. An autoregulatory feedback loop directs the localized expression of the *Drosophila* CPEB protein Orb in the developing oocyte. *Development*, 128(7), pp.1159–1169.

Teixeira, D. & Parker, R., 2007. Analysis of P-body assembly in *Saccharomyces cerevisiae*. *Molecular biology of the cell*, 18(6), pp.2274–2287.

Teixeira, D. et al., 2005. Processing bodies require RNA for assembly and contain nontranslating mRNAs. *RNA*, 11(4), pp.371–382.

Tekotte, H. & Davis, I., 2002. Intracellular mRNA localization: motors move messages. *Trends in genetics : TIG*, 18(12), pp.636–642.

Tharun, S. & Parker, R., 2001. Targeting an mRNA for decapping: displacement of translation factors and association of the Lsm1p-7p complex on deadenylated yeast mRNAs. *Molecular cell*, 8(5), pp.1075–1083.

Tharun, S. et al., 2000. Yeast Sm-like proteins function in mRNA decapping and decay. *Nature*, 404(6777), pp.515–518.

Theurkauf, W.E. & Hazelrigg, T.I., 1998. In vivo analyses of cytoplasmic transport and cytoskeletal organization during *Drosophila* oogenesis: characterization of a multi-step anterior localization pathway. *Development*, 125(18), pp.3655–3666.

Theurkauf, W.E. et al., 1992. Reorganization of the cytoskeleton during *Drosophila* oogenesis: implications for axis specification and intercellular transport. *Development*, 115(4), pp.923–936.

Thio, G.L. et al., 2000. Localization of *gurken* RNA in *Drosophila* oogenesis requires elements in the 5' and 3' regions of the transcript. *Developmental Biology*, 221(2), pp.435–446.

Thomsen, G.H. & Melton, D.A., 1993. Processed Vg1 protein is an axial mesoderm inducer in Xenopus. *Cell*. 74(3), pp. 433-441

Thore, S. et al., 2003. X-ray structure and activity of the yeast Pop2 protein: a nuclease subunit of the mRNA deadenylase complex. *EMBO reports*, 4(12), pp.1150–1155.

Tiruchinapalli, D.M. et al., 2003. Activity-Dependent Trafficking and Dynamic Localization of Zipcode Binding Protein 1 and *β-Actin* mRNA in Dendrites and Spines of Hippocampal Neurons. *Journal of neuroscience*. 23(8), pp. 3251-3261

Tomari, Y. et al., 2004. RISC assembly defects in the *Drosophila* RNAi mutant armitage. *Cell*, 116(6), pp.831–841.

TOMPA, P. & CSERMELY, P., 2004. The role of structural disorder in the function of RNA and protein chaperones. *FASEB journal : official publication of the Federation of American Societies for Experimental Biology*, 18(11), pp.1169–1175.

Toretsky, J.A. & Wright, P.E., 2014. Assemblages: functional units formed by cellular phase separation. *The Journal of Cell Biology*, 206(5), pp.579–588.

Tran, D.H. & Berg, C.A., 2003. *bullwinkle* and *shark* regulate dorsal-appendage morphogenesis in *Drosophila* oogenesis. *Development*, 130(25), pp.6273–6282.

Trcek, T. & Singer, H. R., 2010. The cytoplasmic fate of an mRNP is determined cotranscriptionally: exception or rule? *Genes & Development*, 24(17), pp. 1827–1831.

Trcek, T. et al., 2011. Single-Molecule mRNA Decay Measurements Reveal Promoter- Regulated mRNA Stability in Yeast. *Cell*, 147(7), pp.1484–1497.

Trcek, T. et al., 2012. Single-mRNA counting using fluorescent in situ hybridization in budding yeast. *Nature Protocols*, 7(2), pp.408–419.

Trcek, T. et al., 2013. Temporal and spatial characterization of nonsense-mediated mRNA decay. *Genes & Development*, 27(5), pp.541–551.

Tucker, M. et al., 2002. Ccr4p is the catalytic subunit of a Ccr4p/Pop2p/Notp mRNA deadenylase complex in Saccharomyces cerevisiae. *The EMBO journal*, 21(6), pp.1427–1436.

Tucker, M. et al., 2001. The transcription factor associated Ccr4 and Caf1 proteins are components of the major cytoplasmic mRNA deadenylase in Saccharomyces cerevisiae. *Cell*, 104(3), pp.377–386.

Tyagi, S. & Kramer, F.R., 1996. Molecular beacons: probes that fluoresce upon hybridization. *Nature Biotechnology*. 14(3), pp. 303-308

Ulitsky, I. et al., 2012. Extensive alternative polyadenylation during zebrafish development. *Genome research*, 22(10), pp.2054–2066.

Updike, D. & Strome, S., 2010. P granule assembly and function in *Caenorhabditis elegans* germ cells. *Journal of andrology*, 31(1), pp.53–60.

Vale, R.D., 2003. The molecular motor toolbox for intracellular transport. *Cell*. 112(4), pp. 467-480

Valegård, K. et al., 1990. The three-dimensional structure of the bacterial virus MS2. *Nature*, 345(6270), pp.36–41.

Valkov, E. et al., 2012. ScienceDirect.com - Biochimica et Biophysica Acta (BBA) - Gene Regulatory Mechanisms - Structural basis for the assembly and disassembly of mRNA nuclear export complexes. *Biochimica et Biophysica Acta (BBA) - Gene Regulatory Mechanisms*, 1819(6), pp.578–592.

Van Buskirk, C., Hawkins, N.C. & Schupbach, T., 2000. Encore is a member of a novel family of proteins and affects multiple processes in *Drosophila* oogenesis. *Development*, 127(22), pp.4753–4762.

Van De Bor, V. et al., 2005. *gurken* and the I Factor Retrotransposon RNAs Share Common Localization Signals and Machinery. *Trends in Cell Biology*, 9(1), pp. 51–62.

van Dijk, E. et al., 2002. Human Dcp2: a catalytically active mRNA decapping enzyme located in specific cytoplasmic structures. *The EMBO journal*. 21(24), pp.6915-6924

van Eeden, F.J.M., 2001. Barentsz is essential for the posterior localization of *oskar* mRNA and colocalizes with it to the posterior pole. *The Journal of Cell Biology*, 154(3), pp.511–524.

van Hoof, A. et al., 2002. Exosome-mediated recognition and degradation of mRNAs lacking a termination codon. *Science*. 295(5563), 2262-2264

Vanzo, N. et al., 2007. Stimulation of endocytosis and actin dynamics by Oskar polarizes the *Drosophila* oocyte. *Developmental Cell*, 12(4), pp.543–555.

Vanzo, N.F. & Ephrussi, A., 2002. Oskar anchoring restricts pole plasm formation to the posterior of the *Drosophila* oocyte. *Development*, 129(15), pp.3705–3714.

Vendra, G., Hamilton, R.S. & Davis, I., 2007. Dynactin suppresses the retrograde movement of apically localized mRNA in *Drosophila* blastoderm embryos. *RNA*, 13(11), pp.1860–1867.

Venken, K.J.T. et al., 2011. MiMIC: a highly versatile transposon insertion resource for engineering Drosophila melanogaster genes. *Nature Methods*, 2(9) pp. 737-743.

Vereshchagina, N. & Wilson, C., 2006. Cytoplasmic activated protein kinase Akt regulates lipid-droplet accumulation in *Drosophila* nurse cells. *Development*, 133(23), pp.4731–4735.

Vereshchagina, N. et al., 2008. The protein phosphatase PP2A-B' subunit Widerborst is a negative regulator of cytoplasmic activated Akt and lipid metabolism in *Drosophila*. *Journal of Cell Science*, 121(20), pp.3383–3392.

Wang, C. & Lehmann, R., 1991. Nanos is the localized posterior determinant in *Drosophila*. *Cell*, 66(4), pp.637–647.

Wang, J.T. et al., 2014. Regulation of RNA granule dynamics by phosphorylation of serine-rich, intrinsically disordered proteins in *C. elegans*. *eLife*, 3, p.e04591.

Wang, S. & Hazelrigg, T., 1994. Implications for *bcd* mRNA localization from spatial distribution of Exu protein in *Drosophila* oogenesis. *Nature*, 369(6479), pp. 400–403.

Wang, Z. & Kiledjian, M., 2001. Functional link between the mammalian exosome and mRNA decapping. *Cell*, 107(6), pp.751–762.

Wasserman, J.D. & Freeman, M., 1998. An autoregulatory cascade of EGF receptor signaling patterns the *Drosophila* egg. *Cell*, 95(3), pp.355–364.

Waterman-Storer, C.M. & Karki, S., 1995. The p150Glued component of the dynactin complex binds to both microtubules and the actin-related protein centractin (Arp-1). *Proceedings of the National Academy of Science*. 92(5), pp. 1634-1638

Weber, S.C. & Brangwynne, C.P., 2012. Getting RNA and Protein in Phase. *Cell*, 149(6), pp.1188–1191.

Webster, P.J. et al., 1997. Translational repressor bruno plays multiple roles in development and is widely conserved. *Genes & Development*, 11(19), pp. 2510–2521.

Weeks, D.L. & Melton, D.A., 1987. A maternal mRNA localized to the vegetal hemisphere in Xenopus eggs codes for a growth factor related to TGF-β. *Cell*. 51(5), 861-867

Weil, T.T., 2014. mRNA localization in the *Drosophila* germline. *RNA biology*, 11(8), pp.1010–1018.

Weil, T.T., 2015. Post-transcriptional regulation of early embryogenesis. *F1000Prime Reports*, 7.

Weil, T.T. et al., 2008. Changes in *bicoid* mRNA Anchoring Highlight Conserved Mechanisms during the Oocyte-to-Embryo Transition. *Current Biology*, 18(14), pp.1055–1061.

Weil, T.T., Forrest, K.M. & Gavis, E.R., 2006. Localization of *bicoid* mRNA in Late Oocytes Is Maintained by Continual Active Transport. *Developmental Cell*, 11(2), pp.251–262.

Weil, T.T., Parton, R.M. & Davis, I., 2010a. Making the message clear: visualizing mRNA localization. *Trends in Cell Biology*, pp.1–11.

Weil, T.T., Parton, R.M. & Davis, I., 2012a. Preparing individual *Drosophila* egg chambers for live imaging. *Journal of visualized experiments : JoVE*, (60).

Weil, T.T., Parton, R.M., Herpers, B., et al., 2012b. *Drosophila* patterning is established by differential association of mRNAs with P bodies. *Nature Structural & Molecular Biology*, 14(12), pp.1305–1315.

Weil, T.T., Xanthakis, D., et al., 2010b. Distinguishing direct from indirect roles for *bicoid* mRNA localization factors. *Development*, 137(1), pp.169–176.

Wells, S.E. et al., 1998. Circularization of mRNA by eukaryotic translation initiation factors. *Molecular cell*. 2(1), pp. 135-140

Wharton, R.P. & Struhl, G., 1989. Structure of the *Drosophila* BicaudalD protein and its role in localizing the the posterior determinant nanos. *Cell*, 59(5), pp.881–892.

Wieschaus, E., Marsh, J.L. & Gehring, W., 1978. s(1)KlO, a Germline-Dependent Female Sterile Mutation Causing Abnormal Chorion Morphology in *Drosophila melanogaster*. *Roux's archives of developmental biology*. Information missing

Wilczynska, A. et al., 2005. The translational regulator CPEB1 provides a link between dcp1 bodies and stress granules. *Journal of Cell Science*, 118(Pt 5), pp.981–992.

Wilhelm, J.E., 2003. Cup is an eIF4E binding protein required for both the translational repression of *oskar* and the recruitment of Barentsz. *The Journal of Cell Biology*, 163(6), pp.1197–1204.

Wilhelm, J.E. & Vale, R.D., 1993. RNA on the move: the mRNA localization pathway. *The Journal of Cell Biology*, 123(2), pp.269–274.

Wilhelm, J.E. et al., 2000. Isolation of a ribonucleoprotein complex involved in mRNA localization in *Drosophila* oocytes. *The Journal of Cell Biology*, 148(3), pp. 427–440.

Wilkie, G.S. & Davis, I., 2001. *Drosophila* wingless and pair-rule transcripts localize apically by Dynein-mediated transport of RNA particles. *Cell*, 105(2), pp.209–219.

Wilkie, G.S. et al., 1999. Transcribed genes are localized according to chromosomal position within polarized *Drosophila* embryonic nuclei. *Current biology : CB*, 9(21), pp.1263–1266.

Wilsch-Bräuninger, M., Schwarz, H. & Nüsslein-Volhard, C., 1997. A sponge-like structure involved in the association and transport of maternal products during *Drosophila* oogenesis. *The Journal of Cell Biology*, 139(3), pp.817–829.

Wippich, F. et al., 2013. Dual specificity kinase DYRK3 couples stress granule condensation/dissolution to mTORC1 signaling. *Cell*. 152(4), pp. 791-805

Wolf, N., Priess, J. & Hirsh, D., 1983. Segregation of germline granules in early embryos of *Caenorhabditis elegans*: an electron microscopic analysis. *Journal of embryology and experimental morphology*, 73, pp.297–306.

Wolke, U. et al., 2002. Multiple levels of post transcriptional control lead to germ line-specific gene expression in the zebrafish. *Current biology : CB*, 12(4), pp.289–294.

Wong, L.C. & Schedl, P., 2011. Cup blocks the precocious activation of the orb autoregulatory loop. *PLoS ONE*, 6(12), p.e28261.

Wong, L.C. et al., 2011. The functioning of the *Drosophila* CPEB protein Orb is regulated by phosphorylation and requires casein kinase 2 activity. *PLoS ONE*, 6(9), p.e24355.

Wu, B., Chao, J.A. & Singer, R.H., 2012. Fluorescence Fluctuation Spectroscopy Enables Quantitative Imaging of Single mRNAs in Living Cells. *Biophysical Journal*, 102(12), pp.2936–2944.

Wu, B., Chen, J. & H, S.R., 2014. Background free imaging of single mRNAs in live cells using split fluorescent proteins. *Scientific reports*.

Wu, K.Y. et al., 2005. Local translation of RhoA regulates growth cone collapse. *Nature*, 436(7053), pp.1020–1024.

Wu, X., Tanwar, P.S. & Raftery, L.A., 2008. *Drosophila* follicle cells: morphogenesis in an eggshell. *Seminars in Cell and Developmental Biology*, 19(3), pp.271–282.

Yan, N. & Macdonald, P.M., 2004. Genetic interactions of *Drosophila melanogaster arrest* reveal roles for translational repressor Bruno in accumulation of Gurken and activity of Delta. *Genetics*, 168(3), pp.1433–1442.

Yang, L. et al., 2010. An adaptive non-local means filter for denoising live-cell images and improving particle detection. *Journal of structural biology*, 172(3), pp.233–243.

Yildiz, A. et al., 2004. Kinesin walks hand-over-hand. *Science*, 303(5658), pp.676–678.

Yisraeli, J.K. & Melton, D.A., 1988. The material mRNA *Vg1* is correctly localized following injection into *Xenopus* oocytes. *Nature*, 336(6199), pp.592–595.

Yisraeli, J.K., Sokol, S. & Melton, D.A., 1990. A two-step model for the localization of maternal mRNA in *Xenopus* oocytes: involvement of microtubules and microfilaments in the translocation and anchoring of Vg1 mRNA. *Development*, 108(2), pp.289–298.

Yoon, B.C. et al., 2012. Local translation of extranuclear lamin B promotes axon maintenance. *Cell*, 148(4), pp.752–764.

Yoon, C., Kawakami, K. & Hopkins, N., 1997. Zebrafish *vasa* homologue RNA is localized to the cleavage planes of 2- and 4-cell-stage embryos and is expressed in the primordial germ cells. *Development*, 124(16), pp.3157–3165.

Yoshida, S. et al., 2004. PKA-R1 spatially restricts Oskar expression for *Drosophila* embryonic patterning. *Development*, 131(6), pp.1401–1410.

Zaessinger, S., Busseau, I. & Simonelig, M., 2006. Oskar allows *nanos* mRNA translation in *Drosophila* embryos by preventing its deadenylation by Smaug/CCR4. *Development*, 133(22), pp.4573–4583.

Zhang, F. et al., 2012. UAP56 Couples piRNA Clusters to the Perinuclear Transposon Silencing Machinery. *Trends in Cell Biology*, 151(4), pp.871–884.

Zhang, H.L. et al., 2001. Neurotrophin-induced transport of a beta-actin mRNP complex increases beta-actin levels and stimulates growth cone motility. *Neuron*, 31(2), pp.261–275.

Zhao, T. et al., 2012. Growing Microtubules Push the Oocyte Nucleus to Polarize the *Drosophila* Dorsal-Ventral Axis. *Science*, 336(6084), pp.999–1003.

Zimyanin, V., Lowe, N. & St Johnston, D., 2007. An oskar-dependent positive feedback loop maintains the polarity of the *Drosophila* oocyte. *Current biology : CB*, 17(4), pp.353–359.

Zimyanin, V.L. et al., 2008. In Vivo Imaging of *oskar* mRNA Transport Reveals the Mechanism of Posterior Localization. *Cell*, 134(5), pp.843–853.

Chapter 10: Appendices

Appendix A: Primers

Name	Sequence	Purpose
DNA splint	CGCATAGCTACAGCTGTTTTTTTTT	Aids ligation of the RNA anchor to the poly(A) tail of the mRNA
RNA anchor oligonucleotide	CAGCUCUAGCUAUGCGCACCGAGUCAGAUCAG	Provides a uniform sequence from which to reverse - prime
RT anchor primer	CTGATCTGACTCGGTGCGCA	sPAT PCR reverse outer primer
Anchor primer	TGCGCATAGCTACAGCTGTTTT	sPAT PCR-reverse inner primer
grk outer primer	ATTTAGTTGCAAAAGACGCACAAGT	*grk* specific (forward) outer primer for sPAT and poly(A) mapping
grk inner primer	TAGCGCTTACTCCAGTTACCAG	*grk* specific (forward) inner primer for sPAT and poly(A) mapping

Appendix B: Stellaris FISH probes

Each line represents the sequence of a single probe (5' to 3'). Probes were designed using the Biosearch Stellaris Probe Designer Organism chosen was *Drosophila melanogaster*, masking level of 5, maximum of 48 probes, 20mer oligonucleotides, 2 nucleotide minimum spacing.

Stellaris *grk* probe:

CGCACGTCGGAAAAGAGACT
TGCTCCACTTTGATTTTAGG
ATCTAAAGAGCAGCAAGCGC
CTGTAGAAGGCTTCGACATT
GGATTTTATGGAGCTGCTAT
CTACACACTTGCATCTCCTT
GTCGCAACAGAAGCTGAAAC
CTGGCCGCAAATGCAATTTG
AGGGGTCTAAACGATCGAGG
GTCCACCACTAGGAAAACTG
ATATTGATTGGGTGGACCGA
ATTGGAAAACGCTTGGGGTG
CCGAGTAAATGGGATTTGCA
GCGACAATTGTTGAGAGCAC
CGGCTCGAACAACAATCTGT
CGTATGCTCTCGGAGAAGTA
TGCTGATGCTGCACAATTTT
CAGGCGATTGAGCAACTCAA
ATTGGGATCCGTATCGGGAT
AATGGAGTCGTCTGCGTTTG
ACTGGATCCGAGAATTATCC
TGATTGGTGTGCTGCTTTCG
TGTTGTCACTGTCTCGGAAT
CGGTGTGGGTAACAGTTTCG
CTGGACGAACTGGGGTCAGG
AGCATCTGAATCTCTGTCTC
TATTGTAAGCTTCGCTGCAG
ATCGGATGCTGGAAGCAGTG
GCAGGAATGGAAGACTGTGT
CATCGTAGTCGTTAACGCAG
CACCATTCCAGCTCTTGTAG
TGTTGGAGGCGAATAGATGT
AAGGAGAAGACGATGTGCGC
GACGACAGCATGAGGAGTAC
GGCTGCGAAGAGAACGTAGA
GCACATTGCGGAGCATGAAA
TTATGCAGGTGTAGTTGCTG
GCATCTGACAAAAAAGCGCT
GGTGAAACCAAATTGTTTCC
CCAACAAAGAGGAGGCTTAT
ATGGTCAACAAGAATTTGCC
TACGCTGCGCAACGTAAAGA
AACTTGTGCGTCTTTTGCAA
AGCTCCAACGAAAGCTTCAA
CTGGAGTAAGCGCTAAGATT
AAATAATCACTTGTCCTGGT
ATCCTCTTCTTTAATACACT
ATTCTGTTTCGAGTCGAGTC

48 probes total, conjugated to Cal Fluor 590 (red).

Stellaris *grk* sense:

GGGACTCGACTCGAAACAGA
ACACTCTGTTACATTGTGTA
GTTACCAGGACAAGTGATTA
TGTAATCTTAGCGCTTACTC
TGTAATCTTAGCGCTTACTC
CTTTTGAAGCTTTCGTTGGA
CGCACAAGTTAGTATTTGCT
GGATTTTCTATTTAGTTGCA
ACGTTGCGCAGCGTAAAATT
TGGCAAATTCTTGTTGACCA
TATAAGCCTCCTCTTTGTTG
GGAAACAATTTGGTTTCACC
GCTTTTTTGTCAGATGCTGA
CAACTACACCTGCATAAGCA
TTTTCATGCTCCGCAATGTG
GAATGGCGCACATCGTCTTC
TACATCTATTCGCCTCCAAC
CCTACAAGAGCTGGAATGGT
CTCTGCGTTAACGACTACGA
AGCATCCGATGGTGAACAAC
CAATACTAGCTTTTGCCTGA
GACAGAGATTCAGATGCTGC
CGAAACTGTTACCCACACCG
ATTCCGAGACAGTGACAACA
CGAAAGCAGCACACCAATCA
TAATTCTCGGATCCAGTACC
TGCGGATCCGGAACAGGATG
CAAACGCAGACGACTCCATT
TGCAGCGCAAGCAACTGGAG
TTGAGTTGCTCAATCGCCTG
CAGCAGCAGATCCAGGAGAC
AAATTGTGCAGCATCAGCAC
TTACTTCTCCGAGAGCATAC
TCACAGATTGTTGTTCGAGC
CGTGCTCTCAACAATTGTCG
AATCCCATTTACTCGGATTT
CCAAGCGTTTTCCAATGATG
GTCCACCCAATCAATATTTT
TTTTCCTAGTGGTGGACAAT
TTTAGACCCCTTCATTGACT
GACGCCAAATTGCATTTGCG
AGTATGTTTCAGCTTCTGTT
CCACAAGGAGATGCAAGTGT
CCATATAGCAGCTCCATAAA
TAATGTCGAAGCCTTCTACA
GCTTGCTGCTCTTTAGATTA
AAGTGGAGCAGAGAAGAGCC
TGCGCGCAACAAGACCTAAA

48 probes total, conjugated to Cal Fluor 590 (red).

Stellaris *grk* scrambled probe:

AGTCTCTTTTCCGACGTGCG
CGCAACAAGACCTAAAATCA
AAGTGGAGCAGAGAAGAGCC
CGCTTCCCGCGCTTGCTGCT
CTTTAGATTAACTAATTAAT
TACTTGCCTGATATATAAAA
TGATTCACGAGTCATTATAA
TAATTATAATGTCGAAGCCT
TCTACAGGCCATATAGCAGC
TCCATAAAATCCACAAGGAG
ATGCAAGTGTGTAGTATGTT
TCAGCTTCTGTTGCGACGCC
AAATTGCATTTGCGGCCAGC
ACGCCGCTCGATCCCTCGAT
CGTTTAGACCCCTTCATTGA
CTCAGTTTTCCTAGTGGTGG
ACAATCGGTCCACCCAATCA
ATATTTTTCGGAGCGCCACC
CCAAGCGTTTTCCAATGATG
CAAATCCCATTTACTCGGAT
TTTCAAAGTAATTTTCGTGC
TCTCAACAATTGTCGCCGTC
ACAGATTGTTGTTCGAGCCG
AATCTTACTTCTCCGAGAGC
ATACGCTGAAAATTGTGCAG
CATCAGCACAGCCACATGCA
CGAGCATGCGCACGAGCTGC
AGCAGCAGATCCAGGAGACC
GCGGTTGAGTTGCTCAATCG
CCTGGAGCTGCAGCGCAAGC
AACTGGAGGCCTCGGCCCAG
GAGGAGGCAGACCAGCTGCA
TCCCGATACGGATCCCAATC
CGGACTCGGGCGGCCAACTG
CCAAACGCAGACGACTCCAT
TGCTGCGGATCCGGAACAGG
ATGGGATAATTCTCGGATCC
AGTACCGACACCTGGTTGGC
CAGCGAAAGCAGCACACCAA
TCACTGATTCCGAGACAGTG
ACAACACCCGAAACTGTTAC
CCACACCGGAGAACCGCCAC
CTGACCCCAGTTCGTCCAGC
ACGCCTGACTCCACGACTCC
CAGCCCGAACGACAAGGAGA
CAGAGATTCAGATGCTGCCC
TGCAGCGAAGCTTACAATAC
TAGCTTTTGCCTGAACGGCG

48 probes total, conjugated to Cal Fluor 590 (red).

Stellaris *grk* intron probe:

GGTGATCCAAAAGCTTTTCA
CATTTTCTGTCGCACGAACG
ATAGAACATTTTAGCGCCTC
CAGGTGGAGATTATGTACGT
GGCAATACTGGCCGTAATAT
AGCTTTTTTTGTGGGAGAGC
CAGTTTTTTCGACGCTAGAA
ATGATTTGTTGTAGCTGTTT
AGTATATAATCAGCACTGCA
CAGGATTTTACACAGTTTTC
ACTTCATTCATCATCCACGA
AGTTTGTTCATAAGGACAGT
AGCTTTCAGTTTTTAGTGCG
CGTTGTAAAGCTCAAGTTGA
TTTCCAGTGATCGCAAAGAT
ATACAGAAGAAGGTGTGCGA
TGCTAGAGTAGAGTACCTAC
GACTTCTGTGAATGGATGGC
ATCCGTTCCATACAACACAG
ACTGGGTACAGACTAATAGA
ATGAGTTCATTTAGTTACCA

21 probes total, conjugated to Quasar 670 (far red).

Stellaris *grk* intron sense:

TGAACTCATTGATCATTGCA
ATCTATTAGTCTGTACCCAG
GTGTTGTATGGAACGGATGG
TCCATTCACAGAAGTCTCTT
GTACTCTACTCTAGCATAGC
ACACCTTCTTCTGTATTCTG
TGTATCTTTGCGATCACTGG
TGTACTTCAACTTGAGCTTT
ATTTCAAAAGTTGCCGCACT
CCATAGGGAGACATTTTTAT
TATTAGCTTTCTGTTCGTGG
ACTTCCTTGAAAACTGTGTA
GCAGTGCTGATTATATACTT
GGCTCTCCCACAAAAAAAGC
CCAATATTACGGCCAGTATT
TACGTACATAATCTCCACCT
TGGAGGCGCTAAAATGTTCT
TGCGTTCGTGCGACAGAAAA
GCTTTTGGATCACCAATTTT

19 probes total, conjugated to Quasar 670 (far red).

MS2-12 probe:

CTAGGCAATTAGGTACCTTA
ACATGGGTGATCCTCATGTT
AGACATGGGTGATCCTCATG
CTAATGAACCCGGGAATACT
AGGCAATTAGGTACCTTAGG
ATGGGTGATCCTCATGTTTT
AGACATGGGTGATCCTCATG
CTAATGAACCCGGGAATACT
AGGCAATTAGGTACCTTAGG
ATGGGTGATCCTCATGTTTT
AGACATGGGTGATCCTCATG
CTAATGAACCCGGGAATACT
AGGCAATTAGGTACCTTAGG
ATGGGTGATCCTCATGTTTT
AGACATGGGTGATCCTCATG
CTAATGAACCCGGGAATACT
AGGCAATTAGGTACCTTAGG
ATGGGTGATCCTCATGTTTT
AGACATGGGTGATCCTCATG
CTAATGAACCCGGGAATACT
AGGCAATTAGGTACCTTAGG
ATGGGTGATCCTCATGTTTT
CATGGGTGATCCTCATGTTT
ATGAACCCGGGAATACTGCA

24 probes total, conjugated to either Cal Fluor 590 (red) or Quasar 670 (far red) depending on the experiment.

MS2-12 sense:

AACATGAGGATCACCCATGT
AACATGAGGATCACCCATGT
TAAGGTACCTAATTGCCTAG
TAAGGTACCTAATTGCCTAG
AACATGAGGATCACCCATGT
AACATGAGGATCACCCATGT
TAAGGTACCTAATTGCCTAG
TATTCCCGGGTTCATTAGAT
AACATGAGGATCACCCATGT
AACATGAGGATCACCCATGT
TAAGGTACCTAATTGCCTAG
TATTCCCGGGTTCATTAGAT
AACATGAGGATCACCCATGT
AACATGAGGATCACCCATGT
TAAGGTACCTAATTGCCTAG
TATTCCCGGGTTCATTAGAT
AACATGAGGATCACCCATGT
AACATGAGGATCACCCATGT
TAAGGTACCTAATTGCCTAG
TATTCCCGGGTTCATTAGAT
AACATGAGGATCACCCATGT
AGGTACCTAATTGCCTAGAA

22 probes total, conjugated to Cal Fluor 590

Appendix C: Fly strains

Group/Genotype	Description	Source
***Wild-type* strains**		
OrR	Wild type stock (all experiments)	
w^{1118}	Wild type stock (for imaging)	Bloomington (6326)
yw	Wild type stock (for imaging)	
MS2 lines		
grk - $(MS2)^{12}$/Cyo	*grk* mRNA with 12 MS2 stem loops	Jaramillo et al 2008
grk - (MS2)-24/Cyo	*grk* mRNA with 24 MS2 stem loops	This work (strain 8B)
osk MS2-10/TM3, Sb	*osk* mRNA with 10 MS2 stem loops	Zymanin et al 2008
MCP-FP lines		
Pnos-NLS-MCP-GFP	GFP tagged MCP protein driven by germline specific promoter	Gift from E. Gavis
Pnos-NLS-MCP-mCherry/ TM3, Ser	mCherry tagged MCP driven by germline specific promoter	Hayashi et al 2014, Weil et al 2012
P body markers		
Me31B::GFP	Me31B protein trap GFP line	Buszczak et al 2007, CG4916
Tral::YFP	Tral protein trap GFP line	Gift from D. St Johnston, CG10686
Growl::GFP	Growl protein trap GFP line	Buszczak et al 2007, CG14648
eIF4E::GFP	eIF4E protein trap GFP line	Buszczak et al 2007, CG4035
Sqd::GFP	Sqd protein trap GFP line	Norvell et al 2005, CG16901
YPS::GFP	YPS protein trap GFP line	Buszczak 2007, ZCL1503

Group/Genotype	Description	Source
Cup::YFP	Cup protein trap YFP line	D. St Johnston, CG11181
Fluorophore tagged trans-acting factors		
Heph::GFP	Heph protein trap GFP line	Besse et al 2009
BicD::GFP	BicD protein trap GFP line	Pare et al 2000
UAP56-GFP	P element insertion of GFP tagged UAP56 driven by the *UAP56* promoter	Meignin & Davis 2008
Vas-GFP/TM3	P element insertion of GFP tagged Vasa driven by the *vas* promoter	Nakamura et al 2001
Btz-GFP/Cyo	P element insertion of GFP tagged Btz driven by α4-tubulin	Gift from D. St Johnston (Van Eeden et al 2001)
Mutant lines		
me31B$^{\Delta 1}$ FRT40A/Cyo	For generating *me31b* null heat shock germline clones	Nakamura et al 2001
me31B$^{\Delta 2}$ FRT40A/Cyo	For generating *me31b* null heat shock germline clones	Nakamura et al 2001
aret^{PD}/Cyo	Weak *aret* mutant allele	Schupbach et al 1991
aret^{PA}/Cyo	Intermediate *aret* mutant allele	Schupbach et al 1991
aret^{QB}/Cyo	Strong *aret* mutant allele	Schupbach et al 1991
sqd^{1}	*sqd* mutant for all isoforms	Kelley et al 1993
cup^{1355}	Weak (Class III) *cup* mutant	Karpen et al 1992
cup$^{\Delta 212}$	*cup* mutant with eIF4E interaction domain specifically disrupted	Nakamura et al 2004
orb^{mel}	Weak *orb* mutant	Christerson & McKearin 1994

Group/Genotype	Description	Source
grk^{2B6}/*Cyo*	*grk* mRNA null mutant	Neuman-Silberberg & Schupbach 1993
grk^{2E12}/*Cyo*	*grk* protein null mutant	Neuman-Silberberg & Schupbach 1993
Heat shock marker lines		
hsFLP/w ; gfp-vas FRT40A/Cyo	Marker for generating *me31B* germline clones	Gift from A. Nakamura
Overexpression lines		
Maternal tubulin: Gal4-VP16	Ubiquitous expression driver for *UAS* lines	Weil et al 2012
UASp grk3A	For overexpression of *grk*	Bokel et al 2006
UASp-orb	For overexpression of *orb*	Li et al 2012
UASp-SypGFP2	For overexpression of *Syp* isoform F tagged with GFP	McDermott et al 2012
UASp-bru-1	For overexpression of *aret*	Snee et al 2007
Deficiency lines		
Df(2L)esc-P2-0/Cyo amos [Roi-1]	Second chromosome deficiency covering *aret*	Bloomington (3130)
Balancer lines		
yw; Pin/Cyo	Balancer stock (chromosome II)	
yw; Ly/TM3, Sb	Balancer stock (chromosome III)	
Gla/Cyo ; pri/TM6, Tb	Balancer stock (chromosomes II and III)	

Appendix D: Antibodies

DSHB, Developmental Studies Hybridoma Bank

Name	Dilution	Source
Primary antibodies		
anti-Grk mouse monoclonal 1D12	1:300	DSHB (Neuman-Silberberg and Schupbach 1996)
anti-Orb mouse monoclonal 4H8	1:30	DSHB (Lantz et al 1994)
anti-Sqd mouse monoclonal A 2G9	1:2000	DSHB (Norvell et al 1999)
anti-Me31B mouse monoclonal	1:1000	Gift from A. Nakamura (Nakamura et al 2001)
anti-Bruno rat polyclonal	1:300	Gift from A. Ephrussi (Filardo and Ephrussi 2003)
anti-Osk rabbit polyclonal	1:500	Gift from A. Ephrussi (Vanzo and Ephrussi 2002)
anti- α Ribo-490 human polyclonal	1:300	Gift from J. Van Minnen
Sheep anti-DIG (Fab fragments)	1:400	Roche (11214667001)
Mouse anti-DIG HRP conjugate	1:1000	PerkinElmer (NEF832001EA)
Secondary antibodies		
Donkey anti-mouse IgG (H+L), Alexa Fluor 488 conjugate	1:500	Life technologies, A-21202
Donkey anti-mouse IgG, Alexa Fluor 568 conjugate	1:500	Life technologies, A10037
Goat anti-Rat IgG (H+L), Alexa Fluor 568 conjugate	1:500	Life technologies, A-11077
Goat anti-Rabbit IgG (H +L), Alexa Fluor 568 conjugate	1:500	Life Technologies, A-11011

Name	Dilution	Source
Donkey anti-sheep IgG (H +L), Alexa Fluor 488 conjugate	1:400	Life technologies, A-11015
Donkey anti-sheep IgG (H +L), Alexa Fluor 568 conjugate	1:400	Life technologies, A-21099
GFP-booster	1:200	Chromotek (gba488)
RFP-booster	1:200	Chromotek (rba594)

Appendix E: Imaging parameters

Widefield imaging of live MS2 and protein trap egg chambers

The live cell filter set was used with the Quad/mCherry polychroic.

Subject of imaging	Excitation filter	Exposure (ms)	Bulb intensity (%)	Acquisition rate (fps)
*grk*GFP*	GFP	300	100	3
*grk*mCherry*	mCherry	300	100	3
P body protein traps	GFP/YFP	50	50	7
Fluorescently labelled trans-acting factors	GFP	50-100	50-100	3-9
P body protein traps (ring canal imaging)	GFP/YFP	50	50	1 frame/30s

For imaging *grk*mCherry* with GFP trap lines, imaging parameters were: mCherry excitation, 100% bulb intensity, 300 ms exposure. GFP excitation, 50% bulb intensity, 50 ms exposure. 2 fps final capture rate. In all cases, images were acquired on one Z plane only.

Widefield imaging of egg chambers with antibody staining/FISH

The live cell filter set was used with the Quad/mCherry polychroic.

All slides were imaged in multiple Zs with the size and position of the Z stack altered to capture the region of interest within each sample.

Subject of imaging	Excitation filter	Exposure (ms)	Bulb intensity (%)
Antibodies with Alexa 568/sm-FISH Cal Fluor 590	mCherry	100	100
Antibodies with Alexa 488	GFP	100	100
*grk*GFP*	GFP	300	100
*grk*mCherry*	mCherry	300	100
Fixed P body protein traps	GFP/YFP	50	50
sm-FISH probes with Qasar 670	Cy-5	200	100

Imaging of live MS2 and protein trap egg chambers on the OMX V3

All samples were imaged in multiple Zs with the position of the Z stack altered to capture the region of interest within each sample.

Subject of imaging	Excitation filter	Exposure (ms)	Laser intensity (%)	Z planes per stack (0.2 μm steps)	Acquisiton rate (fps)
*grk*GFP*	GFP	5	50	5	15
*grk*mCherry*	mCherry	5	100	5	5
Me31B::GFP	GFP	1	30	25	7

3D-SIM imaging of Orb antibody and *Me31B::GFP* on the OMX V3

Imaging parameters were as follows: SI experiment, sequential acquisition, All Z then channel, 0.125 μm Z steps, 10 Z sections. 488 settings: 80ms exposure, 1% laser. TRITC settings: 120ms, 10% laser.

Appendix F: Image analysis protocols

Scoring for presence of MS2 labelled RNA in the nurse cells.

mRNA particles were defined as between 200 and 500nm in diameter, regular spherical shape, and a fluorescence intensity of >1.5 x the background intensity of the nurse cell cytoplasm. Egg chambers were scored for the number of particles in the nurse cell cytoplasm (particles in nuclei were excluded) and classed as containing >10 particles, 1-9 particles, or no particles. In the nurse cell cytoplasm of most egg chambers, there were also large fluorescent assemblies. These “Large assemblies” were defined as being any one of; larger than 500nm, irregular in shape, lower than of 1.5x brightness of cytoplasmic background, and moving with cytoplasmic streaming. Egg chambers without mRNA particles were further sub-classed into those which contained large assemblies and those which contained none.

Tracking RNA in nurse cells

Particle tracking was performed in SoftWorx. All egg chambers which met the following criteria were used: healthy egg chamber morphology/cytoplasmic streaming, data in the correct stage and focal plane, and sample containing moving RNA particles (judged by eye). A 40μm x 40μm region was defined in the nurse cell cytoplasm in between the two nurse cell nuclei closest to the nurse cell - oocyte boundary. Within this region every particle during the first 50 frames of the movie was scored as follows: particles which did not move at all are “static”. Particles which moved but did not move for more than 5 frames in the same direction in one continuous movement are “paused”. Particles which moved for more than 5 frames in the same direction in one continuous movement are “Actively transported”. The same

definitions were applied to *Me31B::GFP* egg chambers, with another category added for “Large bodies”; assemblies of Me31B larger than 1μm in diameter.

For measuring particle speeds, a 10μm x 10μm region was defined in the nurse cell cytoplasm in the same region of nurse cell cytoplasm as above. Within this region the whole time series was observed. Any mRNA particles which moved were tracked and the number of static particles was recorded. Both the average velocity over a run (μm/s) and run length (μm) was recorded. Velocities and run lengths were statistically compared using a two tailed t-test

Co-transport analysis of *grk* and P body proteins in nurse cells

Egg chambers co-expressing *grk*-MS2 labelled mRNA and P body protein traps were imaged on the Deltavision microscope and analysed using SoftWorx. In a given egg chamber, all actively transported *grk* particles over the whole time series were tracked. The channel in which the fluorescent protein was imaged was then checked for particles on the same trajectory, and both channels were viewed simultaneously to see if particles on the same trajectory colocalised. Particles were deemed to be moving together when they ran over the same trajectory, started/stopped the run together and moved in or out of the plane of focus at the same point. I also recorded when *grk* mRNA particles which did not move with P bodies began a run at a P body, ended a run at a P body, or moved “through” a P body during a run. The percentage of *grk* particles which displayed each behaviour was recorded, and a total percantage of those which interacted with P bodies (moving with, from, to or through them) and those which did not (none of the above) was calculated.

Analysing colocalisation of FISH labelled *grk* and P bodies

Egg chambers were imaged with *grk* labelled with sm-FISH on the Deltavision microscope. All analysis was performed in SoftWorx. A 10 um x 10 um region in the nurse cell cytoplasm nearest to the oocyte was scored in the shallowest Z plane. *grk* particles were classed as; in the P body core when all pixels of the particle centroid were entirely within a P body; at the edge when any pixels of the particle centroid were within a P body; not associated with P bodies when there was no overlap between the particle centroid and the P body. Results were compared by a Chi-square test, detailed in Table 7-4

Quantification of Orb expression levels from *cup* mutant and *UAS-orb* egg chambers

Image analysis was performed with FIJI (ImageJ 1.45r). For each egg chamber, an average intensity projection of 3 Z slices (0.6μm) at the plane of brightest fluorescence intensity in the oocyte was used for analysis. Intensity along a transect through the image was defined by a region of interest at 10 pixels width, 500 pixels length placed along the anterior-posterior axis of a representative egg chamber. The average fluorescence intensity of the 10 width pixels was plotted for each of the 500 length pixels and expressed as a line graph. All values were normalised to the highest signal intensity in the oocyte cortex to remove variability in fluorescence from microscope bulb hours, antibody penetrance, and DSHB antibody batch.

To assess the fluorescence intensities in various regions of the egg chamber from numerous samples, the mean fluorescence and standard deviation of a 50x50 pixel box was taken from each region (oocyte centre, front row nurse cells, second row nurse cells, third row nurse cells). For the oocyte cortex, a custom ROI was defined around the cortex as visible by Orb fluorescence. A 50x50 box was placed outside

the egg chamber for a dark signal reading, which was subtracted from all values. Values were then normalised to the oocyte cortex mean for each egg chamber, and the mean values of each region of 10 egg chambers per genotype used for statistical analysis with a two tailed t-test.

Appendix G: Supplementary movies legends

In all movies, the playback speed is limited to 20fps. The rate of acquisition varies in some of the movies, giving the appearance of faster or slower moving particles in some instances. Orientation of egg chambers is noted in the figure legends.

Supplementary movies are on a USB flash drive at the back of the Thesis.

Chapter 3

Movie 3-1: *grk* particles are visible in the nurse cells of *grk*GFP* egg chambers

Small, bright, highly motile puncta are visible in the nurse cells of *grk*GFP* egg chambers. Static, paused, and actively transported *grk* particles are visible (note the particle undergoing a long run and looping back on itself from 2s onwards). This movie is a magnified view of the nurse cells and does not show the oocyte. Image series is deconvolved. Movie acquired at 3fps and played back at 20fps.

Movie 3-2: *grk* particles in the oocyte are brighter than those in the nurse cells

In *grk*GFP* egg chambers, individual particles in the nurse cells are less bright than particles in the oocyte. The contrast has been increased to highlight the nurse cell particles, which has caused signal saturation (white regions) at areas of high *grk* density in the oocyte. Posterior (oocyte) is oriented to the left, dorsal to the bottom. Image series is deconvolved. Movie acquired at 3fps and played back at 20fps.

Movie 3-3: Particles are not visible in the nurse cells of *MCP-GFP* egg chambers

In egg chambers expressing only *MCP-GFP* (in this instance 2 copies) no bright, small puncta are visible in the nurse cells. Large, slow moving assemblies are visible, particularly around the nurse cell nuclei. This movie is a magnified view of the nurse cells and does not show the oocyte. Image series is deconvolved, and has been contrasted for best display. Movie acquired at 3fps and played back at 20fps.

Movie 3-4: *grk* particles are visible in the nurse cells of *grk*mCherry* egg chambers

Small, bright, highly motile puncta are visible in the nurse cells of *grk*mCherry* egg chambers. Although these particles are visible, they are significantly harder to visualise than those in *grk*GFP* egg chambers, and visualising particles undergoing long runs is more challenging. Posterior (oocyte) is oriented to the top. Image series is deconvolved. Movie acquired at 3fps and played back at 20fps.

Movie 3-5: Particles are not visible in the nurse cells of *MCP-mCherry* egg chambers

In egg chambers expressing only *MCP-mCherry* no bright, small puncta are visible in the nurse cells. Large, slow moving assemblies are visible, particularly around the nurse cell nuclei. This movie is a magnified view of the nurse cells and does not show the oocyte. Image series is deconvolved, and has been contrasted for best display. Movie acquired at 3fps and played back at 20fps.

Movie 3-6: *osk* particles are visible in the nurse cells of *osk*GFP* egg chambers

Small, bright, highly motile puncta are visible in the nurse cells of *osk*GFP* egg chambers. Static, paused, and actively transported *osk* particles are visible. There appears to be a higher density of *osk* particles than *grk* particles in the nurse cell cytoplasm, and there are far more static particles. Many of these static particles are enriched in areas around the nurse cell nuclei. This movie is a magnified view of the nurse cells and does not show the oocyte. Image series is deconvolved. Movie acquired at 3fps and played back at 20fps.

Movie 3-7: *osk* particles are visible in the nurse cells of *osk*mCherry* egg chambers

Small, bright, highly motile puncta are visible in the nurse cells of *osk*mCherry* egg chambers. These particles are significantly harder to visualise than those in *osk*GFP* egg chambers, and there are many large fluorescent assemblies of MCP-mCherry in the nurse cell cytoplasm. This movie is a magnified view of the nurse cells and does not show the oocyte. Image series is deconvolved. Movie acquired at 3fps and played back at 20fps.

Movie 3-8: *grk* dynamics in nurse cells visualised using the OMX

Using the OMX V3, *grk* particles can be readily visualised with high contrast in the nurse cell cytoplasm. Some particles are visible undergoing long runs (bottom left and top left). However, the image bleaches quickly and the signal rapidly deteriorates. This movie is a magnified view of the nurse cells and does not show the oocyte. Image series is deconvolved. Movie acquired at 15fps and played back at 15fps. The particles in this movie appear to be moving much slower because of the higher rate of acquisition.

Movie 3-9: *grk*mCherry* fluorescence bleaches quickly on the OMX V3

Using the OMX V3, particles of *grk*mCherry* can be visualised in the oocyte, but this fluorescence bleaches extremely quickly (in this case signal is completely lost by 3s and is effectively lost within 1s). Posterior (oocyte) is oriented to the top right. Image series is deconvolved and is a 1μm maximum intensity projection. Movie acquired at 5fps and played back at 20fps.

Movie 3-10: Many *grk* particles are visible in the nurse cell nuclei in *grk*GFP-24* egg chambers

In early stage *grk*GFP-24* egg chambers (stage 6 shown here), large numbers of *grk* particles, some of which are as bright or brighter than those in the oocyte, are visible in the nurse cell nuclei. Some *grk* mRNA is still visible in the oocyte, but appear to be at a lower density than in *grk*GFP* egg chambers. Posterior (oocyte) is oriented to the left. Image series is deconvolved. Movie acquired at 3fps and played back at 13fps.

Movie 3-11: Few *grk* particles are visible in the nurse cell nuclei in *grk*GFP* egg chambers

In early stage *grk*GFP* egg chambers (stage 6 shown here), *grk* particles are visible in the nurse cell cytoplasm and the oocyte, but few particles are visible in the nurse cell nuclei. This movie is equally contrasted to Movie 3-10. Posterior (oocyte) is oriented to the bottom. Image series is deconvolved. Movie acquired at 3fps and played back at 13fps.

Movie 3-12: *grk* particles which are exported from the nurse cell nuclei in *grk*GFP-24* egg chambers do localise to the oocyte DA corner

In later stage *grk*GFP-24* egg chambers (stage 9 shown here), some *grk* particles do localise to the DA corner. However, this is far fewer than in *grk*GFP* egg chambers. Note the high density of *grk* particles in the nurse cell nucleus (top right), which is not seen in *grk*GFP* egg chambers. The large, bright fluorescent objects in the oocyte are autofluorescent yolk particles. Posterior (oocyte) is oriented to the bottom left, dorsal (oocyte nucleus) to the bottom right. Image series is deconvolved. Movie acquired at 3fps and played back at 13fps.

Movie 3-13: There is a high density of *grk* particles localised to the DA corner of the oocyte in *grk*GFP* egg chambers

In later stage *grk*GFP* egg chambers (stage 9 shown here), the majority of *grk* particles localise to the DA corner of the oocyte. Note the absence of particles in the nurse cell nucleus (top right) at this late stage. The large, bright fluorescent objects in the oocyte are autofluorescent yolk particles. Posterior (oocyte) is oriented to the left, dorsal (oocyte nucleus) to the top. This movie is equally contrasted to movie 3-12. Image series is deconvolved. Movie acquired at 3fps and played back at 13fps.

Movie 3-14: *grk* particles are more difficult to visualise using *td-MCP-GFP* constructs

Particles are visible in the oocyte of *grk*tdGFP* egg chambers, but they are less bright than those in *grk*GFP* egg chambers. No particles are visible in the nurse cells of these egg chambers. Posterior (oocyte) is oriented to the left, dorsal (oocyte nucleus) to the top. Image series is deconvolved. Movie acquired at 3fps and played back at 18fps.

Movie 3-15: The number of fluorescent assemblies is increased in *td-MCP-GFP* expressing egg chambers

Numerous bright, large assemblies of td-MCP-GFP protein are visible in the nurse cell cytoplasm of *td-MCP-GFP* egg chambers. Posterior (oocyte) is oriented to the left. Image series is deconvolved. Movie acquired at 3fps and played back at 20fps.

Chapter 5

Movie 5-1: Me31B particles are highly dynamic in the nurse cell cytoplasm

Me31B particles can be seen moving in the nurse cell cytoplasm of *Me31B::GFP* egg chambers. Static, paused, and actively transported Me31B particles are visible, as well as large foci. Note the less dynamic particles in the oocyte and at the oocyte DA corner. Posterior (oocyte) is oriented to the bottom left, dorsal (oocyte nucleus) to the bottom right. Image series is deconvolved. Movie acquired at 3fps and played back at 20fps.

Movie 5-2: Me31B assemblies move through ring canals

Large Me31B assemblies can be seen moving through a ring canal (centre left) at speeds not indicative of active transport. Note that particles which move through the ring canal appear to move rapidly out of the Z plane as they are picked up by the cytoplasmic streaming/seething. Posterior (oocyte) is oriented to the left, dorsal (oocyte nucleus) to the top. Movie acquired at 1 frame/30s and played back at 9fps.

Movie 5-3: Growl assemblies move through ring canals

Large Growl assemblies can be seen moving through two ring canals at speeds not indicative of active transport. Note that most particles which move through the ring canal move rapidly out of the Z plane as they are picked up by the cytoplasmic

streaming/seething, although some can be seen moving with the cytoplasmic flow. Posterior (oocyte) is oriented to the left, dorsal (oocyte nucleus) to the top. Movie acquired at 1 frame/30s and played back at 9fps.

Movie 5-4: Me31B particles can be visualised using the OMX V3

All classes of Me31B particles (Static, paused, and actively transported Me31B particles are visible, as well as large foci). *Me31B::GFP* labelled particles are very bright and photostable, and so can be imaged over multiple Zs for long time courses. (this movie is 43s long). Posterior (oocyte) is oriented to the top. Image series is deconvolved and is a 4μm maximum intensity projection. Movie acquired at 7fps and played back at 20fps.

Movie 5-5: Me31B particle motility it abolished in egg chambers from Colcemid fed females

When females are fed with Colcemid, particles in the nurse cells are completely static. Note the increase in number of large bodies, most likely due to Me31B aggregation under nutrient stress. Posterior (oocyte) is oriented to the bottom right. Image series is deconvolved. Movie acquired at 7fps and played back at 20fps.

Movie 5-6: Me31B particle motility it normal in egg chambers from control fed females

When females are fed with yeast supplemented with the equivalent volume of ethanol to those treated with colcemid, motility of Me31B particles in the nurse cells is normal. Image series is deconvolved. Posterior (oocyte) is oriented to the top left. Image series is deconvolved. Movie acquired at 7fps and played back at 20fps.

Movie 5-7: Me31B particle motility in control, 24h fed egg chambers

Me31B particles in the nurse cells are dynamic in egg chambers from 2 day fed females. Posterior (oocyte) is oriented to the right, dorsal (oocyte nucleus) in the centre (image is taking from a dorsal view). Image series is deconvolved. Movie acquired at 3fps and played back at 20fps.

Movie 5-8: Me31B particle motility is abolished in starved egg chambers

Me31B particles in the nurse cells are no longer dynamic in egg chambers from stavred females. Posterior (oocyte) is oriented to the right, dorsal (oocyte nucleus) in the centre (image is taking from a dorsal view). Image series is deconvolved. Movie acquired at 3 fps and played back at 20fps.

Movie 5-9: Me31B particle motility is restored in 12 h re-fed egg chambers

Me31B particles motility in the nurse cells is restored in egg chambers from starved females which are re-fed on yeast for 12h. Posterior (oocyte) is oriented to the right, dorsal (oocyte nucleus) in the centre (image is taking from a dorsal view). Image series is deconvolved. Movie acquired at 3fps and played back at 20fps.

Movie 5-10: Vasa particles are dynamic in the nurse cells

In *Vasa-GFP* egg chambers, particles are visible undergoing long runs in the nurse cells. 3 particles can be visualised moving in a highly processive, unidirectional fashion along the same track in the folds in this nurse cell nucleus. This is a close up of one nurse cell nucleus. Image series is deconvolved. Movie acquired at 9fps and played back at 20fps.

Movie 5-11: Btz particles are dynamic in the nurse cells

In *Btz-GFP* egg chambers, particles are visible undergoing long runs in the nurse cells. 2 “strands” of particles are visible moving in a highly processive, unidirectional fashion along the same track in the folds in this nurse cell nucleus. Both can be seen moving from the central region of the nurse cell nuclear envelope (middle of frame) out into the nurse cell cytoplasm. One is moving from the top to the left, the other from the bottom to the right. This is a close up of one nurse cell nucleus. Image series is deconvolved. Movie acquired at 4fps and played back at 20fps.

Appendix H: Publications

Parton, R. M.*, **Davidson, A**.*, Davis, I., & Weil, T. T. (2014). Subcellular mRNA localisation at a glance. *Journal of Cell Science*, *127*(Pt 10), 2127–2133. doi:10.1242 jcs.114272

* These authors contributed equally to this work

© 2014. Published by The Company of Biologists Ltd | Journal of Cell Science (2014) 127, 2127–2133 doi:10.1242/jcs.114272

CELL SCIENCE AT A GLANCE

Subcellular mRNA localisation at a glance

Richard M. Parton[1,*], Alexander Davidson[1,*], Ilan Davis[1] and Timothy T. Weil[2,‡]

ABSTRACT

mRNA localisation coupled to translational regulation provides an important means of dictating when and where proteins function in a variety of model systems. This mechanism is particularly relevant in polarised or migrating cells. Although many of the models for how this is achieved were first proposed over 20 years ago, some of the molecular details are still poorly understood. Nevertheless, advanced imaging, biochemical and computational approaches have started to shed light on the cis-acting localisation signals and trans-acting factors that dictate the final destination of localised transcripts. In this Cell Science at a Glance article and accompanying poster, we provide an overview of mRNA localisation, from transcription to degradation, focusing on the microtubule-dependent active transport and anchoring mechanism, which we will use to explain the general paradigm. However, it is clear that there are diverse ways in which mRNAs become localised and target protein expression, and we highlight some of the similarities and differences between these mechanisms.

KEY WORDS: Cell Biology, Develoment, Polarity, mRNA

[1]Department of Biochemistry, University of Oxford, South Parks Road, Oxford OX1 3QU, UK. [2]Department of Zoology, University of Cambridge, Downing Street, Cambridge CB2 3EJ, UK.
*These authors contributed equally to this work

‡Author for correspondence (tw419@cam.ac.uk)

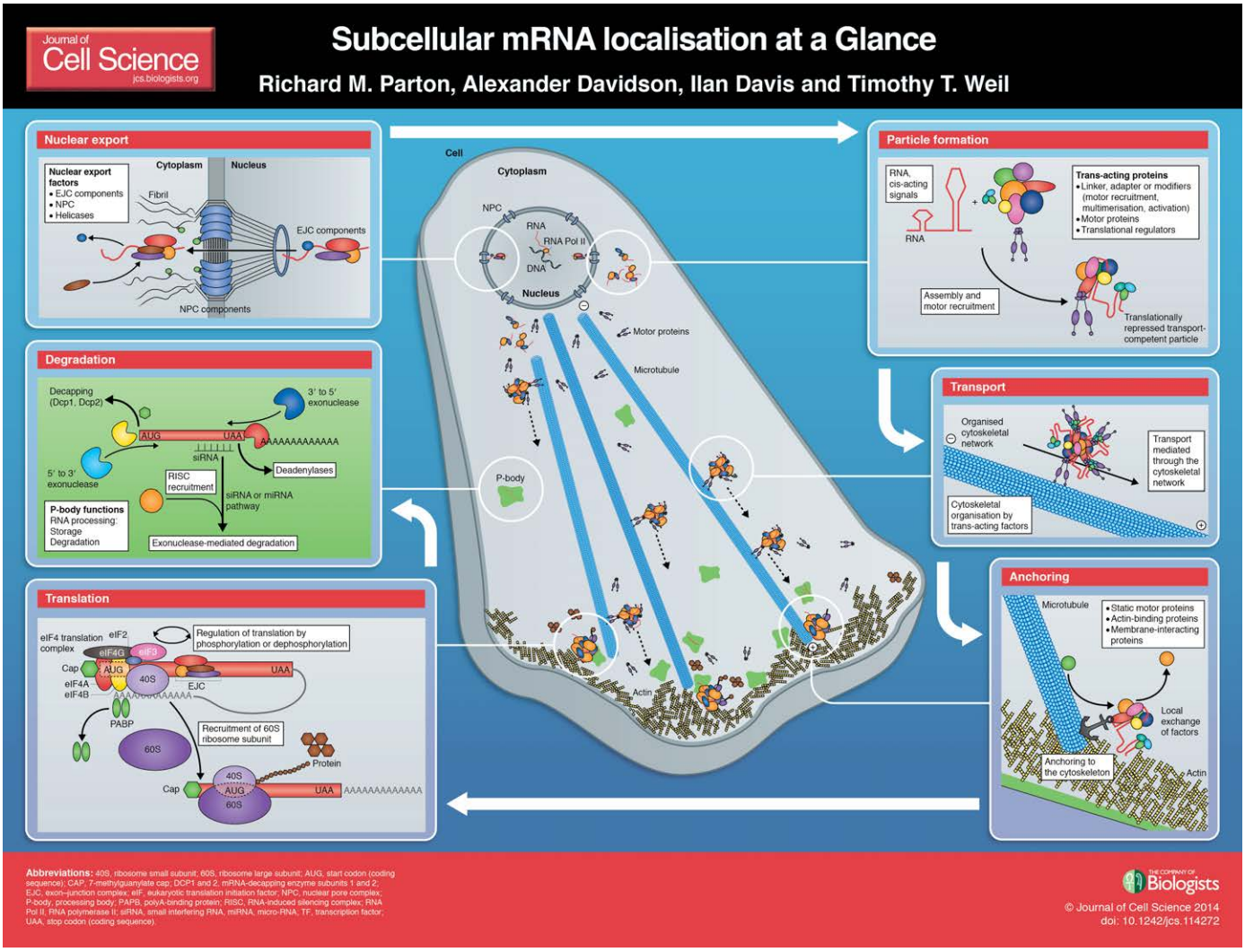

Journal of Cell Science

Journal of Cell Science (2014) 127, 2127–2133 doi:10.1242/jcs.114272

Introduction

mRNA localisation is a common and conserved means of targeting proteins to their site of function, and is important in a diverse range of cellular and developmental functions (reviewed in Medioni et al., 2012) with clear links to human diseases (Jeibmann et al., 2009).

Throughout their journey, mRNA transcripts never exist alone; they bind to a number of proteins to form mRNA–protein complexes, the ribonucleoprotein (RNP) complexes, (Box 1) (reviewed in Kato and Nakamura, 2012). Furthermore, as RNP complexes travel through the cell, there is evidence for dynamic remodeling of these complexes by different trans-acting protein factors that interact with regulatory cis-acting mRNA sequences (Otero et al., 2001). These interactions dictate the fate of mRNAs, so an understanding of these interactions is crucial for explaining the precise spatio-temporal control of localisation and translation. These biological processes have proven challenging to study because of the diversity of proteins and mRNA sequences involved. However, there has recently been significant progress owing to innovative experimental approaches (Box 2).

In this Cell Science at a Glance article and accompanying poster, we focus on localised coding mRNAs in polarised or migrating cells. Using a mechanism of 'active transport and anchoring' as a basis for comparison, we follow the fate of mRNA from nuclear export, particle formation (see Box 1), transport, anchoring, translation, to degradation (see poster), highlighting some of the recent exciting findings.

Nuclear export

mRNAs start their journey in the nucleus where they are transcribed from DNA (Shandilya and Roberts, 2012). Nascent transcripts are spliced, typically co-transcriptionally, to generate the coding mRNA in a process that removes introns, followed by the deposition of the exon–junction complex (EJC) and other components necessary for export and localisation (Baurén and Wieslander, 1994; Natalizio and Wente, 2013; Saulière et al., 2012). At this point, the emerging mRNAs associate, for the first time, with protein co-factors (Box 1) to form RNP complexes (Holt and Bullock, 2009; Natalizio and Wente, 2013).

A growing theme that emerges from the recent literature is that, even at this early stage, the association of localising mRNAs with proteins in the nucleus can dictate their future fate. First, recent work on the EJC suggests that the formation of RNP multimers through interaction with other EJC complexes and with serine- and arginine-rich (SR) proteins plays a role in packaging mRNAs, and in preparing them for nuclear export (Singh et al., 2012). More generally, a host of protein associations is initiated co-transcriptionally in the nucleus and appears to change continually throughout the different stages of mRNA localisation (Marchand et al., 2012; Rodríguez-Navarro and Hurt, 2011; Tran et al., 2007; Trcek et al., 2010). The formation of RNP complexes is directed by specific regions (cis-acting domains), which typically comprise double-stranded secondary structures including hairpins, stem loops and bulges (Amrute-Nayak and Bullock, 2012; Hamilton et al., 2007; Patel et al., 2012; Wilhelm and Vale, 1993). Second, alternative splicing can redefine or shuffle these cis-acting sequences to generate RNP complexes with varying trans-acting protein composition that dictates differential fates of mRNAs (Horne-Badovinac and Bilder, 2008; Trcek et al., 2010). Third, direct interactions of RNP complexes with the nuclear pore complex (NPC) can be essential for the formation of an export- and localisation-competent RNP complex. For example in *Saccharomyces cerevisiae*, mutants for the nucleoporin protein Nup60p, fail to export *ASH1* mRNA from the nucleus and transcripts that are exported do not localise correctly (Powrie et al., 2011).

Once mRNAs are spliced, RNP complexes become export competent through the addition of further co-factors and diffuse through the interchromatin spaces in the nucleoplasm to the NPC (Mor et al., 2010). At the NPC, a conserved and highly complicated structure, they are exported through interactions with co-factors such as nuclear RNA export factor 1 and NTF2-related export protein 1 (NXF1 and NXT1, respectively) and the transcription export complex (TREX), which are essential for nuclear export (Natalizio and Wente, 2013; Rodríguez-Navarro and Hurt, 2011; Valkov et al., 2012). In *Drosophila* embryos and rat myoblasts, the export path has been shown to be random (Politz et al., 2003; Wilkie and Davis, 2001). However, the exact routes taken by RNP complexes remains an area of debate and may indeed be polarised with respect to the cell. Recent breakthroughs achieved by using 'super registration' fluorescence microscopy approaches, which allow a direct visualisation of mRNA export in transgenic mouse cell lines (Grünwald and Singer, 2010), show that not all nuclear pores are equally active at

Box 1. Particle formation

Biochemical and genetic studies have shown how, for localising mRNAs, particular proteins determine each step of their journey (reviewed in Kato and Nakamura, 2012). Although a diverse array of proteins are involved, these trans-acting factors can be grouped into several classes (see poster).

Understanding the interaction between cis- and trans-acting components, RNP complex composition and remodeling are crucial for understanding the molecular mechanisms underlying mRNA localisation (Otero et al., 2001). Assembly of the multiple proteins required for regulating the translational state of the mRNA has been shown to involve numerous sites of weak interaction and involve modification of the mRNA folding (Chao et al., 2010; St Johnston, 2005). One of the intriguing questions is how the composition of the RNP complexes confers the specific fates of different mRNAs. Although there is evidence that different mRNAs with the same destination are packaged and transported together in the same RNP complex (Lange et al., 2008), it was hypothesised that particles with distinct destinations can be distinguished by certain trans-acting factors that are specific for the particular destination (Cha et al., 2001). It has been difficult to confirm this hypothesis because many mRNA binding proteins associate with a wide range of different transcripts; for example, the highly conserved double-stranded RNA (dsRNA)-binding protein Staufen (Stau) associates with both *oskar (osk)* and *bicoid (bcd)* mRNA in *Drosophila* oocytes (Ephrussi et al., 1991; St Johnston et al., 1989). This notion is further complicated by evidence from biochemical analysis such as the 'atlas' of mammalian mRNA-interacting proteins, which has revealed the enormous diversity of trans-acting factors (Castello et al., 2012).

These complex data suggest an alternative view of the specificity of RNP complexes, in that their flexibility in regulating transcripts is based on an unique complement of overlapping cofactors for each mRNA species (Castello et al., 2012; Castello et al., 2013; Kato and Nakamura, 2012; McDermott et al., 2012). A major remaining question is what precise combination of factors is required for the correct localization and translational regulation of each mRNA species, and how this is modified during the life cycle of the transcripts.

Journal of Cell Science (2014) 127, 2127–2133 doi:10.1242/jcs.114272

Box 2. Imaging techniques to study mRNA localisation

Early studies of mRNA localisation were reliant upon *in situ* hybridisation in fixed material, a slow and laborious method. Recent advances in fluorescent *in situ* hybridisation (FISH) now allow the rapid labeling of single mRNA molecules with high sensitivity and selectivity (Buxbaum et al., 2014; Little et al., 2011). FISH has also been applied to live cells (Santangelo et al., 2009). However, despite these improvements, *in situ* hybridisation remains limited in its application to certain tissues. An alternative approach to label mRNA in live cells is through injection of *in vitro* synthesized RNA that incorporates fluorescent dyes. By using this technique, it has been possible to rapidly screen a range of mutated RNAs to determine the crucial cis-acting sequences that determine mRNA localisation in *Drosophila* embryos and oocytes (Bullock and Ish-Horowicz, 2001; Van De Bor et al., 2005).

A breakthrough in live imaging that also emerges as one of the most useful approaches for *in vivo* study of mRNA localisation is the MS2 bacteriophage RNA stem loop bound by MS2 coat protein fusion to a fluorescent protein (MS2-MCP system). It was originally developed in yeast (Bertrand et al., 1998) but has since been extended to several organisms, including *Drosophila* (Forrest et al., 2003), *Mus musculus* (Park et al., 2014), *Xenopus* (Gagnon et al., 2013) and plants (Hamada et al., 2003). It has also been used to detect nascent mRNA as it is transcribed (Hocine et al., 2013; Yunger et al., 2013). Improvements are directed towards maximising the detection of mRNAs, such as by increasing the number and optimisation of MS2 loops (Lionnet et al., 2011). An alternative construct uses the bacteriophage PP7 and also involves the interaction between a stem loop and a viral coat protein (Wu et al., 2012). Using the MS2 and PP7 systems in combination might allow the tracking of two different species of mRNAs simultaneously and could provide insights into how transcripts segregate.

However, one limitation of the MS2 and PP7 systems is the potential lack of contrast caused by unbound MCP. This may be overcome by targeting MCP to the nucleus (Bertrand et al., 1998), although this would compromise the ability to follow mRNAs in and around the nucleus. Recently, a combination of MS2 and PP7 has been described that drives a highly specific split-fluorescent protein complementation on the mRNA and allows for high-contrast labeling of individual transcripts (Hocine et al., 2013).

Furthermore, different tissues present different challenges for imaging approaches, which could be addressed by using advances in imaging techniques. For instance, fast, sensitive widefield microscopy is useful when imaging fast-moving mRNA particles (Zimyanin et al., 2008), whereas when imaging within thick samples, such as *Drosophila* embryos, multi-photon microscopy can be useful (Sinsimer et al., 2013). Total internal reflection microscopy (TIRF) is ideal for *in vitro* applications because of its high axial resolution (Amrute-Nayak and Bullock, 2012), whereas 3D structured illumination microscopy (3D-SIM) gives axial and lateral super-resolution while being flexible enough to be applied when investigating conventionally prepared materials (Weil et al., 2010a).

the same time. Furthermore, mRNAs were shown to move bidirectionally through the pores, with docking at and release from the nuclear pore being the rate-limiting steps, rather than translocation through the channel. There is also evidence that translocation of a large RNP complex through a channel of limited diameter is facilitated by RNA helicases, which are essential for nuclear export and mRNA quality control (reviewed in Valkov et al., 2012), and can specifically interact with nucleoporins and promote mRNA remodeling (Montpetit et al., 2011).

Interestingly, export through the NPC is not the only path to the cytoplasm. Recently, an alternative mechanism has been discovered in the *Drosophila* neuromuscular junction where large RNP complexes exit the nucleus through vesicular budding (Jokhi et al., 2013; Speese et al., 2012), a process thought to be utilized by some DNA viruses. Regardless of the underlying mechanism, once the mRNA has arrived at the cytoplasmic face of the nucleus, it is ready for the next phase of its journey.

Transport and anchoring

Early studies of mRNA transport in the cytoplasm focused on the overall localisation of transcripts through the visualisation of endogenous mRNA by *in situ* hybridisation (Jeffery et al., 1983; Lawrence and Singer, 1986; Weil et al., 2010a). The subsequent development of the MS2 bacteriophage RNA stem loop bound by MS2 coat protein fusion to a fluorescent protein (MS2-MCP system) and recent imaging advances (see Box 2) combined with the use of mutants that affect transacting protein factors, motors and the cytoskeleton, and also drug treatments, showed that different mRNAs localise by means of different mechanisms (Bertrand et al., 1998; Forrest et al., 2003; Jaramillo et al., 2008; Lerit and Gavis, 2011; Medioni et al., 2012; Takatori et al., 2010). For example, in late *Drosophila* oogenesis, *bicoid* (*bcd*) is localised by active transport and *nanos* (*nos*) is localised by means of diffusion and trapping (Forrest et al., 2003; Weil et al., 2006). Biochemical experiments have supported and expanded our understanding of the trans-acting factors that are required for the regulation of these processes (McDermott et al., 2012; Müller et al., 2011; Snee et al., 2005). The classic view of RNP complexes is that they are composed of higher order mRNA complexes. This certainly appears to be the case for *oskar* (*osk*) mRNA, where multiple mRNA particles associate with each other to form large transport particles or granules (Chekulaeva et al., 2006; Kato and Nakamura, 2012). However, recent research following individual mRNAs indicates that oligomerisation is not obligatory for transport (Amrute-Nayak and Bullock, 2012). In this section, we focus primarily on the current understanding of mRNA localisation along microtubules by means of active motor-dependent transport in polarised cells. This is exemplified by the classic axis-determining mRNAs in *Drosophila* that move on microtubule tracks, with kinesin transporting *osk* mRNA in the plus-end direction and dynein driving *gurken* (*grk*) mRNA transport to the microtubule minus end (MacDougall et al., 2003; Zimyanin et al., 2008).

An essential requirement for localisation is the linkage of the correct motor to the cargo and the connection of this complex to the cytoskeleton. Bicaudal-D (BicD) and Egalitarian (Egl) are two linkers with key roles in axis determination in *Drosophila* oocytes and embryos (Mach and Lehmann, 1997; Bullock and Ish-Horowicz, 2001; Navarro et al., 2004). Egl directly binds to different cis-acting elements that mediate mRNA localisation and BicD regulates the linkage of mRNA cargo to dynein. A recent study provides insight into the molecular mechanism of motor protein recruitment by solving the crystal structure of the cargo-binding domain of BicD (Liu et al., 2013), which shows that cargo binds to the homotypic domain of BicD and releases the auto inhibition of its heterotypic coiled-coil domain, thus allowing this domain to bind to dynein.

Journal of Cell Science (2014) 127, 2127–2133 doi:10.1242/jcs.114272

Work *in vitro* has suggested that the number of motors that are recruited to an RNP complex can be controlled by cis-acting localisation elements in the mRNA (Amrute-Nayak and Bullock, 2012). Similarly, recruitment of multiple copies of the class V myosin Myo4 by She2 has been shown to enhance transport of *ASH1* mRNA along actin in *S. cerevisiae* (Chung and Takizawa, 2010). Additional levels of regulating transport efficiency also exist, for instance mediated by proteins such as Pat1, which interacts with cargo adaptors to regulate the motility of kinesin heavy chain on microtubules and is necessary for *osk* mRNA localisation (Loiseau et al., 2010). The microtubule-associated protein (MAP) ensconsin interacts with microtubules and kinesin-1 to increase efficiency of motor recruitment (Sung et al., 2008). This is different to typical MAPs, which affect cytoskeletal stability and organisation.

The classic model of mRNA localisation poses that it is underpinned by a highly polarised cytoskeletal network (Clark et al., 1994). This model predicts that mRNAs exhibit a concerted directional motion. However, research on the dynamics of RNP complexes often shows a non-uniform rather than continuous, processive movement (Sinsimer et al., 2013). One explanation for this is that the dynein motor is capable of reversing direction (Gross, 2004). Another explanation comes from recent *in vivo* and *in vitro* analysis that has shown that individual mRNA cargos can undergo bidirectional movement owing to transport by multiple motors. In the case of *Vg1* mRNA in frogs, there are different phases of transport during localisation. An initial highly unidirectional dynein-dependent phase is followed by multiple rounds of bidirectional transport for which kinesin-1, kinesin-2 and dynein are required, before transcripts are anchored at the vegetal cortex (Gagnon et al., 2013).

In *Drosophila* oocytes, live imaging of *osk* mRNA and visualisation of microtubules using green fluorescent protein (GFP) tagged to end-binding protein 1 (EB1) revealed an apparently random organisation with subtle bias towards the posterior, rather than the expected highly polarised cytoskeletal network (Parton et al., 2011; Zimyanin et al., 2008). Additional control of transport can be mediated through the regulation of the properties of the tracks themselves (Gardner et al., 2011), such as regulating the extension and catastrophic collapse of microtubules.

Once the mRNA has reached its destination, anchoring is a common mechanism for maintaining mRNA localisation. For example *grk* mRNA is anchored by dynein at the *Drosophila* oocyte dorsal anterior corner, whereas *nos* mRNA that is diffusing in the ooplasm is trapped by actin at the posterior pole (Delanoue et al., 2007; Forrest et al., 2003). In *Xenopus*, *Vg1* mRNA is maintained at the vegetal pole of the oocyte by the actin cytoskeleton (Yisraeli et al., 1990).

Actin has also been implicated in the organisation and function of the microtubule cytoskeleton and has been demonstrated to be of particular importance for the localisation of *bicoid* mRNA (Weil et al., 2010b) and in organising a polarised microtubule cytoskeleton in the *Drosophila* oocyte (Dahlgaard et al., 2007). Actin can also function as a track on which cargoes can be transported. Here, actin not only acts in the short-range localisation of mRNAs, as is the case for *ASH1* mRNA in yeast (Bertrand et al., 1998), but also in long-range vesicle transport in mouse oocytes (Schuh et al., 2011; reviewed in St Johnston, 2005). Together, these examples demonstrate that there is no clear universal mechanism for mRNA transport. The future challenge is to understand to what extent the differential localisation of mRNA species is achieved through distinct transport mechanisms that operate in parallel.

Translation

For effective localised protein expression, mRNAs are kept translationally silent during transport and are activated for translation when they are anchored at their destination. Cis-acting mRNA sequences are almost certainly responsible for both the translational repression of mRNAs and their activation by directing their interaction with trans-acting proteins. Several strategies have been proposed, including the binding of factors that block or mask the interaction of translational activators, either by sequestering these translation activation factors or by occupying their interaction sites on the mRNA. These factors could either physically restrict the access of the translational machinery or act by regulating the length of the poly(A)-tail on the transcripts, whose extension is known to precede translational activation (Rosenthal et al., 1983).

One of the best-studied mechanisms of translational repression involves the eukaryotic translation initiation factor 4E (eIF4E) pathway (Jackson et al., 2010). In this repression pathway, mRNAs are prevented from initiating translation that requires the recruitment of the 40S ribosomal subunit through assembly of eIF4F (eIF4G+eIF4E and eIF4A) at the 5′ cap. Translational repressors can bind directly to the mRNA, thus masking the sites for eIF4E binding. For example, the *Drosophila* protein Bruno interacts with Bruno-response elements on mRNA, thus blocking initiation of translation (Kim-Ha et al., 1995). Alternatively, factors such as the *Drosophila* ovarian protein Cup can bind eIF4E and prevent it from accessing mRNA, thereby inhibiting initiation of translation (Chekulaeva et al., 2006; Nakamura et al., 2004; Piccioni et al., 2005; Wilhelm et al., 2003). Overexpression of eIF4E has been shown to lead to autism-like behavior in mice (Santini et al., 2013), and HIV-1 was shown to be able to maintain virus-specific protein synthesis when eIF4E is downregulated (Sharma et al., 2012). This demonstrates that eIF4E-mediated translational repression is important in a range of cells and circumstances.

A further well-characterised means of controlling the level of proteins synthesis from mRNA is through polyadenylation or deadenylation. In frogs and flies, there are many examples of cytoplasmic polyadenylation elements (CPEs) that reside in the 3′ UTR of mRNA, which are bound by the CPE-binding protein (CPEB) to control translation (Chang et al., 1999; Christerson and McKearin, 1994; Hake and Richter, 1994; Radford et al., 2008). Recently, work in the hippocampus of mice has shown that mutants in which the translational repressor of poly(A)-binding protein (PABP) has been knocked out show an increased translation of Ca^{2+}/calmodulin-dependent protein kinase II alpha (*Camk2a*) mRNA, a factor involved in many signaling cascades that are regulated by Ca^{2+}. Translational activation through the release of PABP-dependent repression has been demonstrated following electrode stimulation and is important for synaptic plasticity and learning (Khoutorsky et al., 2013).

Mouse models have also highlighted the complexity of translational regulation and revealed new means by which kinase activity regulates mRNA translation. For instance, the mouse protein kinase R (PKR)-like endoplasmic reticulum kinase (PERK, also known as EIF2AK3) has been shown to have a key role in brain function by phosphorylating eIF2α (also known as EIF2A), a key regulator of translational activity (Trinh et al., 2012). A unique level of intricacy has been shown to be provided

Journal of Cell Science (2014) 127, 2127–2133 doi:10.1242/jcs.114272

by the interaction of fragile X mental retardation 1 (FMRP, also known as FMR1) protein and the human topoisomerase 3-beta-1 (Top3β, also known as TOP3B) (Xu et al., 2013), as this complex appears to regulate multiple mRNAs in neurons and – in Top3β mutants – there is a reduction in the expression of genes within the neuromuscular junction (NMJ) that are important for neural function. In addition to FMRP, other RNA-binding proteins found in the *Drosophila* nervous system, such as Syncrip (Syp) and Staufen (Stau), have distinct roles in regulation mRNA translation in other stages of development (McDermott et al., 2012; Barbee et al., 2006).

Although non-coding RNAs are thought to primarily have a role in mRNA degradation (see following section), an additional role is emerging in translational regulation. In flies, a reversible mechanism for regulating gene expression through the pathway via microRNA (miRNA) and argonaute 2 (AGO2) (Muddashetty et al., 2011) involves the phosphorylation of *Drosophila* FMR1 at the synapse. The direct targeting of precursor miRNA – a long piece of double-stranded RNA (dsRNA) from which mature miRNAs are generated – to neuronal dendrites has been shown to be mediated by the DEAH-box helicase 36 (DHX36), suggesting that the localisation of precursor miRNA is an important plasticity mechanism (Bicker et al., 2013). Interestingly, an miRNA-independent mechanism for the recruitment of Argonaute-1 (AGO1) to nanos (*nos*) mRNA in the *Drosophila* early embryo has been described that acts through the smaug protein, suggesting that there are different mechanisms of translational regulation that most likely work in concert (Pinder and Smibert, 2013).

The recent characterisation of protein components that are involved in translational repression of mRNAs has revealed that the subcellular organisation of protein complexes contributes to efficient translational regulation (Balagopal and Parker, 2009). Processing bodies (P-bodies) are known locations of mRNA translational control and degradation and have, therefore, been referred to as hubs for RNA metabolism in yeast (Aizer et al., 2008; reviewed in Balagopal and Parker, 2009). It has recently been shown that they are also important in regulating developmentally relevant transcripts. We have also shown that it is important where exactly in P-bodies mRNAs localise because the inside of electron-dense P-bodies does not support translation, whereas their localisation at the P-body edge allows translation to occur (Weil et al., 2012). Other work from yeast suggests that P-bodies are also the place where mRNAs terminate their journey through the cell (Aizer et al., 2008; Brengues et al., 2005).

Degradation

The tight regulation of mRNAs in both space and time ultimately requires mRNA degradation. Although there are several pathways of degradation, the most common is through 5′ to 3′ exonuclease activity, following deadenylation and decapping (reviewed in Decker and Parker, 2012). In yeast, this process is linked with cytoplasmic P-bodies, which are associated with translationally repressed transcripts (Teixeira et al., 2005). These are distinct from stress granules, related cytoplasmic foci that have a similar composition and are likely to share functions. Stress granules assemble under physiological conditions when translation is stalled rather than repressed (Buchan and Parker, 2009). Interestingly, recent research indicates that mRNA can be degraded in a 5′ to 3′ fashion as translation is occurring (Hu et al., 2009), suggesting that the removal of ribosomes and the activity of exonucleases are not necessarily sequential events.

In *Drosophila*, P-body proteins have been found in neurons and oocytes, and have been suggested to be important for regulating transcripts (Barbee et al., 2006; Weil et al., 2012). In the case of *grk* mRNA, these bodies may be involved in regulating the level of transcripts and act as a dosage and temporal control, although degradation was not explicitly demonstrated in our study (Weil et al., 2012). An additional mechanism of mRNA degradation that is relevant for the control of spatially and temporally constrained transcripts is miRNA-mediated degradation. In the case of the maternal to zygotic transition in zebrafish and *Drosophila* embryos, maternal mRNAs are cleared from the embryo by miRNA-mediated deadenylation (Bushati et al., 2008; Giraldez et al., 2006).

Another mechanism of mRNA regulation is at the level of the DNA sequence, which can affect mRNA levels through the control of decay rates. Recent evidence from yeast shows that DNA promoter elements can affect the decay kinetics of their respective mRNAs after nuclear export (Bregman et al., 2011).

The specific mechanisms that regulate the degradation of mRNA transcripts after their final localisation have yet to be extensively studied and, thus, the role of P-bodies as sites of degradation remains to be established, mainly owing to the difficulty in characterising these labile bodies and in observing their interactions with mRNA.

Perspectives

New imaging technologies, bioinformatics and biochemistry have facilitated major advances in our understanding of the composition, motility and translational regulation of RNP complexes. One successful example of these applications is in the analysis of RNP complex composition of nascent transcripts as they are being processed during splicing in the nucleus and at the NPC.

However, many important questions in the field remain unanswered, such as what is the extent of RNP complex remodeling in the cytoplasm and how is it regulated? How prevalent is the function of small non-coding RNA in the translational regulation of mRNAs? Do the numerous regulatory mechanisms facilitate the localisation of diverse transcripts or are they redundant mechanisms to protect crucial biological processes? The challenge will be to place the biochemical information with regard to the components that are involved in the context of *in vivo* data to fully understand the molecular mechanism of mRNA localisation with respect to cell and tissue function.

Acknowledgements

We are grateful to Russell Hamilton and David Ish-Horowicz for critical reading of the manuscript.

Competing interests

The authors declare no competing interests.

Funding

This work was supported by a Wellcome Trust Senior Research Fellowship to I.D. supporting R.M.P. [grant number: 096144], a studentship from the Wellcome Trust to A.D. [grant number: 097304], the University of Cambridge, ISSF to T.T.W. [grant number 097814]. Deposited in PMC for immediate release.

Cell science at a glance

A high-resolution version of the poster is available for downloading in the online version of this article at jcs.biologists.org. Individual poster panels are available as JPEG files at http://jcs.biologists.org/lookup/suppl/doi:10.1242/jcs.114272/-/DC1.

Journal of Cell Science (2014) 127, 2127–2133 doi:10.1242/jcs.114272

References

Aizer, A., Brody, Y., Ler, L. W., Sonenberg, N., Singer, R. H. and Shav-Tal, Y. (2008). The dynamics of mammalian P body transport, assembly, and disassembly in vivo. *Mol. Biol. Cell* **19**, 4154-4166.

Amrute-Nayak, M. and Bullock, S. L. (2012). Single-molecule assays reveal that RNA localization signals regulate dynein-dynactin copy number on individual transcript cargoes. *Nat. Cell Biol.* **14**, 416-423.

Balagopal, V. and Parker, R. (2009). Polysomes, P bodies and stress granules: states and fates of eukaryotic mRNAs. *Curr. Opin. Cell Biol.* **21**, 403-408.

Barbee, S. A., Estes, P. S., Cziko, A.-M., Hillebrand, J., Luedeman, R. A., Coller, J. M., Johnson, N., Howlett, I. C., Geng, C., Ueda, R. et al. (2006). Staufen- and FMRP-containing neuronal RNPs are structurally and functionally related to somatic P bodies. *Neuron* **52**, 997-1009.

Baurén, G. and Wieslander, L. (1994). Splicing of Balbiani ring 1 gene pre-mRNA occurs simultaneously with transcription. *Cell* **76**, 183-192.

Bertrand, E., Chartrand, P., Schaefer, M., Shenoy, S. M., Singer, R. H. and Long, R. M. (1998). Localization of ASH1 mRNA particles in living yeast. *Mol. Cell* **2**, 437-445.

Bicker, S., Khudayberdiev, S., Weiß, K., Zocher, K., Baumeister, S. and Schratt, G. (2013). The DEAH-box helicase DHX36 mediates dendritic localization of the neuronal precursor-microRNA-134. *Genes Dev.* **27**, 991-996.

Bregman, A., Avraham-Kelbert, M., Barkai, O., Duek, L., Guterman, A. and Choder, M. (2011). Promoter elements regulate cytoplasmic mRNA decay. *Cell* **147**, 1473-1483.

Brengues, M., Teixeira, D. and Parker, R. (2005). Movement of eukaryotic mRNAs between polysomes and cytoplasmic processing bodies. *Science* **310**, 486-489.

Buchan, J. R. and Parker, R. (2009). Eukaryotic stress granules: the ins and outs of translation. *Mol. Cell* **36**, 932-941.

Bullock, S. L. and Ish-Horowicz, D. (2001). Conserved signals and machinery for RNA transport in Drosophila oogenesis and embryogenesis. *Nature* **414**, 611-616.

Bushati, N., Stark, A., Brennecke, J. and Cohen, S. M. (2008). Temporal reciprocity of miRNAs and their targets during the maternal-to-zygotic transition in Drosophila. *Curr. Biol.* **18**, 501-506.

Buxbaum, A. R., Wu, B. and Singer, R. H. (2014). Single β-actin mRNA detection in neurons reveals a mechanism for regulating its translatability. *Science* **343**, 419-422.

Castello, A., Fischer, B., Eichelbaum, K., Horos, R., Beckmann, B. M., Strein, C., Davey, N. E., Humphreys, D. T., Preiss, T., Steinmetz, L. M. et al. (2012). Insights into RNA biology from an atlas of mammalian mRNA-binding proteins. *Cell* **149**, 1393-1406.

Castello, A., Horos, R., Strein, C., Fischer, B., Eichelbaum, K., Steinmetz, L. M., Krijgsveld, J. and Hentze, M. W. (2013). System-wide identification of RNA-binding proteins by interactome capture. *Nat. Protoc.* **8**, 491-500.

Cha, B. J., Koppetsch, B. S. and Theurkauf, W. E. (2001). In vivo analysis of Drosophila bicoid mRNA localization reveals a novel microtubule-dependent axis specification pathway. *Cell* **106**, 35-46.

Chang, J. S., Tan, L. and Schedl, P. (1999). The Drosophila CPEB homolog, orb, is required for oskar protein expression in oocytes. *Dev. Biol.* **215**, 91-106.

Chao, J. A., Patskovsky, Y., Patel, V., Levy, M., Almo, S. C. and Singer, R. H. (2010). ZBP1 recognition of beta-actin zipcode induces RNA looping. *Genes Dev.* **24**, 148-158.

Chekulaeva, M., Hentze, M. W. and Ephrussi, A. (2006). Bruno acts as a dual repressor of oskar translation, promoting mRNA oligomerization and formation of silencing particles. *Cell* **124**, 521-533.

Christerson, L. B. and McKearin, D. M. (1994). orb is required for anteroposterior and dorsoventral patterning during Drosophila oogenesis. *Genes Dev.* **8**, 614-628.

Chung, S. and Takizawa, P. A. (2010). Multiple Myo4 motors enhance ASH1 mRNA transport in Saccharomyces cerevisiae. *J. Cell Biol.* **189**, 755-767.

Clark, I., Giniger, E., Ruohola-Baker, H., Jan, L. Y. and Jan, Y. N. (1994). Transient posterior localization of a kinesin fusion protein reflects anteroposterior polarity of the Drosophila oocyte. *Curr. Biol.* **4**, 289-300.

Dahlgaard, K., Raposo, A. A. S. F., Niccoli, T. and St Johnston, D. (2007). Capu and Spire assemble a cytoplasmic actin mesh that maintains microtubule organization in the Drosophila oocyte. *Dev. Cell* **13**, 539-553.

Decker, C. J. and Parker, R. (2012). P-bodies and stress granules: possible roles in the control of translation and mRNA degradation. *Cold Spring Harb. Perspect. Biol.* **4**, a012286.

Delanoue, R., Herpers, B., Soetaert, J., Davis, I. and Rabouille, C. (2007). Drosophila Squid/hnRNP helps Dynein switch from a gurken mRNA transport motor to an ultrastructural static anchor in sponge bodies. *Dev. Cell* **13**, 523-538.

Ephrussi, A., Dickinson, L. K. and Lehmann, R. (1991). Oskar organizes the germ plasm and directs localization of the posterior determinant nanos. *Cell* **66**, 37-50.

Forrest, K. M. and Gavis, E. R. (2003). Live imaging of endogenous RNA reveals a diffusion and entrapment mechanism for nanos mRNA localization in Drosophila. *Curr. Biol.* **13**, 1159-1168.

Gagnon, J. A., Kreiling, J. A., Powrie, E. A., Wood, T. R. and Mowry, K. L. (2013). Directional transport is mediated by a Dynein-dependent step in an RNA localization pathway. *PLoS Biol.* **11**, e1001551.

Gardner, M. K., Zanic, M., Gell, C., Bormuth, V. and Howard, J. (2011). Depolymerizing kinesins Kip3 and MCAK shape cellular microtubule architecture by differential control of catastrophe. *Cell* **147**, 1092-1103.

Giraldez, A. J., Mishima, Y., Rihel, J., Grocock, R. J., Van Dongen, S., Inoue, K., Enright, A. J. and Schier, A. F. (2006). Zebrafish MiR-430 promotes deadenylation and clearance of maternal mRNAs. *Science* **312**, 75-79.

Gross, S. P. (2004). Hither and yon: a review of bi-directional microtubule-based transport. *Phys. Biol.* **1**, R1-R11.

Grünwald, D. and Singer, R. H. (2010). In vivo imaging of labelled endogenous β-actin mRNA during nucleocytoplasmic transport. *Nature* **467**, 604-607.

Hake, L. E. and Richter, J. D. (1994). CPEB is a specificity factor that mediates cytoplasmic polyadenylation during Xenopus oocyte maturation. *Cell* **79**, 617-627.

Hamada, S., Ishiyama, K., Choi, S.-B., Wang, C., Singh, S., Kawai, N., Franceschi, V. R. and Okita, T. W. (2003). The transport of prolamine RNAs to prolamine protein bodies in living rice endosperm cells. *Plant Cell* **15**, 2253-2264.

Hamilton, R. S. and Davis, I. (2007). RNA localization signals: deciphering the message with bioinformatics. *Semin. Cell Dev. Biol.* **18**, 178-185.

Hocine, S., Raymond, P., Zenklusen, D., Chao, J. A. and Singer, R. H. (2013). Single-molecule analysis of gene expression using two-color RNA labeling in live yeast. *Nat. Methods* **10**, 119-121.

Holt, C. E. and Bullock, S. L. (2009). Subcellular mRNA localization in animal cells and why it matters. *Science* **326**, 1212-1216.

Horne-Badovinac, S. and Bilder, D. (2008). Dynein regulates epithelial polarity and the apical localization of stardust A mRNA. *PLoS Genet.* **4**, e8.

Hu, W., Sweet, T. J., Chamnongpol, S., Baker, K. E. and Coller, J. (2009). Co-translational mRNA decay in Saccharomyces cerevisiae. *Nature* **461**, 225-229.

Jackson, R. J., Hellen, C. U. T. and Pestova, T. V. (2010). The mechanism of eukaryotic translation initiation and principles of its regulation. *Nat. Rev. Mol. Cell Biol.* **11**, 113-127.

Jaramillo, A. M., Weil, T. T., Goodhouse, J., Gavis, E. R. and Schupbach, T. (2008). The dynamics of fluorescently labeled endogenous gurken mRNA in Drosophila. *J. Cell Sci.* **121**, 887-894.

Jeffery, W. R., Tomlinson, C. R. and Brodeur, R. D. (1983). Localization of actin messenger RNA during early ascidian development. *Dev. Biol.* **99**, 408-417.

Jeibmann, A. and Paulus, W. (2009). Drosophila melanogaster as a model organism of brain diseases. *Int. J. Mol. Sci.* **10**, 407-440.

Jokhi, V., Ashley, J., Nunnari, J., Noma, A., Ito, N., Wakabayashi-Ito, N., Moore, M. J. and Budnik, V. (2013). Torsin mediates primary envelopment of large ribonucleoprotein granules at the nuclear envelope. *Cell Rep* **3**, 988-995.

Kato, Y. and Nakamura, A. (2012). Roles of cytoplasmic RNP granules in intracellular RNA localization and translational control in the Drosophila oocyte. *Dev. Growth Differ.* **54**, 19-31.

Khoutorsky, A., Yanagiya, A., Gkogkas, C. G., Fabian, M. R., Prager-Khoutorsky, M., Cao, R., Gamache, K., Bouthiette, F., Parsyan, A., Sorge, R. E. et al. (2013). Control of synaptic plasticity and memory via suppression of poly(A)-binding protein. *Neuron* **78**, 298-311.

Kim-Ha, J., Kerr, K. and Macdonald, P. M. (1995). Translational regulation of oskar mRNA by bruno, an ovarian RNA-binding protein, is essential. *Cell* **81**, 403-412.

Lange, S., Katayama, Y., Schmid, M., Burkacky, O., Bräuchle, C., Lamb, D. C. and Jansen, R.-P. (2008). Simultaneous transport of different localized mRNA species revealed by live-cell imaging. *Traffic* **9**, 1256-1267.

Lawrence, J. B. and Singer, R. H. (1986). Intracellular localization of messenger RNAs for cytoskeletal proteins. *Cell* **45**, 407-415.

Lerit, D. A. and Gavis, E. R. (2011). Transport of germ plasm on astral microtubules directs germ cell development in Drosophila. *Curr. Biol.* **21**, 439-448.

Lionnet, T., Czaplinski, K., Darzacq, X., Shav-Tal, Y., Wells, A. L., Chao, J. A., Park, H. Y., de Turris, V., Lopez-Jones, M. and Singer, R. H. (2011). A transgenic mouse for in vivo detection of endogenous labeled mRNA. *Nat. Methods* **8**, 165-170.

Little, S. C., Tkačik, G., Kneeland, T. B., Wieschaus, E. F. and Gregor, T. (2011). The formation of the Bicoid morphogen gradient requires protein movement from anteriorly localized mRNA. *PLoS Biol.* **9**, e1000596.

Liu, Y., Salter, H. K., Holding, A. N., Johnson, C. M., Stephens, E., Lukavsky, P. J., Walshaw, J. and Bullock, S. L. (2013). Bicaudal-D uses a parallel, homodimeric coiled coil with heterotypic registry to coordinate recruitment of cargos to dynein. *Genes Dev.* **27**, 1233-1246.

Loiseau, P., Davies, T., Williams, L. S., Mishima, M. and Palacios, I. M. (2010). Drosophila PAT1 is required for Kinesin-1 to transport cargo and to maximize its motility. *Development* **137**, 2763-2772.

MacDougall, N., Clark, A., MacDougall, E. and Davis, I. (2003). Drosophila gurken (TGFalpha) mRNA localizes as particles that move within the oocyte in two dynein-dependent steps. *Dev. Cell* **4**, 307-319.

Mach, J. M. and Lehmann, R. (1997). An Egalitarian-BicaudalD complex is essential for oocyte specification and axis determination in Drosophila. *Genes Dev.* **11**, 423-435.

Marchand, V., Gaspar, I. and Ephrussi, A. (2012). An intracellular transmission control protocol: assembly and transport of ribonucleoprotein complexes. *Curr. Opin. Cell Biol.* **24**, 202-210.

McDermott, S. M., Meignin, C., Rappsilber, J. and Davis, I. (2012). Drosophila Syncrip binds the gurken mRNA localisation signal and regulates localised transcripts during axis specification. *Biol. Open* **1**, 488-497.

Medioni, C., Mowry, K. and Besse, F. (2012). Principles and roles of mRNA localization in animal development. *Development* **139**, 3263-3276.

Montpetit, B., Thomsen, N. D., Helmke, K. J., Seeliger, M. A., Berger, J. M. and Weis, K. (2011). A conserved mechanism of DEAD-box ATPase activation by nucleoporins and InsP6 in mRNA export. *Nature* **472**, 238-242.
Mor, A., Suliman, S., Ben-Yishay, R., Yunger, S., Brody, Y. and Shav-Tal, Y. (2010). Dynamics of single mRNP nucleocytoplasmic transport and export through the nuclear pore in living cells. *Nat. Cell Biol.* **12**, 543-552.
Muddashetty, R. S., Nalavadi, V. C., Gross, C., Yao, X., Xing, L., Laur, O., Warren, S. T. and Bassell, G. J. (2011). Reversible inhibition of PSD-95 mRNA translation by miR-125a, FMRP phosphorylation, and mGluR signaling. *Mol. Cell* **42**, 673-688.
Müller, M., Heym, R. G., Mayer, A., Kramer, K., Schmid, M., Cramer, P., Urlaub, H., Jansen, R.-P. and Niessing, D. (2011). A cytoplasmic complex mediates specific mRNA recognition and localization in yeast. *PLoS Biol.* **9**, e1000611.
Nakamura, A., Sato, K. and Hanyu-Nakamura, K. (2004). Drosophila cup is an eIF4E binding protein that associates with Bruno and regulates oskar mRNA translation in oogenesis. *Dev. Cell* **6**, 69-78.
Natalizio, B. J. and Wente, S. R. (2013). Postage for the messenger: designating routes for nuclear mRNA export. *Trends Cell Biol.* **23**, 365-373.
Navarro, C., Puthalakath, H., Adams, J. M., Strasser, A. and Lehmann, R. (2004). Egalitarian binds dynein light chain to establish oocyte polarity and maintain oocyte fate. *Nat. Cell Biol.* **6**, 427-435.
Otero, L. J., Devaux, A. and Standart, N. (2001). A 250-nucleotide UA-rich element in the 3′ untranslated region of Xenopus laevis Vg1 mRNA represses translation both in vivo and in vitro. *RNA* **7**, 1753-1767.
Park, H. Y., Lim, H., Yoon, Y. J., Follenzi, A., Nwokafor, C., Lopez-Jones, M., Meng, X. and Singer, R. H. (2014). Visualization of dynamics of single endogenous mRNA labeled in live mouse. *Science* **343**, 422-424.
Parton, R. M., Hamilton, R. S., Ball, G., Yang, L., Cullen, C. F., Lu, W., Ohkura, H. and Davis, I. (2011). A PAR-1-dependent orientation gradient of dynamic microtubules directs posterior cargo transport in the Drosophila oocyte. *J. Cell Biol.* **194**, 121-135.
Patel, V. L., Mitra, S., Harris, R., Buxbaum, A. R., Lionnet, T., Brenowitz, M., Girvin, M., Levy, M., Almo, S. C., Singer, R. H. et al. (2012). Spatial arrangement of an RNA zipcode identifies mRNAs under post-transcriptional control. *Genes Dev.* **26**, 43-53.
Piccioni, F., Zappavigna, V. and Verrotti, A. C. (2005). A cup full of functions. *RNA Biol.* **2**, 125-128.
Pinder, B. D. and Smibert, C. A. (2013). microRNA-independent recruitment of Argonaute 1 to nanos mRNA through the Smaug RNA-binding protein. *EMBO Rep.* **14**, 80-86.
Politz, J. C. R., Tuft, R. A. and Pederson, T. (2003). Diffusion-based transport of nascent ribosomes in the nucleus. *Mol. Biol. Cell* **14**, 4805-4812.
Powrie, E. A., Zenklusen, D. and Singer, R. H. (2011). A nucleoporin, Nup60p, affects the nuclear and cytoplasmic localization of ASH1 mRNA in S. cerevisiae. *RNA* **17**, 134-144.
Radford, H. E., Meijer, H. A. and de Moor, C. H. (2008). Translational control by cytoplasmic polyadenylation in Xenopus oocytes. *Biochim. Biophys. Acta* **1779**, 217-229.
Rodríguez-Navarro, S. and Hurt, E. (2011). Linking gene regulation to mRNA production and export. *Curr. Opin. Cell Biol.* **23**, 302-309.
Rosenthal, E. T., Tansey, T. R. and Ruderman, J. V. (1983). Sequence-specific adenylations and deadenylations accompany changes in the translation of maternal messenger RNA after fertilization of Spisula oocytes. *J. Mol. Biol.* **166**, 309-327.
Santangelo, P. J., Lifland, A. W., Curt, P., Sasaki, Y., Bassell, G. J., Lindquist, M. E. and Crowe, J. E., Jr (2009). Single molecule-sensitive probes for imaging RNA in live cells. *Nat. Methods* **6**, 347-349.
Santini, E., Huynh, T. N., MacAskill, A. F., Carter, A. G., Pierre, P., Ruggero, D., Kaphzan, H. and Klann, E. (2013). Exaggerated translation causes synaptic and behavioural aberrations associated with autism. *Nature* **493**, 411-415.
Saulière, J., Murigneux, V., Wang, Z., Marquenet, E., Barbosa, I., Le Tonquèze, O., Audic, Y., Paillard, L., Roest Crollius, H. and Le Hir, H. (2012). CLIP-seq of eIF4AIII reveals transcriptome-wide mapping of the human exon junction complex. *Nat. Struct. Mol. Biol.* **19**, 1124-1131.
Schuh, M., (2011). An actin-dependent mechanism for long-range vesicle transport. *Nat. Cell Biol.* **13**, 1431-1436.
Shandilya, J. and Roberts, S. G. E. (2012). The transcription cycle in eukaryotes: from productive initiation to RNA polymerase II recycling. *Biochim. Biophys. Acta* **1819**, 391-400.
Sharma, A., Yilmaz, A., Marsh, K., Cochrane, A. and Boris-Lawrie, K. (2012). Thriving under stress: selective translation of HIV-1 structural protein mRNA during Vpr-mediated impairment of eIF4E translation activity. *PLoS Pathog.* **8**, e1002612.
Singh, G., Kucukural, A., Cenik, C., Leszyk, J. D., Shaffer, S. A., Weng, Z. and Moore, M. J. (2012). The cellular EJC interactome reveals higher-order mRNP structure and an EJC-SR protein nexus. *Cell* **151**, 750-764.
Sinsimer, K. S., Lee, J. J., Thiberge, S. Y. and Gavis, E. R. (2013). Germ plasm anchoring is a dynamic state that requires persistent trafficking. *Cell Rep.* **5**, 1169-1177.
Snee, M. J., Arn, E. A., Bullock, S. L. and Macdonald, P. M. (2005). Recognition of the bcd mRNA localization signal in Drosophila embryos and ovaries. *Mol. Cell. Biol.* **25**, 1501-1510.
Speese, S. D., Ashley, J., Jokhi, V., Nunnari, J., Barria, R., Li, Y., Ataman, B., Koon, A., Chang, Y.-T., Li, Q. et al. (2012). Nuclear envelope budding enables large ribonucleoprotein particle export during synaptic Wnt signaling. *Cell* **149**, 832-846.
St Johnston, D. (2005). Moving messages: the intracellular localization of mRNAs. *Nat. Rev. Mol. Cell Biol.* **6**, 363-375.
St Johnston, D., Driever, W., Berleth, T., Richstein, S. and Nüsslein-Volhard, C. (1989). Multiple steps in the localization of bicoid RNA to the anterior pole of the Drosophila oocyte. *Development* **107 Suppl.**, 13-19.
Sung, H.-H., Telley, I. A., Papadaki, P., Ephrussi, A., Surrey, T. and Rørth, P. (2008). Drosophila ensconsin promotes productive recruitment of Kinesin-1 to microtubules. *Dev. Cell* **15**, 866-876.
Takatori, N., Kumano, G., Saiga, H. and Nishida, H. (2010). Segregation of germ layer fates by nuclear migration-dependent localization of Not mRNA. *Dev. Cell* **19**, 589-598.
Teixeira, D., Sheth, U., Valencia-Sanchez, M. A., Brengues, M. and Parker, R. (2005). Processing bodies require RNA for assembly and contain nontranslating mRNAs. *RNA* **11**, 371-382.
Tran, E. J., Zhou, Y., Corbett, A. H. and Wente, S. R. (2007). The DEAD-box protein Dbp5 controls mRNA export by triggering specific RNA:protein remodeling events. *Mol. Cell* **28**, 850-859.
Trcek, T. and Singer, R. H. (2010). The cytoplasmic fate of an mRNP is determined cotranscriptionally: exception or rule? *Genes Dev.* **24**, 1827-1831.
Trinh, M. A., Kaphzan, H., Wek, R. C., Pierre, P., Cavener, D. R. and Klann, E. (2012). Brain-specific disruption of the eIF2α kinase PERK decreases ATF4 expression and impairs behavioral flexibility. *Cell Rep.* **1**, 676-688.
Valkov, E., Dean, J. C., Jani, D., Kuhlmann, S. I. and Stewart, M. (2012). Structural basis for the assembly and disassembly of mRNA nuclear export complexes. *Biochim. Biophys. Acta* **1819**, 578-592.
Van De Bor, V., Hartswood, E., Jones, C., Finnegan, D. and Davis, I. (2005). gurken and the I factor retrotransposon RNAs share common localization signals and machinery. *Dev. Cell* **9**, 51-62.
Weil, T. T., Forrest, K. M. and Gavis, E. R. (2006). Localization of bicoid mRNA in late oocytes is maintained by continual active transport. *Dev. Cell* **11**, 251-262.
Weil, T. T., Parton, R. M. and Davis, I. (2010a). Making the message clear: visualizing mRNA localization. *Trends Cell Biol.* **20**, 380-390.
Weil, T. T., Xanthakis, D., Parton, R., Dobbie, I., Rabouille, C., Gavis, E. R. and Davis, I. (2010b). Distinguishing direct from indirect roles for bicoid mRNA localization factors. *Development* **137**, 169-176.
Weil, T. T., Parton, R. M., Herpers, B., Soetaert, J., Veenendaal, T., Xanthakis, D., Dobbie, I. M., Halstead, J. M., Hayashi, R., Rabouille, C. et al. (2012). Drosophila patterning is established by differential association of mRNAs with P bodies. *Nat. Cell Biol.* **14**, 1305-1315.
Wilhelm, J. E. and Vale, R. D. (1993). RNA on the move: the mRNA localization pathway. *J. Cell Biol.* **123**, 269-274.
Wilhelm, J. E., Hilton, M., Amos, Q. and Henzel, W. J. (2003). Cup is an eIF4E binding protein required for both the translational repression of oskar and the recruitment of Barentsz. *J. Cell Biol.* **163**, 1197-1204.
Wilkie, G. S. and Davis, I. (2001). Drosophila wingless and pair-rule transcripts localize apically by dynein-mediated transport of RNA particles. *Cell* **105**, 209-219.
Wu, B., Chao, J. A. and Singer, R. H. (2012). Fluorescence fluctuation spectroscopy enables quantitative imaging of single mRNAs in living cells. *Biophys. J.* **102**, 2936-2944.
Xu, D., Shen, W., Guo, R., Xue, Y., Peng, W., Sima, J., Yang, J., Sharov, A., Srikantan, S., Yang, J. et al. (2013). Top3β is an RNA topoisomerase that works with fragile X syndrome protein to promote synapse formation. *Nat. Neurosci.* **16**, 1238-1247.
Yisraeli, J. K., Sokol, S. and Melton, D. A. (1990). A two-step model for the localization of maternal mRNA in Xenopus oocytes: involvement of microtubules and microfilaments in the translocation and anchoring of Vg1 mRNA. *Development* **108**, 289-298.
Yunger, S., Rosenfeld, L., Garini, Y. and Shav-Tal, Y. (2013). Quantifying the transcriptional output of single alleles in single living mammalian cells. *Nat. Protoc.* **8**, 393-408.
Zimyanin, V. L., Belaya, K., Pecreaux, J., Gilchrist, M. J., Clark, A., Davis, I. and St Johnston, D. (2008). In vivo imaging of oskar mRNA transport reveals the mechanism of posterior localization. *Cell* **134**, 843-853.